TUSCIA UNIVERSITY OF VITERBO

DEPARTMENT OF

AGRICULTURE AND FORESTRY SCIENCE (DAFNE)

Ph.D. RESEARCH PROGRAM IN

PLANT BIOTECHNOLOGY-XXVIII

SINGLET OXYGEN GENERATED BY PSII REACTION CENTERS OF *CHLAMYDOMONAS REINHARDTII* MUTANTS IN RELATION TO BIOSENSORISTIC PURPOSES

SCIENTIFIC SECTOR-DICIPLINARY

(s.s.d. BIO/13)

Ph.D. Dissertation of:

Mehmet Turemis

Coordinator

Prof. Stefania Masci

Tutor

Dr. Maria Teresa Giardi

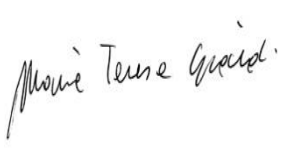

Academic Years 2013-2016

UNIVERSITA DEGLI STUDI DELLA TUSCIA DI VITERBO

DIPERTIMENTO DI

SCIENZE AGRARIE E FORESTALI (DAFNE)

CORSO DI DOTTORATO DI RICERCA IN

BIOTECNOLOGIE VEGETALI – XXVIII CICLO

SINGLET OXYGEN GENERATED BY PSII REACTION CENTERS OF *CHLAMYDOMONAS REINHARDTII* MUTANTS IN RELATION TO BIOSENSORISTIC PURPOSES

SETTORE SCIENTIFICO DISCIPLINARE

(s.s.d. BIO/13)

Tesi di dottorato di:

Mehmet Turemis

Coordinatore del corso

Prof. Stefania Masci

Tutore

Dott. Maria Teresa Giardi

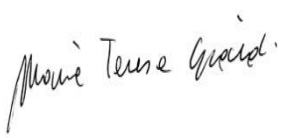

Academic Years 2013-2016

To my loving family

Acknowledgements

This study was carried out in the Biosensor s.r.l (ITALY/Rome) during the years 2013-2016 within the Marie Curie ITN project, "The Singlet Oxygen Strategy: sustainable oxidation procedures for applications in material science, synthesis, wastewater treatment, diagnostics and therapeutics. The research leading to these results has received funding from the European Union's Seventh Framework Program (FP7/2007-2013)/Marie Curie ITN Grant Agreement No. 316975 to Biosensor Srl. Thus, I would like to express my sincere gratitude to Marie Curie research fellowship program for their generous research funding which gave me the possibility to carry out this PhD research in an international environment and gain experience abroad in the private sector. This prestigious grant allowed me to learn new techniques and add valuable publications to my CV.I express my special thanks to my advisor Dr. Maria Teresa Giardi for her supervision, guidance, support and encouragement during my study. With her creative ideas and guidance, I was able to learn how to approach a problem and solve it. It was a great opportunity for me to work with Dr. Maria Teresa Giardi. I would like to thank my PhD coordinator Prof. Stefania Masci and Prof. Renato D'Ovidio, Prof. Carla Perrotta, Dr. Guido Cipriani and Dr. Fabiana Arduini for kindly taking part and precious contributions in my thesis comitee. I want to thank Prof. Dr. Joao Tome and Dr. Venkatramaiah Nutalapati for their help, guidance, and kind encouragement and for everything I learned from them at all stages of my secondment study at University of Aveiro. I would also to thank Dr. Giuseppina Rea for her advices in experiments and her critical views throughout my study.

I am especially thankful to Gianni Basile the general manager of Biosensor s.r.l for his help, support and motivation.

I would like to thank all my friends and colleagues in Biosensor s.r.l. I especially thank to Dr. Gianni Pezzotti, Dr. Giuseppe Rodio, Dr. Laura Moro, Dr. Ivano Manfredonia and Dr. Silvia Silletti for their participation and contribution in my project. I am also thankful to Dr. Laura Moro for always being helpful and support throughout writing my articles and the thesis.

Last, my warmest thanks go to my family for their endless support, patience, helps and encouragement throughout my whole life.

INDEX/TABLE OF CONTENTS

LIST OF ABBREVIATIONS AND ACRONYMS

Abs:	**Absorbance**
AC:	**Alternating current**
ATP:	**Adenosine triphosphate**
BBM:	**Bolds basal medium**
CA:	**Chronoamperometry**
Chl:	**Chlorophyll**
^{3}Chl:	**Triplet chlorophyll**
CNT:	**Carbonnanotube**
CSR:	**Complex space radiation**
DMSO:	**Dimethyl sulfoxide**
DNA:	**Deoxyribonucleic acid**
DOL:	**Degree of labeling**
DPPH:	**1,1-Diphenyl-2-picrylhydrazyl radical**
dsDNA:	**Double stranded deoxyribonucleic acid**
DW:	**Dry weight**
ECL:	**Electrochemiluminescance**
EU:	**European Union**
FET:	**Field effect transistor**
FITC:	**Fluorescein 5 (6)-Isothiocyanate**
Fm:	**Maximum fluorescence (dark-adapted chlorophyll fluorescence)**
Fv:	**Difference between maximum fluorescence and minimum fluorescence or variable fluorescence**
Fv/Fm:	**The maximum quantum efficiency of photosystem II photochemistry**
GC-MS:	**Gas chromatography-mass spectrometry**
GOD:	**Glucose oxidase**
HL:	**High light**
HPLC:	**High performance liquid chromatography**
HRP:	**Horseradish peroxidase**
I_{50}:	**Half-maximal inhibitory concentration**

ICP-MS:	**Inductively coupled plasma mass spectrometry**
Ig:	**Immunoglobulin**
ISS:	**International space station**
LC-MS:	**Liquid chromatography mass spectrometry**
LED:	**Light emitting diodes**
LL:	**Low light**
LOD:	**Limit of detection**
LPPS:	**Liquid phase peptide synthesis**
MALDI-TOFMS:	**Matrix-assisted laser desorption/ionization with time-of-flight mass spectroscopy**
MIP:	**Molecularly imprinted polymers**
NA:	**Nucleic acid**
NADPH:	**Nicotinamide adenine dinucleotide phosphate**
NMR:	**Nuclear magnetic resonance**
O^2:	**Oxygen**
$_1O^2$:	**Singlet oxygen**
ODNs:	**Oligodeoxyribonucleotides**
OEC:	**Oxygen evolving complex**
PCR:	**Polymerase chain reaction**
PSI:	**Photosystem I**
PSII:	**Photosystem II**
PTFE:	**Polytetrafluoroethylene**
TAP:	**Tris-acetate-phosphate**
TEAC:	**Trolox equivalent antioxidant capacity**
QCM:	**Quartz crystal microbalance**
QA:	**Plastoquinone A**
QB:	**Plastoquinone B**
QD:	**Quantum dot**
R^2:	**Coefficent of variation**
RC:	**Reactive center**
RNA:	**Ribonucleic acid**

ROS:	**Reactive oxygen species**
RSD:	**Relative sdard deviation**
SE:	**Standard error**
SPE:	**Screen-printed electrode**
SPPS:	**Solid phase peptide synthesis**
SPR:	**Surface plasmon resonance**
ssDNA:	**Single strand deoxyribonucleic acid**
UV:	**Ultraviolet**
Vj:	**Relative variable fluorescence at the characteristic point J**

LIST OF SYMBOLS

%:	**Percentage**
^{o}C:	**Degree Celsius**
cm:	**Centimeter**
cm^2:	**Square centimeter**
Da:	**Dalton**
g:	**Gram**
h:	**Hour**
Hz:	**Hertz**
kHz:	**Kilohertz**
ml/s:	**Milliliter per second**
mm:	**Millimeter**
µg:	**Microgram**
µL:	**Microliter**
µm:	**Micrometer**
µmol:	**Micromol**
mM:	**Millimolar**
µM:	**Micromolar**
µA:	**Micro ampere**
µg/L:	**Microgram per liter**
m:	**Meter**
nm:	**Nanometer**
ppb:	**Parts per billion**
s:	**Second**
w/v:	**Weight per volume**
v/v:	**Volume per volume**
V:	**Volt**

ABSTRACT

SINGLET OXYGEN GENERATED BY PSII REACTION CENTERS OF *CHLAMYDOMONAS REINHARDTII* MUTANTS IN RELATION TO BIOSENSORISTIC PURPOSES

With the advent of the 21st century, public awareness on issues related to human and animal health, food safety, or environmental pollution has increased considerably and a great deal of research and substantial investments have focused on the development of novel tools for continuous in situ environmental monitoring. In this respect, the use of microalgae as a biological tool for monitoring and assessment of environmental toxicants is an application that has attracted much interest. Among photosynthetic organisms sensitive to pesticide classes, the unicellular green alga *Chlamydomonas reinhardtii* and *Chlorella vulgaris* are some examples revealed to be a smart bio-sensing element useful for the realization of analytical devices. Intact algae cell-based biosensors preserve photosystem functionality, and perform sensitive detection at parts per billion (ppb) levels of herbicide. However, they provide a slow response and sometimes-low sensitivity. Beside, their analytical application is sometimes hampered, among other problems, by their relative instability in non-physiological or extreme environmental conditions. The main challenge is the preservation of the algal photosynthetic functionality when integrated with non-biological electronic components or operated under fluctuating environmental conditions. In fact, photodynamic reactive oxygen species (ROS) reactions are determinative in reactions damaging the photosynthetic apparatus of *Chlamydomonas reinhardtii*, causing a short half-life that is a problem for biosensor applications. High light illumination of photosynthetic organisms stimulates the production of singlet oxygen ($_1O^2$) by photosystem II and causes photooxidative stress. It is known that photo-inhibitory damage of Photosystem II (PSII) under various conditions can result in the formation not only of $_1O^2$ but also of other ROS. In *Chlamydomonas reinhardtii*, reducing the formation of $_1O^2$ and ROS thus lessening the photooxidative membrane damage (including the RC protein) and increasing the stability and

sensitivity for biosensor applications is of special interest. The ability to produce new algal biomediators, with a broad structural stability, can be expected to lead biosensing for food control or environmental monitoring.

The main goal of this PhD thesis was increasing the stability and sensitivity of PSII from algae for the detection of different subclasses of pollutants under extreme environmental conditions (high light, salinity etc.) using various ways such as symbiosis, site directed mutagenesis of D1 protein, UV mutagenesis and synthetic biomimetic approach.

Firstly, an optical biosensor based on algal biomediators for monitoring of marine pollutants was developed. The algae-protozoa symbiotic association between *Chlorella vulgaris* and the ciliate *Tetrahymena pyriformis* was deeply studied as a potential biomediator for biosensor development, showing enhanced resistance to the salinity of marine water when compared with free-living algae strains. The symbiosis was adapted to grow into microfluidic flow cells with integrated detectors for real-time detection of marine pollutants by fluorescence analysis of photosynthetic photosystem II. An integrated symbiotic association of *Paramecium-Chlorella*-based biosensor was successfully developed for real-time monitoring of marine water quality and evaluation of biotoxicity.

Secondly, an optical/amperometric biosensor based on algal cells immobilized in calcium alginate gel was developed. Various *Chlamydomonas reinhardtii* strains mutated at the level of photosynthetic D1 protein were used as biomediators to quantify the capacity of the carotenoid xanthophylls to protect the photosynthetic apparatus from photoinhibition. The highly sensitive and selective biosensor was used for studies on cell physiology aimed to determine the antioxidant and light filtering effects of the xanthophyll astaxanthin. The biosensor was proved to be suitable for the determination of the exogenous supplied astaxanthin showing in a short time a reliable response with a detection limit of 3 µM. This technique revealed the photo-protective effect of astaxanthin-enriched extracts of *Haematococcus pluvialis* in algal cells. The results suggest that in algae astaxanthin exploits both filtering and antioxidant effects at different light intensities. This bioinspired approach

can provide new insights into biological, biomedical, environmental and agricultural research applications and nutraceutical studies.

We also projected and realized a biosensor platform, which combines an optical system, intimately, integrated with an array of biomediators able to provide a helpful tool for safety management of the milk. Optical feature selection of various enzymes was performed for monitoring compounds of various chemical classes and metabolic markers of cow's wellness. The detection of selected analytes was evaluated through biomediators of *Chlamydomonas reinhardtii* cells, and acetylcholinesterase, tyrosinase, urease, β-galactosidase and D-lactate dehydrogenase enzymes. The analyses were performed by fluorescence that for the algal cells was based on chlorophyll a fluorescence emission while for enzymes was guaranteed by the use of fluorescein 5(6)-isothiocyanate or 5(6)-carboxynaphthofluorescein.

Furthermore, a novel fluidic setup based on simple fluid mechanics laws has been realized with no moving components when pump is on. It yields a fluctuation-free outcome signal that we compare with those produced by commercial peristaltic pumps. Evidence of the readout amperometric enhanced signal is shown thus confirming the successful implementation of more reliable biosensors and electrochemical signal transduction devices. Such stable and oscillation free amperometric signals are very desirable in view of biosensors integration in environmental monitoring platforms equipped with advanced communication technologies.

In addition, two set of *C. reinhardtii* mutants, able to quench $_1O^2$ and other ROS produced under extreme conditions, were produced in collaboration with U. Johanningmeier (Uni of Halle). First set was mutated by site-directed mutagenesis (antiox-mutants): antioxidant peptides able to quench $_1O^2$ and variety of free radicals introduced in the D1 protein of Photosystem II. The second set was produced by UV-mutagenesis. The mutated strains were characterized to select more resistant strains to be used as biological element for environmental monitoring under extreme conditions.

In this study, total lipid and phenol content of two set of *Chlamydomonas reinhardtii* mutants (Antiox and UV mutants) were determined. The in-vivo and in-vitro antioxidant capacity of the antiox-mutants were evaluated using different assay and in the presence of $_1O^2$ precursors. The mutants have reduced lipid and phenol content compared to the wild type *Chlamydomonas reinhardtii*. However, they showed better resistant to stress conditions such as high light, $_1O^2$ and H_2O_2. UV mutants have showed longer half-life. The produced mutants revealed to be a promising candidate for improved environmental monitoring on earth.

We also described the use of biomimetic peptides of the photosynthetic plastoquinone binding niche of the green alga *Chlamydomonas reinhardtii* for pesticide measurement in environmental samples. Three biomimetic peptides containing the plastoquinone-binding site in a loop shaped by two alpha helices were designed and characterized. Natural sequence of 70 aminoacid-peptide was modified to increase the solubility in aqueous solvents by adding two histidine in the N- and C-terminus. A cysteine was included in two of the modified peptides (S264C or S268C) and labeled with commercial carboxylated quantum dots (peak emissions 710 nm) by carbodiimide reaction coupling and fluorometric detection was performed. The results confirmed that mutation S264C conferred resistance to atrazine and diuron, while the change S268C increased the sensitivity. This work demonstrates the interest to replace whole microalgae cells or their photosynthetic apparatus (thylakoids, isolated reaction centers) by much smaller fragments such as D1 peptide mimics. This approach might improve the system in terms of sensitivity, but also in terms of stability (oligopeptides being much more stable than the whole three-dimensional protein molecule) and facilitate the commercialization for environmental monitoring.

English is an international language that allows us to communicate with scientists from all over the world and writing a manuscript is important since it is a form of written communication in science. In this occasion, as a part of my training to improve my writing skills and enhance my knowledge on biosensors, we presented a review focuses on bioassay development based on the

simultaneous use of quantum dots and magnetic beads. Due to the outstanding characteristics of both particles for biosensing applications and the large number of publications using a combined approach, we aim to provide a comprehensive overview of the literature on different bioassays. The improvement of current approaches together with novel multiplex detection systems and nanomaterials-based research, including the use of multimodal nanoparticles, will contribute to simpler and more sensitive bioanalyses.

The optical and electrochemical biosensors, that were constructed and optimized within this doctoral thesis, have the advantage of being user friendly, low cost and portable analytical tools, which facilitates a future transfer to the market of environmental and agrifood monitoring.

CHAPTER 1

Introduction

1. Biosensors

Over the past decade, many important technological advances have provided us with the tools and materials needed to construct biosensor devices. Since the first invention of the Clark Oxygen Electrode sensor, there have been many improvements in the sensitivity, selectivity, and multiplexing capacity of the modern biosensor. Before the various types of biosensor technologies and application are discussed, it is first important to understand and define ‘‘biosensor’’ (Perumal, 2014).

A biosensor is a self-contained integrated device that is capable of providing specific quantitative or semi-quantitative analytical information using a biological recognition element (biochemical receptor) that is retained in direct spatial contact with a transduction element. However, a common working definition is that a biosensor is an analytical device that uses biological macromolecules to recognize an analyte and subsequently activate a signal that is detected with a transducer (Cullum and Sumner, 2010). Once the interaction of the biochemical receptor with the analyte is converted into a signal detectable by the transduction system, the signal is send to a readout or display by appropriate electrical equipment (Farré et al., 2009, Thévenot et al., 2001, Justino et al., 2010). The biosensor consists of three parts: the first element is the biomediator a biologically derived material e.g. tissue, microorganisms, organelles, cell receptors, enzymes, antibodies, nucleic acids, and biological sensitive elements created with genetic engineering, or a biomimic system e.g. aptamers, MIPs, etc. The second element is the transducer e.g. physicochemical, optical, piezoelectric, electrochemical, etc. that transforms the signal resulting from the analytes interaction with the biological element into a signal that can be measured and quantified. The third element is the associated electronics or signal processor, responsible of the visualization results in a user-friendly way. There is a need for a simple, rapid and reagentless method for specific determination, both qualitative and quantitative, of various compounds in various applications. Hence, it is paramount to have fast and accurate chemical intelligence, which is particularly conspicuous in human health care.

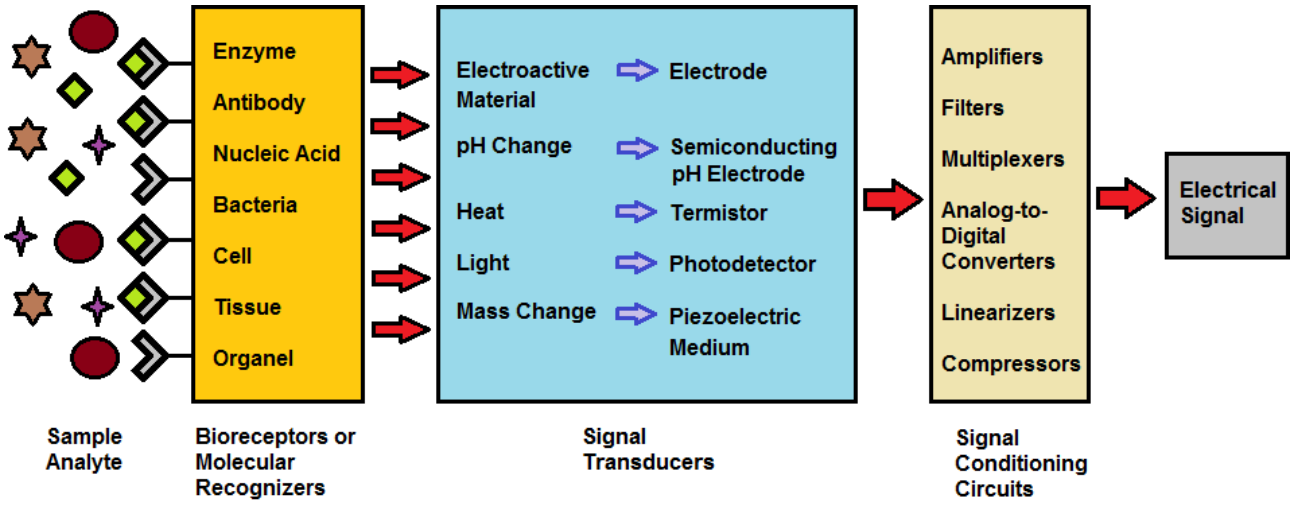

Fig. 1. The Principle of a biosensor

1.1. Classification of biosensors

Biosensors can be classified according to either the biorecognition principle used for sensing (e.g. enzymes, nucleic acids, antibody or whole cells) or the transduction element employed (e.g., electrochemical, optical, piezoelectrical or thermal). Some authorities subdivide biosensors into affinity biosensors and catalytic biosensors based upon the activity of the biorecognition element. Thus, *affinity biosensors* have as their fundamental property the recognition (binding) of the analyte by the biorecognition element (for example, antibody-antigen), whereas *catalytic biosensors* have as their biorecognition element proteins (or microorganisms) that not only bind the analyte but also catalyze a reaction involving the analyte to produce a product (for example, glucose biosensors) (Cullum and Sumner, 2010).

According to the transducer type, biosensors can be classified in four different groups (Frachiolla et al., 2013) As described above, the transducer is the portion of the biosensor responsible for converting the biorecognition event into a measurable signal. It is possible to exploit a change in a number of physical and chemical properties (mass, temperature, electrical properties, and optical properties) to allow for different transduction formats. Although a variety of transducer methods have

been feasible toward the development of biosensor technology, the most common methods are electrochemical and optical followed by piezoelectric.

1.1.1. Optical detection

Due to a number of advantages, optical transduction is one of the most widely used biosensor transduction formats. For example, optical transduction can be very rapid where the limiting factor for the speed of detection is often a diffusion-limited process of the biomolecular recognition event, rather than the optical transducer. Another advantage of optical transduction is that the interferences that can hinder electrochemical transduction measurements (such as voltage surges, harmonic induction, corrosion of electrode elements, and radio frequency interferences) are not present. Some of the disadvantages of using optical transduction formats include detection challenges when analyzing turbid samples and the cost associated with detection system components.

A wide variety of optical transduction formats have been employed, where changes of the interaction of light with the biomolecular system are used to produce a measurable signal. These changes can be based on differences in refractive index, production of chemiluminescent reaction products, fluorescence emission, fluorescence quenching, radiative and nonradiative energy transfer, temporal changes in optical emission properties, and scattering techniques, well as other optical effects.

These effects can be monitored using a variety of optical platforms including total internal reflectance and evanescent wave technologies, interferometric, resonant cavities, and biochip devices. The following paragraphs review the most common as well as most popular emerging optical transduction formats: fluorescence, chemiluminescence, and surface plasmon resonance (Cullum and Sumner, 2010).

1.1.1.1. Fluorescence

Fluorescence is the most popular form of optical transduction due to the high sensitivity that is fundamental to this type of optical process. Another advantage of fluorescence-based methods is that they generally do not have the interference issues that SPR and other refractive index based methods possess. However, in most cases, the intrinsic sample fluorescence is not sufficient for analysis, and a fluorogenic reporter is used to label an affinity reagent to create a bioreporter. By monitoring the intensity of the fluorogenic reporter, it is possible to determine the presence and concentration of the target analytes, as illustrated in the bioassay techniques already described. It is also possible to monitor shifts in the wavelength of the fluorophore reporter, as well as energy transfer phenomena, and time dependence of the fluorescence emission, all of which can be related to binding interactions depending on the assay employed. The distinguishing features between biosensors, besides the above mentioned properties that can be monitored, include the optical detection format used. For example, it is possible to utilize fiber-optic probes to immobilize bioreceptors at the tip of the fiber and use total internal reflectance properties of the fiber to transmit excited and emitted light. Total internal reflectance can also be employed in an evanescent wave format, where a residual amount of (evanescent) light at the reflectance point that escapes is used to excite immobilized bioreceptors only in close proximity to the surface, rather than in bulk solution. This format allows for controlled excitation and can allow for minimal fluorescence background.

However, a key disadvantage is the lack of evanescent excitation power and sometimes poor coupling of the emission when using similar collection geometries. Fluorescence detection can be used with a wide variety of detection formats. For example, it is routinely coupled with flow cytometry and microfluidic platforms or imaging array systems such as biochips that utilize spatial patterning of biological recognition elements to match fluorescence location to target species (Cullum and Sumner, 2010).

1.1.2. Electrochemical

Electrochemical transduction is one of the most popular transduction formats employed in biosensing applications. One of the main advantages of biosensors that employ electrochemical transduction is the ability to operate in turbid media and often in complex matrices. Another distinct advantage of electrochemical transduction is that the detection components are inexpensive and can be readily miniaturized into portable, low-cost devices.

In general, electrochemical-based sensing can be divided into three main categories: potentiometric, amperometric, and impedance. Potentiometric sensors typically rely on a change in potential caused by the production of an electroactive species that is measured by an ion selective electrode. For a biosensor system, this change in electroactive species concentration is usually brought about by an enzyme. In an amperometric sensor system, a change in current is directly measured. Electrochemical sensors based on impedance most commonly utilize impedance spectroscopy since controlled AC electrical stimulus over a range of frequencies is used to detect variations in the sensor surface properties (that is, charge transfer and capacitance at the interface layer). In this way, the resistance to flow of an alternating current is measured as voltage/current. For example, metabolic changes (for example, growth) have been shown to correspond to an increase or decrease in impedance. Some of the many variations of potentiometric, amperometric, and impedance biosensors that provide for improved biosensor performance include field effect transistors (FET) and electrochemiluminescence (ECL) (Cullum and Sumner, 2010; Chaplin, 2000).

1.1.3. Mass-sensitive

Biosensors that are based on mass-sensitive measurements detect small mass changes caused by chemical binding to small piezoelectric crystals. Initially, a specific electrical signal can be applied to the crystals to cause them to vibrate at a specific frequency. This frequency of oscillation depends on the electrical signal frequency and the mass of the crystal. As such, the binding of an analyte of

interest will increase the mass of the crystal and subsequently change its frequency of oscillation, which can then be measured electrically and used to determine the mass of the analyte of interest bound to the crystal (Morrison, 2008). The main advantage to the piezoelectric transduction (that is, mass sensor) approach includes the ability to perform label-free measurements of the binding events, including real-time analysis of binding kinetics (Cullum and Sumner, 2010).

1.1.4. Thermal/Calorimetric

Calorimetric sensors utilize thermistor probes to monitor changes in temperature due to exothermic chemical reactions. This change in temperature can be correlated to the amount of reactants consumed or products formed. Many biological reactions are exothermic (for example, enzyme reactions), and hence calorimetric detection allows for a near-universal transduction format. One key disadvantage of this approach is that environmental temperature fluctuations must be shielded from the sensor system. Calorimetric biosensors traditionally have been large and bulky, although advances in silicon microfabrication technologies and microfluidics have allowed for miniaturization and improved performance.

1.2. Different types of bioreceptors

The key to specificity for biosensor technologies involves bioreceptors. They are responsible for binding the analyte of interest to the sensor for the measurement. These bioreceptors can take many forms and the different bioreceptors that have been used are as numerous as the different analytes that have been monitored using biosensors. However, bioreceptors can generally be classified into five different major categories. These categories include: 1) antibody/antigen, 2) enzymes, 3) nucleic acids/DNA, 4) cellular structures/cells and 5) biomimetic (Dinh, 2007). Enzymes have been the most widely used bioreceptor molecules in biosensor applications, with antibodies and

protein receptor molecules increasingly incorporated in biosensors. The specificity of a biosensor comes from the specificity of the bioreceptor molecule used (Lee and Mutharasan, 2005).

Enzymes: Enzyme based biosensors were the earliest biosensors, introduced by Clark and Lyons in 1962 – an amperometric enzyme electrode for a glucose sensor which used a ‘‘soluble’’ enzyme electrode. Since the first biosensor, enzyme based biosensors have faced a massive growth in usage for various applications up to the present. Enzymes are very efficient biocatalysts, which have the ability to specifically recognize their substrates and to catalyze their transformation. These unique properties make the enzymes powerful tools to develop analytical devices (Perumal and Hashim, 2014).

In biocatalytic recognition mechanisms, the detection is amplified by a reaction catalyzed by macromolecules called biocatalysts. The lock and key and induced fit hypothesis can apply to explain the mechanism of the enzyme action, which is highly specific for this type of biosensor. This high specificity of enzyme–substrate interactions and the usually high turnover rates of biocatalysts are the origin of sensitive and specific enzyme-based biosensor devices. This specific catalytic reaction of the enzyme provides these types of biosensor with the ability to detect much lower limits than with normal binding techniques (Perumal and Hashim, 2014).

The catalytic activity of enzymes depends upon the integrity of their native protein conformation. If an enzyme is denatured, dissociated into its subunits, or broken down into its component amino acids, its catalytic activity is destroyed (Dinh, 2007). Ideally, enzyme catalytic action can be influenced by several factors such as the concentration of the substrate, temperature, presence of a competitive and non-competitive inhibitor and pH. Essentially the Michaelis– Menten equation can be used to further explain the detection limit of the enzyme based biosensor. Some recent studies have shown that enzyme based biosensors can be used to detect cholesterol, food safety and environmental monitoring, heavy metals and also pesticides. (Perumal and Hashim, 2014).

Antibodies: An antibody is a complex biomolecule, made up of hundreds of individual amino acids arranged in a highly ordered sequence. They represent one of the major classes of proteins. They constitute about 20% of the total plasma protein and are collectively called immunoglobulins (Ig). An antigen can be any macromolecule that induces an immune response. The antibody binds reversibly with a specific antigen. Unlike the enzyme proteins, the antibodies do not act as catalysts. The way in which an antigen and its antigen-specific antibody interact may be understood as analogous to a lock and key fit, by which specific geometrical configurations of a unique key enables it to open a lock. In the same way, an antigen-specific antibody "fits" its unique antigen in a highly specific manner. This unique property of antibodies is the key to their usefulness in immunosensors where only the specific analyte of interest, the antigen, fits into the antibody-binding site.

DNA/nucleic acid: The use of a nucleic acids sequence for a specific diagnostics application was developed in the early 1953 and is still growing widely. Biosensors based on DNA, RNA and peptide nucleic acid gain their high sensitivity and selectivity from the very strong base pair affinity between complementary sections of lined — up nucleotide strands (Borgmann et al. 2011). Nucleic acid (NA) — based biosensors integrate an NA (natural and biomimetic forms of oligo- and polynucleotides) as the biological recognition element. Nowadays, mainly synthetic oligodeoxyribonucleotides (ODNs) are used as probes in the DNA hybridization sensors (Monosik, 2012). The highly specific affinity binding's reaction between two single strand DNA (ssDNA) chains to form double stranded DNA (dsDNA) is utilized in the nucleic acids based biosensor which appoints the nucleic acids as the biological recognition element. This biosensor possesses a remarkable specificity to provide analytical tools that can measure the presence of a single molecule species in a complex mixture (Perumal and Hashim, 2014).

Biomimetic receptors: An artificial (man-made) receptor that is fabricated and designed to mimic a bioreceptor is often termed a biomimetic receptor. Several different methods have been developed over the years for the construction of biomimetic receptors. These methods include genetically

engineered molecules, artificial membrane fabrication and molecular imprinting. Recombinant techniques, which allow for the synthesis or modification of a wide variety of binding sites using chemical means, have provided powerful tools for designing synthetic bioreceptors with desired properties (Dinh, 2007).

Cells: These bioreceptors are based on biorecognition either by an entire cell/microorganism or by a specific cellular component that is capable of specific binding to certain species (Monosik, 2012; Dinh, 2007). Microorganisms offer a form of bioreceptor that often allows a whole class of compounds to be monitored. Generally, these microorganism biosensors rely on the uptake of certain chemicals into the microorganism for digestion. Often, a microorganism ingests a class of chemicals therefore allowing a class-specific biosensor to be created. Microorganisms such as bacteria and fungi have been used as indicators of toxicity or for the measurement of specific substances. For example, cell metabolism (e.g., growth inhibition, cell viability, and substrate uptake), cell respiration or bacterial bioluminescence have been used to evaluate the effects of toxic heavy metals. Whole mammalian tissue slices or in vitro cultured mammalian cells are used as biosensing elements in bioreceptors.

Photosytnhetic organisms such as plant tissues and microalgae are also used in plant/algae-based biosensors since they are effective catalysts because of the enzymatic pathways they possess. In general, their use is associated to the environmental monitoring and in particular to pesticides, herbicides and heavy metals (Scognamiglio et al. 2010; Giardi and Pace, 2005).

It is know that photosynthesis in green microalgae and higher plants occurs into chloroplasts that are called cellular organelles, which contain membrane-made closed structures (thylakoids) tightly leant one to the other to form piles named grana. Within thylakoid membranes, the chlorophyll is associated in complexes containing up to 250 molecules among which only a few number are directly involved in the photochemical reactions producing ATP all the other ones are used as light-harvesting antennae. The antennae have the function to collect and convey the light to the producing

molecules of the ATP. The Photosynthetic apparatus is composed of two photosystems named Photosystem I (PSI) and II (PSII), present in the thylakoids (**Fig. 2**). As shown in the figure, PSI and PSII are constituted by the ensemble of several proteins and pigment protein complexes that work in concert in order to build up functional units of metabolic importance. These interactions lead to the generation of a transmembrane proton gradient necessary to ATP synthesis and to the production of the reducing power necessary to NADPH biosynthesis (Foyer et al 2012). The chlorophylls of the light-harvesting complex of PSII absorb the light radiation and transfer it to the pigment P680 (primary electron donor of PSII). A group of pigments that are excitonically coupled constitutes this pigment. In fact when they absorb a photon act as a single molecule. P680 is the strongest biological oxidizing agent known at present (Giardi and Pace, 2005).

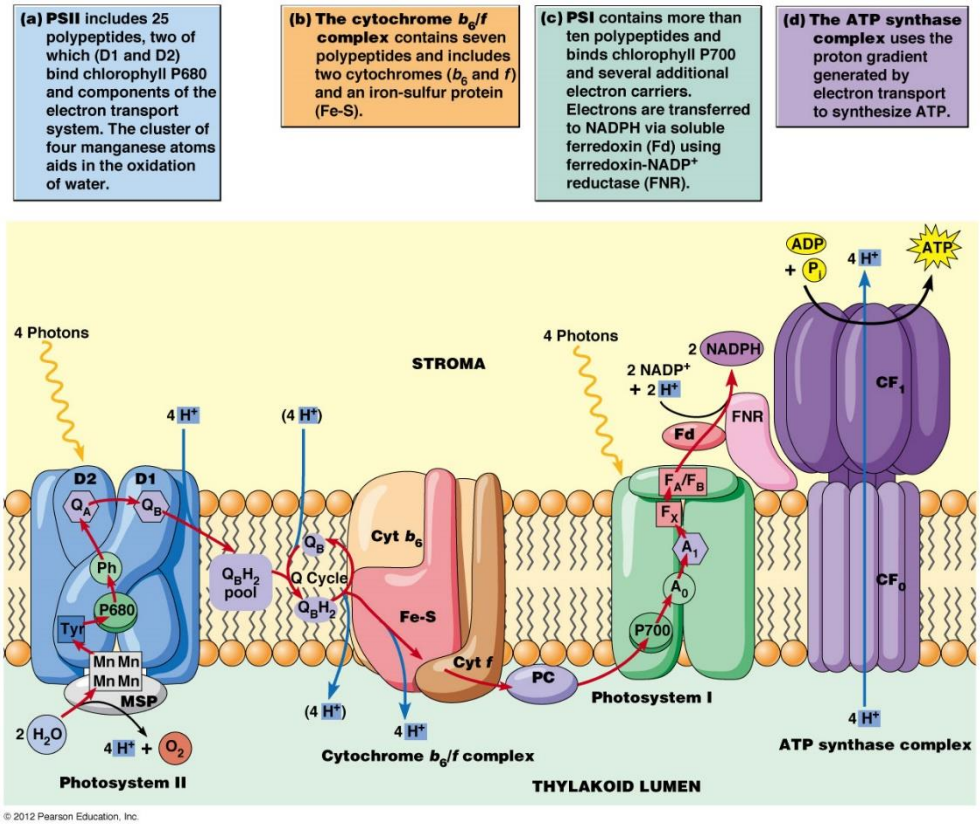

Fig. 2. The Photosynthetic apparatus is arranged in the Photosystem I (PSI) and II (PSII) present in the thylakoids. PSII composed by D1 and D2 proteins and Oxygen Evolving Complex (OEC), Q_A and Q_B binding site.

When the light arrived to PSII, chlorophyll-protein harvesting complexes absorb it then it is funneled to the photochemically active reaction center composed by the subunits D1, D2 and Oxygen Evolving Complex (OEC). Here photoexcitation converts P680 into the oxidized form P680+ thus triggering a single electron transfer first to a pheophytin cofactor then to a plastoquinone molecule Q_A located in D2 and finally to a second plastoquinone Q_B in the D1 protein as shown in the **Figure 2.**

As mentioned above, using photosynthetic organisms and organelles it is possible to detect herbicides presence in waters, environment or agrifood products because herbicides act directly on the photosynthetic system inhibiting the photosynthetic process. About 30% of herbicides including phenylurea, triazine and phenolic herbicides inhibit photosynthetic electron flow by blocking the PSII quinone-binding site and thus modifying chlorophyll fluorescence. Various amperometric and some optical biosensors are developed to detect various kind of herbicides. (Campas et al. 2008; Scognamiglio et al. 2010).

The phenomenon of autofluorescence in photosynthetic organisms is particularly important for our present work. The capture of light energy for photosynthesis is enhanced by networks of pigments in the chloroplasts arranged in aggregates on the thylakoids. These aggregates are called antenna complexes. Evidence for this kind of picture came from research by Robert Emerson and William Arnold in 1932 when they measured the oxygen released in response to extremely bright flashes of light. They found that some 2500 molecules of chlorophyll was required to produce one molecule of oxygen, and that a minimum of eight photons of light must be absorbed in the process. The model that emerges is that of some 300 chlorophyll molecules and 40 or so betacarotenes and other accessory pigments acting as a light harvesting antenna surrounding one chlorophyll a molecule that is a part of an action center. A photon is absorbed by one of the pigment molecules and transfers that energy by successive fluorescence events to neighboring molecules until it reaches the action center where the energy is used to transfer an energetic electron to an electron acceptor. The fluorescence model would suggest that each transferred photon has a longer wavelength and lower

quantum energy with some energy being lost to heat. When a photon reaches the chlorophyll a in the reaction center, that chlorophyll can receive the energy because it absorbs photons of longer wavelengths than the other pigments. Two types of chlorophyll centers have been identified, and are associated with two protein complexes identified as Photosystem II and Photosystem I (**Fig. 2**).

Essentially, the living cell based biosensor is a unique biosensor in contrast to other types of biosensor that contain materials extracted from living things. These types of biosensor have a number of pros and cons. The detection limit of this biosensor is mainly determined by the natural environmental conditions in which the cell can stay alive for a long period in order to control the physical and chemical parameters of the environment. However, the major limitations of the cell based biosensor are the stability of the cell, which depends on various conditions such as sterilization, lifetime, biocompatibility and etc. Another issue that governs the success of cell-based sensors depends primarily on selectivity, in which the cell based sensor has poor selectivity due to the multireceptor behaviour of the intact cells (Belkin and Gu, 2010). Despite these pitfalls, the cell-based biosensor is still favoured by researchers due to the advantages over the enzyme-based biosensor. The cell-based biosensors are less sensitive to inhibition by solutes and are more tolerant of suboptimal pH and temperature values than the enzyme based biosensor, though they must not exceed a narrow range because of the possibility of cell death. A longer lifetime can be expected than with the enzymatic sensors and they are much cheaper because the active cells do not need to be isolated (Struss et al., 2010). The literature indicates that cell based sensors have become emerging tools for medical diagnostics (i.e., such as disease detection), environmental analysis, food quality control, chemical–pharmaceutical industry and drugs detection. Similarly, it was reported that the cell based biosensor is envisioned to be an emerging frontier in the area of nano-diagnotics due to their attractive characteristics.

1.3. Biosensor characteristics

Biosensors are characterized by eight parameters (Lee and Mutharasan, 2005). These are:

(1) Sensitivity is the response of the sensor to per unit change in analyte concentration.

(2) Selectivity is the ability of the sensor to respond only to the target analyte. That is, lack of response to other interfering chemicals is the desired feature.

(3) Range is the concentration range over which the sensitivity of the sensor is good. Sometimes this is called dynamic range or linearity.

(4) Response time is the time required for the sensor to indicate 63% of its final response due to a step change in analyte concentration.

(5) Reproducibility is the accuracy with which the sensor's output can be obtained.

(6) Detection limit is the lowest concentration of the analyte to which there is a measurable response.

(7) Life time is the period over which the sensor can be used without significant deterioration in performance characteristics.

(8) Stability characterizes the change in its baseline or sensitivity over a fixed period.

1.4. Considerations in biosensor development

Once a target analyte has been identified, the major tasks in developing a biosensor involve:

1. Selection of a suitable bioreceptor or a recognition molecule

2. Selection of a suitable immobilization method

3. Selection and design of a transducer that translates binding reaction into measurable signal

4. Design of biosensor considering measurement range, linearity, and minimization of interference, and enhancement of sensitivity

5. Packaging of the biosensor into a complete device

The first item above requires knowledge in biochemistry and biology, the second and third require knowledge in chemistry, electrochemistry and physics, and the fourth requires knowledge of kinetics and mass transfer. Once a biosensor has been designed, it must be packaged for convenient manufacturing and use. The current trend is miniaturization and mass production. Modern IC (integrated circuit) fabrication technology and micromachining technology are used increasingly in fabricating biosensors, as they reduce manufacturing costs. Therefore, an interdisciplinary research team, consisting of the various disciplines identified above, is essential for successful development of a biosensor (Lee and Mutharasan, 2005).

2. Singlet oxygen production in photosystem II

When higher plant, algae and cyanobacteria are exposed to highlight intensity illumination, PSII activity is inhibited in a process called photoinhibition. Photo-inactivation of PSII is considered to be caused by damage to the D1 protein, one of the two proteins, which formed a heterodimer with the D2 protein. It is widely accepted that D1 damage is caused by two distinct mechanisms of photoinhibition i.e. the so called acceptor and donor side mechanism. In the acceptor side photoinhibition, over-reduction of the primary electron acceptor QA leads to its release from the binding site in the D2 protein. In donor side photoinhibition, the formation of long-lived highly oxidizing molecules $P680^{\bullet+}$ /$TyrZ^{\bullet}$ leads to the oxidation of the organic components such as proteins and lipids (Yadav and Pospisil et al., 2012).

It has been reported that different types of reactive oxygen species (ROS) are formed in both the acceptor and the donor side photoinhibition. In the acceptor-side photoinhibition, singlet oxygen

($_1O^2$) is considered the main ROS responsible for PSII damage. It is generated by the interaction of molecular oxygen and triplet chlorophyll formed by the charge recombination of the triplet radical pair ^{3}[P680$^{\bullet+}$ Pheo$^{\bullet-}$]. Trebst and co-workers provided evidence that $_1O^2$ is the important damaging species during photoinhibition of *Chlamydomonas reinhardtii* cells (Trebst et al., 2002). A special case is when herbicides are bound to PSII. Under these conditions electron transfer can take place only as far as $QA^{-\bullet}$ and charge recombination is the main outcome of light-induced charge separation. It was pointed out recently that the stimulated charge recombination occurring in herbicide-treated PSII could be an important factor in the herbicidal action mediated by $_1O^2$. This suggestion was based on a number of experimental observations and theoretical considerations (Fufezan et al., 2002):

1. Different herbicide classes have different influences on the photoinhibition of PSII. Phenolic herbicides increase photodamage, while with 3-(3,4-dichlorophenyl)- 1,1-dimethylurea (DCMU) and other urea- and triazine-type herbicides photodamage is less marked although all of these herbicides bind to the QB-binding site and inhibit forward electron transport.

2. Different classes of herbicides influence the charge recombination measured by differential changes in the thermoluminescence emission temperature. Phenolic herbicides decrease the emission temperature while urea- and triazine type herbicides increase it.

3. Herbicide binding influences the midpoint potential (*E*m) of the QA/$QA^{-\bullet}$ redox couple in PSII with phenolic herbicides lowering the *E*m by 45 mV, while DCMU raises the potential by 50 mV (Krieger-Liszkay et al., 1998).

Correlating these factors it was suggested that herbicides modulate the recombination pathway within PSII and thus the degree of $_1O^2$-mediated photodamage. It is predicted that $_1O^2$ will be generated in herbicide-treated PSII and, importantly, that the yield will be greater when phenolic herbicides are used compared to other classes of herbicide. It is known that photoinhibitory damage of PSII under various conditions can result in the formation not only of $_1O^2$ but also of other reactive oxygen species. In *Chlamydomonas reinhardtii*, reducing the formation of $_1O^2$ and ROS thus

lessening the photooxidative membrane damage and increasing the stability and sensitivity for biosensor applications is of special interest. The ability to produce new algal biomediators, with a broad structural stability, can be expected to lead biosensing for food control or environmental monitoring.

3. Genetic engineering to improve sensitivity and selectivity of biomediators for biosensor development

Nowadays, genetic engineering allows the modification of specific nucleotide sequences of an organism genome to obtain proteins with novel improved properties, and innovative biotechnological approaches make it possible to integrate these systems, or their functional sub-structures, into artificial assemblies for specific applications such as environmental monitoring. Several biomediators have been already developed exploiting molecular biological techniques to produce enzymes and/or protein with improved features in the detection of specific analytes (Wang et al., 2009).

In the context of the photosynthesis-based biosensors, activities in different research areas allowed the design and development of engineered photosynthetic microorganisms with improved sensitivity and stability features to be used as bio-recognition elements for the detection of environmental contaminants. Different approaches, such as space research and physical elicitations, have been applied to select microorganisms with improved tolerance to extreme environmental conditions. The newly selected organisms generated for biosensor purposes were able to maintain a stable photosynthetic efficiency and an increased oxygen evolution capacity (Rea et al., 2008).

In particular, researchers carried out modifications of the D1 reaction center proteins, as they play a crucial role in electron tunneling-mediated charge separation and transmembrane electric field generation, acting principally on reduction, release and migrations of (plasto) quinones. Random mutagenesis targeted to the D1-encoding psbA gene was exploited as a directed evolution strategy to

produce a huge mutant library of *Chlamydomonas* carrying novel D1 proteins with different aminoacidic composition. In addition, thanks to the support of bioinformatics studies, site-directed mutagenesis was also exploited to generate specific point mutations in the D1 protein, in order to modify the properties of the PQ/atrazine binding affinity.

Various mutant strains has been produced and used for biosensing approach so far. *Chlamydomonas* D1 random and site-directed mutants were produced by particle gun bombardments of the chloroplast genome (Przibilla et al., 1991). The Del1 *Chlamydomonas* strain was used as a recipient host for the mutant's generation (Preiss et al., 2001). This strain has a defined deletion in the chloroplast-encoded psbA gene and is unable to grow photoautotrophically, as it cannot produce a functional D1 protein. Acetate is needed as carbon source as minimal media do not support its growth. Minimal media were used to select photosynthetically active colonies generated after the integration of the psbA variant produced both by random and site-directed PCR (Dauvillee et al., 2004). Selected mutants were then characterized by analyzing their photosynthetic performance and the sensitivity and/or resistance to different classes of herbicides assessed (Tibuzzi et al., 2007; Rea et al., 2009; Giardi et al., 2009; Scognamiglio et al., 2009). After the characterization, the best performing mutants were immobilized on screen-printed electrodes and integrated in amperometric or optic transduction systems. Both electrochemical and optical devices were arranged in multi-arrayed setups.

4. Microalgae PSII based biosensors as useful bioanalytical tools for herbicide detection

The exploitation of herbicides for weed control is vital to increase the yields and productivity in agriculture. Without the use of herbicides, it would have been impossible to fully mechanize the production of cotton, sugar beets, grains, potatoes, and corn. Therefore, given the harmful economic implications of poor harvesting, herbicide production is the principal driver of the farming industry.

However, the continuous and massive application of these compounds can negatively affect human health and ecosystems. These consequences result in an increased demand for risk assessment and prompt the regulatory agencies to update legislation aimed at controlling environmental contaminations. In this scenario, it is essential to develop analytical devices able to detect the low levels of herbicide contaminants defined by the EU directives, and to distinguish among different classes of compounds.

A major difficulty in estimating environmental quality related to herbicides contamination is due to seasonal change of field application and the extremely low levels of the maximum admissible concentrations set by the European commission. Several methods, which partially satisfying these requirements have been already developed. In this context, chromatographic techniques, such as gas chromatography (GC) and high performance liquid chromatography (HPLC) with UV and/or mass spectrometry (MS) detection, surely represent the most trustworthy and common techniques used to monitor the presence of herbicides. The classical analytical techniques are unlikely to provide adequate sensitivity, while advanced instrumental methods are highly sensitive, but generally expensive, require skilled operators and are not easily amenable to on-site field-testing. Herbicides usually represent a very small fraction of the whole sample under investigation, so pre-treatments such as clean up and/or pre-concentration steps are required to make their identification possible. Consequently, the qualitative and quantitative analysis of herbicide residues is time consuming and involves high costs. Because of the large numbers of samples to be measured, the necessity of expensive equipment, organic solvents and laborious sample preparation, the development of a fast, automated and inexpensive test is of great interest. These concerns encouraged researchers to seek out alternative methods providing the desired analytical information.

Studies in the framework of the development of biosensors for the detection of environmental pollutants exploit photosynthetic microorganisms or parts of them, such as thylakoids. Photosynthetic systems are naturally occurring anisotropic supramolecular arrangements of proteins and small

molecules that are able to harvest light energy and funnel it towards building up biomass and releasing oxygen. For these purposes, photosynthetic organisms are equipped with multi-enzymatic complexes embedded in thylakoid or free membranes known as photosystems. The hierarchical organization of these pigment-protein complexes is at the basis of their unique efficiency. Functional and structural knowledge of photosynthetic systems has been steadily increasing, and as a result, fundamental and applied research have made it possible to integrate biological photosystems or their functional sub-structures into artificial assemblies in order to get them to carry out their tasks in a controlled environment for specific applications.

In PSII if the electron transfer from the reaction center to the quinone pool is blocked, such as during the binding of the photosynthetically active pesticides, these parameters change dramatically and can be monitored by electro-optical analysis in a pesticide concentration dependent manner. Currently, in parallel to traditional analytical methods, novel detection systems have been already developed based on biosensor technology, which provides rapid, inexpensive and reliable tools for herbicide monitoring and screening analyses, to answer the concern on this issue. An optical biosensor based on the green photosynthetic alga *Chlamydomonas reinhardtii* described by Tibuzzi and coworkers was employed to monitor several classes of herbicides, such as atrazine, diuron, ioxynil, terbuthylazine, prometryn and linuron, in a low concentration range (10^{-8}-10^{-10} M) (Tibuzzi et al., 2007). In particular, a miniaturized optical biosensor instrument was designed and produced using multiarray fluorescence measurements of several biomediators in series, for applications in environmental monitoring and agrofood analysis. In the work by Rea and coworkers, a computational study was performed to design and construct a set of mutant strains from the green photosynthetic alga *C. reinhardtii*, with higher sensitivity towards several classes and subclasses of herbicides (Rea et al., 2009). An in silico study was performed to predict mutations within the D1-D2 heterodimer which improve its specificity, sensitivity, and binding affinity for atrazine. In detail, taking advantage of the high sequence homology observed between *Thermosynecococcus elongatus* D1 and D2

proteins and the corresponding proteins from *C. reinhardtii* (87% and 89% amino acid sequence identity, respectively), the three-dimensional structure of the latter proteins was homology modelled. Based on this model, a series of D1 and D2 mutants were generated in silico and the atrazine affinity of wild type and mutant proteins was predicted by binding energy calculations to identify mutations able to increase PSII affinity for atrazine.

New advances in the same context were achieved in amplifying the range of recognition elements and measurement of a significant number of different classes of environmental pollutants. These advances occurred through the development of a biosensing system, which uses sets of mutant organisms with different affinities towards pesticides. Giardi and coworkers presented a library of functional mutations in the unicellular green alga *C. reinhardtii* for preparing biomediators (Giardi et al., 2009). Exploiting bioinformatics to design new mutant strains resulted in the construction of microorganisms, which showed different limits of detection for diazines, triazines and urea herbicides, underlined the high potential of bioinformatics and molecular biology in the design of desired biological material suitable for biosensor use.

Scognamiglio and coworkers (Scognamiglio et al., 2009) assembled a multi-biomediator fluorescence biosensor based on a new versatile portable instrument. The biosensor instrument was composed of a 24-cell array configuration able to host different mutant strains for the detection of a variety of herbicide classes such as triazines, diazines and ureas. As we can observe from the described advances in biosensor technology, the main features of a successful biosensor are characterized by the interchangeable recognition elements, which provide the versatility to measure large numbers of analytes. Buonasera and coworkers was constructed a biosensing platform to provide an analytical tool applicable to the daily pre-screening of a broad spectrum of samples (Buonasera et al., 2010). The platform combined the most used transduction systems for biosensors, amperometric and optical systems, and used genetically modified microorganisms as versatile biomediators, allowing detection of different subclasses of herbicides. It represented a sensitive,

reliable, and low-cost system able to detect water pollutants such as atrazine, diuron, linuron, and terbuthylazine down to 10^{-8}-10^{-10} M. Combining the amperometric and optical detection systems, the platform was able to determine the toxicological potential of samples, through the determination of the biomediator physiological activity inhibition. Fluorescence modification and current reduction were related to the concentration of herbicide quantified by a dedicated data acquisition software. In addition, the opportunity to use a wide range of biological materials made the platform a good candidate for the development of a biosensor with required features.

In this thesis, we focused on the development of new types of bio-sensing elements for building up a platform of modular biosensors with the best features in terms of versatility, stability, life-time and long-term activities, sensitivity and selectivity, detection limits, linear range, reproducibility and low cost, which can be easily adopted for the simultaneous detection of several herbicides. We developed an array of novel whole-cell biosensors based on the activity of engineered photosystem II with improved sensitivity and stability features, and biomimetic peptides as sensing elements. The new complex biosensors array based on both optical and electronic transduction for multi-parameter detection. It will be able to monitor the herbicide levels and to diagnose their biological impact. This improvement should provide the impetus for the technological transfer from laboratory devices to in-field operation systems. The new devices will lead to a tremendous breakthrough in the detection of contaminants and quality control in risk assessment sectors by providing a rapid broad-spectrum screening tool.

References

Belkin, S., Gu, M.B., 2010. Whole Cell Sensing Systems I: Reporter Cells and Devices. Springer, Heidelberg.

Buonasera, K., Pezzotti, G., Scognamiglio, V., Tibuzzi, A., Giardi, M.T., 2010 New platform of biosensors for prescreening of pesticide residues to support laboratory analyses., J. Agric. Food Chem. 58, 5982–90. doi:10.1021/jf9027602.

Campas M., Carpentier, R., Rouillon, R., 2008. Plant tissue-and photosynthesis-based biosensors. Biotechnology Advances 26, 370-378.

Cavalcanti, A., Shirinzadeh, B., Zhang, M. & Kretly, L.C. (2008). Nanorobot hardware architecture for medical defense. Sensors. 8(5), 2932–2958.

Chaplin, M.F., 2000. Biosensors, in: Walker, J.M., Raply, R. (Eds.), Molecular Biology and Biotechnology. RCS Publishing, pp. 513-546.

Cullum, D.S., Sumner, J., 2010. Biosensors and Bioelectronics, in: Armstrong R.E., Drapeau, M.D., Loeb, C.A., Valdes, J.J. (Eds.), Bio-Inspired Innovation and National Security Biosensors. National Defense University Press, pp. 77-103

Dauvillee, D.; Hilbig, L.; Preiss, S., Johanningmeier, U. (2004). Minimal extent of sequence homology required for homologous recombination at the psbA locus in *Chlamydomonas reinhardtii* chloroplasts using PCR-generated DNA Fragments. Photosynthesis Research, 79(2): 219-224.

Dinh, T.V., 2007. Biosensors and Biochips, in: Ferrari, M., Bashir, R., Wereley, S. (Eds.), BioMEMS and Biomedical Nanotechnology. Springer US, pp. 1-20. DOI: 10.1007/b136241

Farré, M., Kantiani, L., Pérez, S., Barceló, D. 2009. Sensors and biosensors in support of Eu directives. Trends Anal Chem. 28 (2): 170-85.

Foyer, C.H., Neukermans, J., Queval, G., Noctor, G., Harbinson, J., 2012. Photosynthetic control of electron transport and the regulation of gene expression. Journal of Experimental Botany 63 (4), 1637-1661.

Fufezan, C., Rutherford, A.W., Liszkay, A.K. (2002). Singlet oxygen production in herbicide-treated photosystem II. FEBS Letters 532, 407-410.

Frachiolla, N.S., Artuso, S., Cortelezzi, A. 2013. Biosensors in Clinical Practice: Focus on Oncohematology. Sensors 13, 6423-6447. DOI: 10.3390/s130506423

Giardi, M.T., et al., 2009. Optical biosensors for environmental monitoring based on computational and biotechnological tools for engineering the photosynthetic D1 protein of *Chlamydomonas reinhardtii*. Biosens. Bioelectron. 25, 294–300. doi:10.1016/j.bios.2009.07.003

Giardi, M.T., Pace, E. 2005. Photosynthetic proteins for technological applications. TRENDS in Biotechnology 23 (5), 257-263.

Justino, C.I.L., Rocha-Santos, T.A., Duarte A.C. 2010. Review of analytical figures of merit of sensors and biosensors in clinical applications. Trends Anal Chem. 29 (10): 1172-83.

Krieger-Liszkay, A. and Rutherford, A.W. (1998). Biochemistry 37, 17339-17344.

Lee, Y.H., Mutharasan, R., 2005. Biosensors, in: Wilson, J.S. (Eds.), Sensor Technology Handbook. Elsevier Inc., USA, pp. 161-180.

Monosik, R., Stredansky, M., Sturdik, E., 2012. Biosensors-classification, characterization and new trends. Acta Chimica Slovaca 5 (1), 109-120, DOI: 10.2478/v10188-012-0017-z

Morrison, D.W.G. et al. 2008. Clinical applications of Micro-and Nanoscale Biosensors, in: Gonsalves, K.E., Laurencin, C.L., Halberstadt, C.R., Nair L.S. (Eds.), Biomedical Nanostrucutres. John Wiley and Sons Inc. pp. 433-454

Perumal, V., Hashim, U. 2014. Advances in biosensors: Principle, architecture and applications. Journal of Applied Biomedicine 12, 1-15.

Preiss, S.; Schrader, S. & Johanningmeier, U. (2001). Rapid, ATP-dependent degradation of a truncated D1 protein in the chloroplast. European Journal of Biochemistry, 268(16): 4562-4569.

Przibilla, E.; Heiss, S.; Johanningmeier, U., Trebst, A. (1991). Site-specific mutagenesis of the D1 subunit of photosystem II in wild-type *Chlamydomonas*. The Plant Cell, 3: 169-174.

Rea, G., Polticelli, F., Antonacci, A., Scognamiglio, V., Katiyar, P., Kulkarni, S.A., Johanningmeier, U., Giardi, M.T., 2009. Structure-based design of novel *Chlamydomonas reinhardtii* D1-D2 photosynthetic proteins for herbicide monitoring. Protein Sci. 18, 2139–51.

Rea, G.; Serafini, A.; Margonelli, A.; Faraloni, C.; Zanini, A.; Bertalan, I.; Johanningmeier, U. and Giardi. M.T. (2008). Ionizing radiation impacts photochemical quantum yield and oxygen evolution activity of photosystem II in photosynthetic microorganisms. International Journal of Radiation Biology, 84 (11): 867-877.

Scognamiglio, V.; Raffi, D.; Lambreva, M.; Rea, G.; Tibuzzi, A.; Pezzotti, G.; Johanningmeier, U., Giardi, M.T. (2009). Chlamydomonas reinhardtii genetic variants as probes for fluorescence sensing system in detection of pollutants. Analytical and Bioanalytical Chemistry, 394(4): 1081-1087.

Scognamiglio, V., Pezzotti, G., Pezzotti, I., Cano, J., Buonasera, K., Giannini, D., Giardi, M.T., 2010. Biosensors for effective environmental and agrifood protection and commercialization: from research to market. Microchim Acta 170 (3), 215-225.

Struss, A.K., Pasini, P., Daunert, S., 2010. Biosensing systems based on genetically engineered whole cells. In: Zourob, M. (Ed.), Recognition Receptors in Biosensors. Springer, New York, pp. 565–598.

Thévenot DR, Toth K, Durst RA, Wilson GS. Electrochemical biosensors: recommended definitions and classification. Biosens Bioelectron 2001 Jan; 16 (1): 121-31.

Tibuzzi, A., et al., 2007. A new miniaturized multiarray biosensor system for fluorescence detection. J. Phys. Condens. Matter 19, 395006. doi:10.1088/0953-8984/19/39/395006

Trebst, A., Depka, B. and Holla«nder-Czytko, H. (2002) FEBS Lett. 516, 156^160.

Wang, H., Nakata, E. & Hamachi I. (2009). Recent progress in strategies for the creation of protein-based fluorescent biosensors. Chembiochem: a European Journal of Chemical Biology, 10(16): 2560-2577.

Yadav DK., and Pospisil P (2012) Evidence on the Formation of Singlet Oxygen in the Donor Side Photoinhibition of Photosystem II: EPR Spin-Trapping Study. PLoS ONE 7(9): e45883. doi:10.1371/journal.pone.0045883

CHAPTER 2

“An optical biosensor based on microalga-paramecium symbiosis for improved marine monitoring”

Turemis, M., Rodio, G., Pezzotti, G., et al. “A novel optical biosensor based on microalga-paramecium symbiosis for improved marine monitoring” Submitted to Sensors and Actuators B: Chemical.

Abstract

Unprecedented increases in anthropogenic pollution of marine environments have made the development of sensitive, cheap and adaptable early warning systems absolutely crucial for on-site monitoring of chemical contaminants. Biosensors based on algae cells might constitute a promising and cost-effective alternative for environmental analyses since they are able to provide rapid toxicity information in the case of pollution, while assessing the harmful effects of the contaminants on the ecosystem.

In this work, an optical biosensor based on an array of algal biomediators for monitoring of relevant marine pollutants was developed. The potential of the algae-protozoa symbiotic association between *Chlorella vulgaris* and the ciliate *Tetrahymena pyriformis* as a sensitive biomediator for biosensor development was assessed, showing enhanced resistance to the salinity of marine water in comparison with free-living algae strains. The symbiotic algal cells immobilized in calcium alginate gel was adapted to grow into innovative microfluidic flow cells with integrated detectors for real-time detection of marine pollutants by fluorescence analysis of photosynthetic photosystem II. The fluorescence response of free and immobilized symbiotic cells was examined in the presence of three commonly found pesticides: simazine, atrazine and diuron, alone or in combination, and the results were compared by liquid chromatography-mass spectrometry. The limits of detection for the three herbicides were 1.35, 0.44 and 0.25 µg/L, respectively, and 0.13 µg/L for the mixture.

In summary, an autonomous integrated symbiotic association of Paramecium-*Chlorella*-based biosensor was successfully developed for real-time monitoring of marine water quality and evaluation of biotoxicity.

1. Introduction

The marine environment is continuously challenged by the input of around 250,000 types of chemical compounds, mostly through human and industrial activities. These chemicals enter the marine environment via direct inputs, riverine contributions and atmospheric deposition (Sun et al., 2016; Talvitie et al., 2015)

In the case of herbicides for weed control, the use of atrazine in European Union (EU) countries was banned in 2004 but it remains extensively applied in United States and around sixty other countries worldwide (Sass and Colangelo, 2006). Similarly, the EU limited the use of simazine and diuron due to their potential threat to human health. In spite of the regulations, they are still found in soil and waters in many parts of Europe due to their persistence and accumulation. The highest diuron concentrations reported in European rivers and ground waters were 0.86 and 0.28 µg/L, respectively (Loos et al., 2008, 2010). Analyses in water samples from careening areas of several ports showed concentrations of atrazine up to 0.82 µg/L, while diuron presence reached up to 0.21 µg/L, in both cases being the Mediterranean the most polluted sea (Munaron et al., 2012; Nödler et al., 2014). These are recent examples demonstrating the wide distribution of herbicides in marine environments revealing the threats to living organisms (DeLorenzo ME, 2012)

Monitoring approaches for marine water contaminants are typically based on chemical analysis in combination with biomarker assays and ecosystem monitoring (Galloway, 2006; Hamza-Chaffai, 2014). Chemical analyses enable precise and accurate assessment of individual compounds, although demand extensive sample preparation and costly instruments and are usually limited to *ex-situ* collection at individual locations. In addition, they fail to provide information about the bioavailability of pollutants, their effect on living organisms and their synergistic or antagonistic behavior in mixtures (Brayner et al., 2011). Biomarker analysis is widely developed to assess potential effects of chemical exposure to native organisms living at contaminated sites, but it is time and labor intensive, demands on-site recovery of the organisms and has increasing costs depending

on the complexity (Schirmer et al., 2010). Therefore, in order to protect our aquatic environment, improve human safety and reduce the economic impact, it is desirable to develop innovative marine biosensors and other advanced observing technologies that will improve our ability to monitor waters with greater efficiency.

Although biosensors present a great potential for marine environment monitoring, most of the published works have focused in analyses of fresh and wastewater, mainly because of the highly demanding working environment that seawater constitutes (Kröger et al., 2002; Kröger and Law, 2005). In order to face the challenges posed by marine environments, biosensors need to be fully automated, very robust (resistant to physical impacts, high corrosion and biofouling), drift-free or with accurate calibration in case of drift, with minimal power consumption, user-friendly and enough sensitive to measure pollutants frequently found at very low concentrations. Several examples of biosensor development for marine measurements of eutrophication, pesticides, anti-biofouling agents, polycyclic aromatic hydrocarbons, endocrine disruptors, trace metals, organism detection, algal toxins, etc. have been described in the literature (for a review, see Kröger and Law, 2005). Biosensor strategies for pesticide detection in marine ecosystems are mainly based on the use of enzymes, such as cholinesterases (Sturm et al., 1999), immunosensor approaches (Belkhamssa et al., 2016) or sensors based on the use of intact microorganisms, such as bacteria (Ranjan et al., 2012) or algae (Tonnina et al., 2002)

Algal photosystem reporters are robust and react very broadly to toxicity (Giardi and Pace, 2006). The concept of bioreporting with living algal cells most frequently relies on measurement of the fluorescence of photosystem II (PSII), which is extremely sensitive to disruption by a variety of toxicants (Buonasera et al. 2011). The algal cells are small in size and therefore assays based in PSII fluorescence can be downscaled and parallelized in micro-engineered fluidics units with integrated optic detectors (Buonasera et al., 2011; Tibuzzi et al., 2007). This provides an optimal choice to incorporate in autonomous systems for real-time, on line and *in situ* measurements of marine water quality, displaying excellent sensitivity, reproducibility and accuracy.

However, hypo- and hyper-saline conditions affect many sites involved in the photosynthetic process, bring significant changes in the performance of the algae, and may influence biosensor response. Therefore, it is important to select the most appropriate strains to improve the stability and adaptability of the microalgae into the water sources in which they are intended to be used.

Some green algae from *Chlorella* genus are able to establish symbiosis with protists like paramecia as well as with bacteria, some flatworms and cnidaria (Fujishima, 2009; Summerer et al., 2008). The most famous algal symbiosis is the one between the ciliate *Paramecium bursaria* and the unicellular green alga *Chlorella vulgaris* (Fujishima, 2009). *Tetrahymena pyriformis* is a free-living ciliate paramecium with a small cell size between 40 and 60 μm and an elongated form. The symbiosis determines various benefits for both the paramecium and the alga. For the symbiotic algae, the host can supply the algae with nitrogen components and carbon dioxide. Algal carbon dioxide fixation is enhanced by the host extracts. On the other hand, the algae can supply the host with photosynthetic products, mainly maltose and sugars.

Inside the host cell, the algae show a higher rate of photosynthetic oxygen production than in the isolated form, thereby guaranteeing an oxygen supply for the paramecia (Kodama and Fujishima, 2011). The host symbiotic algae can receive protection against UV damage by the paramecium, which contains protecting substances and confers capability to thrive in sunlight UV-exposed waters (Kodama and Fujishima, 2011). Furthermore, alga-bearing paramecium cells can divide better than the alga-free cells, showing a higher survival rate than the alga-free cells under various stressful conditions. It is therefore expectable that the mutualistic relationship between *Chlorella* and *T. pyriformis* could be used for further improvement of algae based biosensors for marine monitoring.

The general aim of the present work was to evaluate various strains as biomediators and the sensitivity of free-living and symbiotic algae to natural seawater. Thus, we studied for the first time an endosymbiosis mechanism that involves the green alga *C. vulgaris* and protozoa for its possible application for biosensoristic purposes. Symbiotic microalgae were integrated in a micro-device including a microfluidics chip, optical illumination and detector elements. The biosensor was tested

in marine water samples spiked with different types and concentrations of herbicides highly used in aquaculture, and finally validated in comparison with liquid chromatography coupled to mass spectrometry (LC-MS) results.

2. Materials and methods

2.1. Chemicals and solutions

All reagents were purchased as high purity grade products from Sigma-Aldrich (St. Louis, Mo, USA). Solid analytical standards of atrazine (ref. 45330), cypermethrin (36128), diuron (45463), irgarol 1051 (46105), linuron (36141), molinate (36171) and simazine (32059), all from the Pestanal® line, were purchased from Sigma-Aldrich (Steinheim, Germany) and dissolved in methanol (HPLC grade, 99.9% minimum purity) to obtain concentrated stock solutions. Herbicides working solutions were diluted with deionized water and the residual methanol concentration kept lower than 0.5% v/v. The measuring buffer consisted of 50 mM Tricine, 20 mM Calcium chloride ($CaCl_2$), 5 mM Magnesium chloride ($MgCl_2$), 50 mM Sodium chloride (NaCl) and 70 mM sucrose, pH 7.2. The storage buffer consisted of 50 mM Tricine, 20 mM $CaCl_2$, 5 mM $MgCl_2$ and 70mM sucrose, pH 7.2. The composition of Tris-Acetate-Phosphate medium (TAP), pH 7.2, was the one described in (Harris, 1989).

2.2. Strains, culture conditions and production of mutants

Several microalgal strains from culture collections were selected among different taxonomic groups in order to test their potential use as biosensors for toxicity measurement in marine environment. Chlamydomonas strains were grown in liquid Tris-Acetate-Phosphate (TAP) medium (Harris, 1989) and *Chlorella vulgaris* (H 1987) in Bold's Basal Medium at 50 μmol m^{-2} s^{-1} light intensity, 25°C temperature and 150 rpm agitation. The *Chlamydomonas reinhardtii* intron-less (IL) strain contains the wild type psbA gene without introns and represents the control reference strain.

Its derivative Del1 mutant has a defined deletion in the psbA gene and was used as a recipient strain to obtain D1 site-directed mutants by particle gun transformation, as previously reported (Johanningmeier and Heiss, 1993). Site-directed mutagenesis and PCR were performed as previously described (Johanningmeier and Heiss, 1993; Xiong et al., 1998). The Chlamydomonas mutants I163N, F255N, A251C and A250R on D1 protein target site were selected because of their high sensitivity to pesticides (Giardi et al., 2009). For symbiosis, 10 mL of the three days-old algae culture of *C. vulgaris* (Fott and Novakova 1969, CCAP 211/11D, a freshwater strain) were inoculated in 100 mL of TAP, mixed with paramecia *Tetrahymena pyriformis* CCAP 1630/1W grown in liquid Chalkley's medium.

2.3. Lipid analyses method

The content of lipids was determined by gravimetric analysis (Huang et al., 2009) and expressed as percentage of lipids per dried biomass. About 20 mg lyophilized algae powders were mixed with 2 ml of chloroform, 2 ml of methanol and 1 ml of 5% NaCl solution. The mixture was vortexed for 2 min and centrifuged at 8000 g for 4 min at 10 ^{o} C. Chloroform layer was collected carefully. The same processes were repeated three times and all chloroform collected were mixed together, dried in oven at 60 ^{o}C, and kept in a vacuum desiccator before weighing with electronic balance. Six samples from each typical pattern of growth were measured and the relative standard deviation calculated. Lipids in the symbiotic form were measured up to 90 and 120 days of culture.

2.4. Fluorescence and optical instrumentation and parameters

Fluorescence was measured using a sensor fluorimeter developed *in house* by Biosensor Srl (Rome, Italy), assembling electronic boards (Microsis, Rome, Italy) with fluidics generated by a peristaltic pump or gravity fluidics. (**Fig. 1A**) The prototype instrument is a modular transducer for biosensors, able to perform simultaneous and autonomous fluorescence measurements of several

biomediators. The instrument contains one module with six miniaturized cells assembled in series for performing, simultaneously six tests of fluorescence on microorganisms. The module is hermetically closed and thermally isolated to avoid any contamination.

In each cell, the measurement system is composed of two red, two white light-emitting diodes (LEDs) and an optical fluorescence detector. The fluorimeter provides inputs of 500 μmol photons m^{-2} s^{-1} red light for 11 s at 650 nm and measured the fluorescence emission by photodiode at 680 nm. The red light covered a surface of 1 cm^2, resulting in highly reproducible measurements averaged over 1000 points. In each measurement cell, the living conditions are provided by two white light LEDs that are switched on continuously for 7 h out of a 24 h period, and guarantee the photoperiod necessary for the algae survival. The intensity of the white lights can be set up to a maximum of 250 μmol m^{-2} s^{-1} as measured at center of each cell. Once the command run is executed, the measurement starts and an integrated fluidic system allows automatic sampling into the flow cell with 6 parallel cavities, containing the biomediator (when immobilized algae into a calcium-alginate gel in use) is mounted above the fluorescence induction analyzer (**Fig. 1B**). The immobilized biomediator allows repeated use after regeneration with the aid of white survival LED and regeneration buffer for long-time measurement. The instruments can work directly by rechargeable battery at 12 V, ensuring autonomy and avoiding problems of fails in electricity.

The sensor allows determination of the main chlorophyll fluorescence parameters: minimum fluorescence (F_0) is calculated using an algorithm that determines the line of best fit for the initial data points recorded at the onset of illumination. This line was extrapolated to time zero to determine F_0; maximum fluorescence (F_M) was the maximum value achieved during recording; F_v was the variable component of fluorescence. Measuring fluorescence at 2 ms gives F_{2ms} and the corresponding fluorescence level at step J, $V_J = (F_{2ms}-F_0)/(F_M-F_0)$ that refers to the rate of reoxidation of plastoquinone A (Q_A) in its reduced form (Q_A^-) with respect to its reduction. The measurement of optical density at 750 nm was conducted by using a UV-Vis spectrophotometer (TU-1880 Double Beam, China).

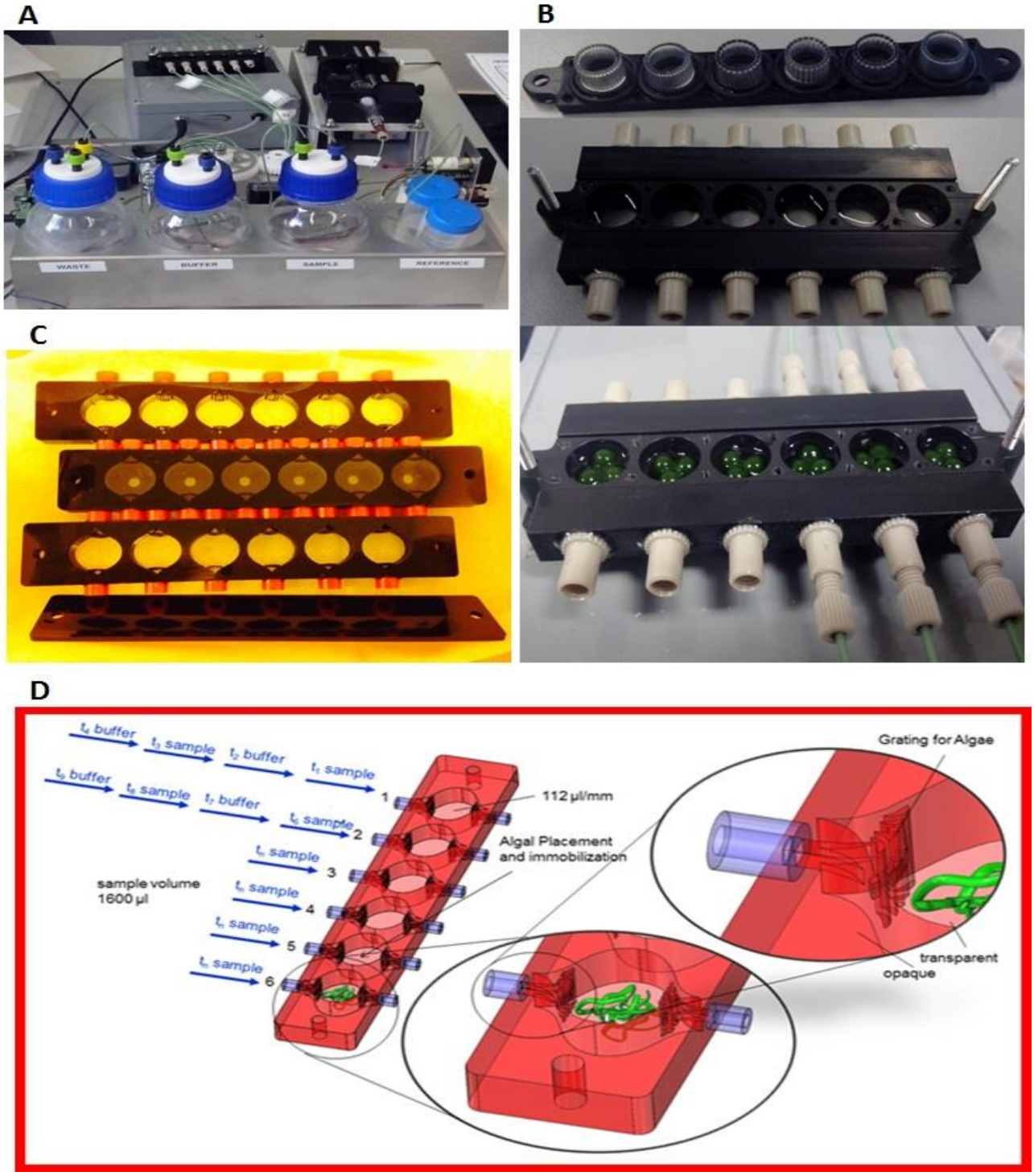

Fig. 1. Optic instrument set up with fluidics unit connected, developed by Lionix (Netherlands, www.lionixbv.nl) and Biosensor Srl (Italy, www.biosensor.it). B) Flow cell with six parallel channels containing the algal biomediator immobilized into a calcium-alginate gel. C) Flow cell design with six channels (MicroTec©, Germany, www.microtec-d.com). D) Schematic representation of the flow cell with six channels and measurement proposal.

2.5. Design and production of microfluidic chips

MicroTec (Duisburg, Germany) designed and produced different microfluidic cartridges suitable to hold immobilized algae bio-reporters and allow the access of seawater, but avoiding the cells to go out of the container, while preserving the maximum fluorescence activity. Microfluidic flow cells, made by MicroTec's Rapid Micro Product Development-Mask technology, encase the algae substances (**Fig. 1B, C and D**).

2.6. Preparation of immobilized algae bio-reporter for fluorescence measurements

Prior to immobilization of microalgae, microchips were sterilized under UV-light for 15 min and then autoclaved (121 °C, 2 atm). In order to immobilize symbiotic microalgae in sodium-alginate, an aliquot of algae culture in the exponential phase of growth was collected and centrifuged at 2000 g for 5 minutes at 15°C. The supernatant was discarded and the pellet was washed twice with Tricine-sodium hydroxide (NaOH) 50 mM, pH 7.2. After washing, the supernatant was discarded while the pellet was resuspended with Tricine-NaOH to a final volume of 600 µL and then mixed with 1200 µL of 2% w/v sodium-alginate solution in the same buffer, to obtain a 1.3% w/v alginate. Alginate beads with entrapped algae cells were prepared by dropping algae suspension from syringe into 200 mM $CaCl_2$ solution. Fifty, 100 and 200 µL of suspension, corresponding to 45, 90 and 180 µg of chlorophyll from the algae cells respectively, were loaded into the cavities of microcell. Subsequently, the microchips with the suspensions were immersed in Tricine-NaOH containing $CaCl_2$ 200 mM for 20 minutes prior to use. When not in use, the microcells with algae were kept at 20°C under 50 µmol m^{-2} s^{-1} white light.

2.7. Fluorescence analyses

First measurements were carried out using TAP/seawater in order to obtain the baseline. Fluorescence measurements were performed before and after algal exposure to herbicide using standard instrument settings (10 min dark, 11 s light at 127 arbitrary units), whose periodicity was optimized to obtain a stable photosynthetic response. All experiments were performed in triplicate at room temperature in TAP/seawater medium. Under these conditions, the fluorescence-time response of the biosensor was continuously monitored and recorded. Comparisons among different samples were performed by normalizing the chlorophyll fluorescence and calculating the transient as relative variable fluorescence [$1-V_J$] at any given time. This procedure simplified the analysis by considering only the dynamic accumulation of Q_A^- (Loll et al., 2005). The limits of detection (LODs) were determined based on the 99% confidence interval, which, assuming the normal distribution corresponds to 2.6×standard error of the measurements (σ). Then, using the modified relationship for the Langmuir absorption isotherm, $LOD = 2.6\times\sigma\times I_{50}/(100-2.6\times\sigma)$, where I_{50} is the 50% Inhibitory *Concentration*, as previously reported (Giardi et al., 2009).

2.8. Validation with LC-MS

2.8.1. Sample preparation for LC-MS

In order to test the practical performance of the algal biosensor, several spiked seawater samples were analysed both using the sensor and using liquid chromatography coupled to mass spectrometry (LC-MS). Three series of seawater samples were prepared, (1) spiked with simazine, (2) spiked with diuron, and (3) spiked with a cocktail of biocides which can be typically found in the real sea environment: three herbicides, including a triazine (atrazine), a phenylurea derivative (linuron) and a thiocarbamate (molinate); a triazine algaecide (irgarol 1051); and an insecticide of the pyrethroid group (cypermethrin).

For validation, samples were prepared at blind concentrations ranging from 0.04 to 600 µg/L in IDAEA-CSIC (Spain) by the following procedure: blank seawater was taken in a pristine location of the Mediterranean Sea close to the Ardenya massif (Costa Brava, Catalonia, Spain). Suspended particulate and planktonic materials, which may potentially interfere in the sensor analyses, were removed by centrifugation (3000 g during 10 minutes). Then, fresh standards of biocides were prepared in methanol at 1 µg/µL and sequentially diluted to 100 and 10 ng/µL. Sample fortification was carried out in volumetric flasks minimizing the final amount of methanol in the samples (<0.5% in all the samples except one). After spiking, samples were homogenized in shaker for 20 minutes. Sample manipulation, storage and transport were carried out using only amber glass material, previously rinsed with water, methanol and acetone and heated overnight at 400°C in order to prevent eventual sample contamination, potential light degradation and irreversible sorption of organic contaminants onto the plastic surfaces. Samples were divided in two aliquots: one was analysed by LC-MS and the other was codified, shipped and measured in parallel by Biosensor Srl (Italy).

2.8.2. Determination of contaminants by LC-MS

In order to determine contaminants, 1350 µL of each sample were combined with 150 µL of acetonitrile in injection vials and analysed by LC-MS, using a published instrumental method (**Fig. 2**) (Köck-Schulmeyer et al., 2014). Chromatographic separation was performed using the Acquity UPLC System (Waters, Milford, USA), equipped with a Luna C18 column (length: 15 cm; internal diameter: 2.00 mm; particles size: 5 µm; pore size 100 Å, Phenomenex) and a water/acetonitrile mobile phase, flowing at 0.35 mL/min. The gradient was as follows: initial conditions, 90% of water (kept for 1.5 minutes); then, the percentage of acetonitrile increased until 90% (conditions reached at minute 5.0 and kept for 3.5 minutes); and, finally, the percentage of water was increased until 90% again (conditions reached at minute 9.5). The column was equilibrated during 5 minutes between runs.

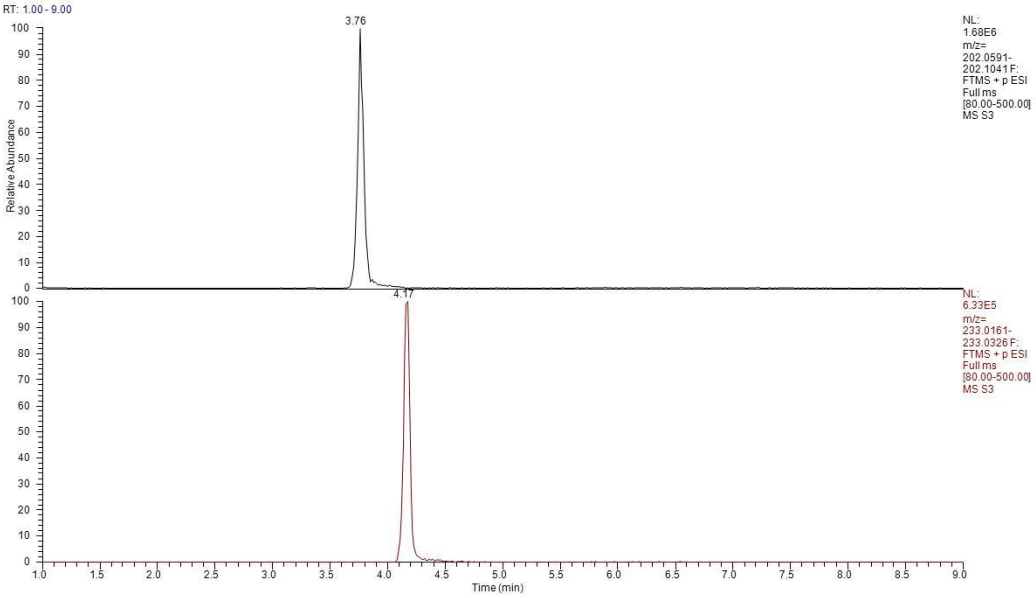

Fig. 2. Chromatograms of two seawater samples fortified with simazine (above) and diuron (below). The respective protonated molecular ions, m/z=202.0854 and m/z=233.0243 were acquired with experimental mass accuracies lower than 0.5 ppm.

The LC was coupled to a Q-Exactive (Thermo Fisher Scientific, San Jose, USA) MS with a hybrid quadrupole-Orbitrap analyser, working with an electrospray ionization source (ESI) operating in positive polarity. ESI conditions were as follows: spray voltage, 2750 keV; capillary temperature and probe heater temperatures, 300 and 375°C, respectively; sheath gas, auxiliary gas and spare gas were set at 40 , 15 and 1 arbitrary units, respectively; and S-Lens radio frequency level was kept at 70. The acquisition was performed in full scan mode (m/z 80–475) with a resolution of 35,000 full width at half maximum (FWHM). Instrument control and data processing were conducted with the Xcalibur 2.2 software (Thermo Fisher Scientific). The statistical analysis was performed with IBM SPSS version 22.

3. Results and discussion

3.1. Selection of salinity resistant algal biomediators based on PSII fluorescence

For biosensing purposes, some of the more relevant characteristics of bioreceptors are stability under operating conditions and sensitivity towards the analytes to be detected. Therefore in order to select suitable microalgae for marine monitoring, algae strains from different taxonomic groups were tested.

In order to understand the behavior and sensitivity of various freshwater algae strains (*C. reinhardtii*, wild-type and mutants I163N, F255N, A251C and A250R; *C. vulgaris*; *Choricystis parasitica* and the symbiosis *C. vulgaris*/*T.pyriformis*, (**Table 1**) to high salinity conditions, fluorescence measurements were carried out in the absence of target molecules, both in standard buffer TAP and in TAP 50% v/v seawater (**Fig.3**). Their sensitivity and response to target molecules were observed by monitoring the changes in the fluorescence emitted by PSII. Non-marine microalgae *C. reinhardtii* strain (IL) and its mutants previously produced as resistant to free radicals (Lambreva et al., 2013) were tested with seawater, resulting stressed in seawater in the short time necessary for the measure (10 min) with a significant increase in the Vj point independent of the analytes tested. The PSII fluorescence was substantially affected in the presence of seawater (43% inhibition), masking in part the effect of biocide presence. In addition, the strain *Chlorella vulgaris* (the fresh water strain H 1987) fluorescence activity was partially affected (11.9% inhibition) by the high salinity, although it was used since potentially it can be adapted to grow in marine water. Surprisingly, the symbiotic form of *C. vulgaris* with *T. pyriformis*, or similarly the *C. minutissima/ C. steinii* rose as a promising candidate to be used for environmental monitoring since the fluorescence response showed the same behavior both in TAP and TAP 50% v/v seawater **(Fig. 3**).

Table 1. Algae from different taxonomic groups tested for their potential use in marine monitoring in TAP: Tris-acetate-phosphate and in Seawater.

Chlorophyceae	**CAUP CCAP strain number or reference**	**Fv/Fm**		**Vj (TAP/seawater)**	
		TAP	**seawater**	**TAP**	**seawater**
Chlamydomonas reinhardtii	Lambreva et al.	0.83	0.79	0.29	0.21
C. reinhardtii mutants: I163N, F255N, A251C, A250R		0.80	0.82	0.30	0.59
Trebouxiophyceae					
Chlorella vulgaris	H 1987	0.75	0.69	0.44	0.50
Choricystis parasitica	H 1983	0.78	0.84	0.47	0.53
C.vulgaris/ Tetrahymena pyriformis	H 1987/ (1630/1W)	0.69	0.72	0.37	0.38

[a] formerly reported as *Chlorella* sp.

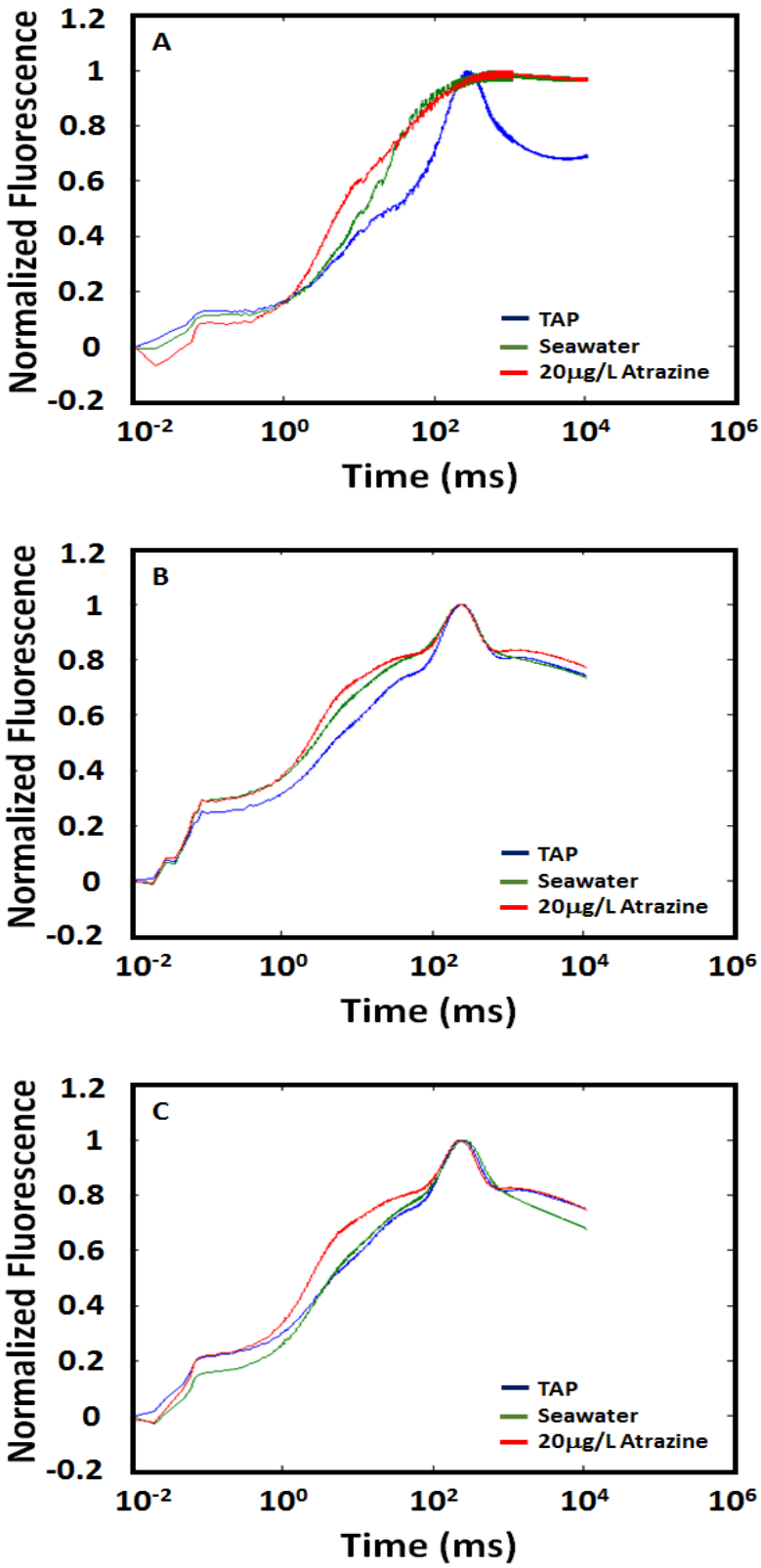

Fig. 3. Normalised PS II fluorescence of non-marine algae strains in Tris-Acetate-Phosphate (blue) and seawater 50% v/v (green) and after 10 min incubation with 20µg/L atrazine. A) *Chlamydomonas reinhardtii*, B) *Chlorella vulgaris* and C) *Chlorella vulgaris/Tetrahymena pyriformis*.

Following, the process of symbiosis was studied in more detail. Symbioses, in general, are defined as two or more species living together in beneficial coexistence. This type of mutualistic interaction plays an important role in maintaining populations living under precarious environmental conditions. In particular, algal chlorella-bearing protozoa are ubiquitous and abundant components in oceanic and freshwater systems of different trophic interactions. In our experiments, the establishment of symbiosis determined changes in different phases both at macroscopic and microscopic level **(Fig. 4)**. Microscopically, the single culture of *C. vulgaris* appeared homogeneous without aggregates (**Fig. 4A**), but two days after addition of paramecia cultures, green aggregates become visible (**Fig. 4B**). The algae inside the body of the paramecium were visible two days after infection. (**Fig. 4D**). After one week the symbiotic culture appeared with high precipitated aggregations (**Fig. 4E**).

For our purpose it is possible to maintain high growth and low aggregation by refreshing the cultures every 2-3 days. It is known that each symbiotic alga is enclosed in a special membrane (perialgal vacuole, PV) derived from the host digestive vacuole (DV) membrane of the protozoan, which protects it by preventing the fusion to the host lysosomes (Kodama and Fujishima, 2011;). Intact algal cells enclosed into perialgal vacuoles can escape from the host cell, and become observable as free algae of increased size in culture medium (Kodama and Fujishima, 2011). The higher salinity tolerance observed for symbiotic algae compared to *Chlorella* alone could be attributed to the existence of PV, with the vacuole membrane closely surrounding the alga in a distance of around 0.05 µm as reported by Reisser and colleagues (Reisser, 1986). In our system, when symbiotic algae were used, the increased salinity tolerance was associated with a high sensitivity to pesticides compared to the non-symbiotic algae (see **Fig. 3**).

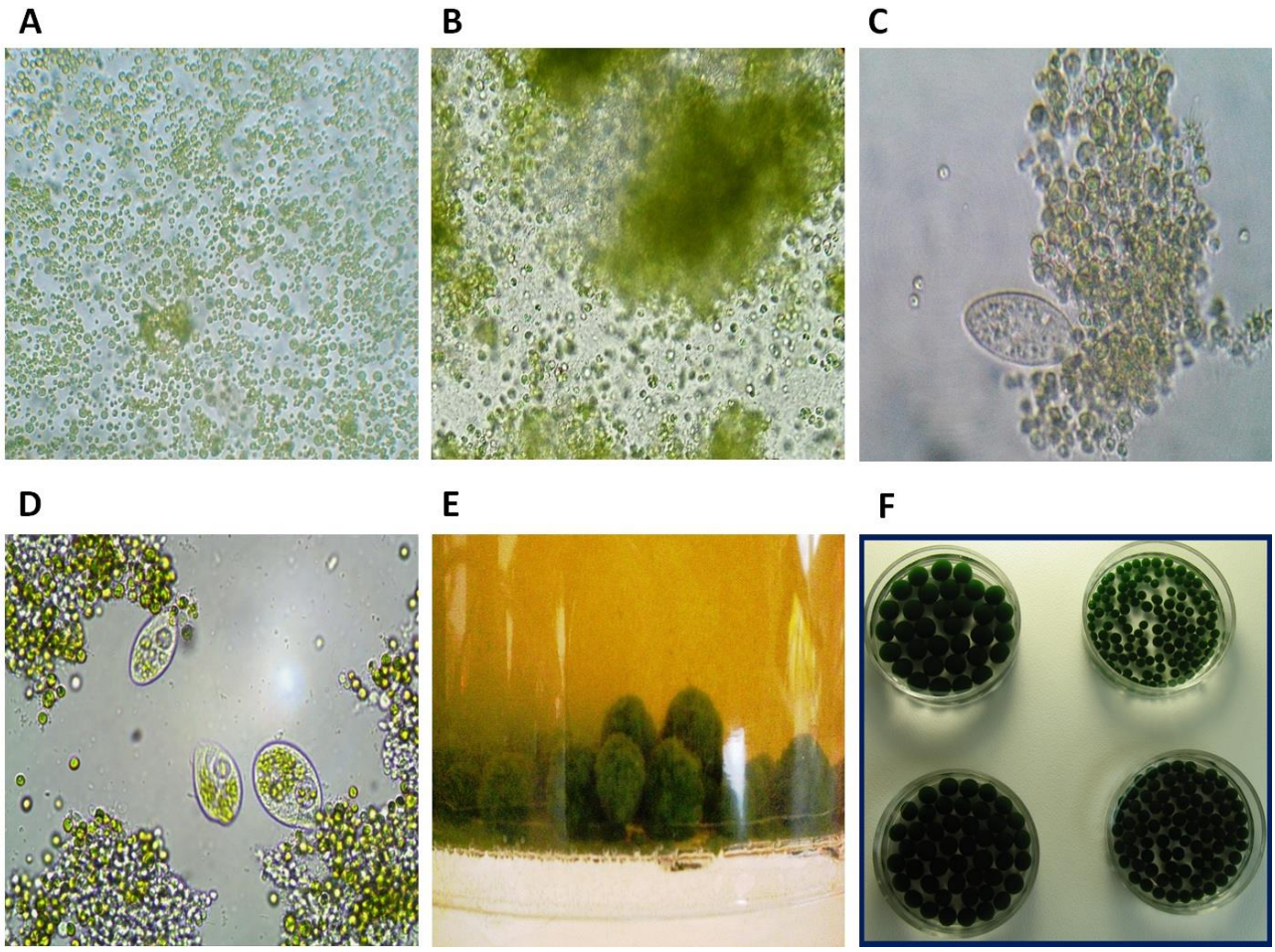

Fig. 4. Microscopic (A-D) and macroscopic (E) symbiosis culture evolution. A) *Chlorella vulgaris* before symbiosis. B) *Chlorella vulgaris* after symbiosis. C) *Tetrahymena pyriformis* before symbiosis. D) Detail of *Tetrahymena pyiriformis* after symbiosis where algal cells can be observed inside the body of paramecium. E) Presence of aggregates after days from symbiosis. F) Symbiotic algae entrapped in calcium-alginate beads using different diameter size tips (range 1-5 mm).

In addition, our study provided some insights into the protection mechanism that constitutes the basis of the symbiotic approach (Kodama and Fujishima, 2009). Some reports have suggested that lipids might be involved in the protection against salt stress [reviewed in (Markou and Nerantzis, 2014)]. Algae can be grouped as halophilic and halotolerant, in both cases producing some metabolites for protection against salt injury and for maintenance of the osmotic balance with the surroundings. The increase in salinity can augment the lipid content of microalgae, as shown by Rao

et al. that demonstrated higher total fat content of alga grown in different salt conditions when compared with control (RAO and RAO, 2007). Increased total lipid content was also reported to act as a storage reserve of energy materials until favorable conditions arise (Asulabh et al., 2012). Therefore we investigated the lipid content of microalgal species and its potential relationship to marine biosensing. After seven days of culture, the percentages of lipids per dried biomass were 47 and 57% in *C. vulgaris* alone and in the Paramecium-*C. vulgaris* symbiont, respectively. After thirty days, these percentages varied to 40% in the alga culture alone, compared with 87% for the symbiotic form. After 90 and 120 days, the content of lipids in the symbiont was 90 and 91%, respectively, but the alga alone was unable to survive. The relative standard deviation for six samples was inferior to 10% (data not shown). In agreement with previous publications, we observed that algae with higher lipid content showed better resistance to salinity and increased response against pesticides, compared to chlorella **(see Fig. 3)**. It is therefore expectable that the high biosensor response observed for the symbiotic form in marine water can be explained by the increased lipid content. In fact, in the case of algae containing lower lipid content, the biosensor response was dominated by salinity stress with diverse effects, such as accumulation of reactive oxygen species and changes in lipid and carotenoid distribution (Tammam et al., 2011), bringing significant variations in the photosynthetic performance of the algae.

3.2. Optimization of algae cells entrapment

To achieve the goal of cost-effective and long-time monitoring of pollution offshore, it is important to reduce the electricity consumption and minimize the space requirements. Miniaturization of the biosensor and development of user-friendly systems become key for this process. In our study, in addition to free algae cells, algal cells entrapped in calcium-alginate within the microcells were also prepared and tested for biosensor measurements. To allow automated reliable sampling, it is required that the microalgae are retained alive within the microcells. For the optimization of the

amount of entrapped algae, several immobilization tests were performed. The micro-cell with 50, 100 or 200 µl of suspension, corresponding to 45, 90 and 180 µg chlorophyll of the entrapped algae cells, respectively, were prepared and tested. The best PSII fluorescence activity was observed when microcell contains 90 µg of chlorophyll from algae cells (data not shown). Moreover, to evaluate PSII fluorescence of algae cells immobilized in various conditions, the cells were entrapped in calcium alginate beads of different sizes by using syringes with different diameter tips (**Fig. 4F**). The algal cells retained their vitality in calcium alginate beads we did not observed any degradation, deformation of the beads or leakage of cell over three month period in TAP medium.

3.3. Design of microfluidic chips and integration of the algae bio-reporter

In order to enable working with immobilized algae, the solution was to encase the algae-alginate gel inside a cage, so that sample liquid flows around the algae but does not flush them away avoiding the blocking of inlet and outlet flows. For that reason, new microfluidic flow cells were designed and fabricated to fulfill the needs of the biosensor system, using immobilized algae with different shapes and sizes (range 1-5 mm) (**Fig. 1B and C**). The results showed that a small shape of the calcium-alginate beads within entrapped algae between 1-2 mm guarantees a better interface between the sample and entrapped algae (data not shown).

3.4. Response of the fluorescence biosensor

The response of the biosensor towards the pesticides simazine, atrazine and diuron was investigated. The variation of PSII fluorescence emitted from illuminated *C. vulgaris/T. pyriformi*s exposed to a range of concentrations of various herbicides was monitored. At least three replicates were made for each tested concentration. We observed an increase in Vj point proportional to herbicide concentration ranging from 2.50 up to 100 µg/L. The representation of the observed inhibition (%) depending on the concentration of pesticide is shown in **Fig. 5A and B**.

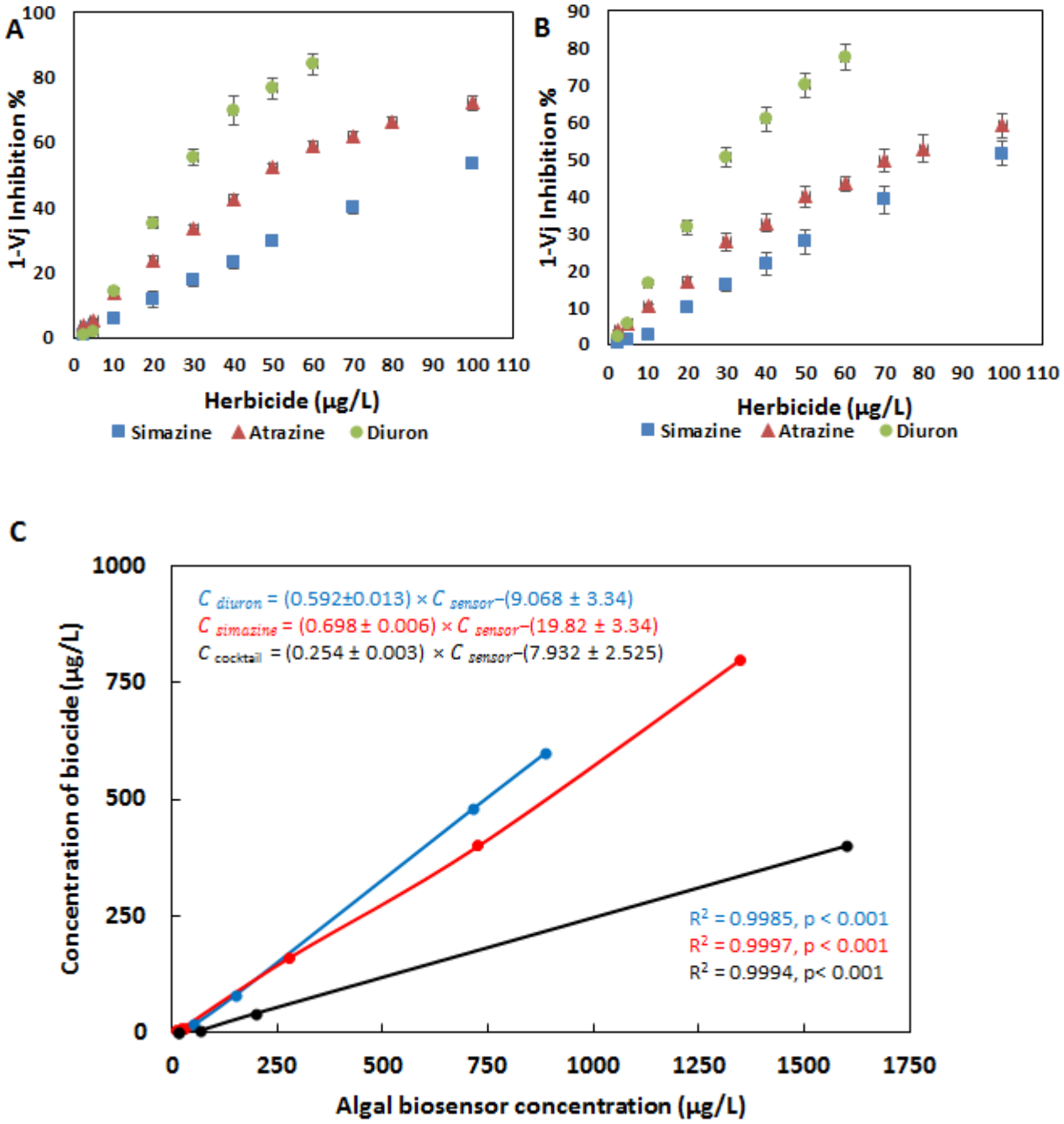

Fig. 5. Calibration plots obtained with symbiotic biosensor. A) Free living and B) immobilized cells. The points represent the average of three measurements calculated for each pesticide concentration. C) Correlations obtained in the analysis of seawater samples fortified with diuron (blue), simazine (red) and cocktail of biocides (black).

The calculated LODs for these three herbicides were 1.35, 0.44 and 0.25 µg/L when free biomediator was used, and 1.55, 0.89, 0.39 µg/L when immobilized biomediator was used, respectively. The

percentage of inhibition followed a linear trend for atrazine, simazine, and diuron in the tested range. The I_{50} values for these three representative herbicides are listed in **Table 2.**

Table 2. Performance of the symbiotic algal biosensor

State of biomediator	Analyte	Linear range (µg/L)	R^2	LOD		I_{30} (µg/L)	I_{50} (µg/L)
				µg/L	M (x10^{-9})		
Free	**Simazine**	2.5-100	0.996	1.35	6.7	53.6	90.1
	Atrazine	2.5-60	0.994	0.44	2.0	28.1	48.4
	Diuron	2.5-40	0.994	0.25	1.1	18.8	28.6
Immobilized	**Simazine**	2.5-100	0.995	1.55	7.7	56.7	93.3
	Atrazine	2.5-60	0.992	0.89	4.1	31.7	53.6
	Diuron	2.5-40	0.992	0.39	1.7	19.6	31.7

R^2, Coefficient of Determination

LOD, Limit of Detection

M, Molarity (mol/L)

I_{30}, Inhibitory *Concentration* 30%

I_{50}, Inhibitory *Concentration* 50%

3.5. Analyses in real world samples

LC-MS analyses of fortified samples, conducted in parallel with biosensor analyses, resulted in concentration values that were ±15% of the spiked concentration, showing no evidences of significant degradation/sorption of the target analytes during the transport and storage of the samples. No diuron or simazine were detected at concentrations smaller than 1 µg/L.

There was a good agreement between the sensor response and the spiked concentrations (**Table 3**). Overall, correlations showed a R^2>0.9985 with statistical significance (P<0.001, α=0.05%) for both diuron and simazine, as shown in **Fig. 5C**. The sensor overestimated the response of these two biocides: the slopes of the correlations were 0.592 ±0.013 L/µg (P<0.001) and 0.698±0.006 L/µg

(P<0.001), for diuron and simazine, respectively, instead of 1.0. No significant correlation was observed between the percentage of methanol (used to dissolve the pesticide) and the biosensor response.

In the environment, organisms are exposed to cocktails of chemicals; it is thus the algal biosensor was tested against samples fortified with a mixture of biocides. The sensor response was positive to the concentration of biocides, and the photosynthetic activity was inhibited even in the ng/L range, a concentration level that is relevant in environmental analyses of sea waters. This could be explained because of the synergistic activity between the fortified analyte and other miscellaneous toxic substances, to which the algae is sensitive (Cedergreen, 2014).The sensor response was linearly correlated with the total concentration of biocides, following the equation:

$C_{cocktail}=(0.254\pm0.003) \times C_{sensor} - (7.932\pm2.525)$, $R^2=0.9994$, $P<0.001$.

Table 3. Analysis of herbicides in blind (spiked) seawater samples and liquid chromatography-based validation results. Cocktail of biocides which can be typically found in the real environment: three herbicides, including a triazine (atrazine), an urea derivative (linuron) and a thiocarbamate (molinate); an algaecide (irgarol 1051); and an insecticide of the pyrethroid group (cypermethrin). Coktail samples contain equal quantity (µg) from each analyte.

Sample	Nominal concentration (µg/L)	Methanol residue (%)	Algal Sensor concentration (µg/L)
Simazine 1	600	0.060	887
Simazine 2	480	0.048	715
Simazine 3	80	0.080	152
Simazine 4	16	0.016	52.3
Simazine 5	8	0.008	31.1
Diuron 1	4	0.040	13.1

Diuron 2	8	0.080	24.7
Diuron 3	800	0.080	1350
Diuron 4	160	0.016	280
Diuron 5	400	0.400	728
Cocktail 1	0.04	0.040	17.2
Cocktail 2	0.40	0.040	16.4
Cocktail 3	4	0.400	68.9
Cocktail 4	40	0.400	199
Cocktail 5	400	4	1600

3.6. Long-term stability and reproducibility of the biosensor

In order to allow automated sampling and reliable measurements, it is desirable that the microalgae are retained within the microcells without any loss of activity over a long period of time. Thus, the storage stability of the immobilized algae was tested by measuring the PSII activity of the immobilized microalgae over 40 days in storage buffer. The biosensor retained approximately 99, 94, 90 and 83% of its initial activity after 3, 10, 20 and 40 days, respectively, as measured by fluorescence. Loss of activity affecting the fluorescence response was observed after 50 days in TAP/seawater (2:1 v/v). Thus, it can be concluded that the life time of the biosensor could be of up to 40 days without significant differences in the analyses.

Moreover, the selected beads of algae (2 mm diameter) were subjected to continuous flow of water, water with pesticide (3 μg/L diuron) and regeneration with methanol solution (5%). The results in terms of (1-Vj) pesticide/(1-Vj) control x 100 are shown in **Table 4** as a continuous set of measures.

Table 4. Continuous set of measurements for *C. vulgaris + Tetrahymena pyriformis* entrapped in calcium-alginate beads after exposure to 3μg/L diuron for 15 minutes.

Algae	**[(1-Vj)P/(1-Vj)C]x100**	**Time of Exposure (min)**	**Treatment and Regeneration**
C. vulgaris + Tetrahymena pyriformis	100	0	-
	135	15	Diuron
	148	15	Diuron
	129	15	Water
	111	15	Water
	110	15	Water
	103	15	Water/MetOH
	141	15	Diuron
	146	15	Diuron
	101	15	Water/MetOH
	139	15	Diuron
	102	15	Water/MetOH

Water/MetOH: 5% v/v methanol in water.

The experiments were repeated in continuous for three days and similar results were obtained with reduction of the entrapped algal activity of less than 5%. Thus, the interaction between the alga and the pesticide is reversible by simple washing. The activity was restored only in part by washing with water while the effect of pesticide can be completely removed by the use of 5% methanol, without affecting the activity of the algae that remains elevated as seen by the high Fv/Fm ratio. Additionally, in order to define how long the set of algae can last under continuous measurement, the fluorescence induction measurements were taken daily showing reproducibility of analyses for about a month.

The reproducibility and repeatability of the proposed biosensor were evaluated by PSII fluorescence measurements. The three microcells containing immobilized or free biomediator were prepared independently at different days showed an acceptable reproducibility with a relative standard deviation (RSD) of 1.8 and 2.1, respectively, for each 5 μg/L of atrazine determination. The

RSDs for each 5 μg/L simazine, atrazine and diuron measurements (n=6) were 1.4, 0.9 and 0.8 for free biomediator and 1.5, 1.4 and 1.1 μg/L for immobilized biomediator, respectively, revealing the good reproducibility of the proposed system.

Conclusions

Increasing pollution of marine environment requires the development of sensitive, cheap and adaptable early warning systems for on-site monitoring of chemical contaminants. In this work, we designed a whole-cell biosensor based on the symbiosis between the alga *C. vulgaris* and the ciliate *T. pyriformis* and adopted a microfluidic chip with the set-up of a smart fluorimeter device for an easy, low-cost and fast pre-screening of toxic contaminants in seawater samples. The LODs of this system for individual PSII inhibitors, in the μg/L range. The combined toxic effects of multiple chemicals have been recognized as an important consideration in ecotoxicology because mixtures of chemicals can have a greater negative impact than the individual constituents of the mixture. Considering this fact for cocktail of biocides, it can reach LODs of ng/L, that is relevant in environmental analyses of sea waters. The symbiotic biomediator has the important advantage of offering long-term resistance in marine water. For biosensing purposes, the use of the symbiotic association has also the advantage to provide a biological material that can be maintained years just by refreshing it, compared to other strains that require preparation of the culture from inoculum every 15-30 days. The present results show that the developed biosensor was effective for the determination of biotoxicity in seawater. The proposed integrated microalgae based biosensor was simple, cheap and rapid in comparison with analytical methods and it could significantly help to reduce the time associated with biotoxicity assays of chemicals and environmental water monitoring.

References

Asulabha K.S., et al, 2012. Effect of Salinity Concentrations on Growth Rate and Lipid Concentration in Microcystis Sp., Chlorococcum Sp. and Chaetoceros Sp. LAKE 2012: National Conference on Conservation and Management of Wetland Ecosystems, 06th-09th November 2012, School of Environmental Sciences, Mahatma Gandhi University, Kottayam, Kerala.

Belkhamssa, N., et al., 2016. Label-free disposable immunosensor for detection of atrazine. Talanta 146, 430–4. doi:10.1016/j.talanta.2015.09.015

Brayner, R., et al., 2011. Micro-algal biosensors. Anal. Bioanal. Chem. 401, 581–97. doi:10.1007/s00216-011-5107-z

Buonasera, K., et al., 2011. Technological applications of chlorophyll a fluorescence for the assessment of environmental pollutants. Anal. Bioanal. Chem. 401, 1139–1151. doi:10.1007/s00216-011-5166-1

Cedergreen N., 2014. Quantifying synergy: a systematic review of mixture toxicity studies within environmental toxicology. PLoS One. 2, 9(5):e96580. doi: 10.1371/journal.pone.0096580

DeLorenzo M.E., Fulton M.H., 2012. Comparative risk assessment of permethrin, chlorothalonil, and diuron to coastal aquatic species. Mar Pollut Bull. 64, 1291–9. doi: 10.1016/j.marpolbul.2012.05.011

Fujishima, M. (Ed.), 2009. Endosymbionts in Paramecium. Microbiology Monographs. Springer Berlin. doi:10.1007/978-3-540-92677-1

Galloway, T.S., 2006. Biomarkers in environmental and human health risk assessment. Mar. Pollut. Bull. 53, 606–13. doi:10.1016/j.marpolbul.2006.08.013

Giardi, M.T., Pace, E., 2006. Photosystem II-Based Biosensors for the Detection of Photosynthetic Herbicides, in: Biotechnological Applications of Photosynthetic Proteins: Biochips, Biosensors and Biodevices. Springer US, Boston, MA, pp. 147–154. doi:10.1007/978-0-387-36672-2_13

Giardi, M.T., et al., 2009. Optical biosensors for environmental monitoring based on computational and biotechnological tools for engineering the photosynthetic D1 protein of Chlamydomonas reinhardtii.

Biosens. Bioelectron. 25, 294–300. doi:10.1016/j.bios.2009.07.003

Hamza-Chaffai, A., 2014. Usefulness of Bioindicators and Biomarkers in Pollution Biomonitoring. Int. J. Biotechnol. Wellness Ind. 3, 19–26. doi:10.6000/1927-3037.2014.03.01.4

Harris, E., 1989. The Chlamydomonas Sourcebook. A Comprehensive Guide to Biology and Laboratory Use. Elizabeth H. Harris. Academic Press, San Diego, CA, 1989. . doi:10.1126/science.246.4936.1503-a

Huang, G.H., et al., 2009. Rapid screening method for lipid production in alga based on Nile red fluorescence. Biomass and Bioenergy 33, 1386–1392. doi:10.1016/j.biombioe.2009.05.022

Johanningmeier, U., Heiss, S., 1993. Construction of a Chlamydomonas reinhardtii mutant with an intronless psbA gene. Plant Mol. Biol. 22, 91–9.

Köck-Schulmeyer, M., et al., 2014. Four-year advanced monitoring program of polar pesticides in groundwater of Catalonia (NE-Spain). Sci. Total Environ. 470–471, 1087–98. doi:10.1016/j.scitotenv.2013.10.079

Kodama, Y., Fujishima, M., 2011. Four important cytological events needed to establish G endosymbiosis of symbiotic Chlorella sp. to the alga-free Paramecium bursaria. Jpn. J. Protozool. 44, 1–20.

Kodama, Y., Fujishima, M., 2009. Infection of Paramecium bursaria by Symbiotic Chlorella Species, in: Fujishima, M (Ed.). Endosymbionts in Paramecium pp 31–55. doi:10.1007/978-3-540-92677-1

Kröger, S., Law, R.J., 2005. Biosensors for marine applications. We all need the sea, but does the sea need biosensors? Biosens. Bioelectron. 20, 1903–13. doi:10.1016/j.bios.2004.08.036

Kröger, S., et al., 2002. Biosensors for marine pollution research, monitoring and control. Mar. Pollut. Bull. 45, 24–34.

Lambreva, M.D., et al., 2013. A Powerful Molecular Engineering Tool Provided Efficient Chlamydomonas Mutants as Bio-Sensing Elements for Herbicides Detection. PLoS One 8, e61851. doi:10.1371/journal.pone.0061851

Loos, R., et al., 2008. EU-Wide Monitoring Survey of Polar Persistent Pollutants in European River Waters.

Environ. Pollut. 157(2), 561-8. doi: 10.1016/j.envpol.2008.09.020

Loos, R., et al., 2010. Pan-European survey on the occurrence of selected polar organic persistent pollutants in ground water. Water Res. 44, 4115–4126. doi:10.1016/j.watres.2010.05.032

Markou, G., Nerantzis, E., 2014. Microalgae for high-value compounds and biofuels production : A review with focus on cultivation under stress conditions A review with focus on cultivation under stress conditions. Biotechnol. Adv. 31, 1532–1542. doi:10.1016/j.biotechadv.2013.07.011

Munaron, D., et al., 2012. Pharmaceuticals, alkylphenols and pesticides in Mediterranean coastal waters: Results from a pilot survey using passive samplers. Estuar. Coast. Shelf Sci. 114, 82–92. doi:10.1016/j.ecss.2011.09.009

Nödler, K., et al., 2014. Polar organic micropollutants in the coastal environment of different marine systems 85, 50–59. doi:10.1016/j.marpolbul.2014.06.024

Ranjan, R., et al., 2012. Development of immobilized biophotonic beads consisting of Photobacterium leiognathi for the detection of heavy metals and pesticide. J. Hazard. Mater. 225–226, 114–23. doi:10.1016/j.jhazmat.2012.04.076

Rao, A.V., Rao, L.G., 2007. Carotenoids and human health. Pharmacol. Res. 55, 207–216. doi:10.1016/j.phrs.2007.01.012

Reisser, W., 1986. Endosymbiotic associations of freshwater protozoa and algae. Prog Protistol 1, 195–214.

Sass, J.B., Colangelo, A., 2006. European Union bans atrazine, while the United States negotiates continued use. Int. J. Occup. Environ. Health 12, 260–7. doi:10.1179/oeh.2006.12.3.260

Schirmer, K., et al., 2010. Transcriptomics in ecotoxicology. Anal. Bioanal. Chem. 397, 917–23. doi:10.1007/s00216-010-3662-3

Sturm, A., et al., 1999. Cholinesterases of marine teleost fish: enzymological characterization and potential use in the monitoring of neurotoxic contamination. Mar. Environ. Res. 47, 389–398. doi:10.1016/S0141-1136(98)00127-5

Summerer, M., et al., 2008. Ciliate-symbiont specificity of freshwater endosymbiotic Chlorella (Trebouxiophyceae, Chlorophyta). J. Phycol. 44, 77–84. doi:10.1111/j.1529-8817.2007.00455.x

Sun, M., et al., 2016. Environmental and human health risks of antimicrobials used in Fenneropenaeus chinensis aquaculture production in China. Environ. Sci. Pollut. Res. Int. doi:10.1007/s11356-016-6733-y

Talvitie, J., et al., 2015. Do wastewater treatment plants act as a potential point source of microplastics? Preliminary study in the coastal Gulf of Finland, Baltic Sea. Water Sci. Technol. 72, 1495–504. doi:10.2166/wst.2015.360

Tammam, A.A., et al., 2011. Effect of salt stress on antioxidant system and the metabolism of the reactive oxygen species in Dunaliella salina and Dunaliella tertiolecta 10, 3795–3808. doi:10.5897/AJB10.2392

Tibuzzi, A., et al., 2007. A new miniaturized multiarray biosensor system for fluorescence detection. J. Phys. Condens. Matter 19, 395006. doi:10.1088/0953-8984/19/39/395006

Tonnina, D., et al., 2002. Integral toxicity test of sea waters by an algal biosensor. Ann. Chim. 92, 477–84.

Xiong, J., et al., 1998. Loss of inhibition by formate in newly constructed photosystem II D1 mutants, D1-R257E and D1-R257M, of Chlamydomonas reinhardtii. Biochim. Biophys. Acta 1365, 473–91.

CHAPTER 3

"A Novel optical/electrochemical biosensor for real time measurement of physiological effect of astaxanthin on algal photoprotection"

Turemis, M., Rodio, G., Pezzotti, G., et al. "A Novel optical/electrochemical biosensor for real time measurement of physiological effect of astaxanthin on algal photoprotection", *Sensors and Actuators B*: Chemical, 241 (2017); 993-1001, DOI: 10.1016/j.snb.2016.10.115

Abstract

An optical/amperometric biosensor based on algal cells immobilized in calcium alginate gel was developed. Various *Chlamydomonas reinhardtii* strains mutated at the level of photosynthetic D1 protein were used as biomediators to quantify the capacity of the carotenoid xanthophylls to protect the photosynthetic apparatus from photoinhibition. The highly sensitive/selective biosensor was used for studies on cell physiology aimed to determine the antioxidant and light filtering effects of the xanthophyll astaxanthin. The biosensor was proved to be suitable for the determination of the exogenous supplied astaxanthin, showing in a short time a reliable response with a detection limit of 3 μM. This technique revealed the photoprotective effect of astaxanthin-enriched extracts of *Haematococcus pluvialis* in algal cells. The results suggest that in algae astaxanthin exploits both filtering and antioxidant effects at different light intensities. This bioinspired approach can provide new insights into biological, biomedical, environmental and agricultural research applications and nutraceutical studies.

1. Introduction

Naturally grown unicellular algae are often subjected to unfavorable conditions such as excess light energy, high or low temperatures, and nutrient deficiency which, especially in combination, can cause photodamage to the photosynthetic apparatus at the level of the D1 protein, the psbA gene product. During evolution, several protection mechanisms against stressful conditions were developed, including among the others, thermal dissipation of excess absorbed light energy, activation of antioxidant enzymes, and accumulation of non-enzymatic antioxidant systems such as protective pigments [1, 2].

Carotenoids are natural pigments synthesized by plants and microorganisms that in recent years have been the major focus of research as essential components of the photosynthetic apparatus, involved in photosystem II (PSII) assembly, functioning and protection. They could act either as antioxidants for deactivation of radical species or as chromophores for filtering the solar light captured by the antenna system of PS II [3-5]. Their protective effect against excess absorbed light energy is particularly important for the PSII D1 protein, which is known to have a rapid and light-dependent turnover also involved in the PSII repair cycle. Krinsky et al. [6-8] proposed that carotenoids prevent damage of excessive irradiance by directly quenching triplet chlorophyll (^{3}Chl) or $_1O^2$ produced during photodynamic reactions. This quenching mechanism requires close proximity between the quencher carotenoid and the photosensitized chlorophyll molecules. A different mechanismof action has been proposed by Fan and coworkers [9] for the red ketocarotenoid astaxanthin: this molecule, belonging to the xanthophyll class, could protect the PSII by acting as a filter that screens excessive irradiance.

An example of this photoprotective mechanism occurs in the green microalga *Haematococcus pluvialis* that under light stress conditions accumulates high amounts of astaxanthin in storage lipids [10]. Recently, Gao and coworkers [11] demonstrated the photoprotective role of astaxanthin in *H. pluvialis* treated with jasmonic acid, and Franceschelli and coworkers [12] reported that astaxanthin

treatment protects against oxidative stress in U937 cells, attenuating lipopolysaccharide-induced toxicity and production of reactive oxygen species (ROS).

Carotenoids in general and xanthophylls in particular are thought to be responsible for the beneficial properties of fruits and vegetables in preventing human diseases. However, humans cannot synthesize carotenoids de novo and depend on diet supply. [13]. Recent reports have attributed several biological functions in humans to astaxanthin, such as protection from cardiovascular diseases, cancer prevention and enhancement of the immune response, and this pigment has also assumed strategical value as nutraceutical supplements [14, 15]. The presence of the hydroxyl and keto endings on each ionone ring confers some unique features, such as the ability to be esterified, a higher anti-oxidant activity, and a more polar configuration than other carotenoids. The structural property of astaxanthin allows it to span the cell cellular membrane bilayer (fat/water) and expose it to aqueous environment. Besides, astaxanthin differs from other antioxidants in its ability to be highly penetrating in the membranes, for instance in the blood brain barrier and in the retina. The use of exogenous astaxanthin as an antioxidant for various cell lines and biomembrane systems have considerably been researched and studied for practical applications [16-18].

At present carotenoids can be detected by using the classical spectrophotometric and chromatographic techniques. Due to high spatial resolution, excellent sensitivity, rapid prototyping, low cost and simple operating, biosensors have emerged as an important tool for measuring several analytes in a wide range of applications including agrifood, environmental, diagnostics and preventive disease research [19]). In addition to their importance in detecting and quantifying analytes, biosensors reflect better the real physiological impact of active compounds on living organisms used as biological biomediators [20]. So far, several computational and molecular biology studies have been carried out on *C. reinhardtii* strains for the design and realization of sensitive and real time PSII II-based biosensing devices [21, 22].

This paper describes the realization of an optical/electrochemical biosensor for the assessment of xantophylls power using a bio-inspired approach. A specific set of mutants of the unicellular green alga *Chlamydomonas reinhardtii* was used as biorecognition element to measure the photoprotective effect of astanxanthin. The mutants host aminoacidic substitution in the PSII D1 protein, and present a highly different xanthophylls content and a different response to photodamage

2. Materials and methods

2.1. Culture growth conditions of *Chlamydomonas reinhardtii* and production of mutants

Chlamydomonas reinhardtii cells were grown at 25°C in Tris-acetate-phosphate (TAP) medium under the continuous illumination of white fluorescent lamps (50 μmol photons $m^{-2}s^{-1}$). Algal cells in the exponential growth phase (OD_{750}=0.50 ± 0.03), were used in all analyses. Construction of the *C. reinhardtii* mutant strain Del1 was reported previously [23]. The Del1 strain was grown in liquid TAP medium to mid-log phase. 2 x 10^7 cells were concentrated onto plain Nylon filters (0.45 μm, 47 mm diameter, MSI, USA) using a filtration device. The filters were placed on plates containing 1.5 % agar in TAP medium and kept overnight in the dark. One microgram of PCR product was precipitated onto tungsten particles [24] loaded onto a carrier and accelerated with a pressurized helium (10 bar pressure for acceleration; 10 cm shoot distance; -1.8 bar vacuum). Photoautotrophic colonies were obtained after 14 days of culture under continuous light at 20 °C. In order to isolate algal strains tolerant to free radical oxidative stress, a cocktail of photoautotrophyc D1 random mutants were selected under stress applied by radiation according to Rea et al [25]. The results revealed that single aminoacidic substitution in the D1 protein could contribute to ionizing radiation tolerance. To exclude the possibility that additional random mutations induced by the radiation exposure in other regions could confer the observed tolerance, a set of the identified amino acid substitutions were introduced into D1 protein by site-directed mutagenesis [22, 25]. The *C.*

reinhardtii wild-type cells 11/32b (Sammlung von Algenkulturen, Grttingen, FRG) with intronless psbA gene (IL) was used as the reference strain in all experiments [26].

2.2. Oxygen evolution and pigments analyses

The oxygen evolution capacity was measured at 24 °C by a Clark-type oxygen electrode (Chlorolab 2, Hansatech, UK) as described previously [22]. The oxygen evolution rate was determined under saturating illumination (300 µmol photons $m^{-2}s^{-1}$), continuous stirring and in the presence of 10 mM $NaHCO_3$, as an additional carbon source. To compare the photosynthetic capacity between the different samples, the same amount of chlorophyll (15µg ml^{-1}) was loaded into an oxygen electrode chamber.

Extraction of pigments was carried out on algal cell pellets using a mixture of methanol: chloroform 1:2 v/v. After homogenization in a glass homogenizer, the suspension was centrifuged for 10 min at 3500 g. The supernatant was washed with distilled water, shaking it for 10 min, and then the organic phase was concentrated by evaporation. The total content of chlorophyll and carotenoids was determined spectrophotometrically [27], while the single pigments were analysed by thin layer silica gel-silufol chromatography (Silufol UV254, Kavalier, Votice, Czech Rep), using a mixture of acetone: benzene: hexane 2:5:5 as a mobile phase. After separation, the pigments were eluted with chloroform: methanol 1:1 and evaporated to dryness [28].

2.3. Astaxanthin extraction from Haematococcus pluvialis cell cultures and UV-Vis quantification

500 mg of dried *H. pluvialis* cells were taken in 3 mL DMSO and mixed with 40 mg of glass beads. The mixture was sonicated for 12 minutes, centrifuged at 4000 rpm for 5 minutes and the supernatant was collected and eventually, filtered on a PTFE filter (4.5 mmesh). The amount of

dissolved astaxanthin in the collected supernatant was estimated by UV-Vis spectrophotometry. A stock solution of 100 µg mL^{-1} astaxanthin was prepared in DMSO and a calibration graph for astaxanthin was drawn for the following concentrations of astaxanthin: 0.4 µg mL^{-1}; 0.8 µg mL^{-1}; 1.6 µg mL^{-1}; 3 µg mL^{-1}; 5 µg mL^{-1}; DMSO was used as the blank; measurements were performed in UV-Vis cells with 1 cm path, at 488 nm. Fifty µL from the supernatant were taken and diluted at 3 mL with 10% (v/v) DMSO; the absorbency at 488 nm was measured and the value obtained was interpolated on the calibration graph to determine the astaxanthin concentration.

2.4. Immobilization of algal cells on the screen printed electrodes

An aliquot of *C. reinhardtii* culture in its exponential growth phase was collected and centrifuged at 2000 g for 5 min at 15°C. The supernatant was discarded and the pellet was washed twice with Tricine-NaOH 50 mM pH 7.2. After washing, the supernatant was discarded while the pellet was suspended in Tricine-NaOH 50 mM pH 7.2 to a final volume of 50 µl, then mixed with 100 µl of 2 % sodium alginate solution (w/v) in the same buffer, to obtain a 1.3% (w/v) alginate. Five µl of suspension, corresponding to 4.5µg chlorophyll of the algae cells, was dropped over a Multi-Walled Carbon Nanotube (CNT) working electrode of the Screen-Printed Electrodes (SPEs) (DRP-110CNT, DropSens, Spain). The CNT-SPE with the spotted material was immersed for 20 min in Tricine-NaOH 50 mM, $CaCl_2$ 200 mM prior to use.

2.5. Biosensor experimental set-up

The device was based on a multiarray system made up in six dynamic cells of two separate and independent sensing modules, optical and electrochemical, integrated in a compact miniaturised sensor with some modifications made to the previously described system [29, 30].

The optical set-up was a fluorimeter hosting excitation light sources in the six cells. In each cell, there was a set of LEDs (Ø 3 mm) with appropriate excitation wavelength and a set of photodiodes for the appropriate emission wavelengths. A 30 sec red light (650 nm, 500 µmol photons $m^{-2}s^{-1}$) was used to excite fluorescence, while illumination with a physiological light or high light of various intensities (in the range 50-1400 µmol photons $m^{-2}s^{-1}$), was applied continually for various periods of time, leaving the samples in the dark for fluorescence measurements. The fluorescence transient registered from samples after the onset of saturating illumination mainly reflected the photoinduced reduction of the PSII electron carriers and transition of the reaction centres to a closed state. The fluorescence rise as a polyphasic curve and the relative variable fluorescence allowed a direct comparison between the samples [31].

The electrochemical sensing module was composed of the electrochemical cell hosting the biological material, directly deposed on the SPEs on the six cells. The washing solution, the electrolytic fluid and sample flow entered and excited through inlet and outlet connections. The electrochemical biosensor set-up was performed under the following conditions: the CNT electrode was polarized at -0.7 V with an Ag/AgCl reference electrode mounted in the flow cell and illumination was provided by the light-emitting diodes. The current intensity was stimulated or inhibited in the algal cells by red or white light. The electrode was continously washed with the measuring buffer, Tricine 50 mM pH 7.0, $CaCl_2$ 20 mM, $MgCl_2$ 5 mM, NaCl 50 mM, sucrose 70 mM. All measurements were performed at a room temperature of 25 ^{o}C.

The device was made up of an electronic control, LED drivers, a pre-processing signal-conditioning module, a flash memory card, with a USB connection in order to permit transmission to the computer data storage.

2.6. Statistical analyses and limit of detection

The fluorescence emission expressed as Fv/Fm was evaluated in three biological replicates (±SE, n=9). The current intensity was averaged on three stable peaks and expressed as the difference between the peak intensity and the baseline. The statistical significance of the differences was evaluated at values of $p \leq 0.05$ values. The limit of detection was calculated on the basis of the signal to noise ratio S/N=3.

3. Results and discussion

This research aimed to develop a biosensor useful to study the photoprotective effect of xanthophylls on the PSII macromolecular assembly in microalgae. It has been previously demonstrated that *C. reinhardtii* is an efficient biosensing element having good stability and photosynthetic performance in immobilized form. In addition, the photochemical properties of this microalga could be efficiently exploited to construct either optical or electrochemical transduction system. In fact, the PSII has the unique capability to emit a variable fluorescence when excited with a short pulse of saturating light that could be opportunely measured providing information on the photosynthesis efficiency. Similarly, it is also possible to amperometrically measure the O_2 reduction currents produced by the light-induced electron transfer chain and water splitting in PSII [32, 33]. The proof-of-concept of this novel-designed biosensor is based on the knowledge that in the presence of excess absorbed energy the D1 protein is photodamaged determining a reduction of the amperometric/fluorescence signals; that damage in the presence of xanthophylls could be prevented or reduced [34, 35].

Algal cells were immobilized on screen-printed electrodes and exposed to highlight stress in the cell module depicted in Figure 1 that contains all the components necessary for algae hosting and stimulations, and the measuring set-up.

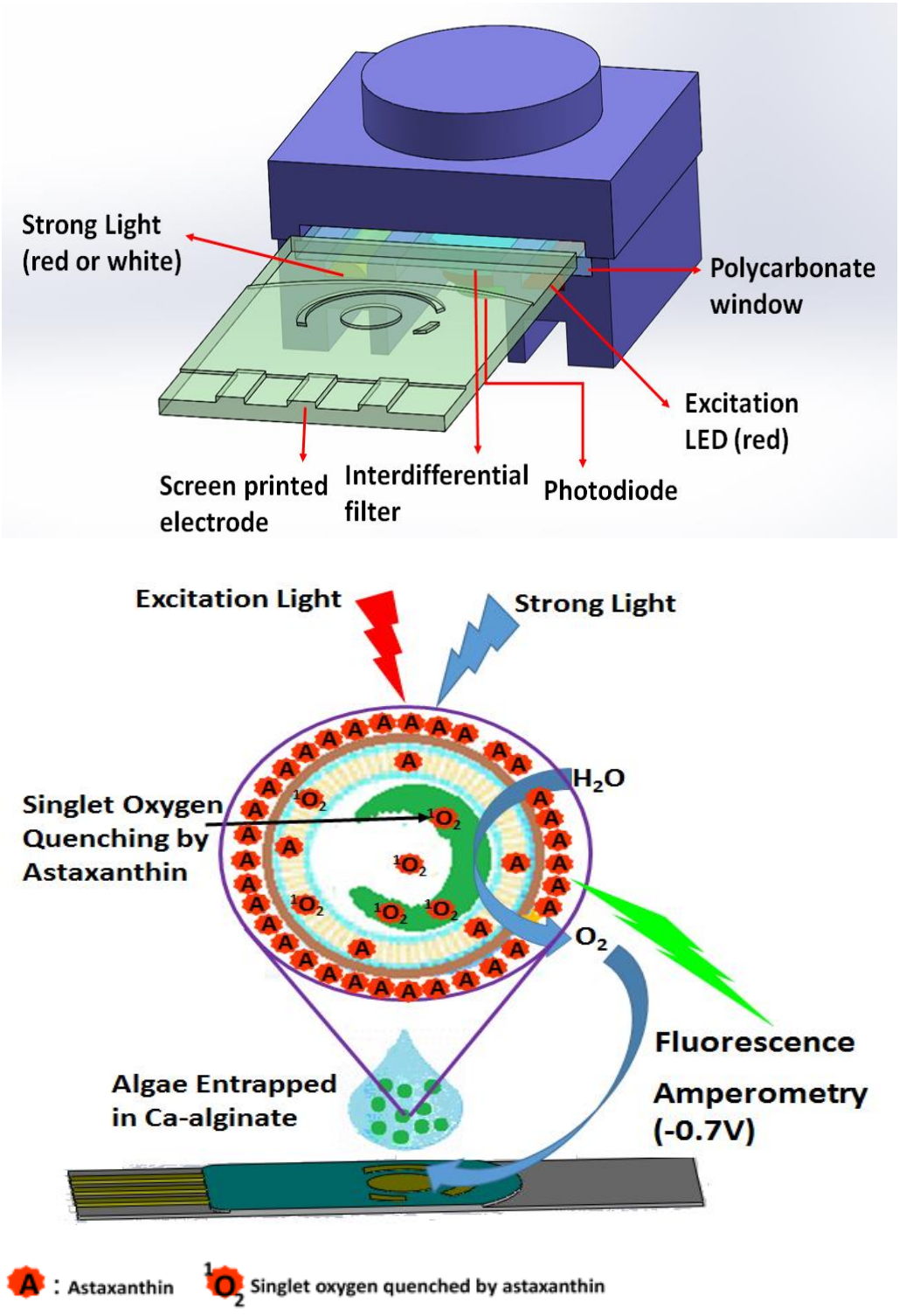

Fig. 1. Sketch of the biomimetic approach showing astaxanthin light filtering activity and quenching of singlet oxygen produced in PS II with strong light. A) Scheme of the amperometric/fluorescence module cell. B) Screen printed electrode used to immobilise the biological material, the optical excitation for measurement, and the high light set-up necessary to induce photodamage.

3.1. Characterization of D1 mutant strains

Since it is known that modifications of D1 protein can promote tolerance to photodamage [36], we produced and selected PSII D1 mutants tolerant to free radical-associated stress induced by ionizing radiation. These mutants were produced by adopting an in vitro directed evolution strategy followed by site-directed mutagenesis experiments to rule out the occurrence of additional mutations induced by the applied selection pressure. The mutants were hence identified by DNA sequencing and characterized as previously reported [22, 25]. The best performing strains were selected to be used as biomediators for the biosensor construction by assessing photosynthetic parameters and accumulation of photoprotective xanthophylls. The main features of the produced mutants are reported in **Table 1**. For our purpose, we chose the strains having a good maximum quantum yield (Fv/Fm) defined by fluorescence induction curves and oxygen evolution rates and as calculated by polarographic techniques. (**Table 1, 2**).

Table 1. Description of mutants hosting aminoacidic replacements in the PSII D1 protein, and photosynthetic oxygen evolution measured by a Clark electrode under saturating illumination (300 µmol photons $m^{-2}s^{-1}$).

	Wild -type and aminoacidic replacements-localization of mutation in D1 protein	**Oxygen evolution µmol O_2 mg $Chl^{-1}h^{-1}$**
IL	**Intronless wild-type**	**90±4**
G207S	**glycine-serine in helix IV**	**130±4**
I163N	**isoleucine–asparagine near to Tyr_{161}**	**151±5**
I281T	**isoleucine-threonine in helix V**	**120±4**
M172L	**methionine-leucine near to EOC**	**110±4**
P162S	**proline-serine near to Tyr_{161}**	**109±5**

Table 2. Fluorescence activity measured as Fv/Fm and sensitivity of *Chlamydomonas reinhardtii* D1 mutants subjected to 10 min white light stress (1400 µmol photons $m^{-2}s^{-1}$), presented as a reduction in percent of the initial Fv/Fm value, in the absence and presence of 10 µM astaxanthin.

Strain	Fv/Fm	light stress	
		% Fv/Fm reduction	% Fv/Fm reduction +10 µM astaxanthin
IL	**0.792±0.01**	**17± 3**	**10± 2**
G207S	**0.753±0.01**	**26 ± 3**	**9± 3**
I163N	**0.790±0.01**	**20 ± 4**	**11± 4**
I281T	**0.710±0.02**	**19 ± 4**	**nd**
M172L	**0.755±0.02**	**0**	**0**
P162S	**0.700±0.02**	**9 ± 7**	**nd**

nd: not determined

Determination of pigment content revealed that in all the mutants, the Chlorophyll a/b and the Chl a+b/carotenoids ratio was lower compared to the control strain IL. However, specific xanthophylls content was greatly increased in M172 and decreased in I163N and G207S (**Fig. 2 A, B**) in comparison to IL. The different content of xanthophylls could be ascribed to the modification of the D1 protein and the corresponding supported electron transfer that it is known to be gene expression regulator [37, 38, and unpublished results].

A set of experiments was hence performed with the biosensor by exposing the selected algae strains to physiological and damaging light conditions to test the photoprotective effect of astaxanthin (**Fig. 1**).

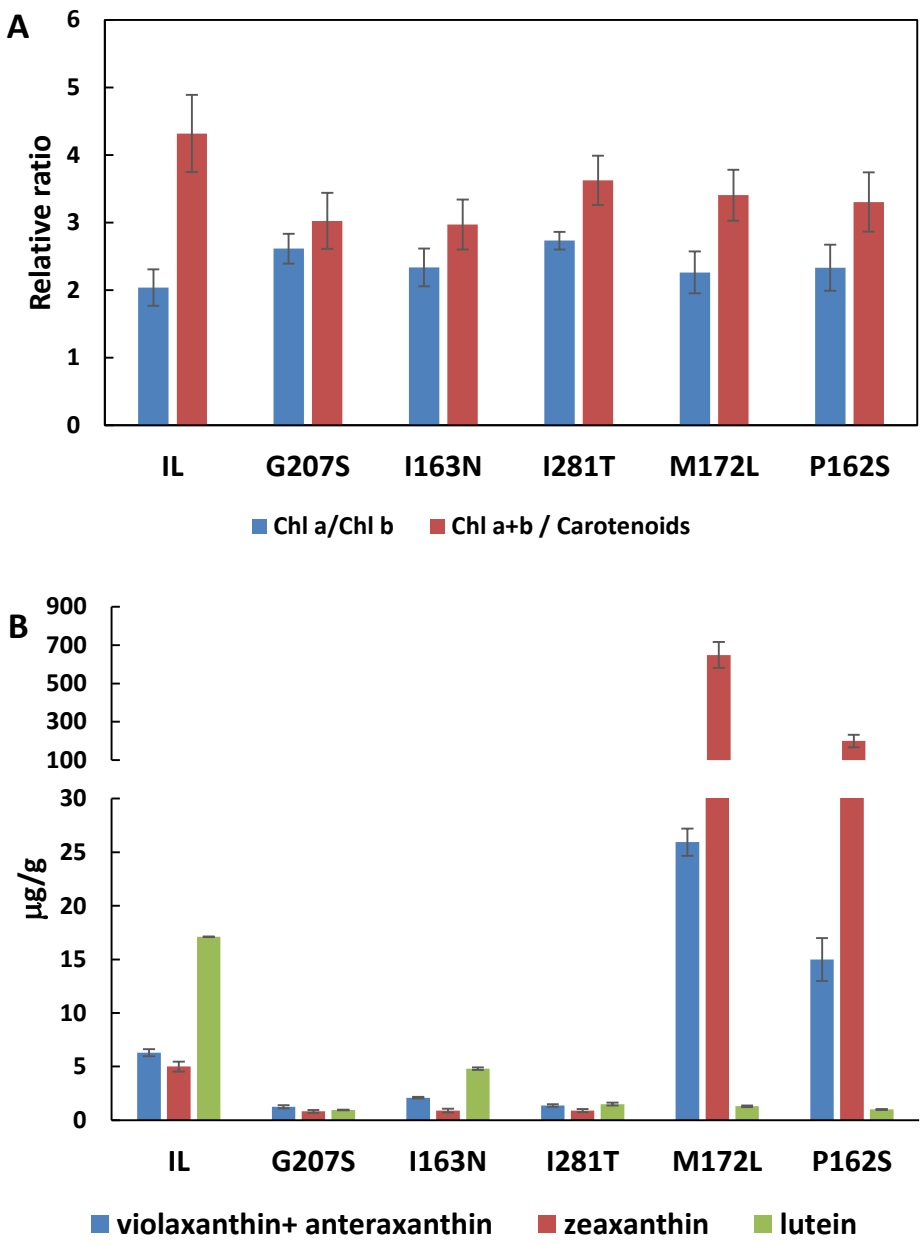

Fig. 2. Pigment analyses of *Chlamydomonas reinhardtii* mutants. A) Chlorophyll a/b and Chl a+b/carotenoids ratios. B) Content of xanthophyll pigments µ/g of alga dried weight. Cells were grown in TAP medium under continuous light 50µmol photons $m^{-2}s^{-1}$ and harvested after three days. Values shown are the mean of three independent experiments.

3.2. Fluorescence-based biosensor for analysis of the alga photoprotection by astaxanthin

The wild-type algal cells entrapped in alginate gels were exposed to physiological light (LL) or high light (HL), with and without exogenous astaxanthin (10 µM), and their fluorescence activity was periodically measured by the biosensor.

The fluorescence activity in physiological light remains stable and a small reduction of Fv/Fm from 0.792 till 0.720 +/- 0.03 was observed in the presence of increasing concentration of exogenous astaxanthin indicating a possible light filter effect (see Time 0 in Fig. 3). When the algae are illuminated with high light, the Fv/Fm value is reduced to 0.393 +/- 0.03 within 40 min of illumination (**Fig. 3**). A protection of PSII is noticed by applying exogenous astaxanthin. This effect is not linear in the tested range of concentrations and it presents a maximum of 49% reduction with 10 µM astaxanthin and a limit of detection of about 3 µM (**Fig. 3**).

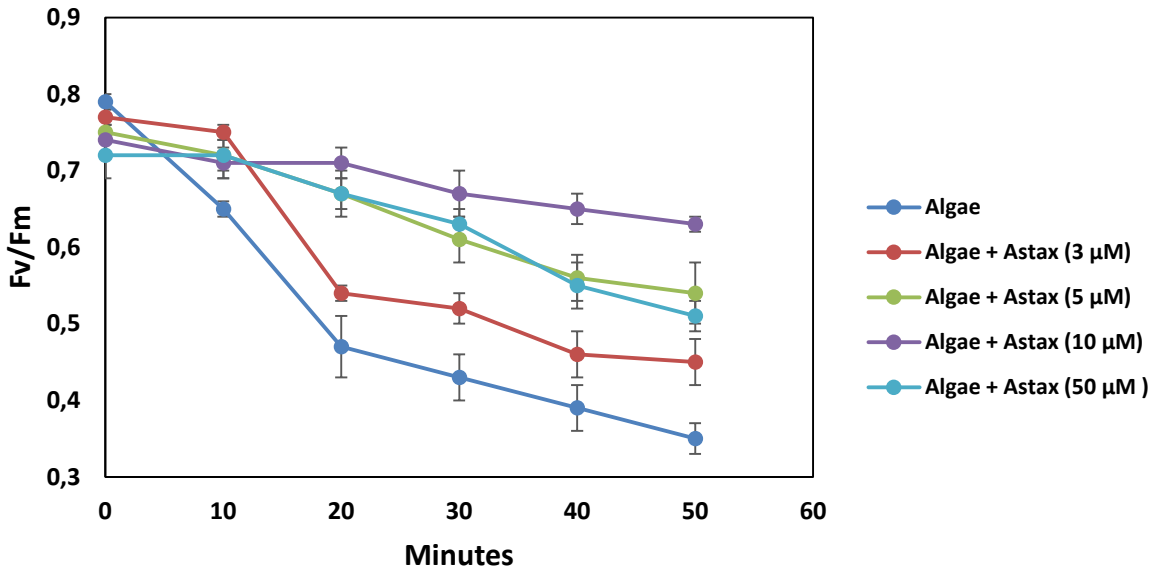

Fig. 3. PSII activity measured by the biosensor as Fv/Fm ratio. The initial Fv/Fm ratio is reported in Table 2. Data are presented as percent of initial value measured under physiological low light (LL, 50 µmol photons $m^{-2}s^{-1}$) or high light (HL, 1400 µmol photons $m^{-2}s^{-1}$) after 1 hour incubation with or without astaxanthin (concentrations: 5 µM, 10 µM, 50 µM)); recovery was measured after 1h in low light. The control samples contain the same methanol (5% v/v) used for dissolution of astaxanthin.

The photosynthetic performance of D1 protein mutants was also measured as Fv/Fm reduction under light stress. In accordance with previous results [28, 39] the sensitivity of the mutants to light stress well correlates with the highest content of the xanthophyll zeaxanthin, being M172L the most resistant strain and G207S the most sensitive one (Table 2). The supply of 10 µM astaxanthin leads to a slight protection, particularly for the mutant G207S that contains less zeaxanthin (Table 2).

3.3. Amperometric-based biosensor for analysis of the alga photoprotection by astaxanthin

According to previous cyclic voltammetry tests, the potential of -0.7 V corresponds to a reduction in the photosynthetically generated O_2 on the electrode [33]. The current intensities generated by algae upon illumination was in the microamperes range, calculated as the difference between current intensities produced in dark and light conditions. After 5 minutes of dark adaptation, the immobilized algae cells were stimulated by an input of 30s of red light and the intensity of the biosensor current peak was recorded. The same measurement was then repeated after algae cells were exposed to light for 40 min in the absence and presence of exogenous astaxanthin. In the wild-type cells (IL) a decrease in the current of light-activated PSII electron transfer was observed by increasing astaxanthin concentrations. This increase was inversely proportional to the astaxanthin concentration providing a limit of detection of 3 µM; this result indicates a possible light filtering effect of astaxanthin on the immobilized cells (**Fig. 4**).

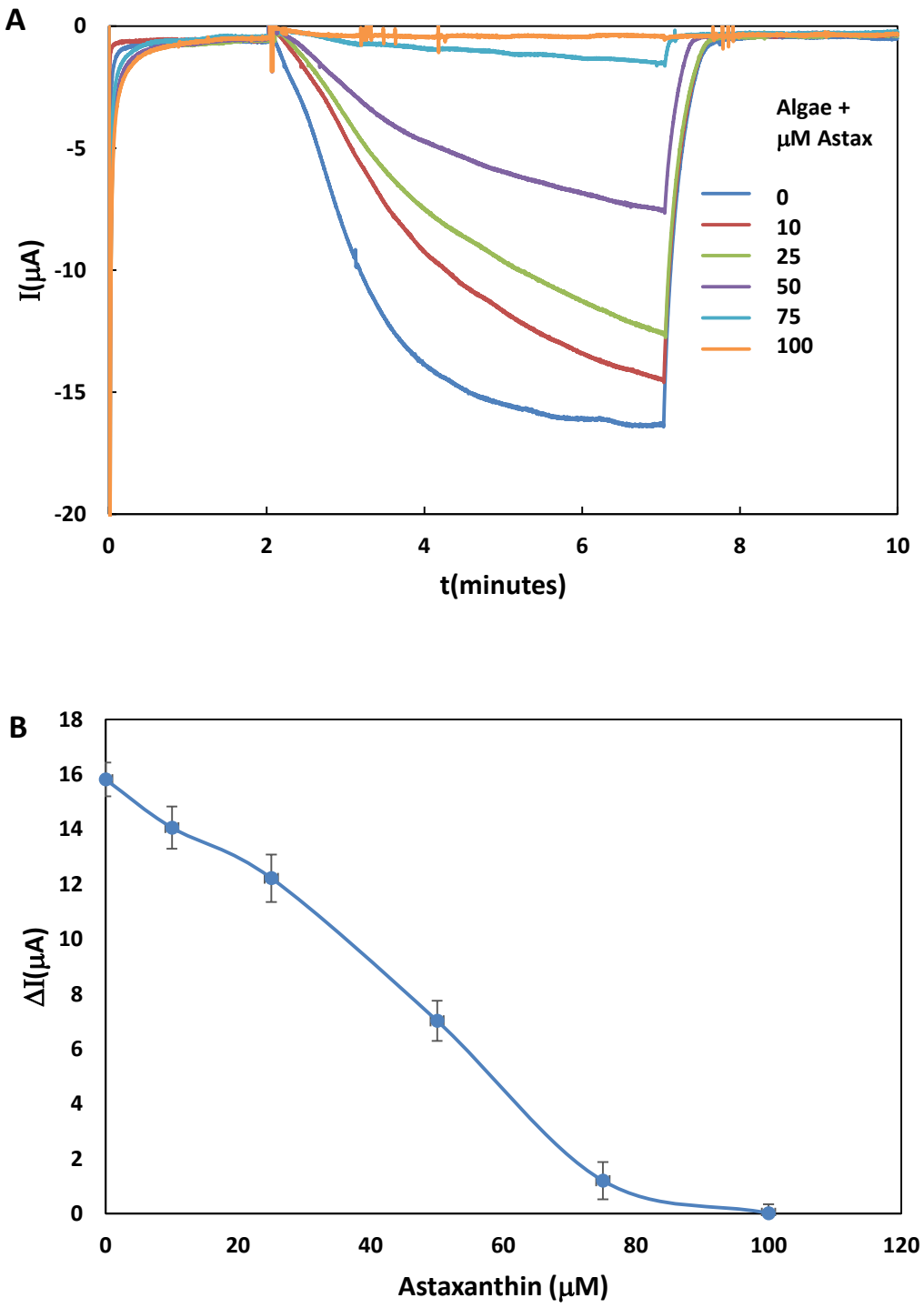

Fig. 4. Amperometric measurements using specific *Chlamydomonas* strains as biomediators (A). Amperometric curves obtained at various astaxanthin concentrations (B). Experimental conditions: 5 min dark and 5 min of white light intensity of 300 μmol photons $m^{-2}s^{-1}$ in presence of various astaxanthin concentrations. The measurements consisted of 3 repetitive cycles of 5 min dark/light. The points represent the average of three measurements calculated for each astaxanthin concentration.

Unexpectedly by increasing the light intensity up to 1400 µmol photons m^{-2} s^{-1}, an increase of the current peak was registered indicating a possible interference by newly produced free radicals generated in these photoinhibitory conditions (data not shown). In fact, under the strong illumination of PSII, endogenous superoxide anion, hydrogen peroxide, and hydroxyl radical are successively produced that could generate more oxygen on the electrode [40]. Instead, exposure of cells to relatively high red light, which specifically inhibits the photosynthetic PSII activity, caused a small reduction of about 0.6 µA in the amperometric peak (**Fig. 5**). Application of exogenous astaxanthin at various concentrations led to protection from red light stress, restoring the amplitude of the amperometric peak at the same control value (**Fig. 5**).

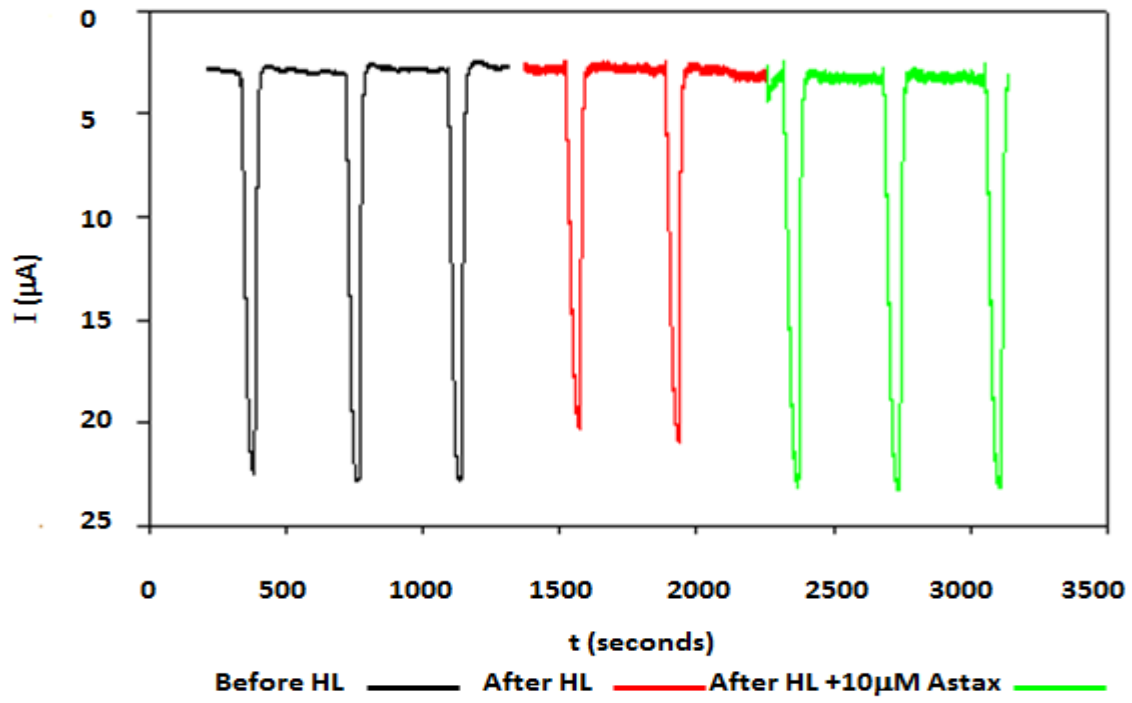

Fig. 5. Amperometric tests using different *Chlamydomonas* strains as biomediator. Experimental conditions: 3 cycles of 5 min dark and 30s of light flash, then high red light intensity of 500 µmol photons $m^{-2}s^{-1}$ in the absence and in presence of 10 µM astaxanthin. Black: before light stress; red: after 10 min light stress; green: after 10 min light stress in the presence of 10 µM astaxanthin.

By performing the same experiments of light stress on the *C. reinhardtii* mutants, a different reduction in the peak was observed. An important effect in activity reduction was observed in the mutant G207S, which has the lowest xanthophyll content (**Fig. 2B**). The introduction of astaxanthin at a concentration of 10 µM leads to a slight but significative protection particularly evident in the G207S mutant (**Table 3**).

Table 3. Effect of 10µM astaxanthin in protection of PSII electron transfer activity measured amperometrically under red light stress of 500 µmol photons $m^{-2}s^{-1}$ for 40 min using *Chlamydomonas reinhardtii* mutants as biomediators.

Strain	**light stress**	
	% ET reduction	**% ET reduction + 10 µM astaxanthin**
IL	**12 ± 2**	**7± 2**
G207S	**40 ± 5**	**30± 3**
I163N	**18±4**	**13±4**
I281T	**25 ± 5**	**15± 5**
M172L	**0**	**0**
P162S	**8± 2**	**3± 2**

ET: electron transport

3.4. Analysis of algal extracts

The proposed method was applied for the determination of spiked astaxanthin in extracted algal H. pluvialis samples. In order to study the matrix effect on the biosensor response we analysed extracts containing different amount of astaxanthin, taken at different alga growth stages. The results were calculated as equivalent synthetic astaxanthin per mg dry weight. In addition, the concentration of astaxanthin in the spiked samples (average of three determinations) and the recovery of astaxanthin by the standard addition were also measured using the proposed biosensor. The results summarized in **Table 4**. were in good agreement with spectrophotometry. The recovery of all measured samples

was between 96.5% and 101.7%. These results indicate that the proposed biosensor system could be applied for astaxanthin analysis in real samples.

Table 4. Astaxanthin recovery in algae extracts by amperometry and spectrophotometry.

Detection Method	**Sample**	**Found astaxanthin in 10 mg dry weight/L (µM)**	**Spiked (µM)**	**Expected (µM)**	**Found (µM ± SD)**	**Recovery (%)**
Amperometry	**Synthetic astaxanthin**	**-**	**50**	**50**	**50.7**	**101.4**
	***Hematococcus* extract in green stage**	**5**	**50**	**55.0**	**53.1**	**96.2**
	***Hematococcus* extract in red stage**	**29,3**	**50**	**79.3**	**80.4**	**102.2**
Spectrophotometry	**Synthetic astaxanthin**	**-**	**50**	**50**	**49.7**	**99.4**
	***Hematococcus* extrac in green stage**	**5.9**	**50**	**55.9**	**56.5**	**101.2**
	***Hematococcus* extract in red stage**	**28.5**	**50**	**78.5**	**80.2**	**103.4**

Note: The carotenoid fraction in the green stage is quite exclusively composed of lutein and β-carotene, while in the red stage, the major carotenoid is astaxanthin.

3.5. Repeatability and stability of the biosensor

The repeatability of the algae based biosensor was evaluated by measuring the responses to 50µM astaxanthin in 5 replicates. The prepared biosensor exhibited good and repeatable performance with a relative standard deviation of 2.4%. To investigate the storage stability of the developed biosensor, screen printed carbon electrode modified with freshly prepared algae were stored under standard indoor illumination (10 µmol m^{-2} s^{-1} light intensity) in storage buffer (PBS, pH 7.0) at 25±2 ^{o}C and its fluorescence and amperometric response (oxygen reduction current) was monitored periodically in fresh buffer solution. The modified electrode retained approximately 99%, 90%, 75% and 20 % of its initial activity after 3, 10, 20 and 40 days respectively. Therefore, it can be concluded that the storage stability of the biosensor is about 20 days for optic/amperometric biosensor, respectively.

3.6. Comparison of biosensors

To the best of our knowledge no previous published work used a similar approach, hence the performance of the proposed biosensor was compared to some xanthophyll sensors previously reported (**Table 5**). For example, in comparison with some chemical sensors [41-20], the detection limit of our biosensor is higher. This could be due to the diffusion limitation of the astaxanthin to the target membrane of algae cell. However, our biosensor present some advantages over the biosensors reported in reference [41, 42] since it allows measurements in aqueous medium. Moreover, our biosensor provided insight into the physiological effect of astaxanthin under various light intensities with combined transduction methods. Finally, this biosensor allows the indirect determination of astaxanthin at low operational potential -0.7 V vs. Ag/AgCl with high sensitivity and elimination of undesirable oxidation of interferents.

Table 5. Comparative performance of sensors and biosensors for astaxanthin determination.

Measurement Technic	**Differantial pulse voltammetry**	**Amperometry**	**Amperometry**	**Amperometry/Optic**
Electrode	**GCE**	**GCE**	**Gold**	**CNT**
Measurement Principal	**Electrooxidation of lutein**	**Electrooxidation of astaxanthin**	**Antioxidant activity against oxidizable phosphatdylcholine**	**Antioxidant activity against PSII activity under high light**
Analyte	**Lutein**	**Astaxanthin**	**Astaxanthin**	**Astaxanthin**
Sorbent/solvent	**Acetonitrile**	**MTBE/MetOH**	**Water**	**TAP**
Linear range (µM)	**0.5-76**	**nr**	**nr**	**10-100**
LOD (µM)	**0.1**	**nr**	**nr**	**3**
Detection Potential	**0.252V**	**0.5V**	**0.385V**	**-0.7V**
Detection time (minute)	**1**	**nr**	**20**	**40**
Referance	**[41]**	**[42]**	**[20]**	**Present work**

nr: not reported

Conclusions

This paper shows the first attempt to develop a biosensor for carotenoid pigments using a bioinspired approach that measures their photoprotective activity on a model alga strain. In accordance with previous works [39,43], the results of our amperometry/fluorescence based biosensing system confirm the strong correlation between zeaxanthin content and protection from

light stress in the D1-protein *Chlamydomonas* mutants. The present results suggest that in algae, astaxanthin exploits both filtering and antioxidant effects in different light conditions. The xanthophyll astaxanthin was tested as exogenous photoprotector of *Chlamydomonas* strains used as biorecognition elements of the biosensor, and showed its photoprotective activity in a μM range, with a limit of detection 3μM. The performance of the biosensor was additionally evaluated in extracted algae samples showing good recovery. The proposed multitransduction biosensor based on algae was novel, cheap and convenient for the evaluation of astaxanthin physiological effect and its detection. Moreover, the developed biosensor set-up could be extended toward monitoring of other physiological important chemicals with the employment of different microorganisms for biological, biomedical, environmental and agricultural research applications.

References

[1] J.B.K. Park, R.J. Craggs, A.N. Shilton, Wastewater treatment high rate algal ponds for biofuel production, Bioresour. Technol. 102 (2011) 35–42. doi:10.1016/j.biortech.2010.06.158.

[2] E. Erickson, S. Wakao, K.K. Niyogi, Light stress and photoprotection in *Chlamydomonas reinhardtii*., Plant J. 82 (2015) 449–65. doi:10.1111/tpj.12825.

[3] J. González-Cruz, C. Pastenes, Water-stress-induced thermotolerance of photosynthesis in bean (*Phaseolus vulgaris L.*) plants: The possible involvement of lipid composition and xanthophyll cycle pigments, Environ. Exp. Bot. 77 (2012) 127–140. doi:10.1016/j.envexpbot.2011.11.004.

[4] P. Jahns, A.R. Holzwarth, The role of the xanthophyll cycle and of lutein in photoprotection of photosystem II, Biochim. Biophys. Acta - Bioenerg. 1817 (2012) 182–193. doi:10.1016/j.bbabio.2011.04.012.

[5] Y. Yin, S. Li, W. Liao, Q. Lu, X. Wen, C. Lu, Photosystem II photochemistry, photoinhibition, and the xanthophyll cycle in heat-stressed rice leaves., J. Plant Physiol. 167 (2010) 959–66. doi:10.1016/j.jplph.2009.12.021.

[6] N.I. Krinsky, Carotenoids, In: Isler O, Guttman G, Solms U (ed). Birkhauser Verlag, Basel 23 (1979) 669-716.

[7] N.I. Krinsky, Carotenoid Protection Against Oxidation, Pure and Applied Chemistry. 51 (1979) 649-660.

[8] N.I. Krinsky, The biological properties of carotenoids, Pure and Applied Chemistry. 66 (1994) 1003-1010.

[9] L. Fan, A. Vonshak, A. Zarka, S. Boussiba, Does astaxanthin protect *Haematococcus* against light damage?, Zeitschrift Fur Naturforsch. - Sect. C J. Biosci. 53 (1998) 93–100.

[10] Z. Hu, Y. Li, M. Sommerfeld, F. Chen, Q. Hu, Enhanced protection against oxidative stress in an astaxanthin-overproduction *Haematococcus* mutant (Chlorophyceae), Eur. J. Phycol. 43 (2008) 365–376. doi:10.1080/09670260802227736.

[11] Z. Gao, C. Meng, X. Zhang, D. Xu, Y. Zhao, Y. Wang, et al., Differential Expression of Carotenogenic Genes, Associated Changes on Astaxanthin Production and Photosynthesis Features Induced by JA in H. pluvialis, PLoS One. 7 (2012) e42243. doi:10.1371/journal.pone.0042243.

[12] S. Franceschelli, M. Pesce, A. Ferrone, M.A. De Lutiis, A. Patruno, A. Grilli, et al., Astaxanthin treatment confers protection against oxidative stress in U937 cells stimulated with lipopolysaccharide reducing O2\n- production, PLoS One. 9 (2014) 1–9. doi:10.1371/journal.pone.0088359.

[13] W. Stahl, H. Sies, Bioactivity and protective effects of natural carotenoids, Biochim. Biophys. Acta - Mol. Basis Dis. 1740 (2005) 101–107. doi:10.1016/j.bbadis.2004.12.006.

[14] A. RAO, L. RAO, Carotenoids and human health, Pharmacol. Res. 55 (2007) 207–216. doi:10.1016/j.phrs.2007.01.012.

[15] Y. Yang, B. Kim, J. Lee, Astaxanthin structure, metabolism, and health benefits, J. Hum. Nutr. Food Sci. (2013) 1–11. http://www.j-scimedcentral.com/Nutrition/Articles/nutrition-1-1003.pdf.

[16] N.M. Lyons, N.M. O'Brien, Modulatory effects of an algal extract containing astaxanthin on UVA-irradiated cells in culture, J. Dermatol. Sci. 30 (2002) 73–84. doi:10.1016/S0923-1811(02)00063-4.

[17] P. Kidd, Astaxanthin Cell Membrane Nutrient with Diverse Clinical Benefits and Anti-Aging Potential, Alternative Medicine Review. 16 (2011) 355-364.

[18] G. Rea, A. Antonacci, M. Lambreva, A. Margonelli, C. Ambrosi, M.T. Giardi, The NUTRA-SNACKS Project: Basic Research and Biotechnological Programs on Nutraceutics, in: M.T. Giardi, G. Rea, B. Berra, eds., Bio-Farms for Nutraceuticals, Springer US, Boston, MA, 2010, pp. 1-16. doi:10.1007/978-1-4419-7347-4.

[19] V. Scognamiglio, A. Antonacci, L. Patrolecco, M. D. Lambreva, S. C. Litescu, S. A. Ghuge, et al., Analytical tools monitoring endocrine disrupting chemicals. TrAC Trends in Analytical Chemistry, 80 (2016) 555-567.

[20] R. Penu, S.C. Litescu, S. A. V. Eremia, I. Vasilescu, G.-L. Radu, M.T. Giardi, et al., Application of an optimized electrochemical sensor for monitoring astaxanthin antioxidant properties against lipoperoxidation, New J. Chem. 39 (2015) 6428–6436. doi:10.1039/C5NJ00457H.

[21] M.T. Giardi, V. Scognamiglio, G. Rea, G. Rodio, A. Antonacci, M. Lambreva, et al., Optical biosensors for environmental monitoring based on computational and biotechnological tools for engineering the photosynthetic D1 protein of *Chlamydomonas reinhardtii*., Biosens. Bioelectron. 25 (2009) 294–300. doi:10.1016/j.bios.2009.07.003.

[22] M.D. Lambreva, M.T. Giardi, I. Rambaldi, A. Antonacci, S. Pastorelli, I. Bertalan, et al., A Powerful Molecular Engineering Tool Provided Efficient *Chlamydomonas* Mutants as Bio-Sensing Elements for Herbicides Detection, PLoS One. 8 (2013) e61851. doi:10.1371/journal.pone.0061851.

[23] S. Preiss, S. Schrader, U. Johanningmeier, Rapid, ATP-dependent degradation of a truncated D1 protein in the chloroplast, Eur. J. Biochem. 268 (2001) 4562–4569. doi:10.1046/j.1432-1327.2001.02383.x.

[24] S.M. Newman, J.E. Boynton, N.W. Gillham, B.L. Randolph-Anderson, A.M. Johnson, E.H. Harris, Transformation of Chloroplast Ribosomal RNA Genes in *Chlamydomonas*: Molecular and Genetic Characterization of Integration Events , Genetics. 126 (1990) 875-888.

[25] G. Rea, M. Lambreva, F. Polticelli, I. Bertalan, A. Antonacci, S. Pastorelli, et al., Directed evolution and in silico analysis of reaction centre proteins reveal molecular signatures of photosynthesis adaptation to radiation pressure., PLoS One. 6 (2011) e16216. doi:10.1371/journal.pone.0016216.

[26] U. Johanningmeier, S. Heiss, Construction of a *Chlamydomonas reinhardtii* mutant with an intronless psbA gene., Plant Mol. Biol. 22 (1993) 91–9. http://www.ncbi.nlm.nih.gov/pubmed/8499620 (accessed January 13, 2016).

[27] H.K. Lichtenthaler, C. Buschmann, Current Protocols in Food Analytical Chemistry, John Wiley & Sons, Inc., Hoboken, NJ, USA, 2001. doi:10.1002/0471142913.faf0403s01.

[28] A.E. Solovchenko, O.B. Chivkunova, I.P. Maslova, Pigment composition, optical properties, and resistance to photodamage of the microalga *Haematococcus pluvialis* cultivated under high light, Russ. J. Plant Physiol. 58 (2011) 9–17. doi:10.1134/S1021443710061056.

[29] V. Scognamiglio, I. Pezzotti, G. Pezzotti, J. Cano, I. Manfredonia, K. Buonasera, et al., Towards an integrated biosensor array for simultaneous and rapid multi-analysis of endocrine disrupting chemicals, Anal. Chim. Acta. 751 (2012) 161–170. doi:10.1016/j.aca.2012.09.010.

[30] M.T. Giardi, G. Pezzotti, (2010) Patent n.0001372480

[31] K. Buonasera, M. Lambreva, G. Rea, E. Touloupakis, M.T. Giardi, Technological applications of chlorophyll a fluorescence for the assessment of environmental pollutants, Anal. Bioanal. Chem. 401 (2011) 1139–1151. doi:10.1007/s00216-011-5166-1.

[32] K. Buonasera, G. Pezzotti, V. Scognamiglio, A. Tibuzzi, M.T. Giardi, New platform of biosensors for prescreening of pesticide residues to support laboratory analyses., J. Agric. Food Chem. 58 (2010) 5982–90. doi:10.1021/jf9027602.

[33] I. Husu, G. Rodio, E. Touloupakis, M.D. Lambreva, K. Buonasera, S.C. Litescu, et al., Insights into photo-electrochemical sensing of herbicides driven by *Chlamydomonas reinhardtii* cells, Sensors Actuators B Chem. 185 (2013) 321–330. doi:10.1016/j.snb.2013.05.013.

[34] A. V. Ruban, Plants in light, Commun. Integr. Biol. 2 (2009) 50–55. doi:10.4161/cib.2.1.7504.

[35] I. Vass, Molecular mechanisms of photodamage in the Photosystem II complex, Biochim. Biophys. Acta - Bioenerg. 1817 (2012) 209–217. doi:10.1016/j.bbabio.2011.04.014.

[36] A. Mattoo, M. Giardi, Dynamic metabolism of photosystem II reaction center proteins and pigments, Physiol. Plant. 107 (1999) 454–461. doi:10.1034/j.1399-3054.1999.100412.x.

[37] C.H. Foyer, J. Neukermans, G. Queval, G. Noctor, J. Harbinson, Photosynthetic control of electron transport and the regulation of gene expression, J. Exp. Bot. 63 (2012) 1637–1661. doi:10.1093/jxb/ers013.

[38] N.J.M. Saibo, T. Lourenco, M.M. Oliveira, Transcription factors and regulation of photosynthetic and related metabolism under environmental stresses, Ann. Bot. 103 (2008) 609–623. doi:10.1093/aob/mcn227.

[39] E.-M. Aro, Book review: “Photoprotection, photoinhibition, gene regulation, and environment” edited by Barbara Demmig-Adams, William W. Adams III and Autar K. Mattoo (Vol 21 in the Series “Advances in photosynthesis and respiration” by Govindjee). Springer, The Neth, Photosynth. Res. 91 (2006) 91–93. doi:10.1007/s11120-006-9091-7.

[40] Y.G. Song, B. Liu, L.F. Wang, M.H. Li, Y. Liu, Damage to the oxygen-evolving complex by superoxide anion, hydrogen peroxide, and hydroxyl radical in photoinhibition of photosystem II., Photosynth. Res. 90 (2006) 67–78. doi:10.1007/s11120-006-9111-7.

[41] Y. Yue, Q. Liang, Y. Liao, Y. Guo, S. Shao, Electrooxidation behavior and electrochemistry determination method of the xanthophylls: Lutein in nonaqueous media, J. Electroanal. Chem. 682 (2012) 90–94. doi:10.1016/j.jelechem.2012.07.029.

[42] S. Buratti, N. Pellegrini, O. V. Brenna, S. Mannino, Rapid electrochemical method for the evaluation of the antioxidant power of some lipophilic food extracts, J. Agric. Food Chem. 49 (2001) 5136–5141. doi:10.1021/jf010731y.

[43] D. Han, Y. Li, Q. Hu, Astaxanthin in microalgae: Pathways, functions and biotechnological implications, Algae. 28 (2013) 131–147. doi:10.4490/algae.2013.28.2.131.

CHAPTER 4

“An optical biosensor based on a multiarray of enzymes for monitoring a large set of chemical classes in milk”

Silletti, S., Rodio, G., Pezzotti, G., Turemis, M et al. “An optical biosensor based on a multiarray of enzymes for monitoring a large set of chemical classes in milk”, Sensors and Actuators B: Chemical, 215 (2015); 607-617, DOI: 10.1016/j.snb.2015.03.092

Abstract

In this paper, we projected and realized a biosensor platform, which combines an optical system, intimately integrated with an array of biomediators able to provide a helpful tool for safety management of the milk. Optical feature selection of various enzymes was performed for monitoring compounds of various chemical classes and metabolic markers of cow's wellness. The detection of selected analytes was evaluated through biomediators of *C. reinhardtii* cells, and acetylcholinesterase, tyrosinase, urease, β-galactosidase and D-lactate dehydrogenase enzymes. The analyses were performed by fluorescence that for the algal cells was based on chlorophyll *a* fluorescence emission while for enzymes was guaranteed by the use of fluorescein 5(6)-isothiocyanate or 5(6)-carboxynaphthofluorescein. The LODs, reported with the units of EU legislation, were 1.1 ng/kg for diuron, 0.6 μg/L for chlorpyrifos, 1.2 μg/L for catechol, 13.8 mg/dL for urea, 0.06g/L for lactose, and 19.5 ppm for D-lactic acid.

1. Introduction

Milk is a staple food that poses several analytical challenges due to its “alive” nature and its position at the interface between the environment and the food chain. Milk quality and safety closely depend on the rearing management, including the farm environment [1, 2].

In Europe, food safety is conceptualized in the “from farm to fork” strategy and regulated by EU legislation, which set the maximum levels for various compounds in foodstuffs [3]. The development of sensors of safety for the presence of chemical pollutants and of quality for the presence of specific metabolites is useful to meet the need of daily milk monitoring performance from feed to pastures.

In order to guarantee the safety of milk, many studies have been focused on analytical methods to detect contaminants and the right step of the production chain in which to perform the analyses. Presently established analytical techniques to monitor chemicals in milk include high performance liquid chromatography (HPLC), gas chromatography-mass spectrometry (GC-MS), inductively coupled plasma mass spectrometry (ICP-MS), capillary electrophoresis, nuclear magnetic resonance (NMR), matrix-assisted laser desorption/ionization with time-of-flight mass spectroscopy (MALDI-TOFMS). Recently a method based on HPLC-tandem mass spectrometry and solid-phase micro extraction in mode headspace coupled to GC–MS has been developed and optimized through multivariate factorial design to determine residues of pesticides in cow's milk [4, 5, 6]. All those techniques require specialized personnel and laboratories.

To prevent problems of contamination at early stage of occurrence it is now important to realize sensors to minimize time and costs of analysis. In the case of biosensors it is possible to make an “early warning” analysis, determining levels of chemical components, comparing sample concentration to the legislative limit, allowing to carry out corrective actions directly during food production. Then, the sample needing further investigation can be directed to more detailed laboratory analyses by HPLC, GC and MS. The biosensor instruments have the advantage of being sensitive,

rapid, inexpensive and highly amenable towards microfabrication, specifically amperometry, potentiometry, impedance and optical based-biosensors [7, 8]. Indeed, several biosensors have been developed as alarm systems for milk monitoring, able to provide information about a single analyte, if present alone, or an indication of total analytes in a real sample. Potentiometric biosensors have been used to monitor urea and lactose in milk [9, 10, 11]. Fluorescence immunosensors have been developed to monitor melamine, a 2,4,6-triammino-1,3,5-triazine with various industrial applications, that has been found as adulteration product in dairy infant formulas to fraudulently increase the apparent protein content [12, 13, 14].

Unfortunately, the number of possible contaminants is enormous and it is difficult to use a specific biosensor for each chemical compound. Thus, there is a need of techniques that can recognize several classes of contaminants at the same time. The development of a biosensor based on an array of different biological recognition elements, able to monitor a wide range of compounds, and the employment of a transduction system integrated together to create a bio-sensing platform, could be an useful strategy to overcome this problem.

Few electrochemical and optic array-based biosensors for simultaneously analysis of multiple samples and multiple analytes have been developed demonstrating the feasibility of this approach. For example, a biosensor array for direct detection of various organophosphates using as biorecognition elements modified organophosphorus hydrolase, and a sol-gel optical-array based biosensor for the simultaneous analysis of multiple markers for Alzheimer's disease have been realized [15, 16]. A biosensor array for in situ monitoring of metabolites in U937 cell cultures has been also reported [17].

With reference to the quality of the farm environment, pesticides may represent a good parameter for monitoring purposes since dairy cows can be exposed through contaminated water and forage. Among these compounds, phenyluree, triazines, organophosphorus and phenolics compounds are highly diffused in feeds [18, 19].

Contamination in milk is complex to monitor, because it can occur at different stages of milk production chain, such as in the farm or during the transport. For detection of some milk pathogens, a few electrochemical biosensors have been already developed [20, 21]. It is known that many microbial contaminations can cause diseases on cows that in turn modify the presence of milk metabolites. One of the most important cow disease that influences milk quality and production is the mastitis, a major endemic disease of dairy cattle, causing an inflammation of the mammary gland and of udder tissue. Milk produced by cows with mastitis has significant changes in protein amount and composition and in general, a higher urea concentration and lower lactose concentration of that produced by healthy cows. Lactic acid concentration is also an important parameter indicating the quality and freshness of milk and its derivatives.

In this paper, we projected and realized a biosensor platform, which combines an optical system, intimately integrated with an array of biomediators able to monitor compounds of various chemical classes to provide a helpful tool for quality and safety management during milk production. We selected fluorescence activity as transducer since it could allow analyses on line through fluidic systems. Being milk a complex mixture of various reactive fat globules, salts, proteins, vitamins, and bioactive substances, the main challenge was to overcome its cross interaction with the biomediators. The other challenge was to find suitable conditions to guarantee fluorescence emission by means of the fluorophores used, that was analyzed during the time from milliseconds until minutes for the various biomediators.

2. Materials and methods

2.1. Chemicals

The following chemicals were obtained from Sigma-Aldrich: diuron (3-(3,4-dichlorophenyl)-1,1-dimethylurea); acetylcholinesterase from *Electrophorus electricus*; acetylthiocholine chloride; tyrosinase from mushroom; catechol (1,2-dihydroxybenzene); urease from *Canavalia ensiformis*;

urea; β-galactosidase from *Aspergillus oryzae*; lactose anhydrous; D-lactate dehydrogenase from *Lactobacillus leichmanii*; D-lactic acid; 5(6)-carboxynaphthofluorescein; FITC (fluorescein 5(6)-isothiocyanate). Chlorpyrifos (O,O-diethyl-O-3,5,6-trichloropyridin-2-yl phosphorothioate) was obtained from Fluka. For the analyses, products from "Centrale del Latte di Roma" were used; for all experiments whole milk was tested while for experiments with β-galactosidase skimmed milk was used.

2.2. Algal biomediator

Cultures of *C. reinhardtii* strain were grown in liquid Tris–Acetate-Phosphate (TAP) medium pH 7.2 at 50μmol photons $m^{-2}s^{-1}$ light intensity, 25ºC temperature and under gently stirring. For fluorescence measurements, Chlamydomonas cultures containing equal quantity of cells (Abs_{750}=1) in each test were incubated with milk (ratio 1:1) and subsequently with herbicide. Fluorescence measurements were carried out after 10min of incubation in the dark. The fluorimeter biosensor device gives inputs of 500μmol photons $m^{-2}s^{-1}$ of red light at 650nm for 11s, provided by 4 LEDs, and measures the fluorescence emission by photodiodes at 680 nm, resulting in highly reproducible measurements averaged over 1000 points. The sensor allows determination of main chlorophyll fluorescence parameters. In order to determine the fluorescence variation in the presence of herbicide, the parameter [1-Vj] was considered that corresponds to $(Fj-F_0)/(Fm-F_0)$, with Fj the fluorescence at step J related to a variation of the slop correlated to the degree of oxidation of the photosynthetic electron acceptor Q_A. F_0 is the basal fluorescence and Fm is the maximum fluorescence. Comparisons among the samples were enabled by normalizing the chlorophyll fluorescence and calculating the relative variable fluorescence [1−Vj] at any given time [22, 23].

2.3. Acetylcholinesterase

In order to use acetylcholinesterase (E.C. 3.1.1.7) as biomediator for the optical biosensor it was necessary to label the enzyme by FITC fluorophore. The labeling protocol requires the solubilization of 0.5mg of FITC in 50µl of DMSO, then the solubilization of 1mg of acetylcholinesterase in 0.5ml of 0.1M $NaHCO_3$ pH 9 and addition drop wise of the solubilized protein to the fluorophore. Then, incubation of the mix at 37°C for 1h in the dark, in order to prevent light exposure of the fluorophore. After equilibrating the column Sephadex G Biogel P with 30 ml of 2mM PBS pH 8, add drop wise the mix protein fluorophore into the column and 2mM PBS pH 8. Collect fraction of about 0.5ml and verify by spectrophotometer the presence of the conjugate protein-FITC by analyzing the spectrum between 220 and 550nm. To determine labeling efficiency, after column separation and before using labeled enzyme in fluorimetric assays, the degree of labeling (DOL) was calculated by the following formula: $DOL = (Amax\ (dye) * MW(prot)/)/[prot] * \varepsilon\ dye$ where A_{max} is the maximum absorbance of fluorophore, MW is the protein molecular weight, ε dye is the molar extinction coefficient of FITC and [prot] is the protein concentration. Protein concentration is calculated by $A = \varepsilon * C$, where A is the absorbance, C is the protein concentration and ε is the protein molar extinction coefficient. For an optimal labeling, DOL value should be as close as possible to one. A stock of 15mM of acetylthiocholine chloride was prepared solubilizing 6mg into 1ml 2mM PBS pH 8. The reaction mix was prepared using 9µl of labeled protein with ABS_{280nm}=1. Thus, 20µl of 5mM acetylthiocoline in 250µl of milk in buffer 2mM PBS pH 8 was added to get the total volume of 500µl. For organophosphorus detection, a stock of 1.4µM chlorpyrifos was prepared in 50% EtOH. Measurements were performed after 10min of dark and 11s of excitation light by blue LEDs (excitation wavelength at 470nm).

2.4. Tyrosinase

In order to use tyrosinase (E.C. 1.14.18.1) as biomediator for the optical biosensor, it was necessary to use FITC as fluorophore. The labeling protocol used is as described before. The reaction mix was incubated 10min in the dark with added catechol and the measurements were performed by 11s of light provided by blue LEDs of excitation wavelength at 470nm.

2.5. Urease

For using urease (EC 3.3.1.5) as biomediator in the optical biosensor, for each measurement 20U of urease was solubilized in 0.1M PBS pH 4.5. The reaction mix was prepared using 100µl of protein above, 25µl of 3.2 µM 5(6)-carboxynaphthofluorescein, 125µl of 0.14M PBS pH 4.5. Measurements were performed after 10min of dark, by 11s of excitation light provided by yellow LEDs with wavelength at 595nm.

2.6. β-galactosidase

The experiments performed with β-galactosidase (EC 3.2.1.23) required FITC as fluorophore and the labeling protocol used was the same reported for acetylcholinesterase. For experiments performed in buffer a stock of 10g/L of lactose was prepared in 0.1M of PBS pH 4.5. The reaction mix was prepared using 50µl of protein with ABS_{280}=1 corresponding to 1.25 U and the 0.1M of PBS pH 4.5 buffer, to get the total volume of 500 µl. To this mix, lactose concentrations between 0.1 and 1g/L were added. For experiments with milk, the mix reaction was prepared using 100µl of labelled protein corresponding to 2.5U, with ABS_{280} =1 and buffer 0.1M of PBS pH 4.5 to get the total volume of 500µl. Measurements were performed after 10min of dark and 11s of light by blue LEDs (excitation wavelength at 470nm).

2.7. D-lactic dehydrogenase

To use D-lactic dehydrogenase (EC1.1.1.28) as biomediator, the reaction mix was prepared using 20µl of 7U/ml of enzyme, 15µl of fluorophore 5(6)-carboxynaphthofluorescein with a concentration of 1mM and 90µl of 75mM PBS pH 8.9. The measurements were performed after 10min of dark incubation with D-lactate (from D-lactic acid, pka 3.86) and 11s of light excitation provided by yellow LEDs with excitation wavelength at 595nm.

2.8. Statistical analyses and LODs

All statistical tests were performed by analysis of variance (ANOVA) of measurements carried out in triplicate and the statistical significance of differences was evaluated by P-level≤0.05. The values were calculated by comparing fluorescence values in a biomediator incubated with or without milk, and in addition with or without analytes with respect to the control.

For enzymes, the LODs were calculated from calibration curves by using the formula 3.3 x (SD of intercept/slope). The limit of detection for diuron was determined on the basis of 99% confidence interval, which assuming the normal distribution corresponds to 2.6 x standard error of the measurement (σ). LOD was calculated as = 2.6 x σ x I_{50}/(100-2.6 σ) as described by Maly et al. [24].

2.9. Multi-array biosensor-setup

The developed sensor is a multi-array fluorimeter able to recognize florescence emitted during time by various biological elements hosting various excitation light sources (red, yellow and blue LEDs, Kingbright, Taiwan) (**Fig. 1**). It is composed of 6 cells for contemporary measurements on the same milk sample. The optical module is designed according to the strict requirements of matching the geometry and the mechanical features of the cell **(Fig. 1).** The measurement cell is made of inert black Delrin. A set of LEDs (Ø 3 mm) with the appropriate excitation wavelengths are mounted in each well in order to provide a flexible excitation and fluorescence emission measurement for the

biologic compounds. A high-pass filter (Ferroperm optics, Denmark) is coupled to each silicon photodiode (Hamamatsu, Japan) to capture only the spectral range where the fluorescence signal is emitted. The optical head can measure the emitting fluorescence within an area of 5 mm^2 for each well. The optical measurements are performed contemporaneously and independently in each well. The interaction with the species contained in the milk sample occurs in a dynamic mode. The solution flows into each well through some small holes in the chamber in order to mix with the biomediator through mixture valves (Sirai, D301V51-Z031A Ø 1.5 V 12 cc).

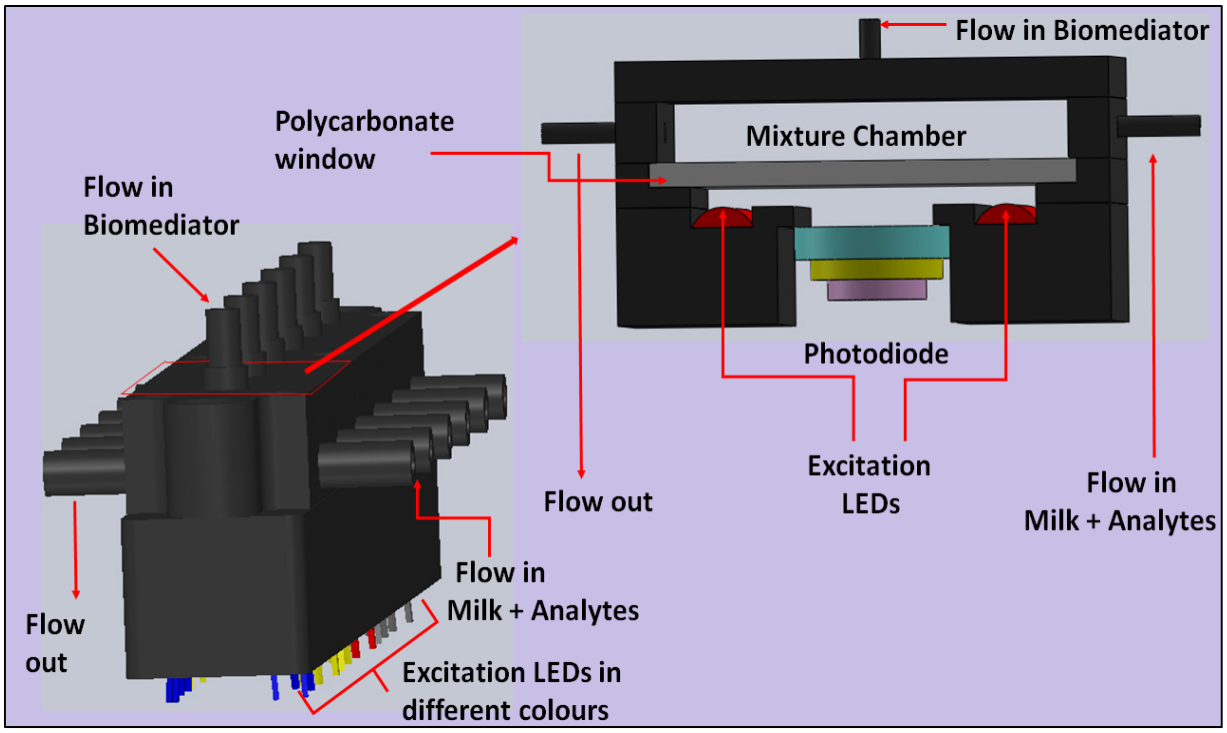

Fig. 1. Scheme of the sensor together with the cells and workflow of on-line measurement and principle of fluorescence measure.

The flow is supplied through tubes of 2mm diameter, by a rotary peristaltic pump of 30×40mm (fabricated in house) with adjustable speed from 100 up to 350µ/min. The pump performs the filling and the discharge of liquids and the air for wells drying. The device is also supplied by a system designed to perform a proper cleaning into the measurement cell, to remove any biological or

chemical material deposited on the surface, and enable compliance with minimum requirements for sterilization.

The electronic control board mounted inside the instrument includes a microcontroller (STMicroelectronics, Italy) for the automatic management of the fluidic system, the LED drivers, pre-processing signal conditioning module for amplification and filtering, timer and flash memory card for data storage in-field applications. The sensor works in a continuous mode and all detected data are stored and transmitted to the computer by a USB cable connection. The sensor modules are modular and easily replaceable to widen the possible application range, while the electronics is fixed, with degrees of freedom in terms of programming the measurement times, amplification range and LED intensity, flow speed, according to the used biologic material and optical heads.

3. Results and discussion

The device was developed in order to obtain a configuration that enables the contemporaneous monitoring of various analytes important for the assessment of milk safety and quality. In **Fig. 1**, the scheme of the biosensor is shown, while the fluorophores used with the relative wavelengths of excitation and emission are reported in **Table 1**.

Attention was focused on the classes of photosynthetic directed herbicides such as triazines and phenyluree, organophosphorus pesticides and phenolic compounds. For pesticides analyses we selected 3 chemicals (diuron, chlorpyrifos, and catechol) which are repeatedly reported in EU legislations (Reg. 852/853/854/882/2004). Moreover, we selected metabolites that can be present in an unusual range in case of cow mastitis such as urea, lactose and lactic acid.

Table 1. List of biomediators and relative fluorophores, with the details of the array of the cells, the specific LEDs color and the wavelengths of excitation (Ex) and emission (Em) for the relative biomediators.

Biomediators	**Fluorophores**	**Cells**	**LED for Ex**	**Wavelength setting (nm)**	
				Ex	**Em**
Algae	Autofluorescent through Chl *a* fluorescence emission	**1**	**red**	**630**	**730**
Urease	5-(6)-Carboxynaphthofluorescein	**2**	**yellow**	**595**	**655**
D-Lactic dehydrogenase		**3**			
Acetyl-cholinesterase	Fluorescein 5-(6)-isothiocyanate	**4**	**blue**	**470**	**510**
β-Galactosidase		**5**			
Tyrosinase		**6**			

A preliminary screening was performed among enzymes to select biomediators that can provide selectively the content of the reported analytes through specific reactions as reported in **Table 2** and in the following sections. In this context, the use of microorganisms, like algae, and macromolecules, like enzymes, represents a crucial approach in multi-response bio-sensing system design (**Table 2**).

Table 2. List of selected analytes and relative biomediators with indication of their mechanism of recognition.

Analytes	**Mechanism of Recognition**
Triazine, phenyluree	Algal Q_A/Q_B photosynthetic electron flow inhibition by herbicides by binding of these pesticides to the D1 protein of PSII and modification of fast chlorophyll *a* fluorescence in the microseconds
Organophosphorus	Acetylcholinesterase causes acetylcholine hydrolysis into acetic acid and choline. These pesticides act blocking irreversibly the activity of the acetylcholinesterase enzyme, determining acetylcholine accumulation
Phenolic compounds	Tyrosinase induces the oxidation of phenols using oxygen. In the presence of catechol, benzoquinone is formed and hydrogens removed from catechol combine with oxygen to form water
Urea	Urease belongs to hydrolase enzyme family and catalyzes the hydrolysis of urea to form ammonia and carbamate
Lactose	β-galactosidase enzyme is involved in the hydrolysis of the disaccharide lactose into constituent galactose and glucose monomers
D-Lactic acid	D-Lactic dehydrogenase is a NAD^+ dependent enzyme catalyzing the conversion of D-lactic acid into pyruvate with production of NADH and H^+

The difficulty encountered was to find the conditions that would allow detecting the fluorescence signal in milk; in fact, the first problem is its white color that can reflect light, secondly being a complete food it constitutes a complex matrix that can cross interact with enzymes and/or the fluorophores. For experiments with the unicellular algae *C. reinhardtii*, the optical detection is guaranteed by the auto fluorescence generated by the chlorophyll *a* fluorescence emission (**see Fig. 2**).

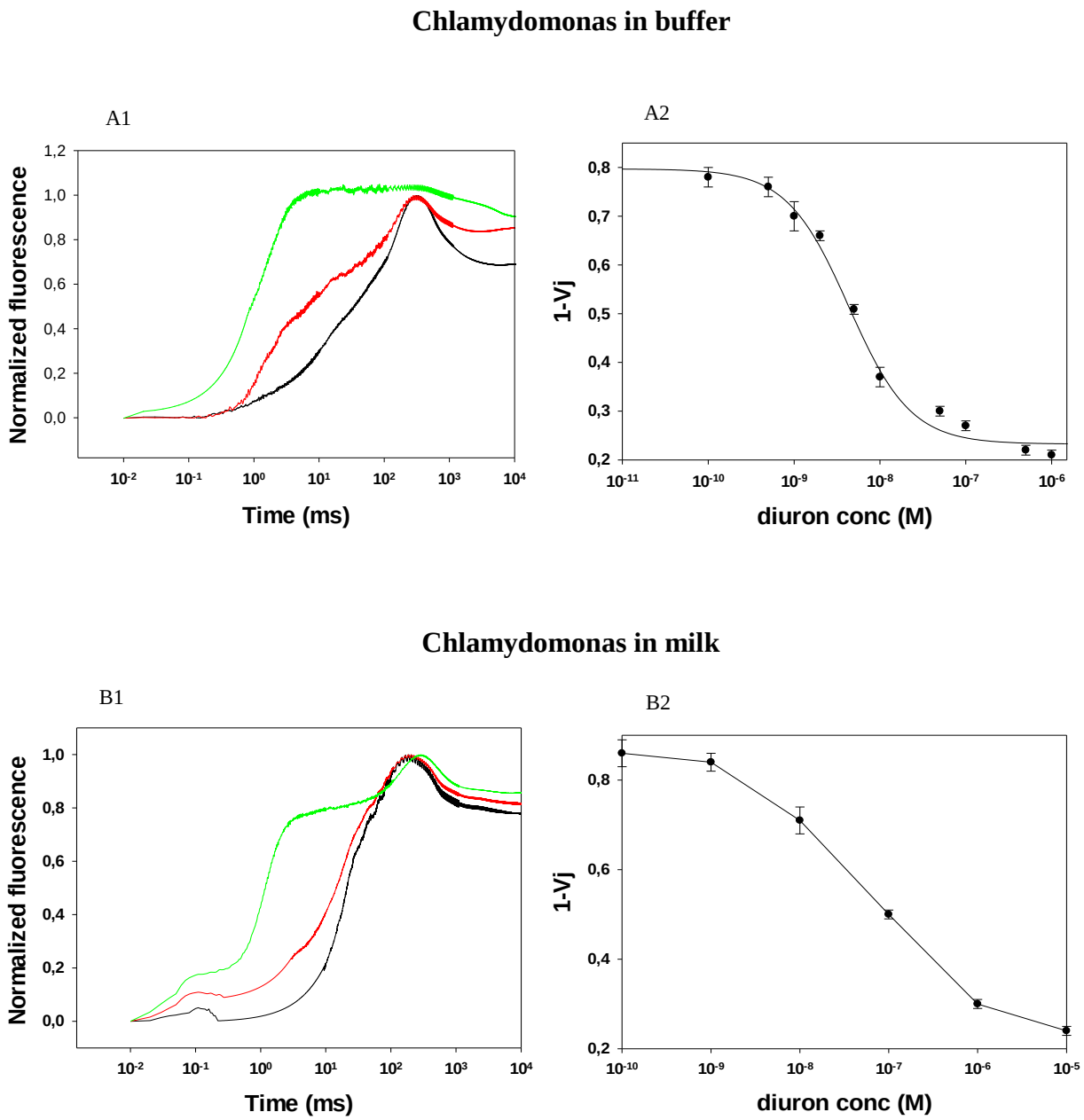

Fig. 2. Data obtained in experiments with unicellular algae *C. reinhardtii* and diuron. (A) Measurements in buffer. (B) Measurements in 50% milk. (1) Fluorescence curves obtained at various diuron concentrations: black without pesticide; red, 10^{-9} M and green, 10^{-6}M of diuron. (2) The points represent the averages of the parameter [1-Vj] = 1-(Fj-F0)/(Fm-F0) calculated for each pesticide concentration. The experiments were performed three times for each concentration and standard error bars are shown for all values. Instrument setting: 10min of dark, red LEDs, 11s of excitation light with intensity of 500µmol photons $cm^{-2}s^{-1}$.

While in order to monitor enzymatic reactions by fluorescence emission, the enzymes were coupled with FITC or 5(6)-carboxynaphthofluorescein, which are environment-sensitive fluorescence probes.

FITC binds proteins stably being able to establish a covalent bond between the thiocyanate radical and the primary amino groups of proteins. Instead the 5(6)-carboxynaphthofluorescein is a dual emission ratiometric pH probe that is functional at near-neutral conditions (pKa=7.6). In its acidic form, this compound absorbs and fluoresces at 509nm and 572nm, respectively. Its basic form has a red-shifted absorption and emission with maxima peaks at 598 and 668nm, respectively [25]. **Figure 3** shows typical fluorescence emission for the enzymes acetylcholinesterase and urease both in buffer and in milk.

In order to determine the progress of the enzymatic reactions, the first experiments were performed spiking the analytes in buffer. Then, experiments were carried out to determine the conditions that can avoid the cross interference caused by milk.

The multi-array biosensor is conceived as an alarm system for possibly revealing the concentrations of the reported analytes on the limits indicated by European legislations. Thus, the limits reported by those regulations were used to identify a range of concentrations under analyses that can be quite narrow, as for urea and lactic acid concentrations (see **Table 3**).

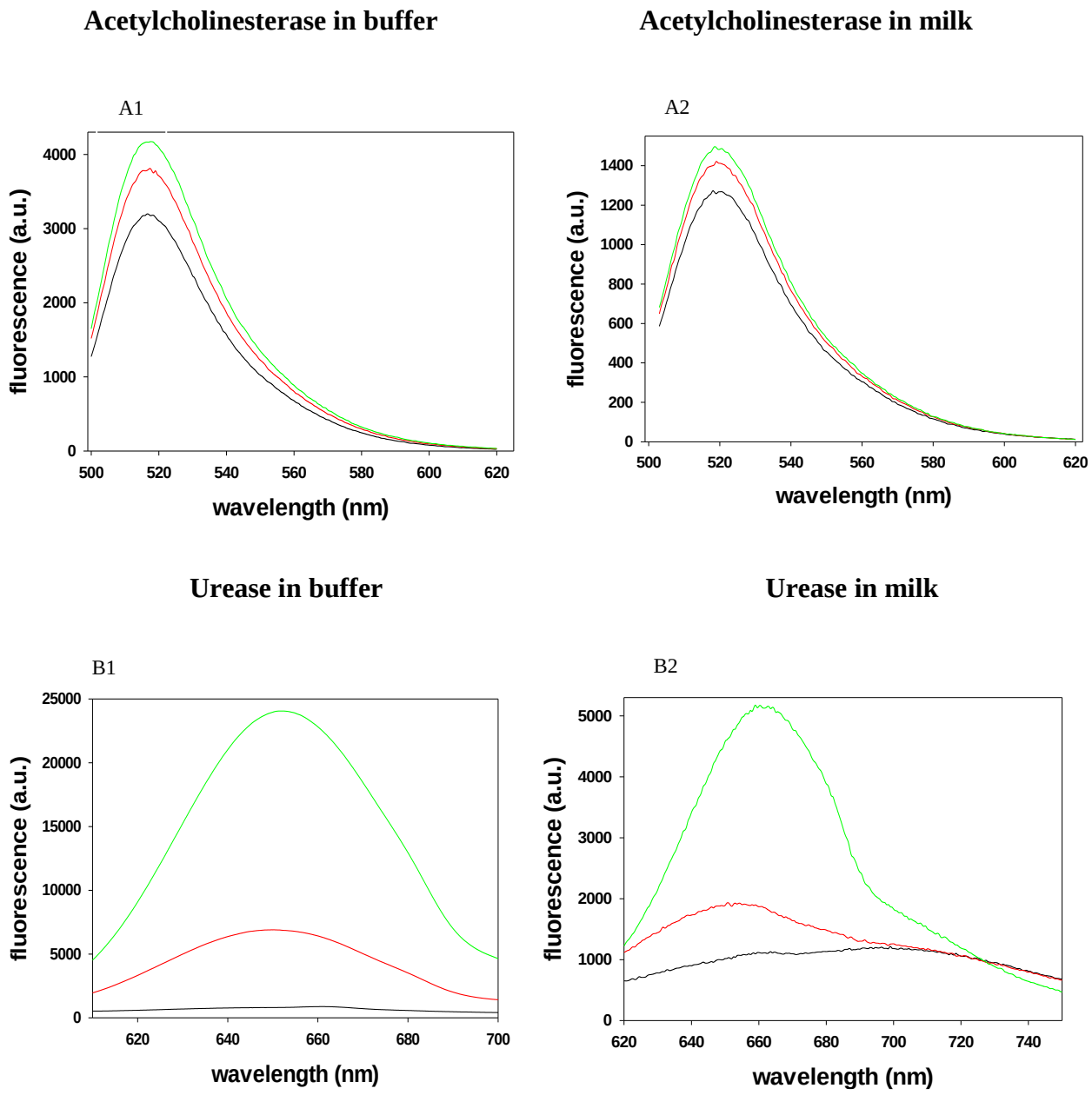

Fig. 3. (A) Fluorescence curves of acetylcholinesterase and chlorpyrifos; (B) urease and urea. (1) Measurements in buffer. (2) Measurements in 50% of milk. Chlorpyrifos concentrations: black, without chlorpyrifos; red, 2.8×10^{-9}M and green, 8.5×10^{-9}M. Urea concentrations: black, without urea; red 24mg/dL and green 30mg/dL of urea.

Table 3. Analytical quality parameters corresponding to the multi-array-based biosensor and standard laboratory analysis. The experiments were performed in 50% milk (Centrale del latte di Roma) with the exception of β-galactosidase that was used in buffer adding skimmed milk of the reported range. Limit of detection LOD calculated by 5 repetitive experiments and relative standard deviation RSD calculated on the slope of working range (WR). LOD for diuron was calculated according to Maly et al. [24] and for enzyme based-biosensors from calibration curves by using the formula 3.3 x (SD of intercept/slope). The limits* are indicated with the same units of measure reported by the EU regulations. LSI**: for algae analysis, spectrofluorimeter Hansatech FMS2, for enzymes: Jasco PF-8200.

Analyte	Limits EU *	Tested range	Em time	LODs					
				MULTI-BIOS	RSD	LSI**	RSD	Linear ranges	Detected in milk
Diuron	0.05-0.1 mg/kg	$0.02x10^{-3}$-2 mg/kg	10 msec	1.1 ng/kg (4.8pM)	5.6	1µM	10	1 nM-1 µM	Spiked
Chlorpyrifos	1 µg/L	0.5-3 µg/L	10 min	0.6 µg/L (1.7nM)	3.7	20nM	2	1.4-8.5nM	
Cathecol	0.02-0.05 µg/kg	0.02-0.06 µg/kg	10 min	1.2µg/kg (9.3nM)	0.5	5 µM	3	5-25nM	
Urea	23-35 mg/dL	12-36 mg/dL	5 min	13.8mg/dL (2.3mM)	4.7	2 mM	6	2.2-6.4mM	25mg/dL
Lactose	45-50 g/L	0.09-1 g/L	5 min	0.06 g/L (170µM)	2.6	120 µM	5	96-576µM	46g/L
D-Lactic acid	30 ppm	15-45 ppm	5 min	19.5ppm (220µM)	4.9	110 µM	5	166-581µM	28ppm

3.1. Algal mechanism for detection of herbicides

Photosynthetic herbicides like triazines and phenyluree are used massively particularly in the maize crops and in addition to acute toxicity from high exposure levels there is concern for their long-term effects such as having endocrine disruptor activity and contributing to Parkinson's disease [23, 26-28]. Therefore, their level in the farm environment is useful as safety management indicator.

For their detection, whole cells of the green alga *C. reinhardtii*, a single-cell bi-flagellated green alga of about 10μm in diameter, were employed. Photosynthetic microalgae are among the most preferred microorganisms for environmental monitoring and screening of food and agricultural products for hazard compounds [29, 30, 31]. The unique features and structural constituents of the photosynthetic systems make them a suitable sensing element in the emerging biosensoristic field mainly due to their ability to conduct charge separation and electron transfer sensitive to the presence of different classes of herbicides [22].

These toxic substances can be straightforwardly detected by photosystem II in few minutes of incubation with the sample, since the presence of herbicides is easily detectable by the rapid decline of the plastoquinone (Q_A) re-oxidation rate reflected by changes in the chlorophyll *a* fluorescence [23, 32]. Thus, the response of the selected strains to photosynthetic herbicides was studied by the chlorophyll fluorescence induction curves (**Fig. 2**).

As previously shown, the accumulation of reduced forms of Q_A is proportional to the herbicide concentration and can be directly evaluated by the increase of the variable fluorescence level at point *J* (Vj), making the value [1-V_J] one of the most sensitive parameter for herbicide toxicity detection [23]. Measurements with a range of herbicide concentrations (diuron is reported in the figure) between 10^{-10} and 10^{-6}M were performed. These experiments show that the presence of diuron, both in buffer and milk, determines a decrease of the [1-Vj] value (see **Fig. 2**).

3.2. Acetylcholinesterase mechanism for detection of organosphosphorus pesticides

Organophosphorus compounds are used in massive way in Europe for pest control, not only in agriculture but also in gardening. They act irreversibly blocking the activity of the acetylcholinesterase enzyme, determining acetylcholine accumulation, harmful for children that are more sensitive to these substances in respect to adults [33, 34, 35]. Chlorpyrifos is one of the organophosphorus most commonly used in agriculture. The safe limit for organophosphorus compounds in water is set to 1µg/L.

Firstly, the carboxynaphthoflurescein was coupled to acetylcholinesterase enzyme in order to sense the pH variation of the solution due to the hydrolysis of the acetylthiocholine into choline and acetic acid. In the presence of organophosphorous compounds, the enzyme activity was inhibited since they covalently block the active site of acetylcholinesterase. This irreversible inactivation leads to an accumulation of acetylcholine and to a variation of pH. Consequently, the pH variation led to a fluorescence variation of the fluorophore that can be correlated to pesticide concentration [36]. However, the analyses performed indicate a good correlation between pesticide concentration and fluorescence variation only in buffer, while in the case of milk no fluorescence emission change was observed varying concentration of analyte (data not shown). Thus, more experiments with acetylcholinesterase were performed using FITC as fluorophore. When pesticide is added, the FITC-labeled acetylcholinesterase shows an increase in fluorescence emission indicating that the binding of pesticide to the enzyme probably determines a conformational change [27]. The results obtained in these experiments show that the presence of chlorpyrifos in the range tested determines an increase of fluorescence emission (data not shown). In milk, fluorescence variation, although significant, results lower compared to the experiments performed in buffer, probably due to the shield effect of milk (**Fig. 4A**).

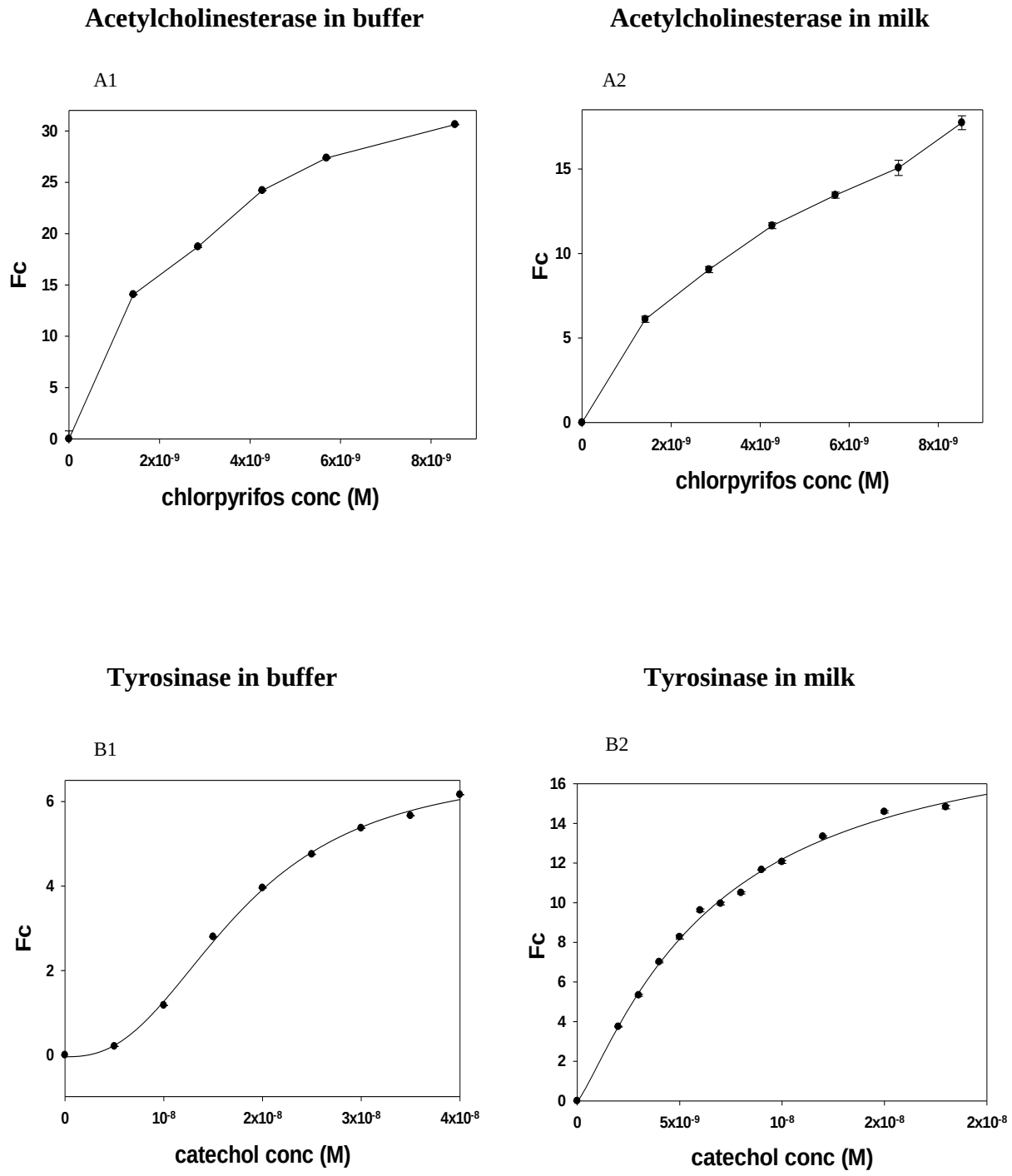

Fig. 4. (A) Experiments with acetylcholinesterase and chlorpyrifos; (B) experiments with tyrosinase and catechol. (1) Measurements in buffer. (2) Measurements in 50% of milk. The points represent the averages of the maximum fluorescence values for each pesticide concentration calculated as Fc = [(F-F0)/F0)x100]. The experiments were performed three times for each concentration with standard error bars shown for all values. Instrument setting: 10 min of dark; LEDs bleu, 11s of light with intensity of 400µmol $cm^{-2}s^{-1}$.

3.3. Tyrosinase mechanism for the detection of phenolic contaminants

Presence of phenolic compounds in the environment is due to their massive use in many application fields as important raw materials and additives for industrial purposes in laboratory processes, chemical industry, chemical engineering processes, wood processing and plastics processing.

They include substances, like bisphenol A and 4-nonylphenol, whose presence and persistence in the environment may cause serious damage to human health. The catechol, the precursor of phenolic compounds used in this work as analyte, is highly consumed (50%) in the production of phenolic pesticides (e.g., nitrophenols, halophenols), the rest being used as a precursor to fine chemicals such as perfumes and pharmaceuticals. European Legislation has established that the maximum concentration of phenolic compounds in food should not exceed the limit value of 0.02-0.05mg/kg. Tyrosinase is a cuproproteic oxidoreductase that catalyzes sequential oxidation steps of phenolic substrates to the respective quinones [37].

Fluorescence was provided by FITC with the same method of labeling indicated for acetylcholinesterase. The experimental results obtained show that 10min after catechol addition, there is a decrease of fluorescence emission that is correlated to the pesticide concentration. The graphs of **Fig. 4B** show Fc absolute values.

3.4. Quality of milk production checked as content of urea, lactose and lactic acid

As previously mentioned, the safety and quality of milk are correlated with cow health. Chemical contaminants may indirectly increase the vulnerability to mastitis through the disruption of the endocrine and immune systems. In its turn, mastitis may affect the excretion of contaminants in milk [38]. Animals with mastitis produce milk of poorer quality and may be identified through the unusual production of metabolites such as great quantity of urea and lactic acid and low amount of lactose.

3.4.1. Urease for analyses of urea content

Urease belongs to hydrolase enzyme family and catalyzes the hydrolysis of urea to form ammonia and carbamate. It is produced by bacteria, fungi, yeast and plants where it catalyzes the urea degradation in order to supply these organisms with a source of nitrogen for growth [39]. Urea is a metabolite produced in liver and kidneys from ammonia, deriving from the degradation of crude proteins in the rumen with a concentration in healthy cows between 23 and 35mg/dL. High concentrations of urea generally accompany typical pathologies of hyperammonaemia (metabolic alkalosis, reduced fertility, lameness, etc.) determining negative quality characteristics. Lower levels of urea in milk are often the result of insufficient protein intake in the diet [40].

Urea concentration in milk was determined using urease with fluorescent probe 5-(6)-carboxynaphthofluorescein, able to sense the pH variation of the solution due to urea hydrolysis. Consequently, the pH variation can led to a fluorescence variation of the fluorophore that can be correlated to urea concentration (**Fig. 5A**).

Urease in buffer **Urease in milk**

A1 A2

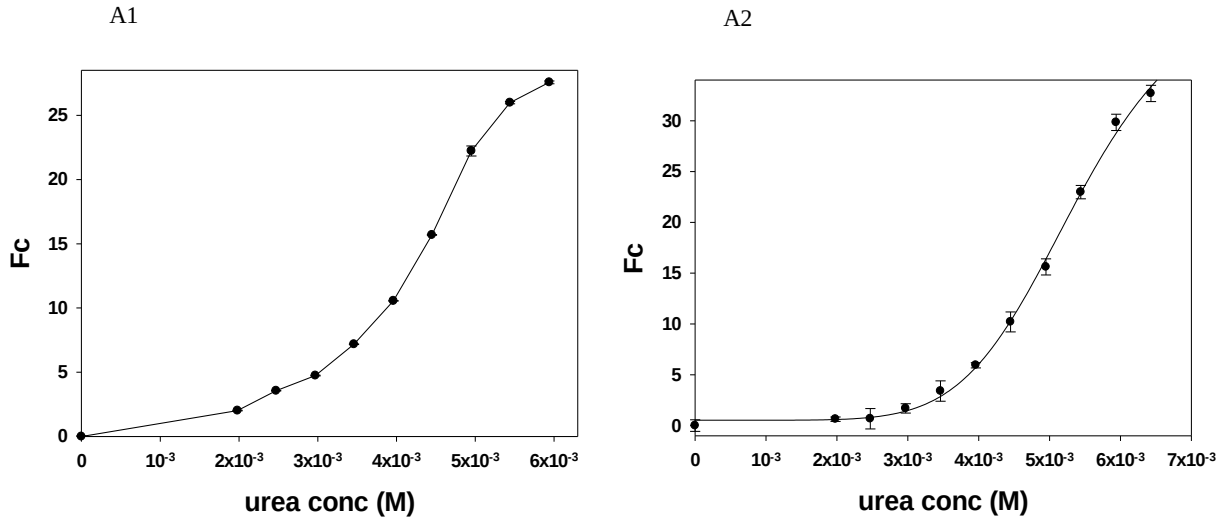

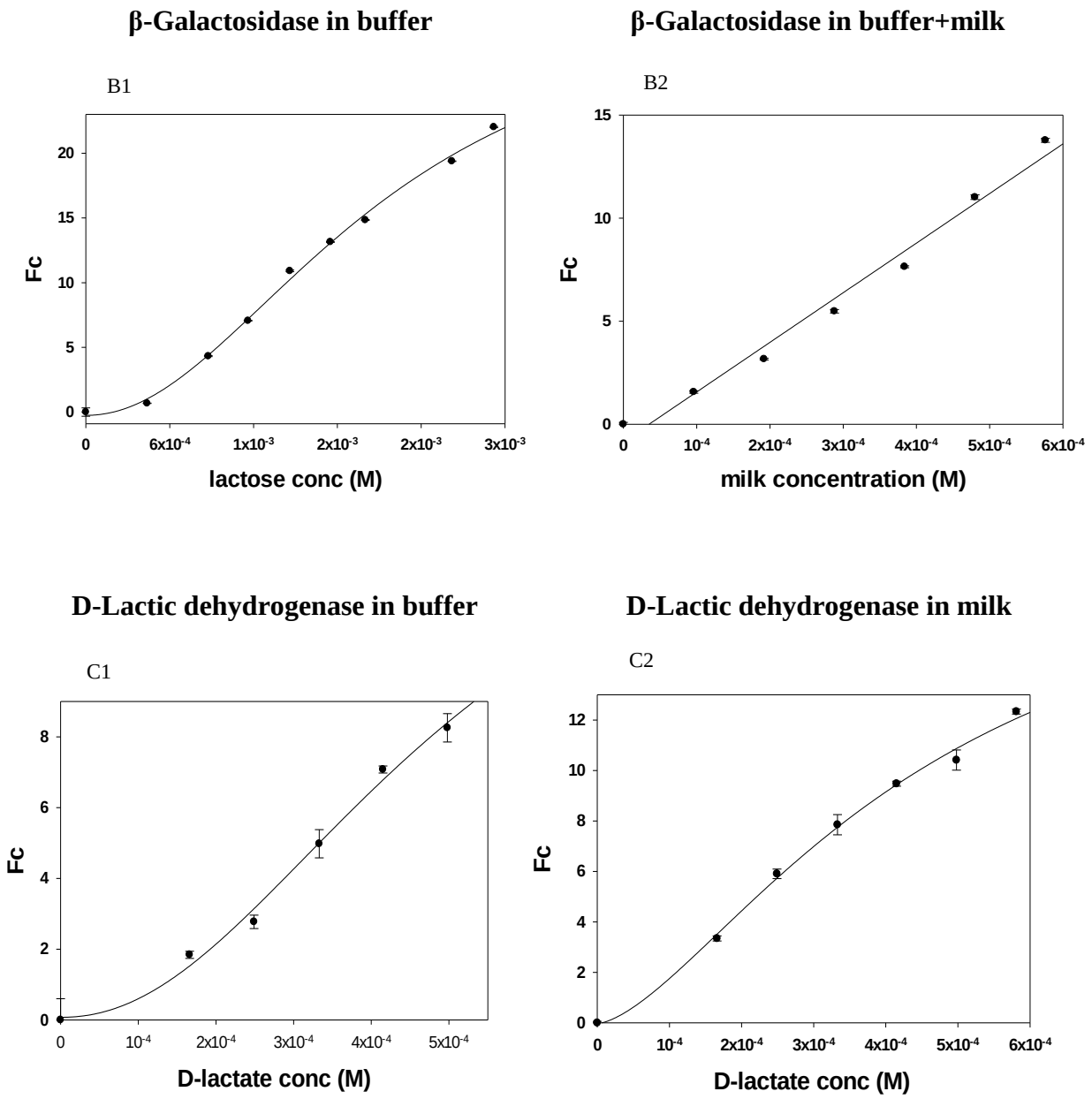

Fig. 5. (A) Experiments with urease and urea; (B) experiments with β-galactosidase and lactose; (C) experiments with D-lactic dehydrogenase and D-lactic acid. (1) Measurements in buffer. (2) Measurements in buffer plus milk. The points represent the averages of the maximum fluorescence values for each analyte concentration calculated as Fc = [(F-F0)/F0) 100]. The experiments were performed three times for each concentration with standard error bars shown for all values. Instrument setting, for urease and D-lactic dehydrogenase: 10min of dark, LEDs yellow, 11s of excitation light with intensity of 100µmol $cm^{-2}s^{-1}$, for β-galactosidase: 10min of dark, LEDs bleu, 11s of excitation light with intensity of 400µmol $cm^{-2}s^{-1}$.

To overcome the problems due to milk interference, buffer concentration used to dissolve the enzyme and the fluorophore was quite increased compared to that for buffer measurements (see section 2.5). The relationship between urea concentration and fluorescence describes a sigmoidal dose response curve, both in buffer and milk. Using the urea concentrations reported in **Table 3**, small but significant variations in fluorescence were obtained. In **Fig. 5A**, it is possible to observe that increasing substrate concentration there is an increase of the fluorescence signal.

3.4.2. β-Galactosidase for analyses of lactose

Lactose is the disaccharide representing the 98% of total carbohydrates present in milk, composed by glucose and galactose linked by a β-1,4 bond. Cow milk has a lactose concentration between 45 and 50g/L, values conserved for all cow types. Drastic reduction of lactose occurs in milk only in case of mastitis [40].

Enzymatic hydrolysis of lactose by β-galactosidase is one of the most popular technologies to produce lactose-reduced milk and related dairy products for consumption by lactose intolerant people. β-galactosidase is widely used in food industry to improve sweetness, solubility, flavor and digestibility of dairy products [41, 42]. For the optical detection system, FITC was used as fluorophore. The experiments in buffer were performed using lactose concentrations between 0.9 and 1g/L, concentrations lower than the optimal values given by EU legislation, because to metabolize 50g/L of lactose, a great amount of enzyme is necessary. Experiments with milk were different that those showed in buffer because adding exogenous lactose no fluorescence variation was obtained, perhaps due to the saturation of the enzyme. Thus, other tests were performed using semi-skimmed and skimmed milk. Positive results were obtained only with skimmed milk, indicating that the fat component may cross interfere with the enzyme. It is possible to see that the increase of the amount of skimmed milk determines a significant increase in fluorescence signal though these differences are not marked (**Fig. 5B**).

3.4.3. D-Lactic dehydrogenase for analyses of D-lactic acid

Last analyte employed was lactic acid since it is an important parameter indicating the quality and freshness of milk and its derivatives. Lactate concentration limit imposed by European legislation is 30ppm corresponding to $3.3x10^{-4}$M. D-lactic dehydrogenase, a NAD^+-dependent enzyme catalyzing the conversion of D-lactic acid into pyruvate with production of NADH and H^+, was used as biomediator. This reaction determines a pH change allowing the use of 5-(6)-carboxynaphthofluorescein as fluorophore. Experiments with D-lactic dehydrogenase were performed in milk and the progress of the reaction was found to be similar to that obtained with buffer where the increase of D-lactate concentration determines a decrease in the fluorescence signal (**Fig. 5C**).

3.5. Performance of the biosensor platform

The performance of the biosensor was studied in order to evaluate the most important parameters of the biosensor, such as limit of detection (LOD), relative standard deviation (RSD%), reproducibility, response time and linear range. The detection performance of the multi-array biosensor for the spiked samples with the selected analytes is reported in **Table 3**.

The performance of the biosensor platform was evaluated against the traditional optical methods with laboratory set-up instrumentations showing good linearity, sensitivity and repeatability in the detection both in standard and real samples. Satisfactory variations were also obtained as the relative standard deviations were in the range 0.5-5.6 %.

In particular the LODs, reported with the same units of EU legislation, were 1.1 ng/kg for diuron, 0.6 μg/L for clorpyrifos, 1.2 μg/L for catechol, 13.8 mg/dL for urea, 0.06 g/L for lactose and 19.5 ppm for D-lactic acid. These limits satisfy the reported EU regulations, a part for the phenolic compound that shows a limit about 20 times higher.

Based on the F0 values, it is possible to extrapolate from the curves the initial value of urea, lactose and lactic acid concentrations that correspond to 25mg/dL, 46g/L and 28ppm, respectively, which are in line with the correct concentrations for a quality milk (**Table 3**). Thus, the developed optical multi-array biosensor provides the possibility of measurements with excellent reproducibility and specificity of the analytes within the EU regulations.

Conclusions

We developed a multi-array biosensor equipped with six wells with three different LEDs (red, yellow and blue) of fluorescence excitation in order to analyze several analytes at the same time. The identification of optimal measurement conditions allowed developing an optical biosensor for simultaneous analyses of various safety and quality parameters in milk. New trends in food industry technology highlight the need of development of transferable tools to empower the food business operators in their responsibility of daily self-monitoring of the food chain originating from the European White Book for Food Safety [3]. Based on the comparative performance of laboratory set-up techniques and the multi-array biosensor, the biosensor platform emerges as a suitable tool for large classes of compounds in fast, simple screening of milk safety/quality.

The effective transfer to the daily use by farm operators will require the corroboration of results robustness under farm conditions as well as the implementation of in-continuous and automated application [43, 44, 45].

References

[1] C. Frazzoli, & A. Mantovani, Toxicants exposures as novel zoonoses: reflections on sustainable development, food safety and veterinary public health, Zoonoses and Public Health 57 (2010) 136-142.

[2] W.L. Claeys, S. Cardoen, G. Daube, J. De Block, K. Dewettinck, K. Dierick, L. De Zutter, A. Huyghebaert, H. Imberechts, P. Thiange, Y. Vandenplas, L. Herman, Raw or heated cow milk consumption: Review of risks and benefits, Food Control 31 (2013) 251–262.

[3] Commission of the European Communities. White Paper on Food safety. Brussels, 12 January 2000; COM (1999) 719 final.

[4] O. Lacina, P. Hradkova, J. Pulkrabova, J. Hajslova, Simple high throughput ultra-high performance liquid chromatography/tandem mass spectrometry trace analysis of perfluorinated alkylated substances in food of animal origin: Milk and fish, Journal of Chromatography A 28 (2011) 4312-4321.

[5] F.M. Rodrigues, P.R.R. Mesquita, L.S. Oliveira, A.M. Filho, P.A.A. Pereira, J.B. Andrade, Development of a headspace solid-phase microextraction/gas chromatography-mass spectrometry method for determination of organophosphorous pesticide residues in cow milk, Microchemical Journal 98 (2011) 56-61.

[6] Martial LeDoux, Analytical methods applied to the determination of pesticide residues in foods of animal origin. A review of the past two decades, Journal of Chromatography A 1218 (2011) 1021-1036.

[7] P.N Patel, V. Mishra, A.S. Mandloi, Optical biosensors fundamentals and trends, JERS 1 (2010) 15-34.

[8] T.F. McGrath, C.T. Elliott, T.L. Fodey, Biosensor for the analysis of microbial and chemical contaminants in food, Analytical Bioanalytical Chemistry 403 (2012) 75-79

[9] U.B. Trivedi, D. Lakshminarayana, I.L. Kothari, N.G. Patel, H.N. Kapse, K.K. Makhija, P.B. Patel, C.J. Panchal, Potentiometric biosensor for urea determination in milk, Sensors and Actuators B: Chemical 140 (2009) 260-266.

[10] N. Verma, M. Singh, A disposable microbial based biosensor for quality control in milk, Biosensors and Bioelectronics 18 (2003) 1219-1224.

[11] Z. Cao, W. Huang, T. Wang, Y. Wang, W. Men, M. Ma, S. Li, Effects of parity, milk production and milk components on milk urea nitrogen in Chinese Holstein, Journal of Animal and Veterinary Advances 9 (2010) 688-695.

[12] H. Dai, Y. Shi, Y. Wang, Y. Sun, J. Hu, P. Ni, Z. Li, A carbon dot based biosensor for melamine detection by fluorescence resonance energy transfer, Sensors and Actuators B: Chemical 202 (2014) 201-208.

[13] H.X. Juan, Z.X. Hong, Z. yan, L.L. Hua, L. Feng, S. Lei, S.H. Chang, Melamine detection in dairy products by using a reusable evanescent wave fiber-optic biosensor, Sensors and Actuators B: Chemical 204 (2014) 682-687.

[14] J. Liu, J. Ren, Z. Min Liu, Ben. Heng Guo, A new comprehensive index for discriminating adulteration in bovine raw milk, Food Chemistry 172 (2015) 251-256.

[15] M. Ramanathan, A.L. Simonian, Array biosensor based on enzyme kinetics monitoring by fluorescence spectroscopy: Application for neurotoxins detection, Biosensor and Bioelectronics 22 (2007) 3001-3007.

[16] R. Doong, P. S. Lee, K. Anitha, Simultaneous determination of biomarkers for Alzahimers disease using sol-gel-derived optical array biosensor, Biosensor and Bioelectronics 25 (2010) 2464-2469.

[17] C. Boero, M. A. Casulli, J. Olivo, L. Foglia, E. Orso, M. Mazza, S. Carrara, G. De Micheli, Design, development, and validation of an in-situ biosensor array for metabolite monitoring of cell cultures, Biosensor and Bioelectronics 61 (2014) 251-259.

[18] A. Mantovani & C. Frazzoli, Risk assessment of toxic contaminants in animal feed, CAB Reviews: Perspectives in Agriculture, Veterinary Science, Nutrition and Natural Resources 5 (2010) 1-14.

[19] W.J. Fisher, B. Schilter, A.M. Tritscher, R.H. Stadler, Contaminants of milk and dairy products, Contamination resulting from farm and dairy practices, Encylopedia of Dairy Sciences Second Edition, (2011) 887-897.

[20] L. Yang, R. Bashir, Electrical/electrochemical impedance for rapid detection of foodborne pathogenic bacteria, Biotechnology Advances 26 (2008) 135-150.

[21] M. Van der Spiegel, P. Sterrenburg, W. Haasnoot, H.J. van der Fels-Klerz, Towards a decision support system for control of multiple food safety hazards in raw milk production, Trends in Food Science and Technology 34 (2013) 137-145.

[22] M.T. Giardi, V. Scognamiglio , G. Rea, G. Rodio, A. Antonacci, M.D. Lambreva, G. Pezzotti, & U. Johanningmeier, Optical biosensors for environmental monitoring based on computational and biotechnological tools for engineering the photosynthetic D1 protein of *Chlamydomonas reinhardtii*, Biosensors and Bioelectronics 25 (2009) 294–300.

[23] K. Buonasera, G. Pezzotti, V. Scognamiglio, A. Tibuzzi, M.T Giardi, New platform for prescreening of pesticides residues to support laboratory analyses. Journal of Agriculture and Food Chemistry 58 (2010) 5982–5990.

[24] J. Maly, J. Masojidek, A. Masci, M. Ilie, E Cianci, V. et al., Direct madiatorless electron transport between the monolayer of photosystem II and poly (mercapto-p-benzoquinone) modified gold electrode-new design of biosensor for herbicide detection. Biosensor and Bioelectronics 21 (2005) 923-932.

[25] J. Han, K. Burgess, Fluorescent Indicators for Intracellular pH, Chemical Reviews 110 (2010) 2709-2728.

[26] R. Betarbet, T. B. Sherer, G. MacKenzie, M. G. Osuna, A.V. Panov & J. T. Reenamyre. Chronic systemic pesticide exposure reproduces features of Parkinson's disease Nature neuroscience 3 (2000), 1300-1306.

[27] V. Scognamiglio, G. Pezzotti, J. Cano, I. Manfredonia, K. Buonasera, F. Arduini, D. Moscone, G. Palleschi, M.T. Giardi, Towards an integrated biosensor array for simultaneous and rapid multi-analysis of endocrine disrupting chemicals, Analytica Chimica Acta. 751 (2012) 161-170.

[28] S. Mostafalou, M. Abdollahi, Pesticides and human chronic deseases: Evidences, mechanisms and perspectives, Toxicology and Applied Pharmacology 268 (2013) 157-177.

[29] M. Del Carlo, & D. Compagnone, Recent strategies for the biological sensing of pesticides: From the design to the application in real samples. Bioanalytical Reviews 1 (2010), 159-176.

[30] R. Brayner, A. Couté, J. Livage, C. Perrette, C. Sicard, Micro-algal biosensors, Analytical and Bioanalytical Chemistry 401 (2011) 581–597.

[31] D. Dewez, O. Didur, J. Vincent-Héroux, & R. Popovic, Validation of photosynthetic-fluorescence parameters as biomarkers for isoproturon toxic effect on alga Scenedesmus obliquus, Environmental Pollution 151 (2008) 93-100.

[32] F. Lefèvre, A. Chalifour, L. Yu, V. Chodavarapu, P. Juneau, & R. Izquierdo, Algal fluorescence sensor integrated into a microfluidic chip for water pollutant detection, Lab on a Chip**.** 12 (2012) 787-793.

[33] A. Hildebrandt, R. Bragos, S. Lacote, J.L. Marty, Performance of a portable biosensor for the analysis of organophosphorous and carbamate insecticides in water and food, Sensors and Actuators B: Chemical 133 (2008) 195-201.

[34] D.C. Rodriguez, S. Carvajal, G. Penuela, Effect of chlorpyrifos on the inhibition of the enzyme acetylcholinesterase by cross-linking in water-supply samples and milk from dairy cattle, Talanta 111 (2013) 1-7.

[35] M.T. Muñoz-Quezada, B.A. Lucero, D.B. Barr, K. Steenland, K. Levy, P.B. Ryan, V. Iglesias, S. Alvarado, C. Concha, E. Rojas, C. Vega, Neurodevelopmental effects in children associated with exposure to organophosphate pesticides: A systematic review, NeuroToxicology 39 (2013) 158-168.

[36] H. Tsai, R. Doong, Simultaneous determination of pH, urea, acetylcholine and heavy metals using array-based enzymatic optical biosensor, Biosensor and Bioelectronics 20 (2005) 1796-1804.

[37] V. Scognamiglio, I. Pezzotti, G. Pezzotti, J. Cano, I. Manfredonia, K. Buonasera, G. Rodio, M.T. Giardi, A new embedded biosensor platform based on micro-electrodes array (MEA) technology, Sensors and Actuators B 176 (2013) 275-283.

[38] D. D. Bannerman, M. J. Paape, R. L. Baldwin 6th, C. P. Rice, K. Bialek, A. V. Capuco, Effects of mastitis on milk perchlorate concentrations in dairy cows, J Dairy Sci. 89 (2006) 3011-9.

[39] Balasubramanian, A. & Ponnuraj, K. (2010). Crystal structure of the first plant urease from Jack bean: 83 years of journey from its first crystal to molecular structure. Journal of Molecular Biology. 400, 274-283.

[40] M. Roesch, M.G. Doherr, W. Schären, J.M Schällibaum, W. Blum, Subclinical mastitis in dairy cows in Swiss organic and conventional production systems, Journal of Dairy Research 74 (2007) 86-92.

[41] Z. Grosova, M. Rosenberg, & M. Rebros, Perspectives and applications of immobilized β- galactosidase in food industry: a review, Czech Journal of Food Sciences 26 (2008) 1–14.

[42] Q. Husain, a β- galactosidase and their potential applications: a review, Critical Reviews in Biotechnology 30 (2010) 41–62.

[43] C. Frazzoli, A. Mantovani, L. Campanella, & R. Dragone, System (BEST-integrated toxicity (bio)sensor's system for hazard analysis and management in the food chain and the environment) for environment diagnostic and monitoring and self-control of food chain, including primary production, and relevant method for quick management of hazard, World Intellectual Property Organization, (2010) International Publication Number WO 2010/001432 A1.

[44] www.alert2015.it

[45] C. Frazzoli, A. Mantovani, R. Dragone, Local role of food producers' communities for a Global One-Health framework: the experience of traslational research in an Italian dairy chain. Journal of Agricultural Chemistry and Environment 3(2B) (2014) 14-19].

CHAPTER 5

“Performance Analysis for Steady Flow Generation and Improved Readout Signal in Amperometric Biosensors”

Manfredonia, I., Barbieri, M., Verzicco, R., Stallo, C., Ruggieri, M., Lavecchia, T., Turemis, M., Pezzotti, G “Performance analyses for steady flow generation and improved readout signal in amperometric biosensors. IEEE Sensors Journal, 15 (2015) 9; 5208-5216, DOI 10.1109/JSEN.2015.2439272

Abstract

The use of peristaltic pumps as fluidic distribution microsystems in electrochemical biosensor devices operating with amperometric transducers can result in periodic spikes affecting the output signal. Mechanical components rotating inside the pumps are the main cause of this kind of disturbing noise. A novel fluidic setup based on simple fluid mechanics laws has been realized with no moving components when pump is on. It yields a fluctuation-free outcome signal that we compare with those produced by commercial peristaltic pumps. Evidence of the readout amperometric enhanced signal is shown thus confirming the successful implementation of more reliable biosensors and electrochemical signal transduction devices. Such stable and oscillation free amperometric signals are very desirable in view of biosensors integration in environmental monitoring platforms equipped with advanced communication technologies. An example is reported for their use in data mining systems equipped with a remote control for the real time monitoring of pollutants. The cleanliness and the strength of the signal can adversely affect the reliability of the transmission of relevant information, especially when there are early warning civil purposes referred to a potential harmful contamination (i.e. water bodies pollution).

1. Introduction

Among the electrochemical biosensors, amperometric biosensors are one of the most common, numerous and successfully commercialized devices of biomolecular electronics [1]. An important application of the amperometric biosensor is in environmental monitoring of pesticides [2] thanks to important features, which make them suitable for in field measurements and industrial production. Firstly, amperometric biosensors are more suitable for mass production than potentiometric and conductometric as they show higher stability and selectivity; secondly these biosensors are highly sensitive, rapid and inexpensive [3]. In addition, they display a high degree of reproducibility, which removes the need for repeated calibration. Amperometric measurements often need a buffering solution to be pumped inside a detection cell and mechanical pumping in dynamic mode are the best practiced solution since they do not interfere with the properties of the fluids, even if they are usually associated with flow oscillations [4]. The flow rate in fact is sensitive to time dependent pressure conditions. Peristaltic pumps work by squeezing deformable pipes with rollers moving in a rotary fashion. This produces oscillations in pressure and velocity and the flow rate is pulsatile in time. Sometimes, even syringe pumps can lead to results similar to those of peristaltic pumps in which there are oscillations in the flow rate with consequences on experimental results. In particular, this happens in the case of an inadequate combination of syringe size and the flow rate. The reason for this behavior is essentially mechanical. In a syringe pump, only the mechanical part of the device is responsible for these oscillations. In order to move the piston of the syringe, an electrical engine sets an endless screw in motion, on which the piston carriage is set. At low flow rates, the step-by-step operation of the electrical engine is perceptible when the piston of the syringe pump has to move very slowly to deliver the required flow rate. Indeed the elastic compliance of the system can smooth the flow but at the cost of decreasing the time response of the system. It is also possible to improve the stability of a syringe pump using additional tools, which sometimes are very

expensive. Comparing to other pumps the (linear) peristaltic pump is more accurate, when the pressure difference is below 13.3 Pa (100 mmdHg). Otherwise, piston pump is more preferable [5].

By increasing the number of rollers, it is possible to decrease the pressure oscillations on the output even if this implies more occlusion for the same flow rate thus reducing the lifetime of lining [6]. In mass transfer applications with open circuits (without looping), steady flow has been generated also by gravity-driven pumping to overcome the above-mentioned limitations and some innovative experimental devices are in the literature [7].

For the biosensor devices used in the present investigation (www.biosensor.it), the fluidic module is generally composed by a PTFE tube, commonly known as Teflon that assures no contamination for the samples, and a peristaltic pump, which has to assure a regular distribution of the buffering solution.

2. The amperometric signal

The described system is based on photosynthetic biosensors. Biosensors are made of a biomolecule (biorecognition element) in contact with a signal transducer (optical, electrochemical or mass-sensitive). The biorecognition element can be a microorganism, enzyme, antibody, nucleic acid etc). In the case of photosynthetic biosensors, the biological element is a photosynthetic microorganism or a part of it. The photosynthetic membranes contain complex protein architectures, involved in the electron transfer chain known as photosystems. A model has been depicted by Buonasera. (Buonasera et al., 2010) (**Fig. 1**).

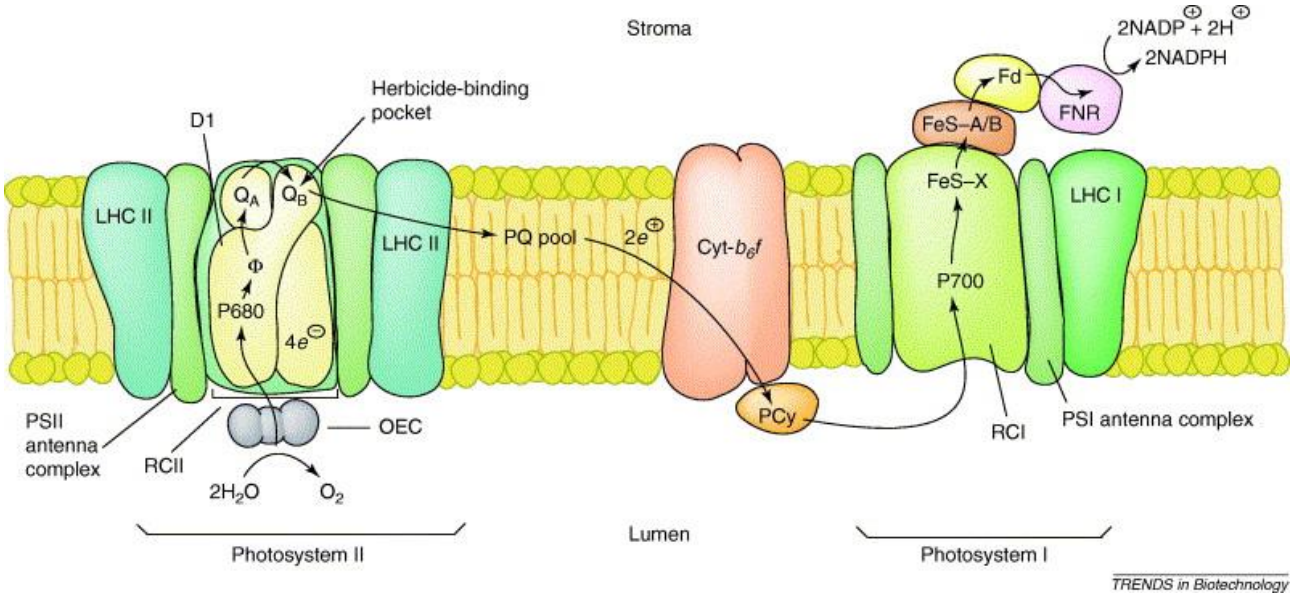

Fig. 1. Photosystem mode

The Photosystem II (PSII) starts the photosynthetic chain absorbing light. Light absorption causes a charge separation and a motion of electrons from the primary acceptor known as quinone A (Q_A) to the secondary acceptor quinone B (Q_B). The biosensing mechanism is based on the total or partial inhibition of this electron transfer due to the presence of chemical interferent species. In particular, when pollutants are present in the sample solution and come into contact with the photosystem, they steak to Q_B inhibiting the transport of electrons from the primary acceptor Q_A to the secondary quinone. This inhibition results in a variation of PSII current that can be monitored by amperometric analysis in pollutants concentration-dependent manner. An easy way to transduce the electric signal due to the photosynthetic activity of a biomediator is the immobilization of it at the working electrode of an electrochemical cell, allowing the monitoring of current arising from the electron motion between Q_A and Q_B. A working potential of -700 mV is needed against an Ag/AgCl reference electrode. The measuring system also requires a light source (about 300 μmol/m2s) to activate the photosynthesis. Light and dark duration (relaxation) is controlled by a photoperiod function. In the dark time no photosynthetic activity occurs, thus the only signal registered is the current due to buffer conductivity (baseline). Once the system is illuminated, the photosynthetic

reaction takes place, releasing electrons at the electrode surface. As a consequence a peak in the output current is detected [8]. In the presence of pollutants blocking the electron transfer, a decrease on the peak current is observed (**Fig. 2**). The rate of the current peaks with and without the pollutant (expressed as percent of inhibition) can be correlated to pollutant concentration[9].

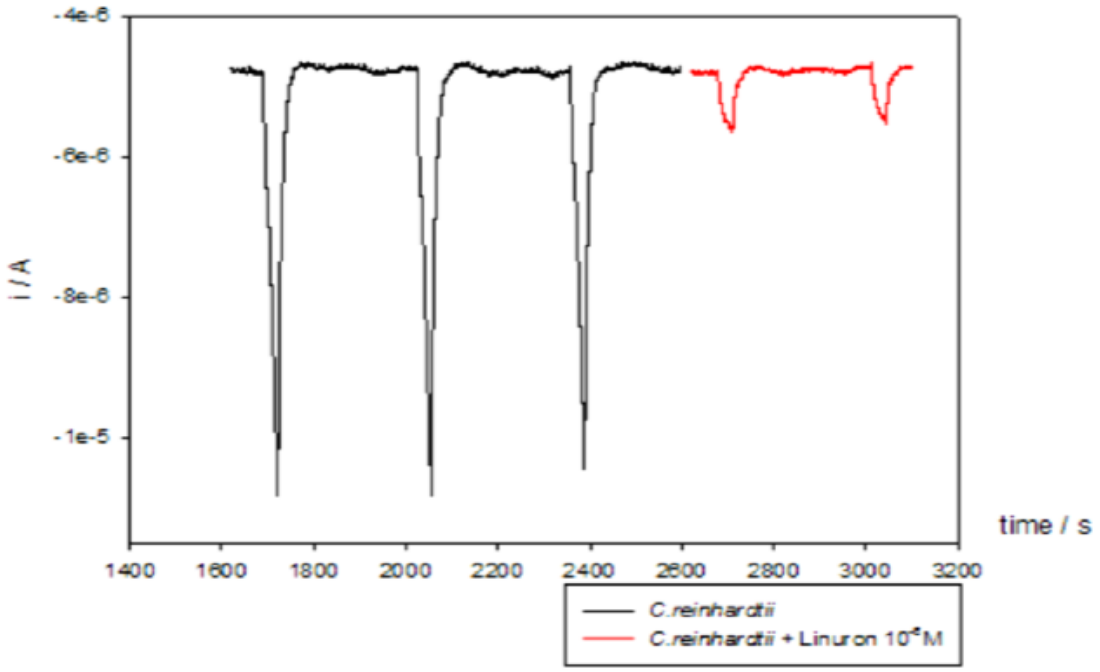

Fig. 2. Example of amperometric signal of photosynthetic material. Red line shows response after contact with Linuron herbicide.

The reliability of amperometric measurements depends on the measuring parameters. At low flow rates, for example, the non-linear friction of the rollers can induce significant oscillations affecting the final signal.

To show the interference created by the pumping system in the previously cited biosensor devices, some measurements have been carried out in laboratory. The results are reported in **Figure 3**:

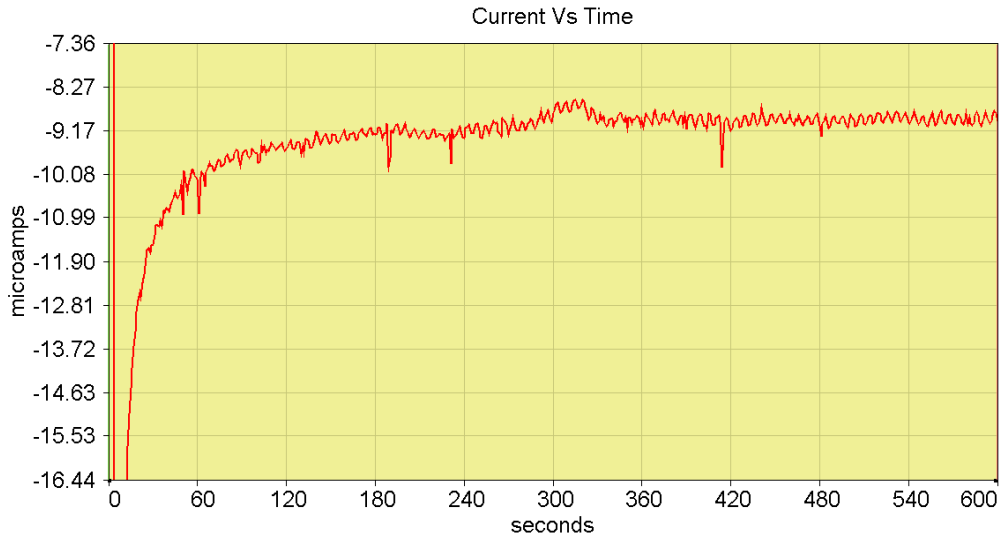

Fig. 3. Amperometric signal obtained with a commercial Gilson peristaltic pump.

Figure 3 shows the signal obtained using a biosensor instrument using an algal biorecognition element (*C. reinhardtii*), in a measurement chamber connected to a commercial pumping unit (Gilson MINIPULS 3®). The MINIPULS 3 peristaltic pump combines a microprocessor-based speed control with a high-torque stepper motor. Chemical resistant pump heads, equipped with 10 stainless steel rollers, set the performance standard in producing smooth, low-pulse flow and reproducible flow rates at high pressure. For the experiment, the flow rate provided is 200 µl/min. The choice of flow rate is the result of a compromise between the best performance in terms of signal-to-noise ratio (S/N) and getting a flow rate avoiding the damage or the complete removal of the immobilized biomaterial. The measured average noise appearing in the curves and highlighted in red is about 0.08 µA. The value of S/N ratio measured for each single replica is found ranging from 2.32 to 2.44 µA. The average S/N ratio calculated from statistics is fixed at 2.39± 0.07 µA.

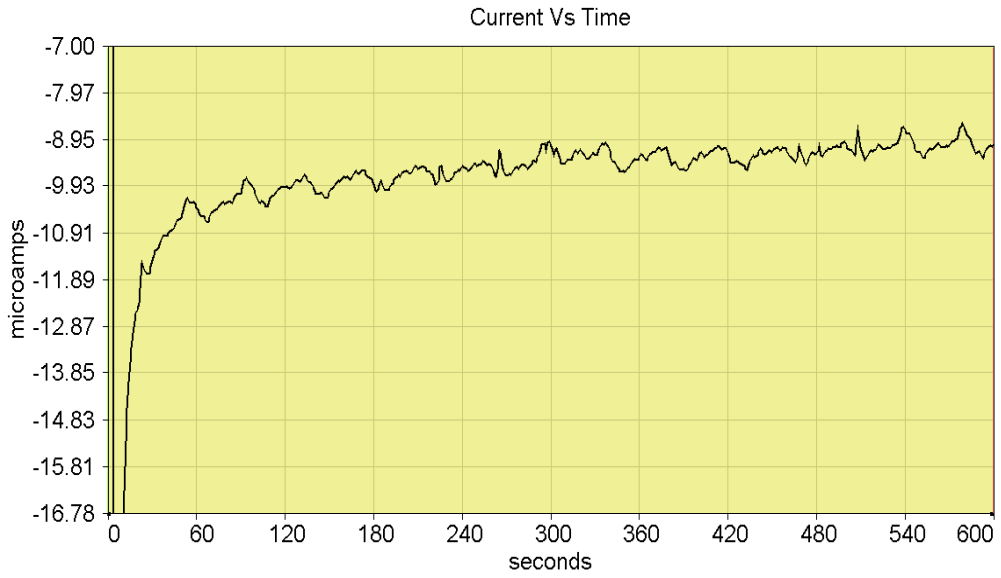

Fig. 4. Amperometric signal obtained with in-house peristaltic pump.

Fig. 4 shows the typical result, obtained by an analogous experiment (same biorecognition element, flow rate, working potential, light source) with an in-house peristaltic pump mounting 6 plastic rollers. In this case, a higher noise appears in the amperometric signal varying from 0.3 to 0.6 μA, while S/N ratio lowers ranging from 1.72 to 2.06 μA. The reduction calculated over the signal component is 20.5 percentage. This accounts for a smaller signal-to-noise level (1.90± 0.15 μA) causing the loss of signal quality. A redoubled standard deviation around the measured current is also found with respect to the first case (0.15 μA against 0.07 μA). These fluctations possess a relatively importance when examining biomediators at low pollutants concentration (see **Fig. 2**). The output current, in these cases, is lowered down but the measured value is in the microamperes (μA) range. As the concentration of pollutant gets higher, the current signal goes further down. For current values ≤ 0.1 μA a percentage error of 60% over the detected value is found.

A comparison between the Gilson MINIPULS 3 system and the in-house built peristaltic pump is clearly shown by overlaying the curves (**Fig. 5**). The overall signal produced by the Gilson pumping system shows a better quality and more regular noise distribution.

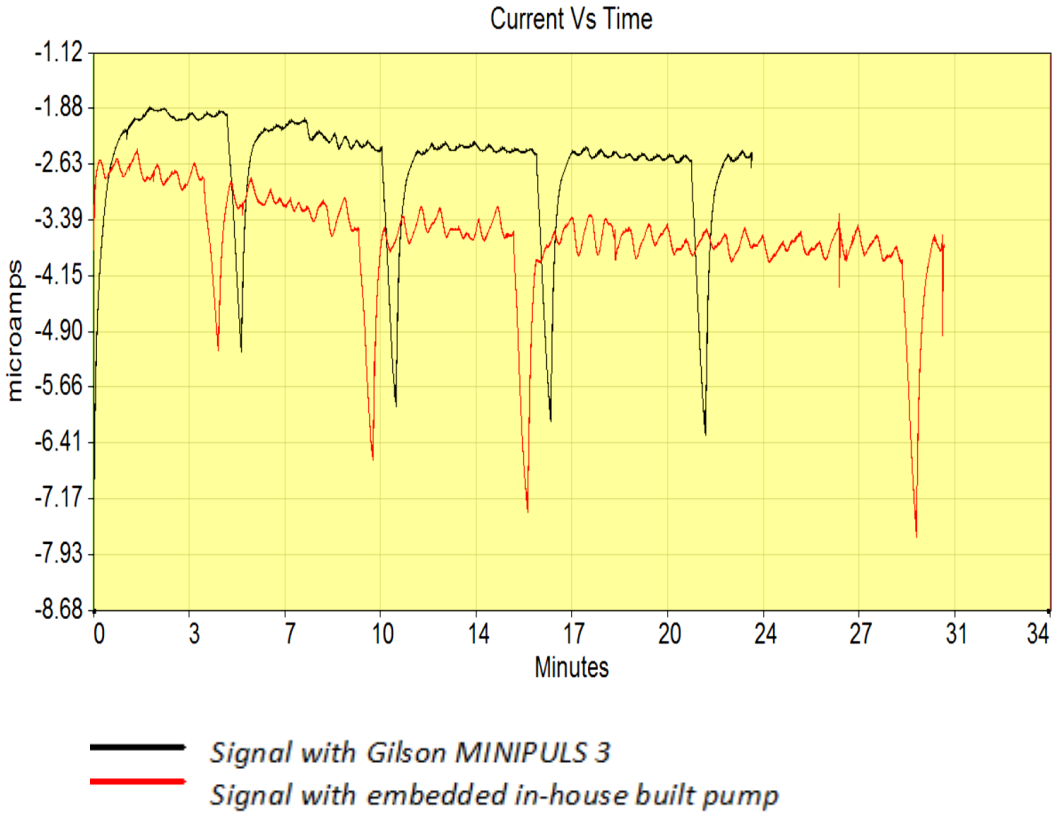

Fig. 5. Comparison between the two peristaltic pumps.

3. New fluidic microsystems

3.1. Peristaltic pump

The absence of mechanical parts in contact with the delivered liquid makes the peristaltic pump particularly suitable to avoid any kind of contamination of the analyzed fluid. In fact, the tubing can be sterilized and the pump can be applied in biomedical applications or food industry when the fluid contamination is an issue.

A peristaltic pump is basically composed by a rotor and by a tube made of a deformable material. The rotating element is equipped with a series of cylindrical rollers that oblige the tube (in blue color) to follow a “U” pattern (**Fig. 6**).

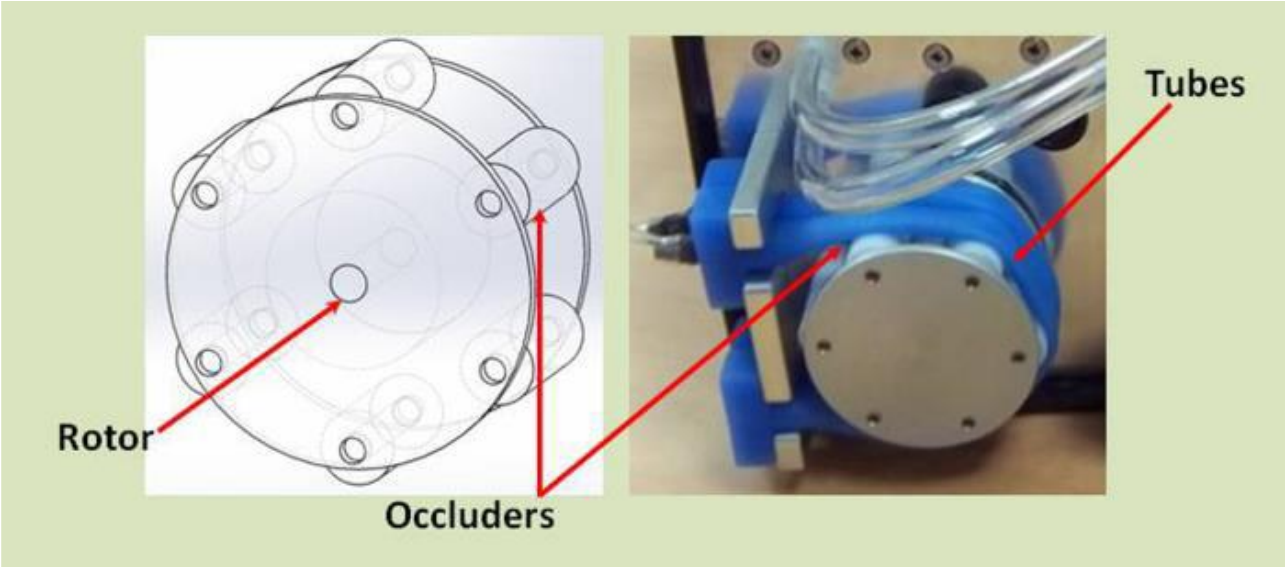

Fig. 6. Peristaltic pump components.

The pumping action occurs thanks to the rotor movement, operated by an electric motor that, through the rollers, pushes the fluid towards the exit of the pump. In order to assure a good functioning it is necessary that the working tube is elastic enough to recover its original shape when relaxed by the occluder.The flow rate can be accurately tuned both working on the tube diameter and modulating the speed of the electric motor connected with the rollers. The possibility of achieving extremely low flow rates, associated with the great constructive simplicity and with the absence of interaction between fluid and mechanical parts, determines the great popularity of the peristaltic pump. Nevertheless, the working principle of the peristaltic pump intrinsically produces a pulsatile flow rate: In fact, the presence of the rollers causes the cyclic interruption of the flow rate as many times in a revolution as from the frequency calculated by:

$$f=\omega/(2\pi\cdot n)=(rpm\cdot n)/60. \qquad (1)$$

Here n is the rollers number, ω the angular velocity in rad/s corresponding to rpm number of revolutions per minute of the rotor. The amplitude of the interruption depends on the rollers size: the smaller is their dimension, the shorter the absence of flow rate will be. Supposing a total reduction of

the flow rate, a square wave shaped trend would result, and the flow rate expression would become the following:

$V=A\omega r\ (1-ln/2\pi r)$ (2)

where A represents the transition area of the fluid, r the distance between the rotor axis and the tube mid-line, n the number of occluders and l their length on the tube axis. From this equation and from (1) we can infer how the rollers number directly affects both the flow rate loss and the tube opening/closure frequency. These oscillations do not allow for a constant flow rate implying a deterioration on the quality of the signal detected by the sensors.

3.2. Mariotte pump

Part of the problems in the measure of the pollutant concentrations by biosensors can be related to the irregular flow rate of the fluid. In order to overcome this issue an alternative pumping system, capable of assuring a constant biosensor feeding is required; this must comply with the need to avoid fluid contamination. Besides these two fundamental requirements a solution aimed at simplifying considerably the system eliminating also the electric motor activating the pump rotor was developed. Among the various potential alternatives, a gravity-driven system has been conceived, giving it the name of the main law it uses. The "Mariotte pump" is able to exploit gravity in order to provide the adequate pressure difference required to assure the expected flow rate. This is achieved by positioning the test tube containing the liquid to be analyzed at a certain height; a valve placed along the PTFE tube, which delivers the liquid to the chamber, regulates the flow rate. One problem is that often only small volumes of fluid are available for the analysis while, on the other hand, an accurate regulation of the flow rate requires the availability of a relatively large reservoir.

Being unpractical to increase volume of fluid to be analyzed, the idea was to employ a secondary fluid to pump the sample liquid into the sensor chamber. In **Figure 7** a scheme of the device is given. The basic system is composed by a water tank, much larger than the test tubes, from

the basis of which a small diameter pipe departs; along the path, a valve and a roller flow rate regulator are present. The pipe ends inside the test-tube, which is sealed. Another pipe connects pneumatically the test-tube A to the test-tube B, containing the liquid to be analyzed. The working principle, though very simple, allows to maintain the examined liquid properties unaltered. Once the outlet valve from the tank is open, water, running through the connecting pipe, feeds the test-tube A, which is initially empty.

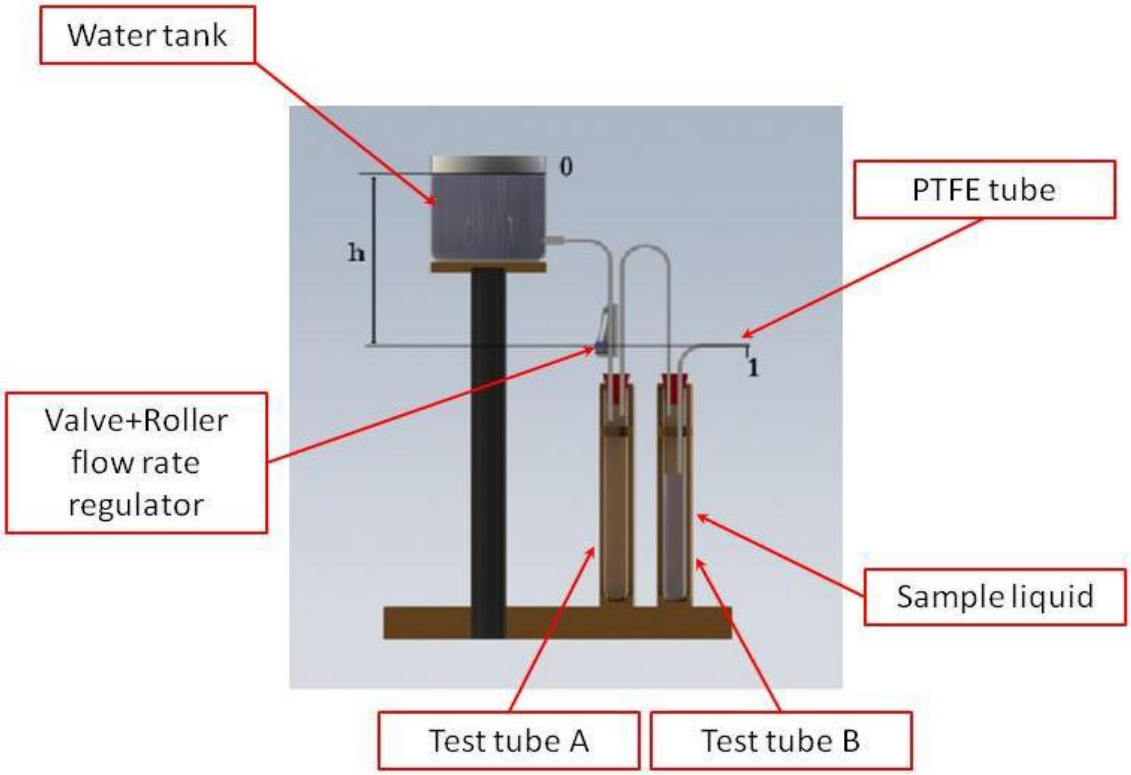

Fig. 7. System of pumping with auxiliary fluid scheme.

The air inside the test-tube A is pushed inside the test-tube B by the pressure increase produced by the incoming liquid. The increasing air pressure in the test-tube B drives the test liquid into the delivery pipe to feed the sensor chamber.

We can write the Bernoulli equation between the sections 0 and 1 to obtain:

$$(p_0/\rho g) + z_0 + (u_0^2/2g) = (p_1/\rho g) + z_1 + (u_1^2/2g) + z_{att} \qquad (3)$$

The terms labeled with the subscript zero are related to the water free surface in the tank while those labeled with the subscript one, represent the characteristics of the flow going out of the pumping system, that is, at the measurement system inlet. The parameter z_{att} represents all the fluid dynamic losses along the path between the section 0 and 1. Considering that the pressure at the two sections as the ambient pressure and assuming $z_1=0$, and $z_0=h$ we can write:

$$h + (u_0^2/2g) = (u_1^2/2g) + z_{att} \qquad (4)$$

The mass flow rate $\dot{m}=\rho A u_1$ becomes:

$$\dot{m} = \rho A\sqrt{2g(h - z_{att}) + u_0^2} \qquad (5)$$

It is now clear that the flow rate is strictly connected to the water level in the tank, that however decreases continuously with velocity u_0 that, even if small, is not completely negligible especially for long lasting measurements. Even if it is only a minor effect, also the pressure losses z_a , caused by the friction, would decrease with the flow rate $\dot{m}$ thus further decreasing the flow rate. In order to solve this issue, keeping the same scheme as the device of **Figure 7**, it is sufficient to replace the open water tank with a sealed one, creating a "Mariotte Box". This device, as simple as barely popular, allows making a piezometric tank, in which the outlet flow rate of the contained liquid remains strictly

constant in time. The construction of the "Mariotte Box" consists of a sealed tank with an external air intake in the liquid. **Figure 8** shows a possible sketch. The presence of the external air intake binds the section 2 to the ambient pressure regardless the effective water level in the tank as long as it is above the air intake; writing again the Bernoulli equation between the sections 1 and 2 we obtain:

$$(p_2/\rho g) + z_2 + (u_2^2/2g) = (p_1/\rho g) + z_1 + (u_1^2/2g) + z_{att} \qquad (6)$$

As before, the pressures $p_1=p_2=p_{atm}$, and considering $z_1=0$ and $z_2=h$, we can write:

$$h + (u_2^2/2g) = (u_1^2/2g) + z_{att} \qquad (7)$$

While the water flows out of the tank, the 0 level decreases but, as long as $z_2>z_0$, the dynamic conditions in section 2 will be such that $u_2=0$ (potential inflow). Equation (7) then becomes:

$$h= (u_1^2/2g) + z_{att} \rightarrow u_1 = \sqrt{2g(h - z_{att})} \qquad (8)$$

Fig. 8. Pumping system with Mariotte Box: overall (left) and section (right).

Now the constancy of h binds $u1$ to a constant value and this yields a time independent mass flow rate $\dot{m}$ that in turn yields a constant $zatt$. Every variable will therefore remain constant as long as $z_2 > z_0$.

The final result is the same as if we would use a very big tank where the free surface velocity and level variation would be negligible. Using the Mariotte Box, however, no approximation is required with the obvious advantage of having a smaller system with a limited quantity of fluid involved. The "downfall" pumping system, relying on the Mariotte Box, allows to achieve both objectives: A constant flow rate and, thanks to the two test-tubes in series, the non contamination of the test fluid. Moreover, this system eliminates all the mechanical elements, both the electrical motor and any mechanism, making the entire instrument simpler and more reliable.

4. Experimental setup construction

In order to evaluate the behavior of the Mariotte pump, a scale prototype has been built which made possible the experimental tests at the desired flow rate. Focusing on the setup of **Figure 8**, a sealed tank is needed with an outlet hole for the fluid and an air intake immersed in the liquid. On the cap and on the side holes have been made to allow the placement of clutches for the connection tubes. A glass container was chosen in place of a PE one (Polyethylene) because of its stiffness. During the functioning in fact, the air volume between the water free surface and the lid attains a pressure below the ambient value. This would cause, in case of a flexible container, a tank deformation with a consequent flow rate variation. Along the delivery tube an on/off tap (red circle and enlarged figure) and a precision flow rate regulator though similar to the one included in an intra venous set used in medical field were placed. The two containers, shown in **Figure 8**, which allow to keep the analyzed fluid uncontaminated during the pumping, are two big glass test-tubes with 20 mm of diameter and 200 mm length, generally used in chemical labs. Tests tubes are closed by rubber truncated conical taps where two holes are drilled for connecting pipe junctions. Support system (**Fig. 9**) for all the components have been manufactured by wood and steel; particularly the higher pillar above which the Mariotte box is placed is made up by a telescopic arm allowing height regulation for the shutter between a minimum value of 450 mm and a maximum value of 750 mm. The delivery pipe of the pump is equipped with an additional tap with the scope of preventing eventual losses of liquid to be analyzed.

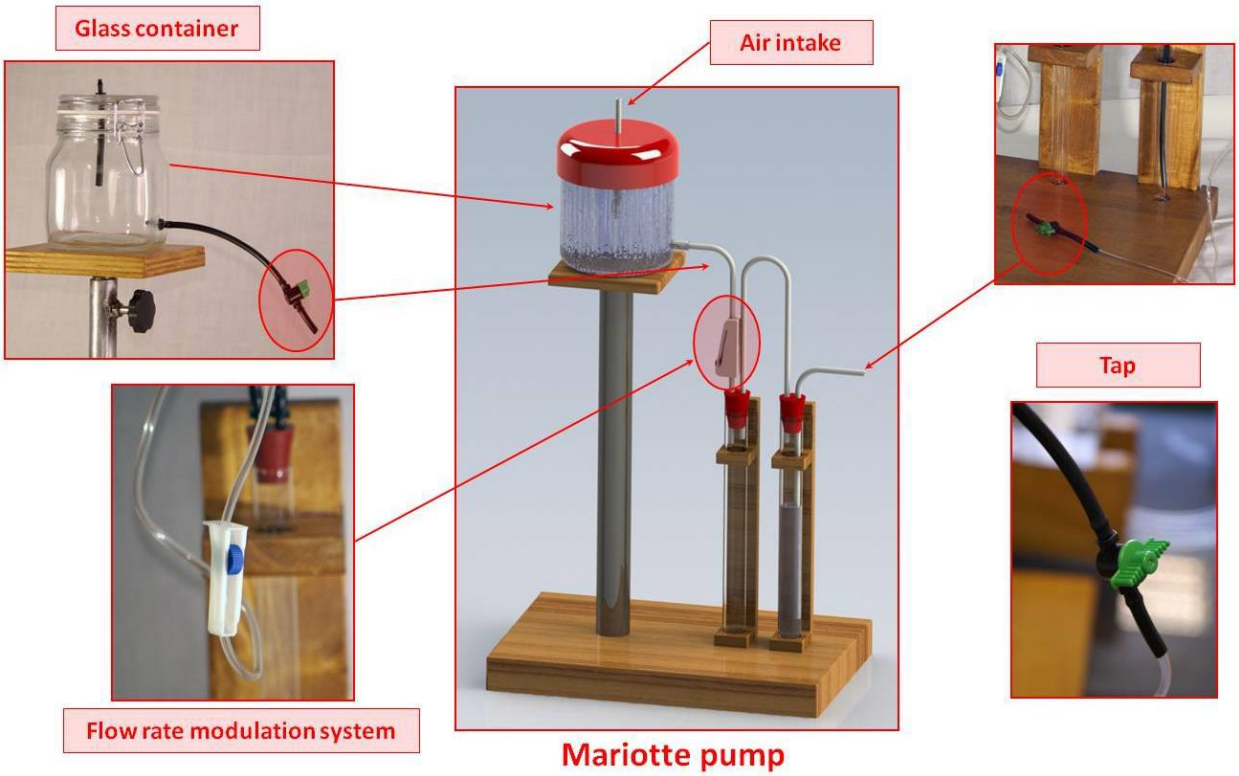

Fig. 9. Mariotte pump

5. Flow rate assessment

As already mentioned, the motivation for the development of a novel pumping system was the presence of a pulsatile flow rate produced by the peristaltic pump. The new system based on the Mariotte box was designed to provide the sensor with a strictly constant flow rate; it was necessary, therefore, to verify whether or not the system performed according to the theory in practice. The flow rate detection was carried out evaluating the liquid level decrease inside the second test-tube, the one containing the liquid to be analyzed, according to the time passed. In order to make a correct assessment of the two indicators, time and level, the emptying was recorded by a high-speed camera (250 fps). As shown in **Figure 10**, the chronometer, the graduated scale and the liquid level are all included in the same frame. The analysis performed allowed assessing optically that liquid level decreases gradually without oscillation suggesting a non-fluctuating trend of the flow rate.

Fig. 10. Measurement system for the flow rate.

Moreover the data, obtained for two different flow rates, P_{Max} e P_{Min}, did not show significant variation of the flow rate during the measurements, exactly how predicted by the Bernoulli relations. The results, reported in **Table 1**, confirm that indeed variations are very limited and, more likely they can be ascribed to measurement approximations. Concerning the latter, we have estimated that our maximum error in evaluating the liquid level in the test-tube is ≈ 1mm (due to the curvature of the free surface) that correspond to ≈ 0.3ml in our test tubes. Since each run lasted at least 15s, the maximum error in the volume flow rate is ≈ 0.02ml/s, which is in between 1% and 4% of our flow rate range. We can therefore conclude that the proposed pumping system is an adequate replacement for the peristaltic pump. Test fluid preservation and flow rate regularity requirements are both satisfied; moreover, as mentioned at the beginning, the absence of mechanical parts and need for external power supply, besides simplifying the system, allows to reduce malfunctions and to considerably contain costs.

Table 1. Flow rates

ID	Δt PMax.	V Pmax (ml/s)	Δt PMin.(s)	V PMin. (ml/s)
1	1.5	1.67	5.6	0.45
2	1.5	1.67	5.9	0.43
3	1.5	1.67	6.2	0.41
4	1.5	1.67	6.2	0.41
5	1.5	1.67	6.7	0.38
6	1.5	1.67	6.5	0.39
7	1.6	1.57	6.9	0.36
8	1.7	1.48	6.9	0.36
9	1.7	1.48	6.9	0.36
10	1.7	1.48	7.1	0.35
Mean		1.66		0.40
Std. Dev.		0.04		0.03

6. Amperometric signal enhancement

In this section, the results obtained on the amperometric measurements after the application of Mariotte pumping system are described. The processes in close proximity to the electrode surface involved in a typical biosensor reaction are rather complex. Thus, it is important to control the variables and parameters that may have a major impact on the signal, affecting the response and the overall performance of a biosensor. As a matter of fact, the design of an appropriate sensor architecture depends on the specific demands arising from the particular analytical task. In biosensors, a limited number of parameters can be controlled. Comparative tests have been fundamental to

demonstrate an evident enhancement in the amperometric curves resulting from the new gravity-driven pumping system. Performance changes have been investigated with a sequence of amperometric tests on three different systems of fluid distribution: a Gilson Minipuls 3 commercial pump (a), a Biosensor's in-house built peristaltic pump (b) and a Mariotte prototype pump (c).

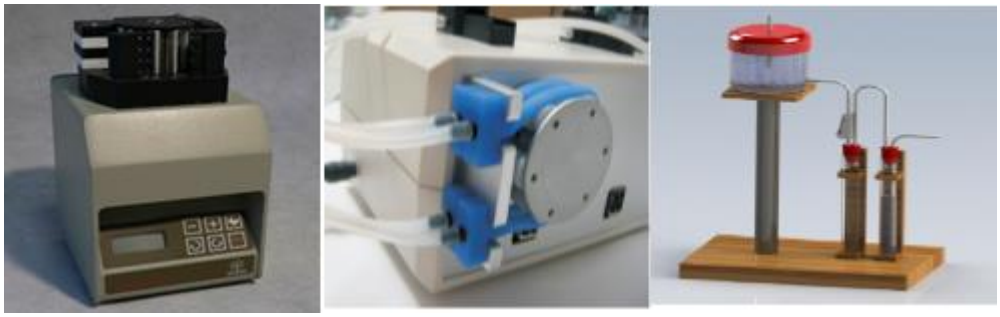

a) b) c)

Fig. 11. Different fluidic distribution devices analyzed.

In each case, the same a buffer solution at the same flow rate and the same flow chamber has been used for the tests. The measuring buffer consisted of 50 mM Tricine, 20 mM $CaCl_2$, 5 mM $MgCl_2$, 50 mM NaCl, 70 mM sucrose, pH 7.2. Optimal concentrations of NaCl and $CaCl_2$ have been experimentally determined by selecting the highest current intensities and signal/noise values. Amperometric measurements have been realized using commercial Screen-Printed Cell (SPE, by DRP-110CNT, DropSens, Oviedo, Spain with a Carbon counter electrode and an Ag/AgCl reference electrode). The whole measuring set-up included a potentiostat (PG581 model, Uniscan Instruments Ltd., Buxton, UK) connected with a notebook to display the curves and a Delrin®-made flow chamber (30 mm in diameter and 25 mm height), hosting the slit for SPE insertion (**Fig. 12 A, B**).

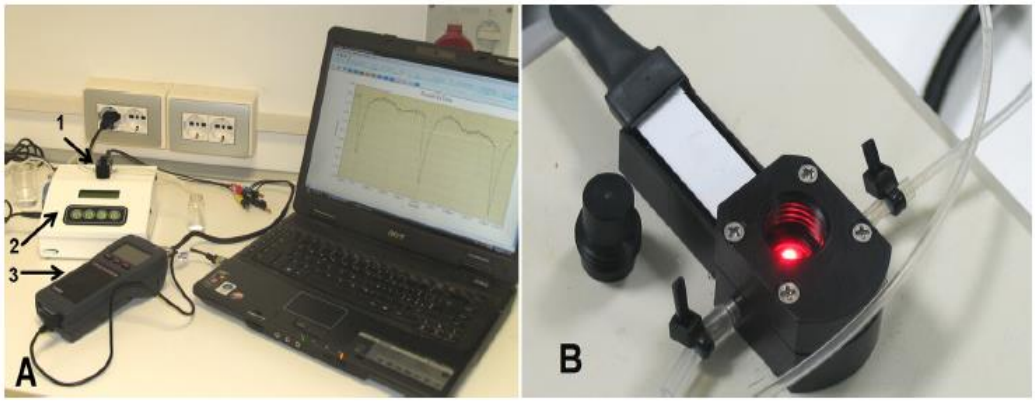

Fig. 12. (A) whole biosensor set-up; (B) Zoom of the flow chamber with switched on red light and SPE (back white surface shown) ready to be inserted.

The above-mentioned apparatus has been also equipped with an electronic control board for data read-out, processing, storage and transfer to a PC laptop. Chronoamperometric (CA) tests have been performed measuring the current intensity against time at an applied potential of −0.70 ± 0.03 V vs. Ag/AgCl and room temperature. An interesting study above the disturbing effect of peristaltic pumps in amperometric recordings has been previously reported by Vergani et al. in 2012 [10]. In this paper authors analyze the current signal resulting from the reduction of potassium ferricyanide 10 mM, injected in one microfluidic chamber [**Fig.13 (a)**]. They observe that when peristaltic pump is on, spikes appear in the detected current. When the pumping system is off, fluctuations are reduced. Electromagnetic interferences of motors are also verified and noise filters applied to remove the disturbing signal of the peristaltic pump. In both cases, the experiments lead to the conclusion, that this type of pumping system strongly disturbs the signal produced by the analyte and the pulsating nature of the peristaltic pump is always responsible for a residual noise that cannot be removed at all.

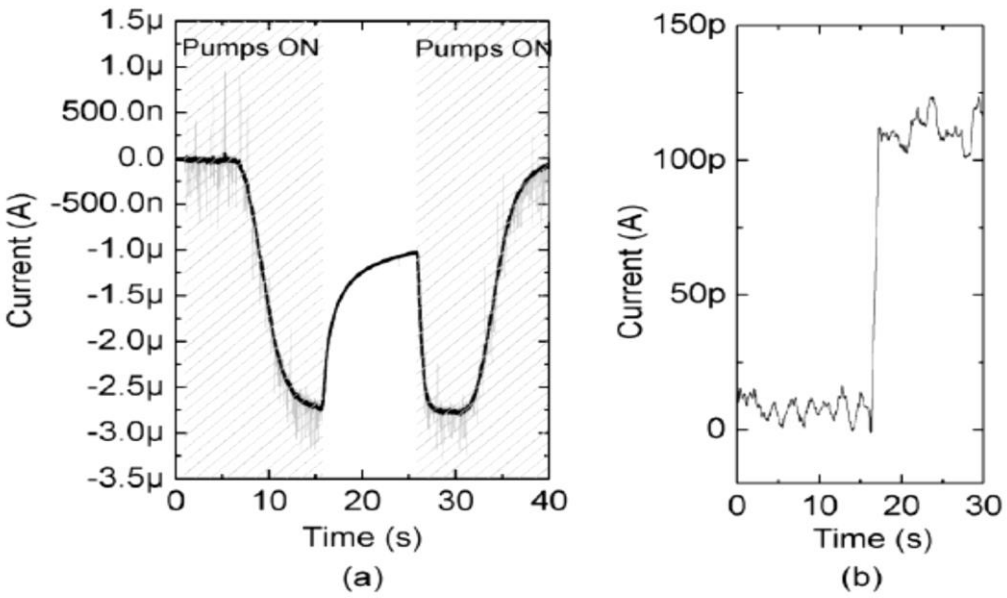

Fig. 13. (a) Amperometric tracking showing the disturbing effect of peristaltic pumping (grey line is the signal acquired at 10 kHz bandwidth whereas the black line is the result of a 5Hz filtration). (b) Response of the system to a 100 pA input current step. The acquired signal has been digitally filtered with 5 Hz bandwidth. From: M. Vergani et al., 2012. Multichannel Bipotentiostat Integrated With a Microfluidic Platform for Electrochemical Real-Time Monitoring of Cell Cultures". IEEE Trans. Biomed. Circuits Syst., Vol. 6, No. 5.

On the basis of Vergani experiment, the comparison between the three pumping systems of **Figure 10** have been performed in the absence of biomediator. This procedure allows to remove the possible signal variability occurring in the case of a different preparation of the biomaterial. **Figure 14** depicts the amperometric registration obtained by the flow injection of buffering solution, into the measuring chamber, via Mariotte pump.

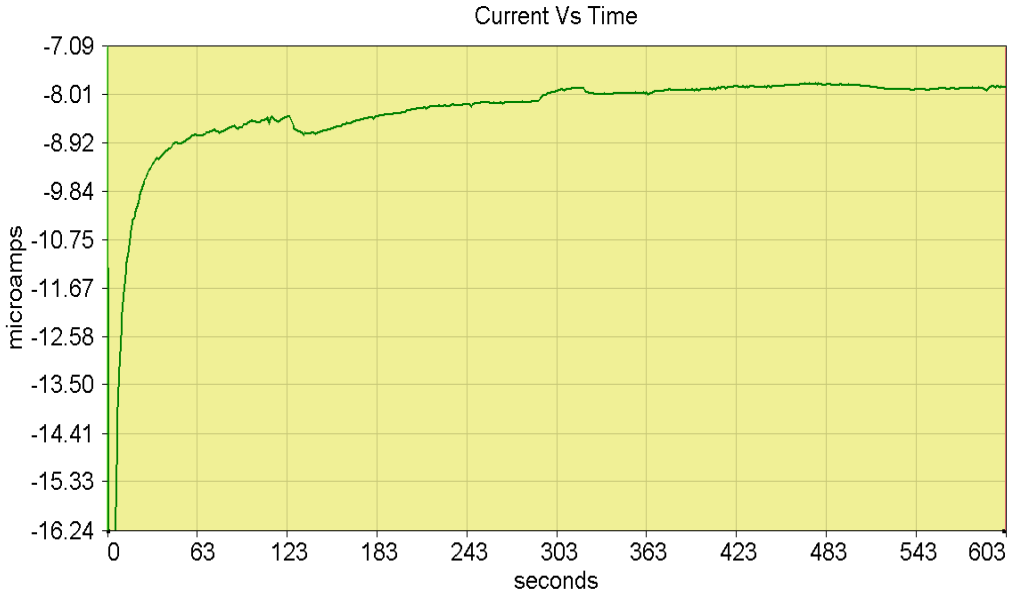

Fig. 14. Experimental results of amperometric signal from experimental fluidic setup

An evident improvement of the readout signal can be observed due to the complete absence of mobile mechanical components, in favor of a fluid motion regulated by the simple pression laws discussed in the previous section.The overlaying of current curves (showed in **Fig. 15**) obtained from Gilson Minipuls 3, Biosensor's in-house built peristaltic pump and Mariotte prototype allows to carry out different considerations.

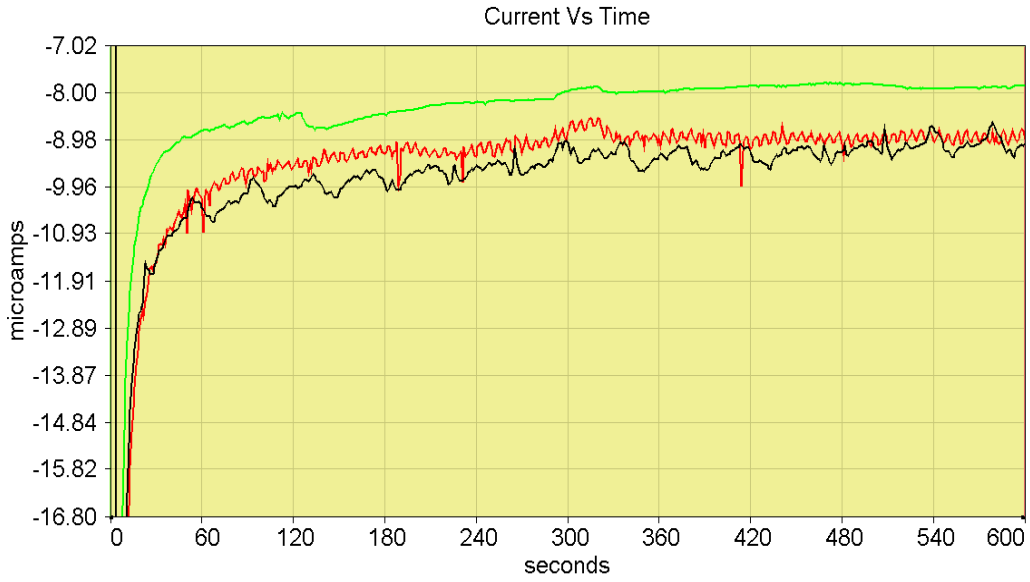

Fig. 15. Overlay of the curves obtained with different flow distribution devices

Firstly, a higher baseline current is registered in the absence of biomediator independently from the pumping system. This allows to hypothesize that the protein cage used to immobilize the photosynthetic element (or the biomaterial itself) is responsible for a diminishing in the electrical conductivity of the working electrode. Secondly, even if the difference between the baseline currents produced by Gilson peristaltic pump and Biosensor's peristaltic pump is reduced, a wide periodic fluctuation is always present in the second device. On the one hand, this indicates the need for further improvements in the mechanical setup of Biosensor's pump and its system of filters for the reduction of noise; on the other hand, attention is required when filtration arrays are applied, to avoid the concrete risk of losing information deriving from the biomediator. A relevant consideration arising from the data analysis of figure 15 is the observation of a current signal in the Mariotte system free from the background noise visible in Gilson and Biosensor's peristaltic pumps. The wider amplitude registered for current perturbation of 0.2 μA is 50% lower than the Gilson Minipuls 3 (0.4 μA) and 75% lower than Biosensor's prototype (0.8 μA). In addition, an increased S/N ratio is expected demonstrating a superior performance on the whole. Indeed, the absence of a biomediator, in this final set of measurements do not allow to calculate the S/N ratio, make a calibration curve and estimate the low detection limit (LOD) or sensitivity. Nevertheless, an improvement of these parameters can be supposed with a deeper analysis of the backgroung current.

Being the metal-solution interface, characterized by metal charged species and oriented dipoles that form the so called electrical double layer, it behaves as a capacitor characterized by a charging current appearing in electrochemical experiments. This current, visible in the first part of fig 15, decays exponentially with a cell time constant (τ), according to eq. 9:

$$I(t)= -(E/Rs) \exp [-t/(\tau)] \qquad (9)$$

with E= Applied potential; Rs= solution resistance. In Mariotte pumping system the decay appear clearly faster than Gilson and Biosensor's devices accounting for a lower interference on the

reduction current, improved signal-to-noise ratio and increased LOD (Limit of Detection) and sensitivity. The displayed results show a very important achievement for this kind of dynamic measurements as the information obtained by the biomediator result enhanced and strengthened by the new fluidic system. Even if additional experiments are required to assess important factors like the influence deriving from the biological materials and from the boundary conditions modifications, we demonstrated that a tangible improvement for the amperometric readout signal of the biosensor instruments was realized.

7. Future development

Although the present results are already relevant and encouraging, further steps aimed at miniaturizing the device and allowing its integration into a portable biosensor instrument have to be taken in the near future. The possibility of an efficient alternative to the classic peristaltic pump distribution system could be an evident breakthrough in the field of biosensors devices, as well as in other laboratory devices embedding fluidic microsystems. Stronger signals make more immediate and easier the interpretation of the information generated by a system, in order to simplify and make more effective the decision process of the involved operators.

Conclusion

A novel fluidic approach for electrochemical measurements based on a test fluid for readout signal cleanliness has been presented. Comparisons with other commercial fluidic systems used in the targeted field have been carried out. Evidence has been shown of an enhanced performance of a novel pumping system resulting in an improved reading of the final signal. The experimental characterization of the system confirmed the theoretical findings and a first functioning prototype device has been built. This device combines the absolute stability of the flow rate feeding the sensor with the non-contamination of the test fluid. In addition, the absence of moving mechanical parts and

need for external power supply, not only simplifies the system but it allows to reduce malfunctions and to considerably contain the cost.

References

[1] S.V. Dzyadevych, V.N. Arkhypova, A.P. Soldatkin, A.V. El'skaya, C. Martelet, N. Jaffrezic-Renault, Amperometric enzyme biosensors: Past, present and future, ITBM-RBM - Volume 29, Issues 2–3, April–May 2008, Pages 171–180;

[2] Palchetti, I., Cagnini, A., Del Carlo, M., Coppi, C., Mascini, M. & Turner, A.P.F., Determination of anticholinesterase pesticides in real samples using a disposable biosensor, Analytica Chimica Acta, 1997, 337, 315-321.

[3] Ivnitski, D., Abdel-Hamid, I., Atanasov, P. & Wilkins, E., Biosensors for detection of pathogenic bacteria, Biosensors & Bioelectronics, 1999, 14, 599-624.

[4] Klespitz, J.; Kovacs, L., "Peristaltic pumps — A review on working and control possibilities," Applied Machine Intelligence and Informatics (SAMI), 2014 IEEE 12th International Symposium on , vol., no., pp.191,194, 23-25 Jan. 2014.

[5] R. Jenkins, H. Harrison, B. Chen, D. Arnold, J. Funk, "Accuracy of intravenous infusion pump in continuous renal replacement therapies", American Society of Artificial Internal Organs, pp. 808-810., 1992.

[6] J. M. Berg, T. Dallas, "Peristaltic Pump", SpringerReference, 2013.

[7] Atencia J, Beebe D J. Steady flow generation in microcirculatory systems. Lab Chip, 2006, 6: 567-574.

[8] K. Buonasera, M. Lambreva , G. Rea, E. Touloupakis, M. T. Giardi. Technological applications of chlorophyll a fluorescence for the assessment of environmental pollutants Anal Bioanal Chem, Springer-Verlag 2011.

[9] K. Buonasera, G. Pezzotti, V. Scognamiglio, A. Tibuzzi, M.T.Giardi, "New Platform of Biosensors for Prescreening of Pesticide Residues To Support Laboratory Analyses". Journal of Agricultural and Food Chemistry, 58, 5982–5990, 2010 .

[10] M. Vergani, M. Carminati, G. Ferrari, E. Landini, C. Caviglia, A. Heiskanen, C. Comminges, K. Zór, D. Sabourin, M. Dufva, M. Dimaki, R. Raiteri, U. Wollenberger, J. Emnéus, M. Sampietro, "Multichannel

Bipotentiostat Integrated With a Microfluidic Platform for Electrochemical Real-Time Monitoring of Cell Cultures". IEEE Trans. Biomed. Circuits Syst., Vol. 6, No. 5, October 2012.

CHAPTER 6

“Automatic Photosystem II based Biodevices to reveal the effect of herbicides on Mutants of Photosynthetic Oxygenic Microorganisms”

Research in progress

1. Brief introduction

In the past few decades, environmental pollution has become one of the world's major concerns. A great number of toxic compounds, originating mostly from industrial effluents, agricultural activities and domestic sewages are principle responsible of environmental pollution. Most of the agricultural water pollution comes from the intensive farming technologies, which use massive amounts of herbicides and fertilizers that produce soil contamination and subsequent pollution of surface and underground water. Herbicides are among the most extensively used chemicals in the world and constitute an important threat to the human wellbeing (Florez et al., 2014). Therefore, early detection of toxic chemical compounds in the environment, particularly in water, and their biological effects on organisms has become increasingly important.

Detection of the pesticides is usually carried out by expensive time-consuming methods, such as, high-performance liquid chromatography (HPLC) or gas chromatography coupled with mass spectrometry (GC–MS), which require highly qualified personnel for the analysis (Rodriguez et al., 2002). The traditional environmental pollution assessments based on chemical analytical methods only provide information about the absolute concentrations of known chemicals in the environmental sample without an adequate interpretation of its toxicity to living organisms. Another disadvantage of chemical methods is the lack of information about the combined toxicity of different compounds such as additive, synergistic or antagonistic effects. Therefore, the development of more convenient alternative methods or parameters for assessment of the presence of pollutants and their toxicity to living organisms has become a major goal in environmental monitoring research (Giardi and Pace 2005).

Microalgae are now widely used as relevant biological indicators in the field of environmental impact studies. Owing to their ubiquity, short life cycles, easiness of culture and high sensitivity to a number of pollutants, these organisms are frequently utilized in ecotoxicological screening of contaminated water (Scognamiglio et al., 2010). Microalgae are especially sensitive to all those

pollutants that work as inhibitors at the photosystem II (PSII) level, such as heavy metals or half of the known pesticides (Brayner et al., 2011).

Among the wide range of microalgae species, which have been employed to develop biosensor technology, Chlamydomonas reinhardtii possess a number of, features that suite perfectly the requirements of an early warning environmental biosensor (Giardi and Piletska, 2006). It is grass organism and easily cultivable having 8 hours doubling time and it can grow with or without carbon source. Beside, it is easily transformable and all 3 genomes are sequenced. Taking advantage of these features, amperometric and optic biosensors based on the green photosynthetic microalgae *C. reinhardtii* have been developed in our lab to be able to detect pesticides in the environmental and food samples (Silletti et al 2015). Recent efforts have focused on increasing the stability and selectivity of PSII from algae for the detection of different subclasses of pollutants (herbicides and heavy metals). This could be achieved in various ways, such as by using the alga *C. reinhardtii* mutated at the QB herbicide-binding site by site-directed mutagenesis. This unicellular alga is easily modifiable by genetically engineering the D1 protein and many mutants have already been selected for their sensitivity or tolerance to herbicides (Johanningmeier et al., 2000; Tibuzzi et al., 2007; Buonasera et al., 2009).

Beyond these achievements, nowadays the market needs a highly specific and precise in situ measurement device able to collect and send the data in real-time for a period of at least one week without maintenance under multi-stressor conditions in a marine or offshore surrounding. The nature of these measurement device demands more robust algal biomediators. Another challenge is the preservation of the algal photosynthetic functionality when integrated with non-biological electronic components or operated under fluctuating environmental conditions. In this context production and the characterization of new-engineered algae strains that have longer half-life and able to tolerate ROS stress becomes essential. In *C. reinhardtii*, reducing the formation of $_1O^2$ and ROS thus lessening the photooxidative membrane damage (including the reactive center protein) and increasing

the stability and sensitivity for biosensor applications is of special interest. Recent advances in photosystem II biochemistry and molecular biology (site-directed mutagenesis) have produced several mutants that are resistant to extreme conditions, characterized by alterations in the amino acid composition of a reaction center protein called D1 (Johanningmeier et al., 2000; Oettmeier et al., 1999). Environmental extremes that negatively impact photosynthesis seem to act primarily at the level of D1 protein metabolism (Mizusawa et al., 2003). In this context, the turnover ability of the D1 protein is of primary importance and its high rate of synthesis and degradation has been conserved throughout evolution because this preserves both the flexibility and the stability of the photosynthetic apparatus against environmental modifications.

The objective of this study is to develop and optimize optical microalgal biosensor for in-situ measurement of currently hard to measure chemical contaminants and biohazards, endowed with specificity to the PSII inhibitors. To this end two set of *C. reinhardtii* mutants, able to quench $_1O^2$ and other ROS, generated under extreme conditions, were produced by site-directed mutagenesis and UV-mutagenesis respectively, integrated into a newly developed single and portable device able to measure and collect PSII fluorescence induction data in real-time for a period of at least two weeks. The biosensor toxicity responses and data for a range of herbicides, such as diuron, atrazine, and irgarol was presented. This biosensor could be used as an early warning system in aquaculture and for assessing the good environmental status of the water sources in compliance with current European policies.

2. Materials and methods

2.1. Chemicals and materials

Glutaraldhyde solution (25% in water), simazine (2,4-Bis(ethylamino)-6-chloro-1,3,5-triazine), and ABTS (2,2′-Azino-bis(3-ethylbenzothiazoline-6-sulfonic acid) diammonium salt) were pucrchased from Fluka (Germany). Trolox (6-hydroxy-2,5,7,8-tetramethylchroman-2-Carboxylic Acid), diuron (3-(3,4-Dichlorophenyl)-1,1-dimethylurea), gallic acid monohydrate (3,4,5-Trihydroxybenzoic acid monohydrate) Rose bengal (4,5,6,7-Tetrachloro-2′,4′,5′,7′-tetraiodofluorescein disodium salt) and DPPH (1,1-diphenyl-2-picrylhydrazyl) were purchased from Sigma-Aldrich. All reagents were analytical grade and were prepared using deionized or distilled water.

2.2. Culture growth conditions of *C. reinhardtii* and production of mutants

C. reinhardtii stock cultures were maintained at 25^{o}C on agar plates prepared with Tris-acetate-phosphate (TAP) medium [Harris, 1989] under continuous white light illumination (50 µmol m^{-2} s^{-1}). Liquid cultures were similarly grown but on TAP liquid medium with agitation at 150 rpm. All experiments were carried out on cell cultures in the mid-exponential growth phase. *C. reinhardtii* wild-type cells 11/32b (Sammlung von Algenkulturen, Grttingen, FRG) with intronless psbA gene (IL) was used as the reference strain in all experiments (Bertalan et al., 2007).

In order to express antioxidative peptides in the green alga *Chlamydomonas reinhardtii*, we engineered a cassette system for the introduction of foreign peptides into the alga in a marker-gene-free transgenic approach. Expression and correct processing of the transgene product was achieved by a translational fusion of the cassette with the D1 subunit of photosystem II, a highly abundant chloroplast protein, which is proteolytically cut at its C-terminal end involving a protease naturally occurring inside the cell. This system has been used now for the introduction of antioxidative peptides

into the chloroplast compartment of *Chlamydomonas.* Coupling directly a foreign peptide to the most highly expressed protein in the chloroplast will allow an increased production of the foreign protein due to the 1:1 ratio with the D1 protein. The peptide is "cut-to-size" by the endogenous protease. **Table 1** shows the mutants hosting the antioxidant peptides placements in the PSII D1 protein C-terminal. Mutants UV150 and UV180 represent strains which were gradually exposed to UV light for a total time of 150 and 180 min UV-B light of 312 nm, distributed over a time period of 9 and 12 months, respectively. They were exposed to a total dose of about 30 and 25 kJ/cm^2 UV light (exact exposure scheme can be given). While the wild type alga does not survive a 45 min daily dose of 7 kJ/ cm^2, the UV180 strain tolerates this dose for 180 min.

Table 1. Mutants hosting the antioxidant peptides placements in the PSII D1 protein C-terminal.

Transformant	**Amino acid sequence of antioxidative peptide**	**Source of peptide**	**Reference**
Aox-m	WYSLAMAASDI	milk	Hernandez et al. 2007
Aox-e	LMSYTWSTSM	egg yolk (mutant of AOX 1)	Park et al. 2001
Aox-f	KSTVPERTHPACPDFN	Hoki (fish)	Kim et al. 2006

2.3. The fluorescence sensor: Monitoring of chlorophyll a fluorescence induction kinetics

An automatic bio-device, Photo II **(Fig. 1)**, designed by Biosensor.srl (www.biosensor.it), was used to measure and store chlorophyll fluorescence induction data (also known as fluorescence transient or Kautsky effect) for the control experiments performed on the ground as previously described (Cano et al., 2011). Different strains of *C. reinhardtii* can be placed in 24 measuring cells

in triplicate/quadruplicate and the fluorescence measurements can be recorded hourly for 20 days. The instrument allowed simultaneous determination of the following chlorophyll fluorescence parameters: F_0, F_m, F_v, the ratio F_v/F_m (where $F_v=F_m-F_0$ is the variable fluorescence), the area below the fluorescence curve, and the time to reach Fm in each sample. F_0 was calculated by using an algorithm that determined the line of best fit for the initial data points recorded at the onset of illumination; the best-fit line was then extrapolated to time zero to determine F_0 (Cano et al., 2011). In each measuring cell, two white light LEDs were programmed to switch on to provide light (50 µmol m^{-2} s^{-1}) for 7 h in a 24-h period, photoperiod necessary for the organisms to grow on Earth.

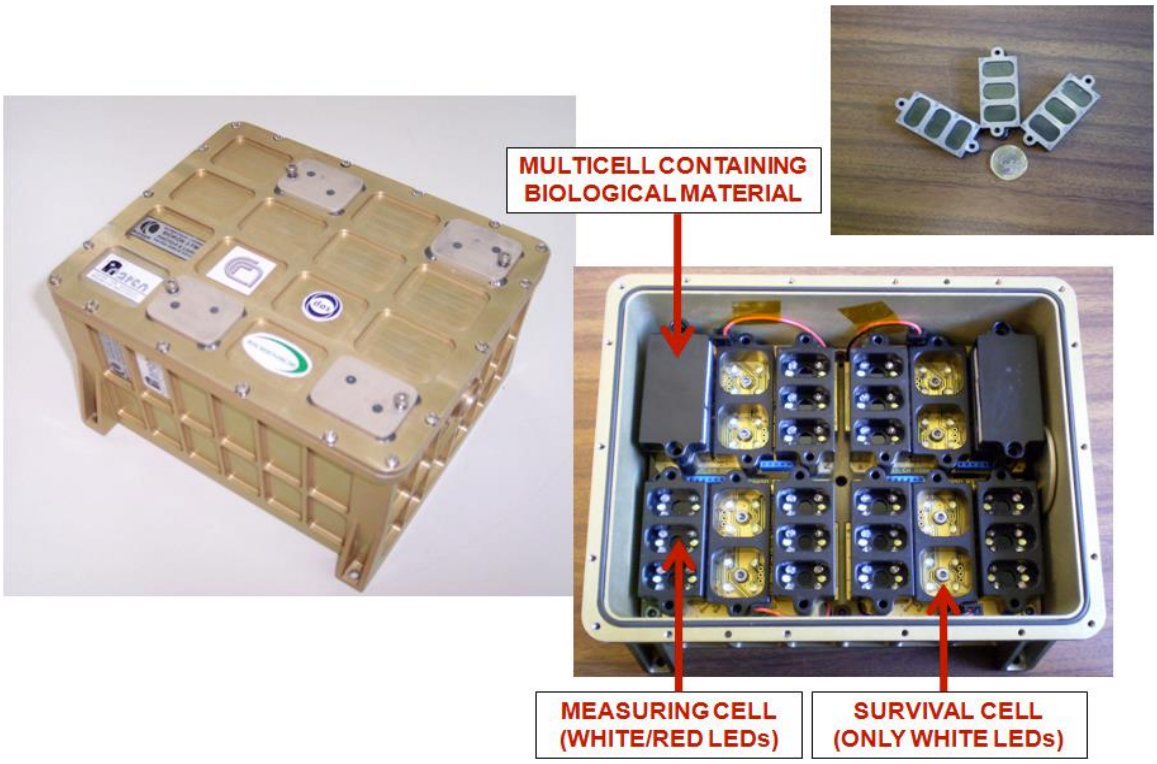

Fig. 1. The Photo II fluorimeter developed for Space missions; the main components are shown and highlighted. External box was built by Kayser-Italia, while electronics were built by Italian companies: Biosensor, Carso and Das.

2.4. Growth rate and chlorophyll content

Optical density (ABS_{750}) and chlorophyll content (ABS_{652}) was measured with an TU-1880 Double Beam UV-Visible spectrophotometer and cells counted using TC10TM automated cell counter (BIO-RAD) to establish growth curves. During the growth of mutants the maximum quantum yield of PSII photochemical reaction (Fv/Fm) was determined with Hansatech fluorescence monitoring system.

2.5. Sample preparation

Cells in exponential growth phase were collected and lyophilized at -50 ºC under vacuum overnight. After measuring exact dry weight (DW) of each sample, the lyophilized material was re-hydrated with bi-distilled water overnight at 4 ºC. Subsequently, samples were centrifuged and pellet frozen in liquid nitrogen. The cells were broken in methanol (1ml for each 10mg of lyophilized material), in presence of $NaHCO_3$ to avoid pH drop due to the cell lyses. Finally, the methanol extracts were centrifuged at 15000 g, at 4 ºC for 15 min., the supernatants were collected and stored at -20 ºC until analysis.

2.6. Determination of total phenolic content

Total phenolic content was estimated as gallic acid equivalent (GAE) according to the Folin-Ciocalteu method. Briefly, 0.1 ml of algae extract was mixed with 0.5 ml of Folin-Ciocalteu reagent (previously diluted 500 fold with distilled water) and the contents were thoroughly mixed. After 1 min, 0.4 ml of saturated sodium carbonate (7.5%) was added and the mixture was mixed thoroughly. After 30 min of incubation at room temperature, the absorbance at 765 nm was measured. Gallic acid (1-10 mg/ml) was used for the standart calibration curve. The results were expressed as gallic acid equivalent (GAE)/g dry weight of microalgae, and calculated as mean value ± SD (n= 4).

2.7. Determination of total lipid content

The gravimetric lipid analysis was carried out according to the method of Huang et al. (2009). 5 mg lyophilized microalgae samples were weighed in a pre-wighed 10ml tubes. 2 ml methanol, 2 ml chloroform and 1 ml NaCl 5% solution were added and the mixture was vortexed for 2 min. Subsequently the mixture was homogenized for 2 min. The homogenized mixture was centrifuged for 4 min at 8000 g in a thermostatic centrifuge at 10 ^{o}C and the lower layer was transferred to a pear-shaped flask with a Pasteur pipette. The extraction and homogenization steps were repeated 3 times and after each centrifugation, the lower $CHCl_3$ phase was added to the first extract. The collected sample was evaporated to dryness. Then the extracted weight recorded and the lipid content was calculated.

2.8. Determination of in-vitro and in-vivo antioxidant activity

2.8.1. 1,1-diphenyl-2-picrylhydrazyl (DPPH) radical scavenging activity assay

The antioxidant activity, based on the extract capacity to scavenge the stable 2.2-diphenyl-1-picrylhydrazyl (DPPH) free radical, was determined as described by Huang et al., 2005. The increasing volumes of cell extract was added to 0.25 ml 0.25mM DPPH methanolic solution. The mixture was vortexed for 1 minute and then the absorption of reaction mixture was measured at 517nm against methanol after 30 min incubation at room temperature in the dark. The antioxidant activity was calculated as the percentage of the DPPH scavenging ability, Scavenging effect (%) = [1- (Asample - Asample blank) / Acontrol]. The IC50 value was defined as the concentration of algae extract required to scavenge %50 of DPPH radicals. Trolox was used as positive control. Results were presented as means of experiments performed for four times ± standard deviation.

2.8.2. Trolox equivalent antioxidant capacity (TEAC) assay

The TEAC assay was measured according to the method of Arts et al. (2003) with slight modification. The ABTS+ radical cation was pregenerated by mixing 7 mM ABTS stock solution with 2.45 mM potassium persulfate and was incubated for 16 h in dark at room temperature until the reaction was completed and absorbance was stable. ABTS+ was diluted with water at room temperature to equilibrate its absorbance to 0.70 (±0.05) at 734 nm. 75µl of diluted samples were mixed with 675µl of diluted ABTS+ solution. The mixutere was allowed to stand for 6 min at room temperature and the absorbance was immediately recorded at 734 nm. Trolox solution (1-10 µg/ml) was used as reference standard. The results were expressed as mmol Trolox/g dry weight of microalgae, and calculated as mean value ± standard error (n = 4). The IC50 value was defined as as the concentration of algae extract required to scavenge 50% of ABTS radical.

3. Results and discussion

3.1. Physiological characterization of *Chlamydomonas* mutants

3.1.1. Chlamydomonas growth culture conditions (OD, chl, cell number, Fv/Fm)

To determine whether mutagenesis have any side effects on the physiological characteristics of the obtained mutants, studies such as growth rate, half-life and chlorophyll content were performed. It was obvious that UV-180 strain clump when grown in liquid media (either minimal or acetat-containing media, makes no difference) therefore it is not used for experiments performed in liquid medium. First, the growth was monitored for a period up to 2 months (**Fig. 2a and 3a**). It was found that mutagenesis did not effect the growth significantly, since very similar trends among the different mutants was obtained compared to the control strain IL. Consistent results were obtained when similar study performed by counting the cell content (**Fig. 2b and 3b**). In another study with mutants, the total chlorophyll content was investigated (**Fig. 2c and 3c)**. Maximum chlorophyll content was

measured as (67.00±2.40), (56.65± 2.26), (63.20±0.70), (66.15±0.55), (63.25±1.05), for IL, antiox-m, antiox-e, antiox-f and UV-150 respectively. Pigment content: Total chlorophyll (Fig. 4a), chlorophyll a (4b), chlorophyll b (4c), total carotenoids including xantophylls and carotenes (4d). Studies on half-life was performed by measuring total photosynthetic quantum yield against time for both cultures in liquid and agar medium (**Fig. 2d,e and 3 d, e).** The results showed that the survival rate was significantly increased for the UV-mutants whereas for the antiox-mutants comparable with the IL. In addition, no gross or microscopic changes detected with morphological evaluation. Taken together it was concluded that the mutagenesis had no detectable adverse effect on characteristic performance of mutants, such as growth or chlorophyll content and half-life except for UV-mutants, which has better half-life compared to IL.

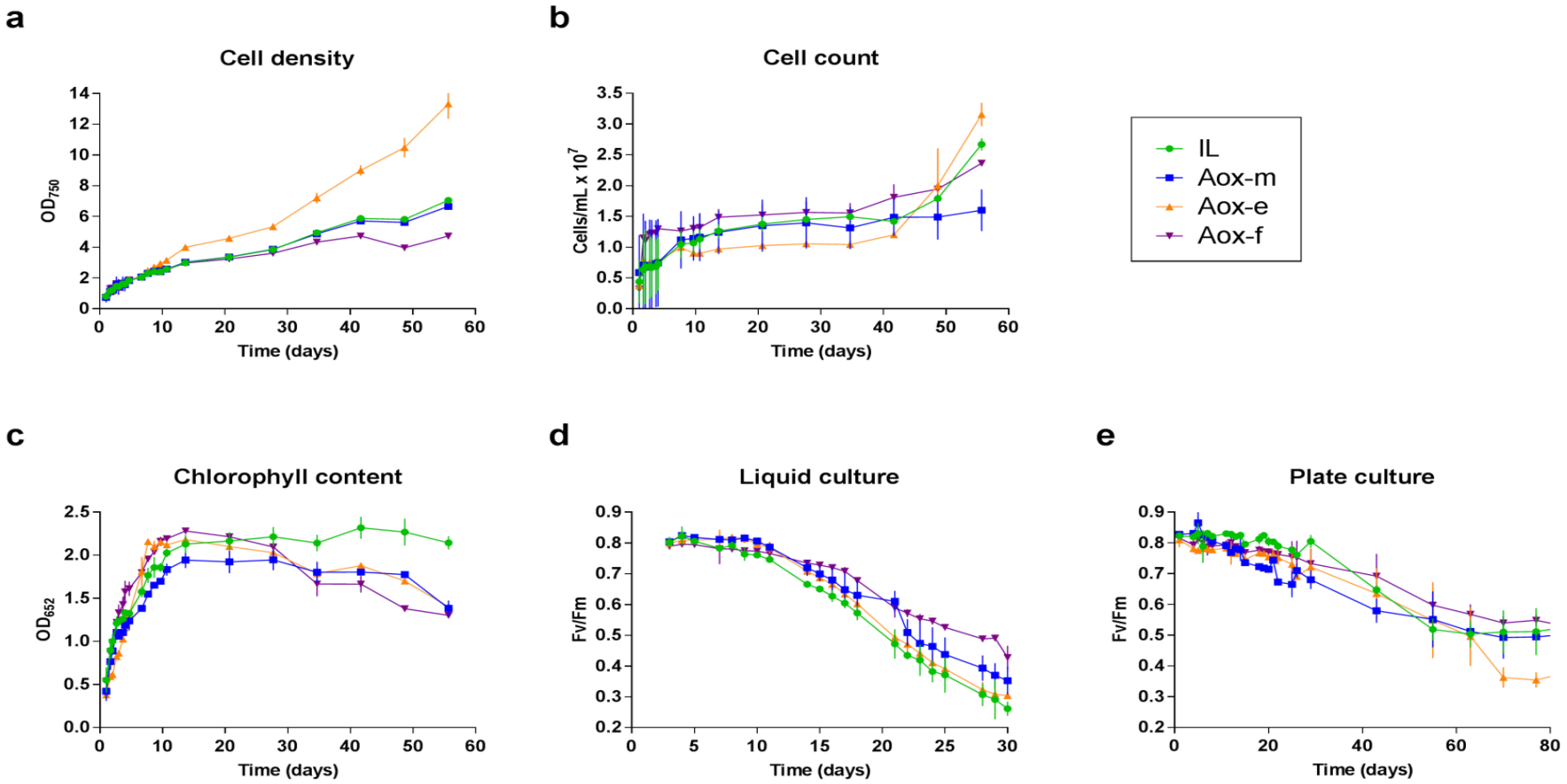

Fig. 2. Physiological characterization of *Chlamydomonas reinhardtii* IL strain and Aox mutants followed for up to 2.5 months. (a) (b) Cell culture growth curves expressed as optical density at 750 nm (OD_{750}) and cell counts, respectively. (c) Chlorophyll accumulation with time expressed as optical density at 652 nm (OD_{652}). (d) (e) Chlorophyll fluorescence expressed as the ratio between Fv, the variable component of fluorescence, and Fm, the maximum value achieved during recording in liquid cultures and agar plates, respectively. Symbols show the average of four independent experiments with error bars indicating the standard deviation.

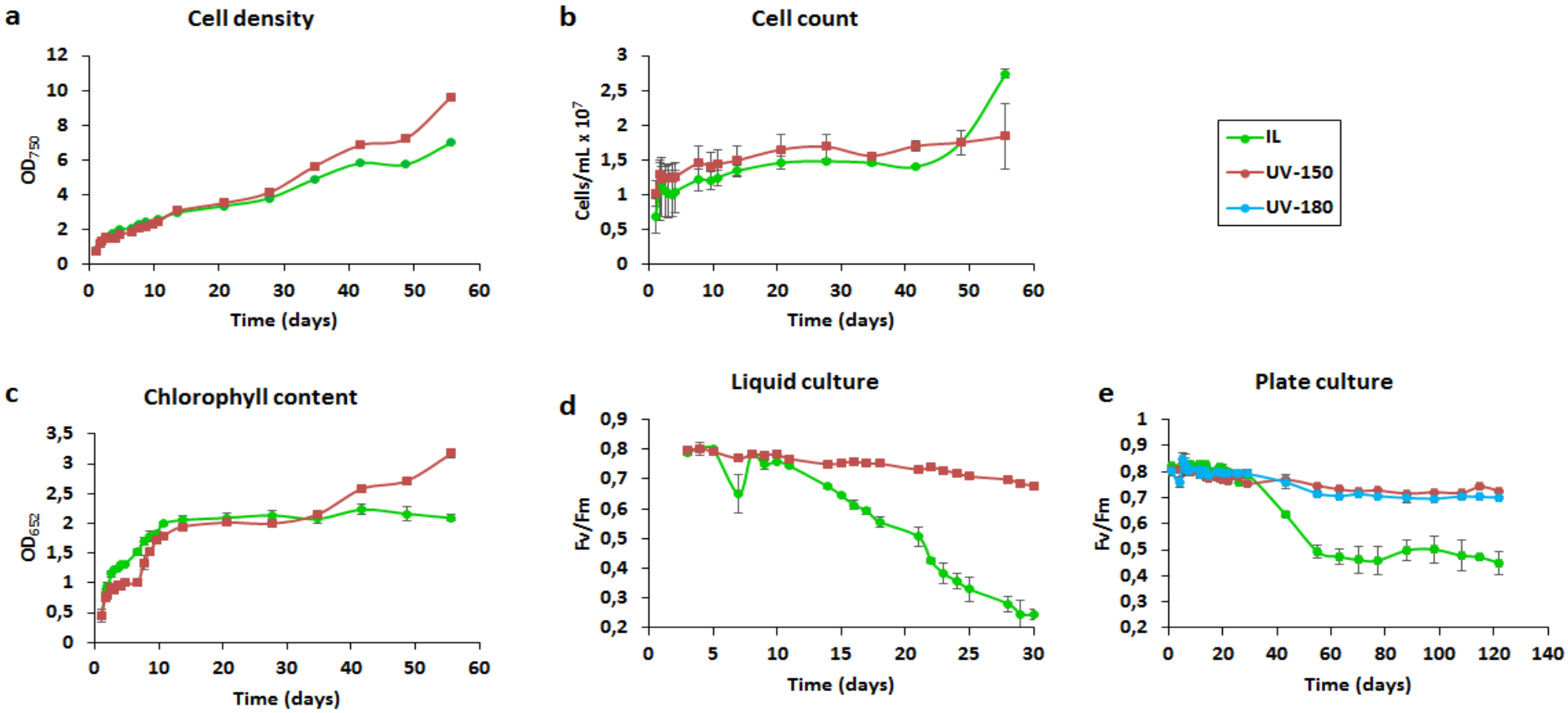

Fig. 3. Physiological characterization of *Chlamydomonas reinhardtii* IL strain and UV mutants followed for up to 4 months. (a) (b) Cell culture growth curves expressed as optical density at 750 nm (OD_{750}) and cell counts, respectively. (c) Chlorophyll accumulation with time expressed as optical density at 652 nm (OD_{652}). (d) (e) Chlorophyll fluorescence expressed as the ratio between Fv, the variable component of fluorescence, and Fm, the maximum value achieved during recording in liquid cultures and agar plates, respectively. Symbols show the average of four independent experiments with error bars indicating the standard deviation.

3.1.2. Total lipid and phenol content

Shetty and friends (Shetty et al., 2015) suggested that microalgal lipids should also be considered when using microalgae as a source of natural antioxidants. Polyphenols like-lipid of microalgae exhibited markedly antioxidant activities and other physiological actions including antibacterial, chemopreventive, UV- protective and antiproliferative effects. They are also known to act as detoxifying agents against heavy metals, and have myriad other bioactivities that could potentially be exploited for use in functional foods (El-Baky et al., 2009). Thus, microalgae lipids also play an important role in protection of microalge under harsh environmental conditions.

In the present study the total lipid content determined in *Chlamydomonas reinhardtii* mutants cultures are shown in **Fig. 3f** and **Fig. 4**. The highest lipid content was recorded for Aox-e culture (28%±1.2) followed by IL (25%±1), antiox-f (23%±0.8). The lowest lipid content was obtained for both Aox-m and UV-150 (21%±0.8). It can be concluded that the mutations slightly effected the total lipid content with the difference in the range of 2 to 4% compared to control IL.

Phenolics are secondary metabolits that play an important role in the maintenance of the microalgae. The presence of phytoconstituents, suc as phenols, flavonoids and tannin in microalgae indicates the possibility of antioxidant activity and this activity will help in preventing a number of diseases through free radical scavenging activity. Phenolic compunds are commonly found in plants and have been reported to have several biological activities including antioxidant properties. Many studies focused on the biological activities of phenolic compounds, which have potential antioxidants and free radical scavengers.

In the present study the phenolic content of the *C. reinhardtii* Aox mutants were evaluated using the Folin-Ciocalteu method and and were expressed as GAE **Fig. 3e and Fig 4**. The highest phenol content was measured for the Aox-e mutant whereas the UV-150 showed the lowest phenol content. Aox-m and Aox-f showed lower phenolic content than the control strain IL.

3.1.3. Antioxidant activity (TEAC, DPPH)

There are many methods to determine antioxidant capacity and they differ in terms of their assay principles and experimental conditions. Consequently, in different methods antioxidants in particular have varying contributions to total antioxidant potential. ABTS radicals and DPPH radicals are stable radical sources and they could provide a ranking order for antioxidants. The TEAC assay, which was the ABTS radical cation decolorization assay, was widely applied to evaluate the total antioxidative activity in both lipophilic and hydrophilic samples (Sheih et al., 2009). The DPPH radical was also one of the few stable radical sources and widely used to test the free radical scavenging ability of various samples (Meenakshi et al., 2012). Decolorization of DPPH suggests the presence of electron and hydrogen donors in algal extracts.

In the present study, we tested the antiox-mutants antioxidative activity in two different, DPPH and TEAC, oxidation systems in comparison with natural antioxidant Trolox. Reaction of the antiox-mutants with ABTS radical was shown in **Fig. 4g** and **Fig 5**. The 50% inhibition concentration (IC50) of the control IL and the antiox mutants in comparison with the standard antioxidant Trolox was reported in **Table 2** and **Table 3**. The control strain IL exhibited the highest ABTS radical scavenging activity with IC_{50} 0.09 mg/ml and the mutant UV150 was the lowest (**Fig. 5**). The control strain IL had the highest antioxidant activity against DPPH radical (IC_{50} 1.59 mg/ml) compared the mutant strains **Fig. 4h and Table 2**

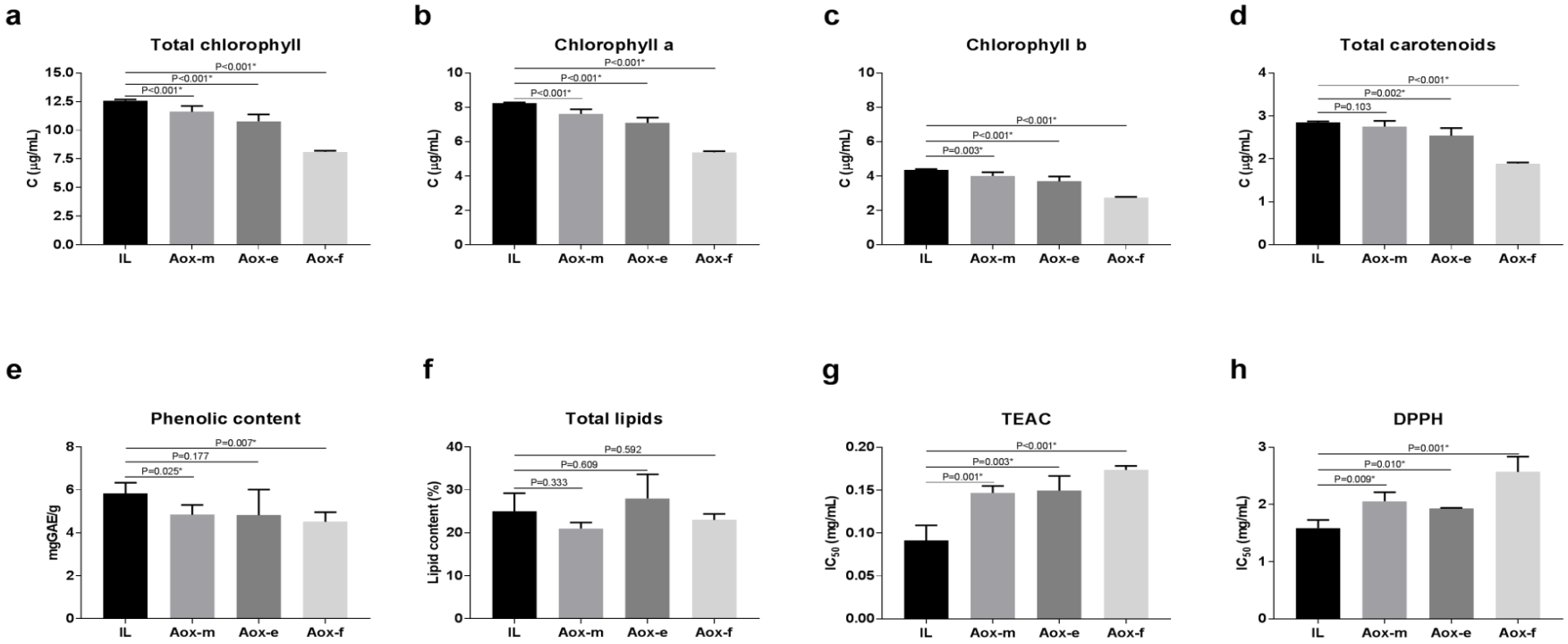

Fig. 4. Pigment identification, composition and antioxidant activity of *Chlamydomonas reinhardtii* IL strain and Aox mutants. (a) Total chlorophyll content. (b) Chlorophyll a content. (c) Chlorophyll b content. (d) Total carotenoids (sum of xanthophylls and carotenes) content. (e) Total phenolic content expressed as gallic acid equivalent (f) Total lipid content expressed in percentage of dry weight. (g) Trolox equivalent antioxidant capacity (h) 1,1-diphenyl-2-picrylhydrazyl (DPPH) radical scavenging activity.

Antioxidant assay	**Alga strain**	**IC_{50}**	**IC_{50} alga/trolox**	**µg trolox/g**
TEAC	IL	0.09	169.91	5.89
	Aox-m	0.15	273.35	3.66
	Aox-e	0.15	277.94	3.60
	Aox-f	0.17	322.96	3.10
	Standard Trolox	0.00054		
DPPH	IL	1.59	1028.18	0.97
	Aox-m	1.96	1267.78	0.79
	Aox-e	1.86	1205.07	0.83
	Aox-f	2.34	1515.80	0.66
	Standard Trolox	0.0015		

Table 2. Trolox equivalent antioxidant capacity and 1,1-diphenyl-2-picrylhydrazyl (DPPH) radical scavenging of the *Chlamydomonas* and its Aox mutant strarins.

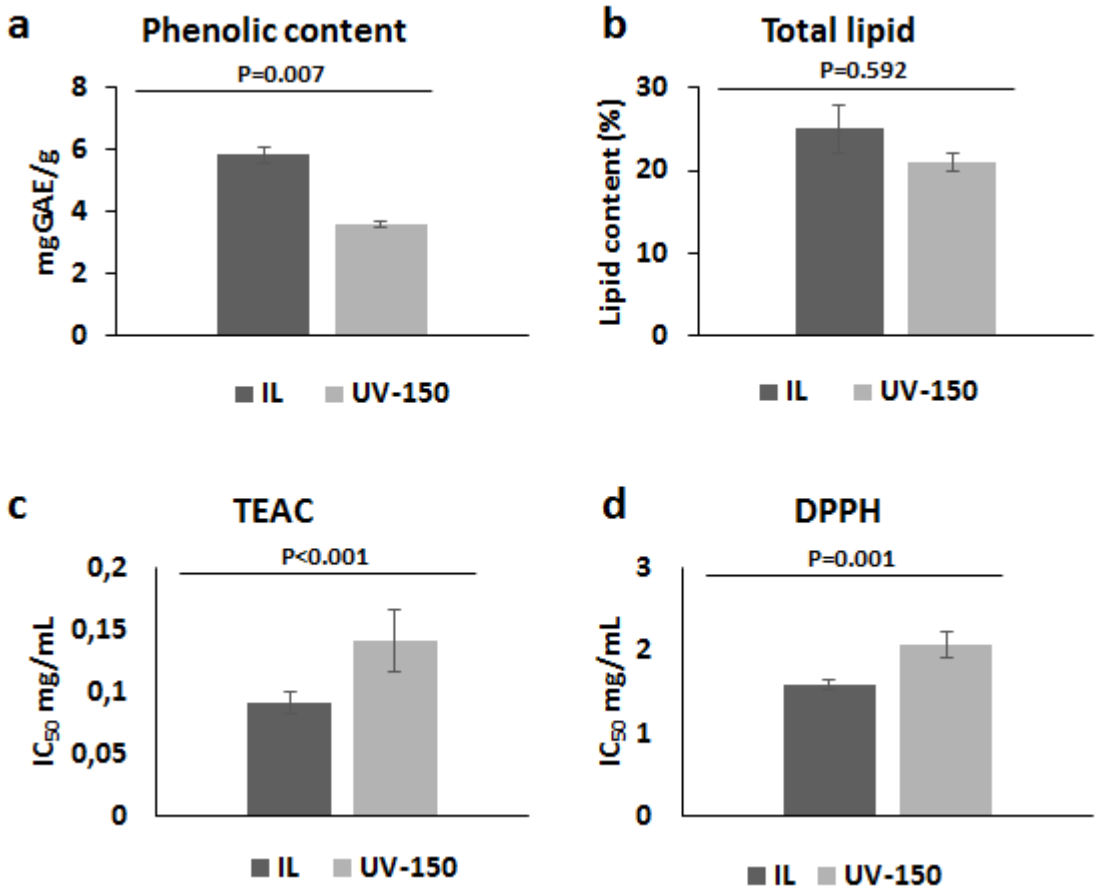

Fig. 5. Composition and antioxidant activity of *Chlamydomonas reinhardtii* IL strain and UV mutants. (a) Total phenolic content expressed as gallic acid equivalent (b) Total lipid content expressed in percentage of dry weight. (c) Trolox equivalent antioxidant capacity (d) 1,1-diphenyl-2-picrylhydrazyl (DPPH) radical scavenging activity.

Table 3. 1,1-diphenyl-2-picrylhydrazyl (DPPH) radical scavenging activity of the Chlamydomonas and its UV-mutant strarins.

Antioxidant assay	**Alga strain**	**IC_{50}**	**IC_{50} alga/trolox**	**µg trolox/g**
TEAC	IL	0.09	169.91	5.89
	UV-150	0.14	263.41	3.80
	Standard Trolox	0.00054		
DPPH	IL	1.59	1028.18	0.97
	UV-150	2.07	1340.21	0.75
	Standard Trolox	0.0015		

3.2. Oxidative stress

It was reported that the changes in ROS, fluctuations in the antioxidants concentrations in photosynthetic cells might have important consequences not only for defense metabolism but also for the regulation of genes associated with adaptive responses. This lower in-vitro antioxidant capacity in atioxidant mutants may be attributed to the continuous release of antioxidant peptides into the thylakoid lumen during D1 protein turnover and therefore suppress the production of enzymes involved in antioxidant defense and other secondary metabolites under optimal conditions. Thus, it is desirable to evaluate the antioxidant properties of selected strains expressing the peptides, since in-vitro antioxidant activity alone does not give real time information about the ability of strains to cope with ROS and especially $_1O^2$ in the presence of stressors affecting photosynthetic light reactions.

3.2.1. Rose Bengal and Oxygen peroxide

Finally, a study with mutants to assess their general in-vivo antioxidant activity was performed in the presence of $_1O^2$ precursors such as a photosynthesizer dye rose bengal and hydrogen peroxide. It was observed that antiox-mutants retained alive on agar whereas wild type (WT) and intronless (IL) wild strain disappeared **Fig. 5**. The results proved that the introduction of foreign peptides into the alga significantly increased the survival rate compared with the reference strain IL.

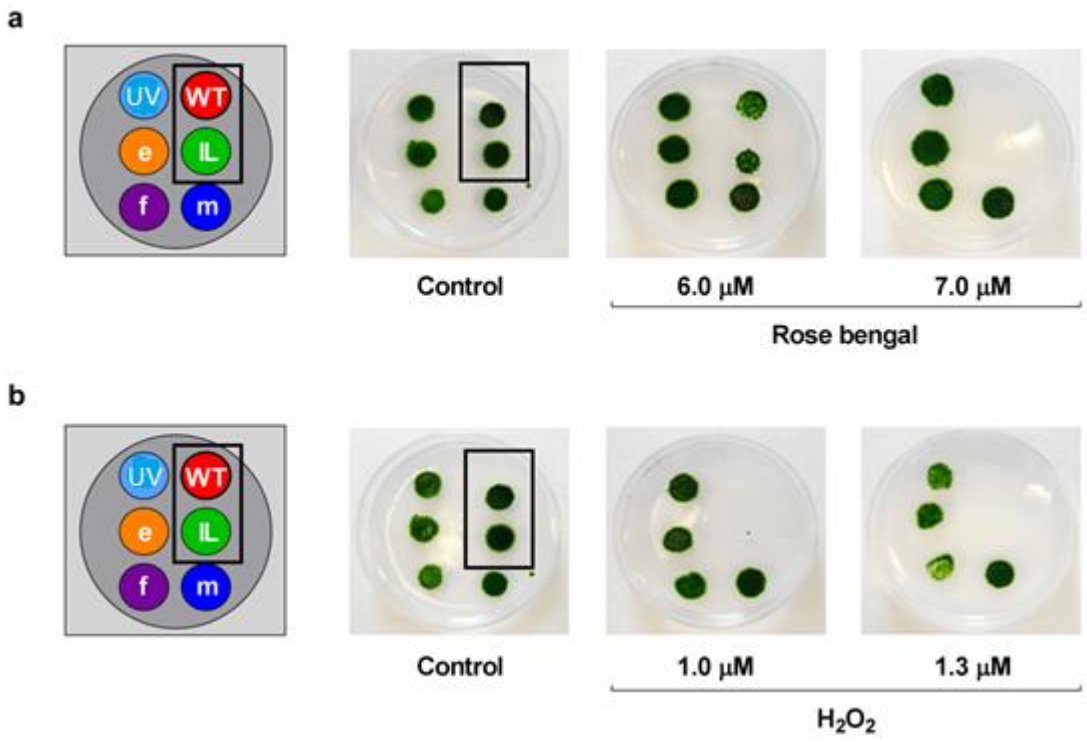

Fig. 5. *Chlamydomonas reinhardtii* controls (wild type, WT; and intronless, IL), antiox (Aox-e0, Aox-e, Aox-f and Aox-m) and UV (150) mutants grown in agar plates containing increasing amounts of substances generating reactive oxygen species: (a) rose bengal, and (b) hydrogen peroxide, H_2O_2.

3.3. Effect of photosynthesis inhibitors (atrazine, diuron, irgarol)

Here we presented the *Chlamydomonas reinhardtti* (IL) and its mutants (Aox-e, Aox-f) response to important PSII inhibitors, such as diuron, atrazine and irgarol under marine ionic strength were investigated. The results were summarized in **Table 4.** The I_{20} result obtained for IL were compared with those of obtained for Antiox mutants. I_{20} values of diuron were determined to be 0.754, 0.529 and 0.072 µg/L for IL, Aox-e and Aox-f respectively. For irgarol, the corresponding results were 0.328, 0.719 and 1.83×10^{-4} µg/L suggesting the hazardous impact of this compound was higher towards Aox mutants than IL. In conclusion, there was significant difference in the response of the each strain, which reflected the fact that mutation improved the sensitivity pattern to toxicants.

Alga strain	Photosynthesis inhibitor	Linear range (μg/L)	R^2	LOD I_{20}	
				μg/L	M (x 10^{-9})
IL	Diuron	5.00-125	0.991	0.754	3.23
	Atrazine	5.00-125	0.995	1.41	6.54
	Irgarol	5.00-125	0.991	0.238	0.939
Aox-e	Diuron	0.500-50.0	0.999	0.529	2.27
	Atrazine	5.00-125	0.981	1.12	5.19
	Irgarol	5.00-125	0.997	0.719	0.284
Aox-f	Diuron	0.500-50.0	0.999	0.072	0.309
	Atrazine	0.500-50.0	0.999	0.084	0.389
	Irgarol	0.500-50.0	0.999	$1.83x10^{-4}$	$7.22x10^{-4}$

Table 4: Inhibition of C. reinhardtti (IL) and mutants (Aox-e and Aox-f) photosynthetic activity induced by various pollutants.

Conclusion

The physiological characteristics and antioxidant activity of the produced antiox and UV mutants of *Chlamydomonas* were studied. The growth of the mutant cultures has the same characteristics except of the UV-180, which clumped in liquid tris-acetate-phosphate medium. Aox-e showed lower chlorophyll content than control strain IL whereas the other mutant's chlorophyll content did not differentiate significantly from IL. The half-life of UV-mutants was increased and for antiox-mutants it did not deviated significantly than control IL. Total phenol and lipid content was decreased at mutant strains. The mutant strains showed lower in-vitro antioxidant activity however, their in-vivo antioxidant activity in the presence of hydrogen peroxide and Rose Bengal was increased

and as a consequence of this benefit the survival rate of the antioxidant mutants on agar plates was extended. Keeping all this interesting results in mind, the produced mutants revealed to be a promising biomediator for improved environmental monitoring under multi-stressor conditions.

The biosensor able to carry out easy, fast and low cost in-situ measurements, replacing more sophisticated, expensive and slower laboratory analytical methods. Real-time results make it an early warning system for the aquaculture industry, beach surveillance and monitoring of water resources. The emergence of a technology based on photosynthetic proteins could benefit those working to develop several commercial devices. The production of mono and/or multi-molecular layers of either natural or engineered photosynthetic systems has become a reality. They can serve as a foundation for the development of commercial biosensors and biochips, photoelectrical and photochemical devices and perhaps alternative computers. Moreover, the proposed biosensors go far beyond the current state-of-the art in terms of stability and robustness parameters in operation by combining innovations in nanotechnology and molecular biology leading to the development new neutraceuticals for bioregenerative life support symstems in space research.

References

Arts, M.J.T.J., Dallinga, J.S., Voss, H.P., Haenen, G.R.M.M., Bast, A., 2003. A critical appraisal of the use of the antioxidant capacity (TEAC) assay in defining optimal antioxidant structures. Food Chemistry 80, 409-414.

Bertalan I., Esposito D., Torzilla G., Faraloni C., Johanningmeier U., Giardi M.T., 2007. Microgravity Science and Technology 19(5), 122-127. DOI: 10.1007/BF02919466

Buonasera K, Pezzotti G, Scognamiglio V, Tibuzzi A, Giardi M.T. 2009. A new platform of biosensors for pre-screening of pesticide residues to support laboratory analyses. J Agric Food Chem

Brayner, R., Coute, A., Livage, J., Perrette, C., Sicard, C., 2011. Micro-algal biosensors. Anal.Bioanal.Chem. 401,581-597. doi: 10.1007/s00216-011-5107-z.

Cano J.B., Giannini D., Pezzotti G., Rea G., Giardi M.T., 2011. Space Impact and Technological Transfer of a Biosensor Facility to Earth Application for Environmental Monitoring. Recent Patents on Space Technology, 1 (1),18-25.

El-Baky, H.H.A., El-Baz, F.K., El-Baroty, G.S., 2009. Production of phenolic compounds from Spirulina maxima microalgae and its protective effects in vitro toward hepatotoxicity model. African Journal of Pharmacy and Pharmacology. 3 (4), 133-139.

Florez, D.V., de la Hera, C., Costas, E., Orellana, G., 2014. Microalgae dual-head biosensors for selective detection of herbicides with fiber optic luminescent O_2 transduction. Biosensors and Bioelectronics 54, 484-491.

Giardi, M.T., Piletska, E.V. (Eds.), 2010. Biotechnological Applications of Photosynthetic Proteins: Biochips, Biosensors and Biodevices, Landes Bioscience-Springer Science and Business, Georgetown, TX

Giardi, M.T, Pace, E. 2005. Photosynthetic proteins for technological applications. Trends Biotech 25:253–267

Giardi MT, Guzzella L, Euzet P, Rouillon R, Esposito D., 2005. Detection of herbicide subclasses by an optical multibiosensor based on an array of photosystem II mutants. Environ. Sci. Technol. 39:5378–5384

Harris, E., 1989. The Chlamydomonas Sourcebook. A Comprehensive Guide to Biology and Laboratory Use. Elizabeth H. Harris. Academic Press, San Diego, CA, 1989. xiv, 780 pp., illus. $145., Science (New York, N.Y.). doi:10.1126/science.246.4936.1503-a

Huang, G.H., Chen, G., Chen, F., 2009. Rapid screening method for lipid production in alga based on Nile red fluorescence. Biomass and Bioenergy 33, 1386–1392. doi:10.1016/j.biombioe.2009.05.022

Husu, I., Rodio, G., Touloupakis, E., Lambreva, M.D., Buonasera, K., Litescu, S.C. et al. 2013. Insights into photo-electrochemical sensing of herbicides driven by *Chlamydomonas reinhardtii* cells, Sensors Actuators B Chem. 185, 321–330. doi:10.1016/j.snb.2013.05.013.

Johanningmeier, U. et al. 2000. Herbicide resistance and supersensitivity in Ala (250) or Ala (251) mutants of the D1 protein in *Chlamydomonas reinhardtii*. Pestic. Biochem. Physiol. 66, 9–19

Meenakshi, S., Umayaparvathi, S., Arumugam, M., Belasubramanian, T., 2012. In vitro antioxidant properties and FTIR analysis of two seaweeds of Gulf of Mannar. Asian Pacific Journal of Tropical Biomedicine. 1 (1), 66-70.

Mizusawa, N. et al. 2003. Degradation of the D1 protein of Photosystem II under illumination in vivo: two different pathways involving cleavage or intermolecular cross-linking. Biochemistry 42, 10034–10044

Oettmeier, W. 1999. Herbicide resistance and supersensitivity in photosystem II. Cell. Mol. Life Sci. 55, 1255–1277

Rodriguez, M., Jr. et al. 2002. Biosensors for rapid monitoring of primary-source drinking water using naturally occurring photosynthesis. Biosens. Bioelectron. 17, 843–849

Scognamiglio, V., Pezzotti, G., Pezzotti, I., Cano, J., Buonasera, K., Giannini, D., Giardi, M.T., 2010. Biosensors for effective environmental and agrifood protection and commercialization: from research to market. Microchim Acta 170 (3), 215-225.

Sheih, I.C., Wu, T.K., Fang, T.J., 2009. Antioxidant properties of a new antioxidative peptide from algae protein waste hydrolysate in different oxidation systems. Biosource Technology. 100, 3419-3425.

Shetty, V., Mokashi, K., Sibi, G., 2015. Variations among Antioxidant Profiles in Lipid and Phenolic Extracts of Microalgae from Different Growth Medium. Journal of Fisheries and Aquatic Science. 10 (5), 367-375. DOI: 10.3923/jfas.2015.367.375

Tibuzzi A, Rea G, Pezzotti G, Esposito D, Johanningmeier U, Giardi M.T. 2007. A new miniaturized multiarray biosensor system for fluorescence detection. J Phys Condens Matter 19:395006–395018

CHAPTER 7

“Development of biomimetic D1 peptides as novel photosynthetic based-biosensors for environmental monitoring”

Research in progress

1. Brief introduction

In the agri-food sector, the discovery of spontaneous D1 mutations in several weed species survived to the extensive use of the PSII herbicide atrazine, laid a foundation for the rationale use of herbicides, and provided insights into the molecular mechanisms underlying the photosynthetic electron transfer. Atrazine competitively inhibits Q_B binding to the D1 protein impairing the natural flux of the electrons to the subsequent acceptors, and inducing an accumulation of the reduced form of Q_A (Giardi et al., 2009). Other poisonous xenobiotics such as triazinic and ureic herbicides affect the photosynthetic electron transfer acting in a similar manner. This amazing feature of PSII to bind different classes of toxic compounds stimulated the design of analytical devices exploiting the photosynthetic activity of whole cells, or their active subcomponents, as bio-recognition elements (Cano et al., 2011; Giardi and Pace, 2006). In this context, although the use of thylakoidal membranes or isolated protein complexes provides high sensitivity, their extraction, purification or in vitro reconstitution procedures are often laborious, expensive and in some cases not always reliable. On the other side, whole cell-based biosensors preserve photosystem functionality, but provide a slow response and sometimes low sensitivity.

In the nanotechnology era, numerous research efforts have been focused on the design of novel biomimetic molecules able to simulate biological processes, such as the binding of specific analytes. These synthetic compounds include peptides, mini-proteins, imprinting polymers or aptamers, and usually derive from a size-minimization strategy, which also aims to fine-tune their sensitivity, selectivity, and robustness properties (Bondi and Pena 2016). The novel products can be exploited as simplified models to deepen the knowledge of the natural macromolecular functions and finding applications as molecular tools in the development of analytical devices, such as biosensors and biochips. Synthetic biomimicry approaches can help to build more robust biorecognition elements for biosensors, overcoming the problem of instability of current biomediators that limits their market applicability (Zhang et al., 2015; Hussain et al., 2013). Synthetic peptides that mimic parts of the

photosynthetic apparatus as biorecognition elements lead to an increased performance for the detection of environmental contaminants, including pesticides able to bind to D1 protein in the photosystem II and inhibit the photosynthetic process. Thus, the combination of computational analysis, molecular biology and biomimicking tools makes possible the use of more stable, sensitive, selective and specific biomediators for the development of effective biosensors (Scognamiglio et al., 2009).

Quantum dots (QDs) are nanostructured semiconductor materials discovered in 1981. They can be covalently bound to biomolecules, such as peptides, oligonucleotides, and proteins for different applications. The small dimensions of QDs and the easy modification of its surface with biomolecules make possible their use as labels for bioassays. In many cases, when they are coated with organic molecules and macromolecules, they can improve aqueous solubility and opportunities for bioconjugation properties, enhance the inherent sensitivity and expand new applications of fluorescence detection (Taoka et al., 2015). QDs and the carboxyl moiety confers water solubility, thus making QDs adaptable to various biologically relevant environments (Zhu et al., 2014). They have generated great interest for optical biosensing because the size controlled luminescence. Compared to other labels, QDs are more stable and cheap and have an important versatility because the different materials and sizes available. The use of QDs instead of enzymatic labels may save a significant amount of analysis time because the enzymatic reaction can be avoided and may save costs because the enzymatic substrates are not necessary (Yerga et al., 2013). With respect to their key features—resistance to photobleaching, large stoke shift and narrow emission spectrum QDs have great potential for dynamic environmental monitoring.

Based on this approach, this work following the previous study by Scognamiglio and coworkers (Scognamiglio et al., 2013), describes the use of biomimetic peptides of the photosynthetic plastoquinone binding niche of the green alga *Chlamydomonas reinhardtii* for pesticide measurement in environmental or food samples. The application of new technologies based on quantum dots,

nanoparticles and magnetic particles that could lead to improved response of the photosynthetic material and, therefore, to increased biosensor sensitivity up to the micromolar range was further explored.

2. Materials and methods

2.1. Reagents and solutions

Carboxyl derivatized nanoparticle QDs with emission maximum at 730 nm were purchased from PlasmaChem GmbH (Germany). Phosphate buffered saline (PBS), 1-[3-(dimethylamino)propyl]-3-ethylcarbodiimide hydrochloride (EDC), N-hydroxy succinimide (NHS) and anhydrous DMSO were purchased from Sigma-Aldrich. The peptides were produced by automated synthesis by GL Biochem Ltd. (Shanghai). The peptides were synthesized by liquid phase peptide synthesis (LPPS) and solid phase peptide synthesis (SPPS) platforms (FlexPeptideTM), and purified to obtain samples with >90% of purity. The synthetic molecules were analyzed by MS/HPLC and sequence confirmation was performed. All reagents were analytical grade and were prepared using deionized or distilled water.

2.2. Instrumentation

The fluorimeter is made up by six innovative measurement cell where for each lodging for the biological material, excitation light source, emission filters are integrated in a compact miniaturized sensor (30 mm external diameter, 20mm height) (**Fig. 1**). The optical module at the bottom is necessary for the excitation considering properties of the fluorophores or quantum dots. It is able to detect variation in emission intensity at fixed wavelength by fluorescent analyses. In relation to quantum dots used it is possible to set the light wavelength excitation and the wavelength of filters. A cuvette that can contain a quantity of liquid ranging from 50 µl up to 200 µl was used for the

measurements. It is possible to connect the instrument to a computer for data analysis. In order to provide saturated light two LEDs were used for each of six cells with different excitation wavelength to provide flexible use of different fluorophores and to target the corresponding maximum light absorption peaks.

Fig. 1. Fluorimeter with six measurement cell (www.biosensor.it)

2.3. Conjugation of biomimetic D1 peptide to QDs nanoparticles

The carboxyl-functionalized QDs were covalently attached to biomimetic peptide by using EDC coupling chemistry. Briefly, QD nanoparticles were activated by mixing 20µl of QD710 stock solution (5 mg/ml) with 6µl of EDC (320mg/ml) and NHS (80mg/ml) in a final volume of 200µl phosphate buffer (50mM, ph:7.4) and incubated for 30 min at room temperature with gentle shaking. The mixture was centrifuged for 3 min at 13500 rpm to precipitate the activated QDs. If necessary, the centrifugation step was repeated to remove residual organic chemicals. The pellet was resuspended in 200µl phosphate buffer and to this 20µl of biomimetic D1 peptide (0.5mg/ml in DMSO) was added and incubated for 2h at room temperature with gentle shaking. At the end of the incubation the mixture was centrifuged for 3 min at 13500 rpm to precipitate the QDs-D1 peptide conjugate. The centrifugation step was repeated to remove unbound biomimetic peptide. Finally the

QDs-D1 peptide conjugate was resuspended in 200µL phosphate buffer and stored in dark at 4ºC when in not use. The efficiency of coupling was found to be 90%.

2.4. Assay procedure and fluorescence measurement

An aliquot of 10 µL of atrazine solution with a serial dilution was mixed with 25 µL of QDs-D1peptide conjugate and incubated for 30 min at room temperature with gentle shaking. After the incubation 165µL of PBS (50mM, pH:7,4) added and fluorescence emission measured by developed fluorimeter. The cuvette (200µL) was filled with final reaction solution and placed into the measurement cell with a fixed set up of 680nm excitation, 730nm emission, 20 A light intensity. Upon the attachment of atrazine to the Q_B binding pocket of D1 biomimetic peptide that leads to a conformational change and results with the variation in the emitted light intensity correlated with atrazine concentration was measured.

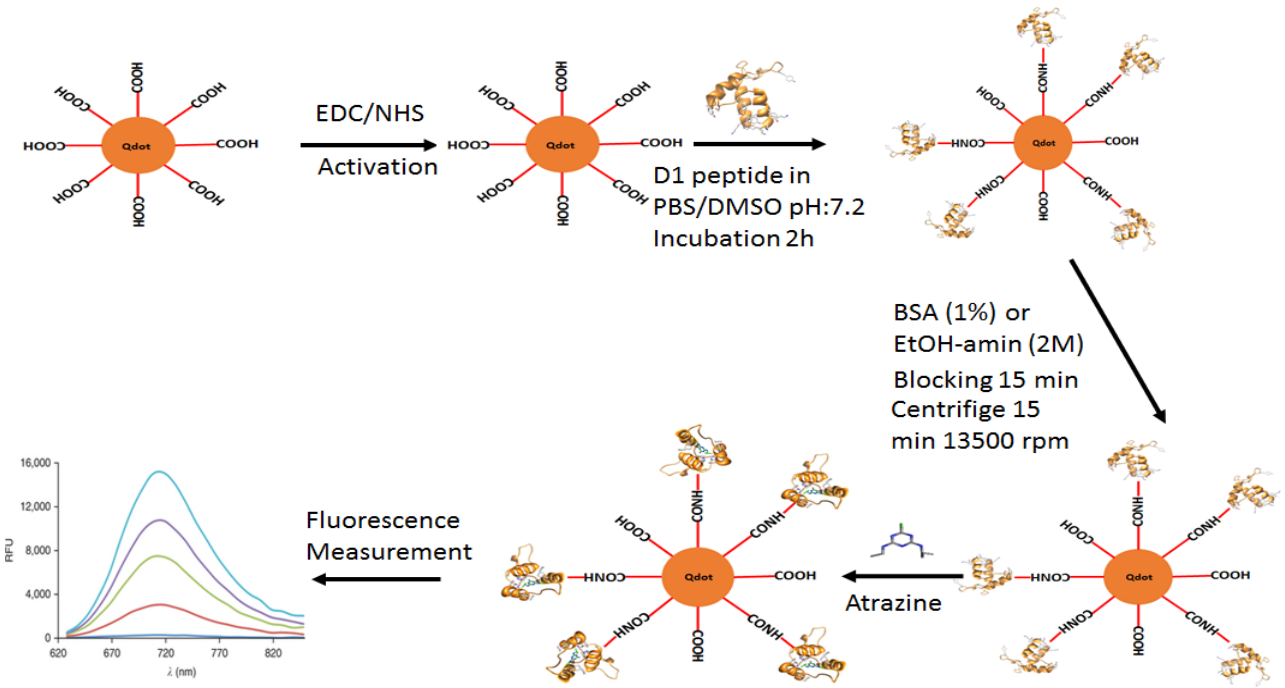

Scheme 1. Schematic representation of covalent coupling of biomimetic D1 peptide to carboxyl quantum dots by carbodiimide method and measurement principle.

3. Results and discussion

A computational strategy has been adopted for designing and minimizing the Q_B binding domain of *C. reinhardtii* as a receptor for atrazine binding. In particular, we explored by in silico/in vitro studies, the structure and binding ability of synthetic peptides that could mimic the Q_B herbicide binding niche of the PSII reaction center D1 protein. The primary sequences of the biomimetic peptides are reported in **Table 1**. In previous studies, we identified point mutations in D1 protein of photosystem II of the alga that increase atrazine binding affinity, particularly the mutant S268C which presents a sensitivity of 1 nM, a 10-fold increase over wild type (Rea et al, 2009; Giardi et al, 2009). After identification of key binding residues, biomimetic peptides containing the plastoquinone-binding site in a loop shaped by two alpha-helices were designed and characterized, showing high stability and affinity for the pesticide atrazine (affinity constant $3.52 \times 10^5\ M^{-1}$ for the selected peptide D1pepmut) (Scognamiglio et al, 2013). Hence, in this study we approached the goal of producing three new synthetic biomimetic peptides in order to increase the solubility in aqueous solvents by adding two histidines in the N- and C-terminus of the 70 aminoacid-peptide. In further steps, a cysteine was included in two of the modified peptides (S264C or S268C). The primary sequences of the biomimetic peptides are reported in **Table 1**.

Table 1. The primary sequences of the produced biomimetic peptides. The aminoacidic substitutions are highlighted in yellow. Green letters indicate the hydrophobic aminoacids.

D1pep70	FSAMHGSLVT SSLIRETTEN ESANEGYRFG QEEETYNIVA AHGYFGRLIF QYASFNNSRS LHFFLAAWPV
D1pepHis	HSAMHGSLVT SSLIRETTEN ESANEGYRFG QEEETYNIVA AHGYFGRLIF QYASFNNSRS LHFFLAAWPH
D1pepS264C	HSAMHGSLVT SSLIRETTEN ESANEGYRFG QEEETYNIVA AHGYFGRLIF QYACFNNSRS LHFFLAAWPH
D1pepS268C	HSAMHGSLVT SSLIRETTEN ESANEGYRFG QEEETYNIVA AHGYFGRLIF QYASFNNCRS LHFFLAAWPH

The peptides were labeled with different types of commercial carboxylated quantum dots (peak emissions from 510 to 710 nm) by carbodiimide reaction coupling and fluorometric detection was performed. In order to test the availability of the biomimetic peptides as biorecognition element, the preliminary investigation was performed with QDs-S264C and QDs-S268C conjugate in 50 mM phosphate buffer solution (PBS), pH 7.4 in the presence of 1 µg/L atrazine. The results confirmed that mutation S264C conferred resistance to atrazine and diuron, while the change S268C increased the sensitivity. When the atrazine concentration were increased, a decrease in the fluorescence intensity was observed. Under the optimal conditions, fluorescence intensity (ΔI) is found to have an inversely linear relationship with the concentration of atrazine over a concentration range of 0.5–10 µg/L **Fig. 2**. These results indicate that the proposed method employing biomimetic peptide S268C as recognition element is acceptable for the determination of atrazine at low concentration levels.

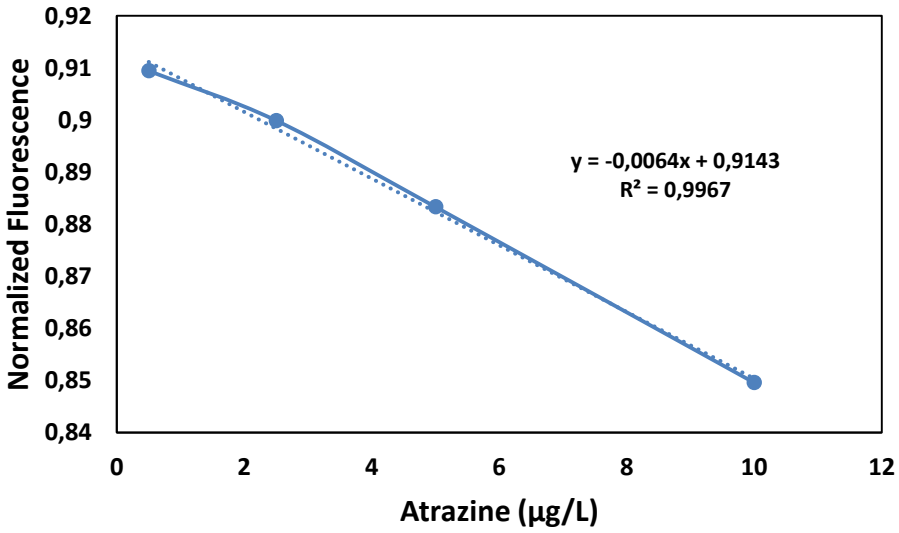

Fig. 2. Calibration plot for atrazine obtained with QDs-D1pepS268C conjugate.

Conclusion

The increasing knowledge of biological natural molecules continuously challenges and stimulates the design of novel and artificial materials with similar biomimetic properties. The recent progress in molecular engineering and nanotechnology witnesses the great interest to create novel molecular structures de novo or by rational design. In particular, the development of biomimetic peptides and small proteins is an expanding area in this research field, which will pave the way to a vast area of future applications. In this paper we described the first attempt to create novel D1-inspired biomimetic molecules with high potential applications in the realization of nanosensor arrays for the detection of herbicides. The synthesized biomimetic molecules were deeply characterized and their structural and functional features studied in response to atrazine binding. In this context, we reported that atrazine binding induces extensive changes in the peptide molecules, resulting in a more stable structure as indicated by fluorescence measurements. We have also documented that D1 peptide mutant S268C shows a high affinity towards atrazine, detecting the herbicide in the micromolar range. Taken together, these results showed that peptides could represent an important alternative as recognition molecules, exhibiting high sensitivity towards target analytes, without the stability and reliability weaknesses often associated with entire native proteins. Future efforts will be dedicated to further improve the peptide binding affinity towards atrazine, as well as to deliver a library of peptide variants with increased selectivity and sensitivity headed for a wide range of herbicides. This achievement will pilot the design of a nanosensor array of biomimetic molecules with different specificities for different chemical species, making these molecules a useful tool as probes in the development of last generation of biosensing systems.

References

Bondi, M.C.M., Pena, E.B., 2016. Analytical applications of biomimetic recognition elements. Analytical and Bioanalytical Chemistry. 408 (7), 1725–1726. DOI: 10.1007/s00216-015-9220-2

Cano J.B., Giannini D., Pezzotti G., Rea G., Giardi M.T., 2011. Space Impact and Technological Transfer of a Biosensor Facility to Earth Application for Environmental Monitoring. Recent Patents on Space Technology, 1 (1),18-25.

Giardi, M.T., Scognamiglio, V., Rea, G., Rodio, G., Antonacci, A., Lambreva, M., Pezzotti, G., Johanningmeier, U., 2009. Optical biosensors for environmental monitoring based on computational and biotechnological tools for engineering the photosynthetic D1 protein of *Chlamydomonas reinhardtii*. Biosens. Bioelectron. 25, 294–300. doi:10.1016/j.bios.2009.07.003

Giardi, M.T., Pace, E., 2006. Photosystem II-Based Biosensors for the Detection of Photosynthetic Herbicides, in: Biotechnological Applications of Photosynthetic Proteins: Biochips, Biosensors and Biodevices. Springer US, Boston, MA, pp. 147–154. doi:10.1007/978-0-387-36672-2_13

Hussain, M., Wackerling, J., Lieberzeit, P.A., 2013. Biomimetic Strategies for Sensing Biological Species. Biosensors. 3 89-107. DOI:10.3390/bios3010089

Rea, G., Polticelli, F., Antonacci, A., Scognamiglio, V., Katiyar, P., Kulkarni, S.A., Johanningmeier, U., Giardi, M.T., 2009. Structure-based design of novel *Chlamydomonas reinhardtii* D1-D2 photosynthetic proteins for herbicide monitoring. Protein Sci. 18, 2139–51.

Scognamiglio, V., Stano, P., Polticelli, F., Antonacci, A., Lambreva, M.D., Pochetti, G., Giardi, M.T., Rea, G., 2013. Design and biophysical characterization of atrazine-sensing peptides mimicking the *Chlamydomonas reinhardtii* plastoquinone binding niche. Phys. Chem. Chem. Phys. 15, 13108.

Zhang, D., Zhang, Q., Lu, Y., Yao, Y., Li, S., Jiang, J., Liu, G.L., Liu, Q., 2016. Peptide Functionalized Nanoplasmonic Sensor for Explosive Detection. Nano-Micro Letters 8 (1), 36-43. DOI 10.1007/s40820-015-0059-z

Zhu, H., Hu, M.Z., Shao, L., Yu, K., Dabestani, R., Zaman, M.B., Liao, S., 2014. Synthesis and Optical Properties of Thiol Functionalized CdSe/ZnS (Core/Shell) Quantum Dots by Ligand Exchange. Journal of Nanomaterials 2014, 1-14. Doi.org/10.1155/2014/324972

Yerga, D.M., Garcia, M.B.G., Garcia, A.C., 2013. Biosensor Array Based on the In-Situ Detection of Quantum Dots as Electrochemical Label. Sensors and Actuators B 182, 184-189.

APPENDIX A

“Better together: strategies based on magnetic particles and quantum dots for improved biosensing”

Moro, L., Turemis, M., Marini, B. et al., “Better together: strategies based on magnetic particles and quantum dots for improved biosensing” Biotechnology Advances, 35 (2017) 1; 51-63 DOI: 10.1016/j.biotechadv.2016.11.007

Abstract

Novel technologies and strategies for sensitive detection of biological responses in healthcare, food and environmental monitoring continue to be a priority. The present review focuses on bioassay development based on the simultaneous use of quantum dots and magnetic beads. Due to the outstanding characteristics of both particles for biosensing applications and the large number of publications using a combined approach, we aim to provide a comprehensive overview of the literature on different bioassays, the most recent advances and innovative strategies on the topic, together with an analysis of the main drawbacks encountered and potential solutions offered, with a special emphasis on the requirements that the transfer of technologies from the laboratory to the market will demand for future commercialization of biodevices. Several procedures used in immunoassays and nucleic acid-based bioassays for the detection of pathogens and biomarkers are discussed. The improvement of current approaches together with novel multiplex detection systems and nanomaterials-based research, including the use of multimodal nanoparticles, will contribute to simpler and more sensitive bioanalyses.

1. Introduction

Novel technologies and strategies for sensitive measurement of biological processes in healthcare, food and environmental monitoring and defense continue to be a priority. In the field of biosensors and bioassays, where labelled specific factors are used to emit a detectable signal, the unique properties of nanomaterials have led to the development of new assays and new transduction mechanisms with increased performance and sensitivity (Bally and Vörös, 2009; Jianrong et al., 2004).

Among the nanomaterials used for biosensing and imaging applications, quantum dots (QDs) have produced one of the most successful stories since their discovery in 1983 (Brus, 1984, 1983). However, it took until 1998 to establish the advantages of QDs for biological applications and biosensing tools (Bruchez et al., 1998; Chan and Nie, 1998). QDs are inorganic nanocrystals of around 1-6 nm with unique optical and chemical properties but complicated surface chemistry (Resch-Genger et al., 2008). Their optical properties are controlled by the constituent material, particle size and size distribution and surface chemistry, and widely rely on method of particle synthesis. Although QDs can be prepared with atoms from groups II-VI, II-V or IV-VI of the periodic table and in many different alloyed versions, the most popularly used are cadmium (Cd)-based QDs (Wegner and Hildebrandt, 2015). Typical QDs are core-only (such as cadmium telluride, CdTe) or core-shell (composed of a core of a semiconductor with a smaller band gap material, enclosed within a shell of another semiconductor material with larger spectral band gap; for example, cadmium selenide core with a zinc sulfide shell, CdSe/ZnS) nanostructures, which can be functionalized with different coatings (Resch-Genger et al., 2008). QDs optical properties include a high quantum yield even in near-infrared wavelengths; narrow, symmetric and size-tunable fluorescence spectra, and extremely broad and intense absorption, enabling a unique flexibility in excitation that overcomes some of the limitations of organic dyes (Esteve-Turrillas and Abad-Fuentes, 2013; Resch-Genger et al., 2008). This kind of nanoparticles therefore presents an additional advantage for multiplexing

approaches, since QDs with different sizes can be excited with a single wavelength of light, resulting in different emission peaks that can be measured simultaneously (Yang and Li, 2006). Their superior stability in comparison with other fluorescence imaging agents also allows longer investigation times for advanced *in vitro* and *in vivo* applications (Wegner and Hildebrandt, 2015). An in-depth description of the preparation, functionalization, properties and applications of QDs is beyond the scope of the present work, and has been extensively discussed in the scientific literature (for a more comprehensive review see Esteve-Turrillas and Abad-Fuentes, 2013; Resch-Genger et al., 2008; Wegner and Hildebrandt, 2015).

Although the unique optical properties of QDs make them a powerful platform in biology and biochemistry, including imaging and sensing purposes, their usage might be limited by two main drawbacks. The first one is their potential toxicity, which has especially delayed the progress towards clinical applications (Yong and Swihart, 2012). QDs cytotoxicity has been demonstrated in several *in vitro* studies, mainly resulting from the release of Cd ions due to degradation, the presence of certain surface-covering molecules, the intracellular distribution and the generation of reactive oxygen species (Chen et al., 2012; Yong and Swihart, 2012). The strategy used for the synthesis of QDs, their hydrodynamic diameter and their surface chemistry are the main factors that determine the cellular interactions. On the other hand, *in vivo* studies about QD toxicity are still scarce and their results are somehow contradictory. Although they accumulate in organs with high blood flow and induce immune responses, no pathological effects have been observed in small animal studies at the concentrations used for imaging applications (Botelho et al., 2016; Chen et al., 2012; Dobrovolskaia and McNeil, 2007; Hauck et al., 2010; Sahu et al., 2014; Su et al., 2011). More extensive long-term studies of QD toxicity and pharmacokinetics are lacking. Meanwhile, novel QD formulations based on indium phosphide or silicon, which eliminate local cytotoxicity caused by the release of Cd ions, are under development in order to improve their optical properties and become an acceptable alternative (Erogbogbo et al., 2011a, 2011b; Yong et al., 2009). Alternatively, QD coating for

example with silica or polyethylene glycol (Zhelev et al., 2006; Painuly et al., 2013) or improved synthetic procedures resulting in more photostable nanocrystals (He et al. 2011; Chen C. et al., 2013) may translate in diminished cytotoxicity. In the case of biosensing applications, the measurements are performed *ex vivo* in samples not containing living cells and require small amounts of QDs, therefore the concerns about cytotoxicity are limited. However, it may pose some difficulties for the approval of regulatory agencies, especially in the cases where the biodevice is expected to be used by the general public.

The second main issue is the strong blinking effect -i.e. random and intermittent light emission that makes individual particles to go dark (nonradiant) only for nanoseconds or remain dark for minutes at a time, or some interval in between-, which limits the applicability of QDs for single molecule fluorescence studies (Nirmal et al., 1996; Rombach-Riegraf et al., 2013). Although several hypotheses have been proposed to explain the blinking phenomenon, the most accepted one is the charging/discharging of the nanocrystal core when lower photoluminiscence intensities correlate with shorter photoluminiscence lifetimes (Galland et al., 2011). Some strategies have been proposed in order to reduce this undesired effect, including the introduction of 'anti-blinking agents' in the solution environment, such as β-mercaptoethanol, which bind to QD surfaces and increase the radiative lifetime; the functionalization of QDs with oligo(phenylene vinylene) (Fomenko and Nesbitt, 2008; Hammer et al., 2006; Hohng and Ha, 2004); or the site-directed binding of QDs to cysteine residues by the presence of thiol groups, which works probably because the dative bond close to the nanocrystal reduces the number of electron traps and therefore increases the radiative pathways (Rombach-Riegraf et al., 2013).Other approaches rely on modifying or tuning internal core/shell structures, instead of introducing surface modifications or surface-mediated interactions, such as the use of optimized synthetic procedures with a slow shell growth rate that eliminate the luminescence photodarkening (Chen O. et al., 2013), or QD heterostructuring by interfacial alloying, thick or "giant" shells, and specific type-II electronic structures (Hollingsworth 2013)

In addition to QDs, magnetic micro- and nanoparticles have acquired unprecedented utility for a wide variety of applications in separation techniques and bioassays. Magnetic beads allow linking to different molecules, including monoclonal antibodies, DNA or other receptors, and coating with streptavidin, protein A, etc., thus ensuring specific interactions with the targets of interest and easy recovery of the material by the use of an external magnet. By providing a solid support for biorecognition, magnetic particles, which commonly consist of magnetic elements such as iron, nickel and cobalt and their chemical compounds and can therefore be manipulated using magnetic field gradients, are able to accelerate the binding kinetics and facilitate analyses in shorter times. Magnetic particles allow the attachment of both ligands and receptors on their surface, thus restricting the conformational freedom and reducing the recognition kinetics when compared with freely diffusing species (Baudry et al., 2006). Magnetic separation is exceptionally efficient because most biological materials are not susceptible to magnetic fields (Hatch and Stelter, 2001). Among other advantages, magnetic beads can be easily separated from the reaction mixture with a magnet and immediately re-dispersed after removal of the magnetic field; they have a large surface area that allows immobilization of large numbers of biomolecules, leading to increased sensitivity without affecting biomolecular activity; and several detection techniques can be applied, ranging from fluorescence to electrochemical, chemiluminescence and colorimetric methods (Wei et al., 2012). Magnetic particles have been successfully applied for targeted drug delivery, bioseparation, biodetection, and labelling and sorting of cells (Labiadh et al., 2015). As an example, immunosensors and other immunoassays, reviewed in detail in following sections, based on magnetic beads and fluorescence detection have shown promising results for sensitive detection of pathogens and disease biomarkers (Chang et al., 2008; Wei et al., 2012; Zhu et al., 2014).

To our knowledge, no previous review has focused on bioanalysisstrategies based on the simultaneous use of QDs and magnetic beads. Due to the outstanding characteristics of both particles for biosensing applications and the large number of publications using the combined approach, we

aim to provide a comprehensive overview of the literature on different bioassays, the most recent advances and innovative strategies on the topic, together with an analysis of the main drawbacks encountered and potential solutions offered, with a special emphasis on the requirements that transfer of technologies from the laboratory to the market will demand for future commercialization ofbioassays. The structure of the present review is established based on the different biorecognition elements (immunoassays and nucleic acid-basedbioassays), the sandwich or competitive approach used, which are further detailed in following sections, and the type of analyte of interest.

2. Immunoassays

Immunosensors are biosensors which exploit antibodies or antigens as specific sensing elements in order to provide concentration-dependent signals. The molecular recognition process consists in the sensing of the specific antigen-antibody binding reaction at the receptor surface, and a consequent signal transfer by measurement of changes in electrochemical, optical, spectroscopic or electrical parameters of the receptor (Jiang et al., 2008). Immunosensors can be distinguished from immunoassays where the transducer is not an integral part of the analytical system, and can be both in label or label-free formats (Jiang et al., 2008).

The first type involves a label, such as an enzyme, nanoparticle, fluorescent or electrochemiluminescent probe, to quantify the amount of antibody or analyte bound to the immunosensor. The most frequent formats of labelled immunosensors are sandwich assays and competitive assays. In the sandwich format, the antigen or antibody is immobilized on the surface of the transducer, capturing the antibody or analyte of interest, respectively. A labelled secondary antibody is added in a second step to bind the previously captured antigen or the primary antibody. After the formation of this immunocomplex, the signal derived from the label increases in proportion to the analyte concentration. In the competitive format, the analyte competes with a fixed amount of

labelled analyte for a limited number of binding sites, thus giving a decrease in signal when the analyte concentration increases and the labelled analyte is displaced (Yang et al., 2016).

In the label-free format, the binding of the analyte and the antibody is detected on a transducer surface without any labels, using either a direct or an indirect strategy, the last one based on a binding inhibition test -i.e. a competitive format. Although simpler and reagent-less, the direct strategy is often unable to meet the demands of sensitive detection (Jiang et al., 2008). However, one work showed a proof-of-principle assay with detection limits around 1 nM by using the direct approach with QDs for measurement of basic fibroblast growth factor and prostate-specific antigen (Wang and Mountziaris, 2013).

2.1. Sandwich format immunoassays

Immunoassays based on the sandwich approach with both magnetic particles and QDs are the most widely used and more frequently reported in the literature. Recent works on the topic are presented throughout the following section according to their intended final application: detection of pathogens, such as bacteria or viruses, or measurement of other biomarkers. **Figure 1** presents a schematic illustration of the different approaches.

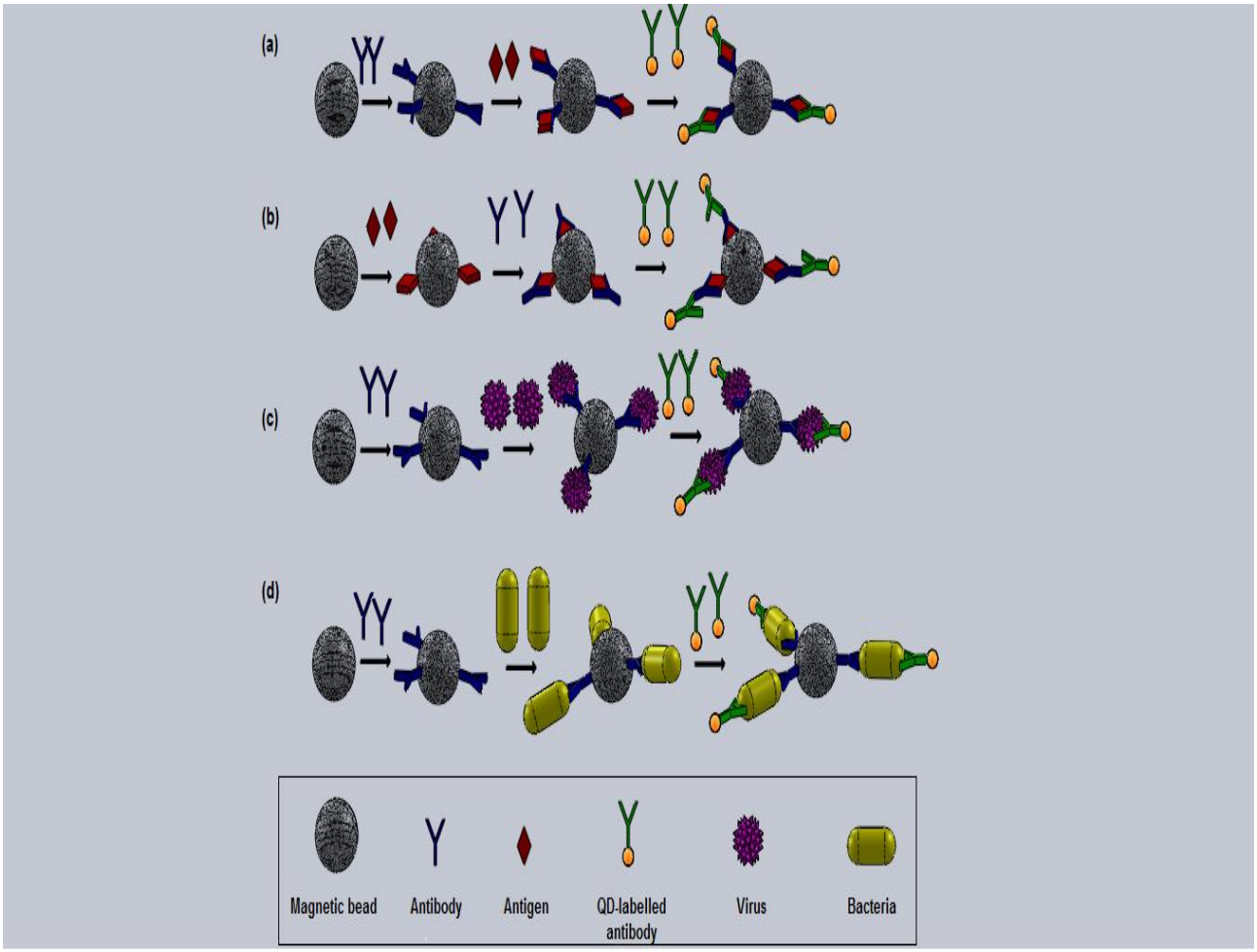

Fig. 1. Schematic representation showing the stepwise formation of immunoassays based on a sandwich approach with magnetic particles and quantum dots for detection of different targets. (a) Immobilized antibodies for antigen detection; (b) immobilized antigens for antibody detection; immobilized antibodies for detection of viruses (c) or bacteria (d).

2.1.1. Detection of bacteria

According to the World Health Organization (WHO), around 600 million -almost 1 in 10 people in the world- fall ill after eating contaminated food and 420,000 die every year (WHO, 2015). Additionally, poor water quality and sanitation are associated with 850,000 deaths per year specially in low- and middle-income countries (WHO, 2014). Due to the growing concern of the risk that food- and water-borne pathogens pose to human health, there is an increasing demand from regulatory agencies to ensure a safe food supply. The implementation of preventive strategies, together with

rapid, sensitive and accurate detection methods are essential tools to improve product safety (Bhunia, 2008). Due to the limitations of conventional microbiological methods, biosensor-based tools offer the most promising solutions for time-efficient, sensitive, specific and labor-saving detection of pathogens in real time or near real time (Law et al., 2014; López-Campos et al., 2012).

Detection of human pathogenic bacteria in cultures, food or water samples is the most frequent and developed application of the sandwich strategy based on magnetic beads and QDs. The first reports come from more than a decade ago, when Su and Li developed an assay based on magnetic particles conjugated with monoclonal biotinylated antibodies against *Escherichia coli* O157:H7 (Su and Li, 2004). In this approach, streptavidin-conjugated QDs were used as labels and a portable device based on a blue light-emitting diode (LED) and a charge-coupled device (CCD)-array spectrometer allowed fluorescence measurement while avoiding the use of expensive instrumentation. Additional advantages were the short assay time of less than 2 hours, the absence of interference with other *E. coli* or *Salmonella* species, the applicability in live cells since it obviates the need for UV radiation, a linear range of 10^3-10^7 colony-forming units (CFU)/mL and a limit of detection (LOD) of around 10^3 CFU/mL, lower than previously used labelling strategies for these bacteria (**see Fig. 2a for more details**). The same group presented an improved assay for detection of *Listeria monocytogenes* in pure cultures with a wide linear range (1-10^7 CFU/mL) and high sensitivity (LOD 2-3 CFU/mL) by the use of magnetic nanoparticles in the enrichment step**.** This work also showed that magnetic nanoparticles present important advantages over larger magnetic beads, since they provide a higher capture efficiency (Wang et al., 2007)**.**

Similar strategies were applied to immunoassays for the detection of *Salmonella typhimurium* in chicken samples (Yang and Li, 2005), *E. coli* in water (Dudak and Boyaci, 2008) and *Staphyloccocus aureus* in bacteria cultures (Yaohua et al., 2014)**,** reaching sensitivities in the order of 10^3 CFU/mL based on conventional fluorometric measurement. By coupling magnetic beads and QDs to two different monoclonal antibodies recognizing different antigenic determinants, Kuang et

al. increased the enrichment efficiency and reduced the LOD to 500 CFU/mL for *Salmonella* in a fast assay (Kuang et al., 2013). In general, all the articles reported no cross-reactivity with other microbial strains, thus confirming the utility of the approach for the detection of specific pathogenic bacteria. Several studies highlighted the difficulties of working with real-world samples (Yaohua et al., 2014; Zhao et al., 2009) due to the presence of complex matrices that can lead to non-specific binding and aberrant signals (Beyer and Biziuk, 2008; Sin et al., 2014). The application of simplification methods might be therefore necessary, which poses a drawback to the application of bioanalysistechnologies in field conditions. In the case of food-borne pathogens, the detection usually requires a pre-enrichment period of 4-48 h, clearly showing the need for new methods to speed food safety assessment.

Due to their particular characteristics, one of the key improvements introduced by the use of QDs is the possibility of simple application of multiplexing strategies (Beloglazova et al., 2014; Wu et al., 2015). Simultaneous detection of more than one species of pathogenic bacteria in culture, such as *E. coli* O157:H7 and *S. typhimurium,* using the double strategy with magnetic particles and QDs was first reported with a LOD of 10^4 CFU/mL (Yang and Li, 2006). Further studies were able to reduce the LOD to orders of magnitude of 10 CFU/mL for the detection of several food-borne pathogens (Wang et al., 2014, 2011, 2012), and the most successful approach detected as low as 10^{-3} CFU/mL of *S. typhimurium*, *Shigella flexneri* and *E. coli* O157:H7 in food matrices (Zhao et al., 2009)**.** Zahavy et al. applied the strategy of immunomagnetic separation followed by QD-labelling for direct fluorescence-activated cell sorting of *Bacillus anthracis* spores and *Yersinia pestis,* both in high and low bacterial concentration samples (Zahavy et al., 2012)**.** Interestingly, bacterial cell sorting can help to improve sensitivity, selectivity and biological viability when further down-stream diagnostic steps are required (Zahavy et al., 2012), for example in the case of bacteria that cannot grow in culture**.**

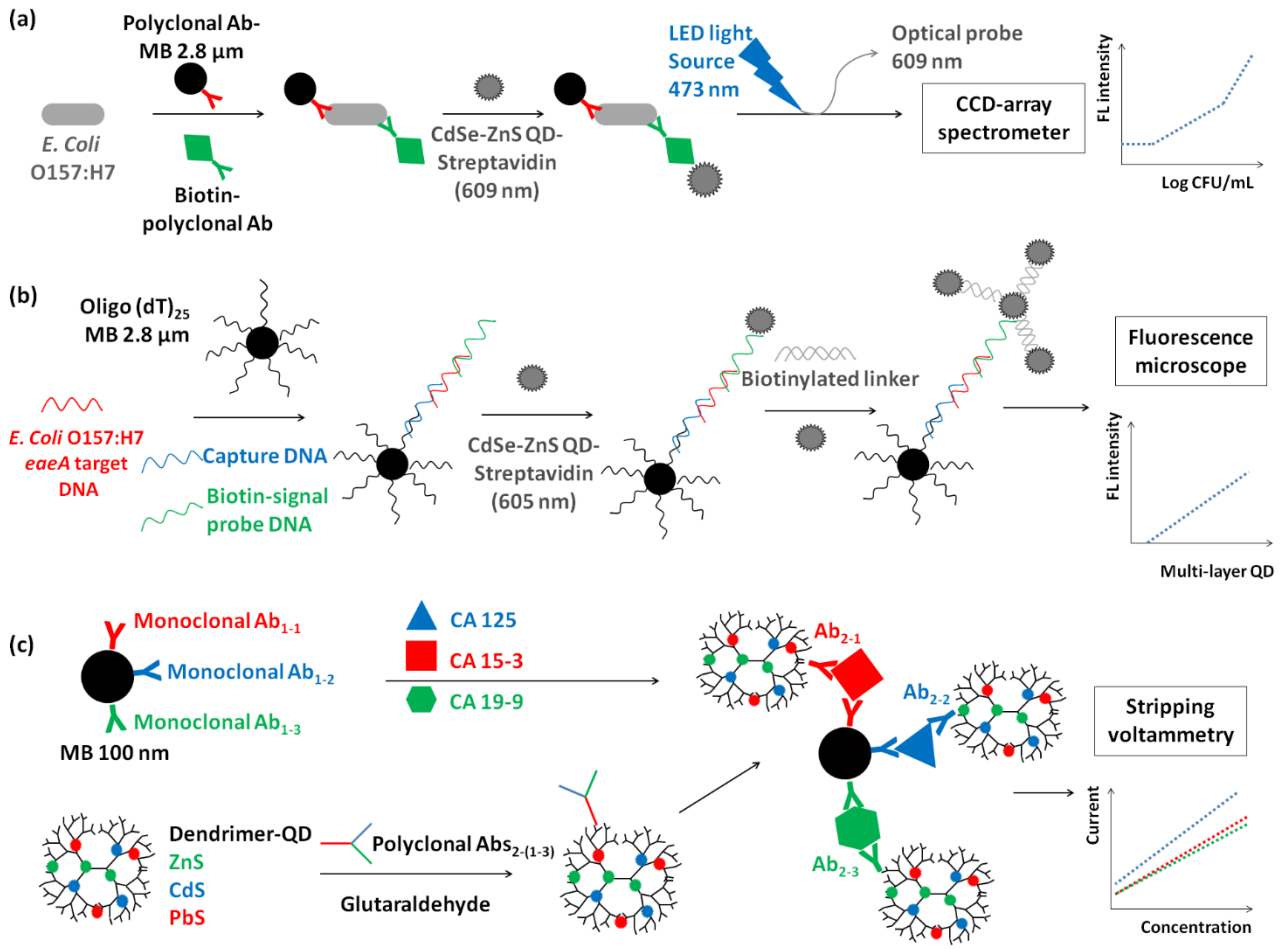

Fig. 2. Specific examples of different bioassays based in the simultaneous use of quantum dots (QDs) and magnetic beads (MBs).

(a) Schematic representation of the immunoassay for detection of *Escherichia coli* O157:H7 based in immunomagnetic separation and QD biolabeling proposed by Su and Li. MBs coated with anti-*E. coli* O157 antibodies (Ab) were employed to selectively capture the target bacteria, and biotin-conjugated anti-*E. coli* antibodies were added to form sandwich immune complexes. After magnetic separation, the immuno complexes were labeled with QDs via biotin-streptavidin conjugation. This was followed by a fluorescence measurement using a laptop-controlled portable device, which consisted of a blue LED and a CCD-array spectrometer. Adapted from Su, X.L., Li, Y., 2004.

b) Schematic representation of the bioassay for rapid detection of *E. coli* O157:H7 using magnetic bead-based DNA detection with multi-layers QD labeling, proposed by Liu and colleagues. MBs were used as the solid support for the binding probe in order to isolate the target DNA from the sample. The detection signals could be amplified by the formation of multi-layers of biotin–streptavidin conjugated QDs based on binding with specific designed biotinlyted linker. Adapted from Liu et al., 2008.

c) Schematic representation of the novel multiplexed stripping voltammetric immunoassay protocol designed by Tang and colleagues for simultaneous detection of multiple biomarkers (cancer antigen 125, CA125; CA15-3; and CA19-9) using dendrimer metal sulfide QD nanolabels as distinguishable signal tags and trifunctionalized MBs as an immunosensing probe. The probe was prepared by means of co- immobilization of monoclonal anti-CA125, anti-CA15-3 and anti-CA19-9 Abs ($Abs_{1-(1-3)}$) on a single MB. The polyamidoamine dendrimer-metal sulfide QD nanolabels containing CdS, ZnS and PbS were synthesized by using in situ synthesis method, which were utilized for the labeling of polyclonal anti-CA125, anti-CA15-3 and anti-CA19-9 detection Abs ($Abs_{2-(1-3)}$), respectively. A sandwich-type immunoassay format was adopted for the simultaneous determination of target biomarkers by anodic stripping voltammetric analysis of cadmium, zinc, and lead components released by acid from the corresponding QD nanolabels. Adapted from Tang et al., 2013.

2.1.2. Detection of viruses

Immunoassays based in magnetic particles and QDs have also been applied for the detection of several viruses. Fast and reliable point-of-care tests using portable devices are becoming crucial tools for patient management and infection control, especially in viral outbreaks (Jangam et al., 2013; Kost et al., 2015) and in a context of spread of emerging viral diseases (Marston et al., 2014). In this sense, novel biosensing technologies appear as a great alternative for ultrasensitive detection of viruses (Chen et al., 2016; Oliveira et al., 2015; Xu et al., 2015).

In 2007, Bruno et al. compared an immunomagnetic sandwich assay labelled with QDs or with home-made phosphorescent nanoparticles for the detection of reovirus in buffer and diluted fecal samples. Both strategies showed a LOD of around 37500 virus particles, although the phosphorescent nanoparticles provided a higher signal intensity in diluted stool, thus being an interesting alternative to explore for this application (Bruno et al., 2007). However, a long magnetic capture phase of more than 30 minutes was necessary due to the adherence of magnetic beads to fecal particulates, again underlining the complexity of working with real samples (Bruno et al., 2007). A subsequent work also applied a co-localization strategy for the detection of Hendra virus based in particles conjugated with viral-specific antibodies, comparing three different systems: luminescent bead-virus-

luminescent protein -similar to the Luminex® Assay-, magnetic bead-virus-luminescent protein or magnetic bead-virus-QD (Lisi et al., 2012). The combination of magnetic separation and QDs improved the assay reproducibility and the signal-to-noise ratio, simplified the detection process, reduced the number of reactions and washing steps and therefore facilitated the development of a portable assay, although it showed a higher coefficient of variation in comparison with the other approaches (Lisi et al., 2012). The authors also demonstrated the portability of the assay in glass capillaries of 2 mm of diameter, where positive samples were discerned directly by the naked eye, and confirmed its applicability for point-of-care testing at the outbreak site**.**

2.1.3. Detection of other biomarkers

The sandwich strategy has been successfully applied to the detection of other markers, including proteins, hormones and drugs. The first successful approach was described by Agrawal et al., reaching as low as fM concentrations for the detection of mouse recombinant interferon alpha by fluorescence microscopy (Agrawal et al., 2007). This work highlighted the potential problem of bead autofluorescence that was overcome by shifting QD emission signals. Zhang et al. developed an immunofluorescence assay that integrated QDs and magnetic carboxyl polystyrene microspheres, showing a detection limit of 4.9 ng/mL in a model of human alpha-fetoprotein (Zhang et al., 2009). This work introduced an important consideration about the size of QD-probes, which could affect the labelling efficiency to microsphere due to steric hindrance.

Interestingly, as an alternative to optical detection methods, electrochemical devices based on QDs instead of enzymes have been used for different applications (Grieshaber, 2008; Vijian et al., 2016; Yue et al., 2013). Zhang et al. constructed a magnetic beads based-electrochemiluminescence immunoassay for detection of human chorionic gonadotropin antigen using QD-functionalized nanoporous platinum-ruthenium alloys as labels (Zhang et al., 2012)**.** With a LOD of 0.8 pg/mL, electrochemiluminescence detection with this approach was simple, rapid, highly sensitivity, easily

controllable, flexible, with acceptable reproducibility and comparable to ELISA in serum samples, pointing towards a promising future clinical application (Zhang et al., 2012). An electrochemiluminescent immunoassay was also developed for detection of aflatoxin M1 in milk, using magnetic graphene oxides as absorbent and antibody-labelled QD-carbon nanotube composites as signal tags (Gan et al., 2013). This methodology showed a LOD of 0.3 pg/mL with excellent reproducibility, undetectable interference with other milk components, stability and possibility of regeneration. Validation in milk samples revealed a higher sensitivity than ELISA techniques (Gan et al., 2013)**.**

A different electrochemical approach used a magneto-controlled stripping voltammetric immunoassay for simultaneous detection of several cancer biomarkers (cancer antigens CA 125, CA 15-3 and CA 19-9) (Tang et al., 2013). This multiplex strategy was based on different dendrimer (synthetic polymers with branched structure)-encapsulated QDs as signal tags and magnetic particles where three primary monoclonal antibodies were co-immobilized for capture. The single-analyte and multiplex modes were compared, showing a similar LOD of 0.005 U/mL, which could meet the requirements for clinical diagnosis. In addition, the assay was cheap, highly specific, reproducible, stable with possibility of regeneration, simple and universal, obviating the need of enzyme substrates and thus emphasizing the convenience of use of QDs for electrochemical detection in biomedical applications (Tang et al., 2013) (**see Fig. 2c for more details**). Electrochemical quantification based on magnetic nanoparticles, QDs and disposable screen-printed electrodes was also applied for the detection of organophosphorylated butyrylcholinesterase (BChE), a biomarker of exposure to organophosphorus agents (Zhang et al., 2013). Under optimized conditions, the authors were able to detect 0.01 nM of the biomarker after 30 minutes incubation, showing acceptable reproducibility and reliability in human plasma**.**

2.2. Competitive format immunoassays

In order to save time and increase specificity, an approach based on a competitive binding process among the sample analyte and an add-in analyte can be exploited. This procedure is commonly used in the competitive enzyme linked immunosorbent assay (ELISA) that often represents the starting platform for many other immunoassat formats. This technique can be applied for the detection of both antigens (proteins, peptides or other macromolecules) and antibodies. In competitive strategies, the signal inversely correlates with the analyte concentration: a higher presence of the sample analyte generates a lower readout signal. The major advantage of the competitive approach is the ability to use crude or impure samples such as complex matrices (blood, urine, saliva, etc.) and still selectively detecting the analytes of interest without requiring any purification steps prior to measurement. Moreover, it is a very flexible method, since both direct and indirect detection approaches can be used. In the first case, the immunochemical recognition is directly detected by measuring the physical changes induced by the formation of the immunocomplex; in the second case, a detectable label is fused to the competing partner (for instance, through a secondary antibody) (**Fig. 3**). The majority of reported bioassaysbased on a competitive approach with QDs and magnetic beads have been designed for antigen detection, rather than antibody detection (**Fig. 3a**).

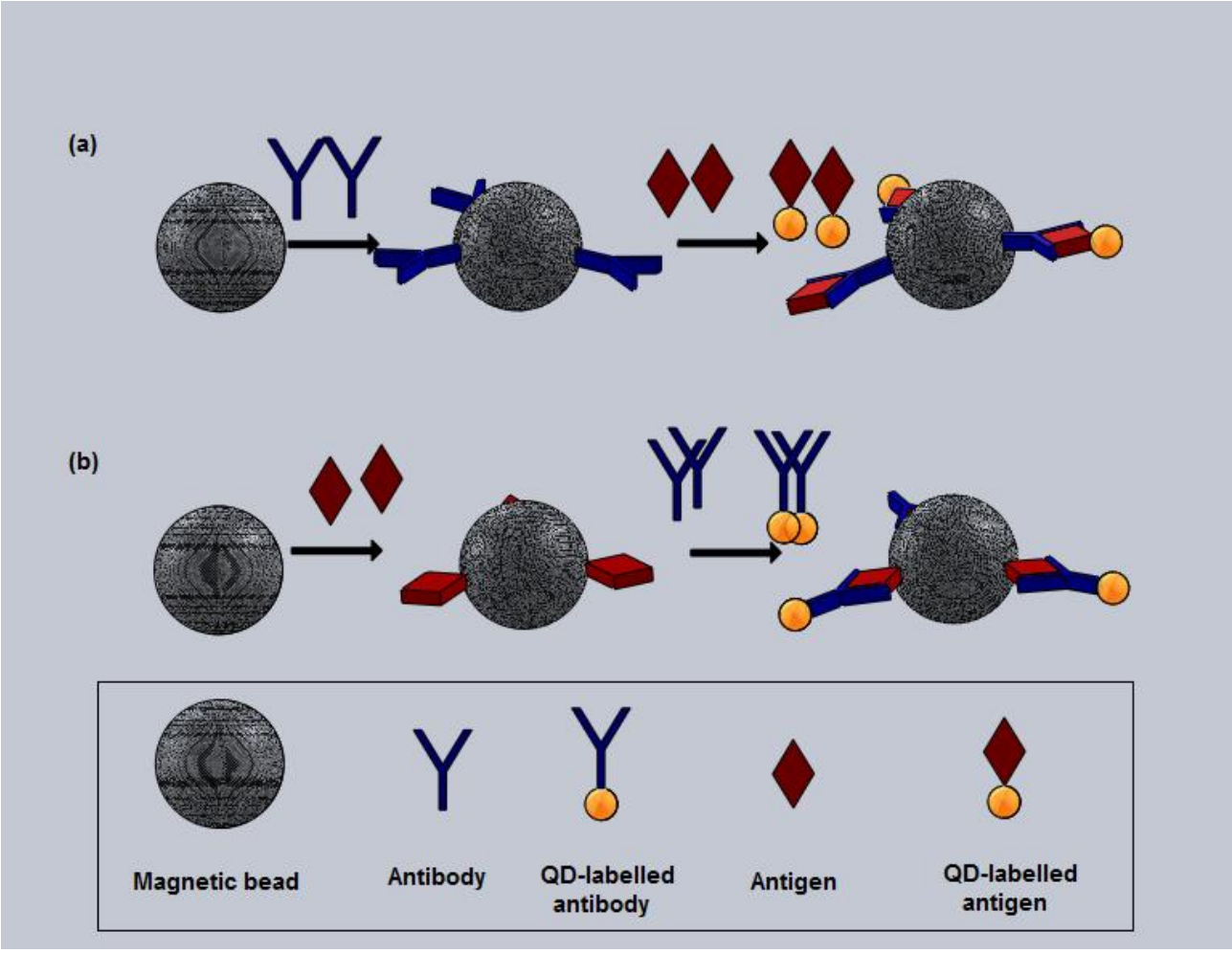

Fig. 3. Schematic representation of competitive-format immunoassays based in a sandwich strategy with magnetic beads for immobilization of capture antibody (a) or antigen (b). A known amount of quantum dot labelled analyte is added simultaneously with the sample, competing with the analyte for the binding sites.

2.2.1. Detection of viruses

The competitive approach is very useful for the rapid identification of pathogen-related antigens with diagnostic purposes, such in the case of a double QD approach used to detect Equine influenza virus (EIV) and Equine infectious anemia virus (EIAV) in blood serum (Wang et al., 2010). EIV or EIAV were conjugated to two kinds of fluorescent magnetic nanoparticles, while the relative antibodies were conjugated to a different wavelength QDs to avoid spectral overlapping. After a first incubation with the QD-labelled antibodies, which interacted with the natural antigens present in the

sample, labelled magnetic antigens were added to compete with the natural antigen and then separated from the sample. Fluorescence was read and used to quantify the natural antigens, with sensitivity in the order of ng/mL.

2.2.2. Detection of other biomarkers

The competitive approach is also useful for the detection of other molecules of interests, such as cellular biomarkers of specific diseases. As an example, Park and colleagues quantified soluble CD40L (sCD40L), a plasma biomarker of cardiovascular disease, with an assay where magnetic beads were coupled with anti-sCD40L specific antibodies. In parallel, QDs were functionalized with an antibody targeting a different epitope of sCD40L, using the protein G as a bridge. When both antibodies recognized sCD40L, the magnetic bead-coupled antibody - sCD40L - protein G - QD-coupled antibody complex was formed. At this point, a molar excess of imidazole (a competitive inhibitor for the interaction between QDs and protein G) was added to detach the QDs from the complex, releasing the QDs in the supernatant where absolute quantification of the sCD40L was achieved through fluorescence measurement with a sensitivity in the range of ng/mL (Park et al., 2013).

Not necessarily, the antigen of interest needs to be recognized by a specific antibody, but also other binding factors, both proteic and non-proteic, can be used in the assay if their affinity for the analyte is strong enough. Electrochemiluminescence strategies have been applied in bioassays able to recognize epidermal growth factor receptor (EGFR) on cell surfaces. CdSe-QDs were functionalized with epidermal growth factor (EGF) coupled to magnetic particles and were used for competitive recognition between add-in recombinant EGFR and EGFR expressed on cell surfaces (Tang et al., 2015).

Moreover, not only peptides or proteins, but also other macromolecules such as carbohydrates, can be detected with a competitive approach. In particular, a competition strategy has been

implemented with the usage of QD technology coupled with magnetic beads for the detection of Thomsen-Friedenreich (TF) antigen, a disaccharide considered as general biomarker for human carcinomas (Li et al., 2013). Li and coworkers experiment design showed that TF-antigen competes with 4-aminophenyl β-d-galactopyranoside (4-APG) conjugated to QDs for binding to peanut agglutinin that was attached to the magnetic beads. This work describes a direct detection where the use of magnetic beads allows an efficient recognition of the partners in a homogeneous phase.

Also inorganic compounds, such as toxins or antibiotics, can be detected with this approach. Wang et al. proposed an interesting QD-based competitive fluoroimmunoassay for the detection of clenbuterol in pig urine, a toxic fattening agent illegally added to animal food, showing acceptable agreement with high performance liquid chromatography. The competitive immunoassay was established through immobilization of an anti-clenbuterol monoclonal antibody to a solid carrier; the authors used iron oxide/gold magnetic nanoparticles of 5-6 nm size. QD nanocrystals were prepared and used to label the clenbuterol antigen. The increased size of the complex antigen-QDs generated a measurable 8 nm red-shifted peak in comparison with the QD alone. The incubation of clenbuterol and clenbuterol antigen-QDs with the magnetic beads was performed over times ranging from 1 to 36 h. After 16 hours, the fluorescence rapidly decayed and the authors attributed this quenching phenomenon to the presence of ions in solution, thus fixing the incubation time to 2 h. The competition between the drug contained in pig urine and the QD-labelled molecule led to an inverse correlation between QD fluorescence intensity and the concentration of the analyte in the solution. This work demonstrated the possibility to use the system within a range of clenbuterol concentrations from 0.5 to 20,000 pg/mL in pig urine, although urine pre-treatment in columns was required (Wang et al., 2009). A competitive QD-magnetic bead-based assay was also developed for the detection of cyanotoxins in drinking water, such microcystin-LR, with a detection limit of 0.03 μg/L (Yu et al., 2011).

A different assay was used to detect pesticides in plasma, such as organophosphorus and nerve agents, exploiting the fact that BChE, an enzyme present in serum, is inhibited by such chemicals (Du et al., 2011). In this assay, two simultaneous measurements were performed: quantification of the enzyme activity and amount of enzyme. For the first measure, magnetic beads were functionalized with BChE-specific antibodies, which recognized the antigens present in the blood sample. At this point, enzyme substrate was added inducing the formation of the thiocholine product, which allowed an electrochemical measurement to determine enzyme activity in proportion to the amount of active, non-inhibited enzyme. In parallel, a second assay was performed exploding magnetic particles functionalized with BChE enzyme itself, and QD-labelled specific antibodies were added in the presence of free-labelled natural BChE contained in the samples; and therefore natural BChE competed with bead-bound BChE for antibody binding. In this way it was possible to calculate the total amount of BChE. The measure of total amount of enzyme was subtracted from the amount of active enzyme, giving as result the amount of inhibited enzyme, which was proportional to the amount of pesticides; the assay reached a sensitivity of 0.5 nM (Du et al., 2011).

Table 1 summarizes and compares the different strategies applied to immunodevices mentioned along the text.

Table 1. Summary of the characteristics of immunoassays based in a sandwich strategy with magnetic beads and quantum dots reviewed along this work.

Biosensor format	Type of analyte	Reference	Measured analytes	Detection system	Limit of detection	Linear range	Time of assay/main incubation	Real-world samples
Sandwich	**Bacteria detection**	Su and Li, 2004	*Escherichia coli* O157:H7	Fluorescence (fiber optic spectrometer)	10^3 CFU/mL	10^3-10^7 CFU/mL	<2 h	No
		Wang et al., 2007	*Listeria monocytogenes*	Fluorescence (fiber optic spectrometer)	2-3 CFU/mL	1-10^7 CFU/mL	1.5 h	No
		Yang and Li, 2005	*Salmonella typhimurium*	Fluorescence (nd)	10^3 CFU/mL	10^3-10^7 CFU/mL	nd	Chicken carcass wash water
		Dudak and Boyaci, 2008	*E. coli*	Fluorescence (spectrofluorometer)	nd	8.9-1.9 x 10^6 CFU/mL	<2 h	Lake and tap water
		Yaohua et al., 2014	*Staphyloccocus aureus*	Fluorescence (fiber optic spectrometer)	10^3 CFU/mL[a]	10^3-10^6 CFU/mL[a]	≈3 h	Lamb wash water
		Kuang et al., 2013	*Salmonella*	Fluorescence (nd)	500 CFU/mL	2.5x10^3-1.95x10^8 CFU/mL	30 min	No
		Yang and Li, 2006	*E. coli* O157:H7 and *S. typhimurium*	Fluorescence (fiber optic spectrometer)	10^4 CFU/mL	10^4 - 10^7 CFU/mL	<2 h	No
		Wang et al., 2012	*E. coli* O157:H7 and *Salmonella*	Fluorescence (spectrofluorometer)	10 CFU/mL	nd	<3h (+24 h with enrichment)	Ground beef
		Zhao et al., 2009	*S. typhimurium*, *Shigella flexneri* and *E. coli* O157:H7	Fluorescence (microscope and spectrofluorometer)	≈10^{-3} CFU/mL	nd	2 h	Apple juice and milk
		Zahavy et al., 2012	*Bacillus anthracis* spores and *Yersinia pestis*	Fluorescence (flow cytometry cell sorting)	10^3 bacteria/mL	10^5-10^7 CFU/mL	5-10 min for sorting of 10^6 bacteria	Swabs spread from local pave ways
		Wang et al., 2014	*S. typhimurium* and *Campylobacter jejuni*	Fluorescence (fiber optic spectrometer)	30-50 CFU/mL	0-10^4 cells/ml pure culture	<2 h	Chicken carcass and ground turkey
	Virus detection	Bruno et al., 2007	Reovirus	Fluorescence (spectrofluorometer)	37500 virus particles	nd	≈2 h	Fecal samples
		Lisi et al., 2012	Hendra virus	Fluorescence (spectrofluorometer)	nd	nd	nd	No
		Wu et al., 2015	Avian influenza H7N9	Fluorescence (spectrofluorometer and microscope)	1.22 ng/mL	2.5-200 ng/mL	1h	Chicken tissue homogenates

	Others	Agrawal et al., 2007	Mouse recombinant interferon alpha	Fluorescence (microscope)	1 to 10 fM	nd	≈2 h	No
		Zhang et al., 2009	Human alpha-fetoprotein	Fluorescence (microscope)	4.9 ng/mL	nd	≈2 h	No
		Zhang et al., 2012	Human chorionic gonadotrophin	Electrochemical (electrochemiluminescence)	0.8 pg/mL	0.005-50 ng/mL	≈3 h	Serum samples
		Gan et al., 2013	Aflatoxin M1	Electrochemical (electrochemiluminescence)	0.3 pg/mL	1-10^5 pg/mL	≈30 min	Milk
		Tang et al., 2013	Cancer antigens CA 125, CA 15-3 and CA 19-9	Electrochemical (voltammetry)	0.005 U/mL	0.01-50 U/mL	≈1.5 h	Serum samples
		Zhang et al., 2013	Organophosphorylated butyrylcholinesterase	Electrochemical (voltammetry) and SPR	0.01 nM	0.02-10 nM	30 min	Plasma samples
Competitive	**Virus detection**	Wang et al., 2010	*Equine influenza* and *Equine infectious anemia* viruses	Fluorescence (spectrofluorometer)	1.2-1.3 ng/ml	0-85 ng/ml	>5 h	No
	Others	Park et al., 2013	Soluble CD40L	Fluorescence (quantum efficiency metrology tool)	5 ng/ml	20-160 ng/ml	>7 h	No
		Tang et al., 2015	Epidermal growth factor receptor	Electrochemical (electrochemiluminescence)	0.005 U/mL	0.01-50 U/mL	≈1 h	Serum samples
		Li et al., 2013	Thomsen-Friedenreich antigen	Fluorescence (spectrofluorometer)	2.44x10^4 µmol/mL	2.44x10^4 - 1.1 µmol/mL	>5 h	Cell lysates
		Wang et al., 2009	Clenbuterol	Fluorescence (spectrofluorometer)	0.5 pg/ml	0.5-20000 pg/ml	2 h	Pig urine
		Du et al., 2011	Organophosphorus and nerve agents	Electrochemical (amperometry)	0.05 nM	0.1-20 nM	≈4 h	Serum samples

SPR= Surface Plasmon Resonance

nd= not described

[a] In bacteria pure culture

3. Nucleic acid-based bioassays

Nucleic acid-based bioassays involve nucleic acid recognition processes, using DNA, RNA or artificial nucleic acids, such as aptamers, as sensing elements (**Fig. 4**). Aptamers are oligonucleotides (or peptides) that bind specific ligands and are derived from an *in vitro* evolution process called Systematic Evolution of Ligands by Exponential Enrichment, or SELEX (Ellington and Szostak, 1990; Tuerk and Gold, 1990). Aptamers could rival antibodies in some therapeutic and diagnostic applications (Chen and Yang, 2015; Toh et al., 2015) and have been successfully used in biosensing and engineering technologies due to their ability to bind a variety of targets and their robustness in terms of synthesis, storage, temperature stability and chemical manipulation (Sefah et al., 2009). For un updated review on aptamer applications, see Tsae and DeRosa, 2015.

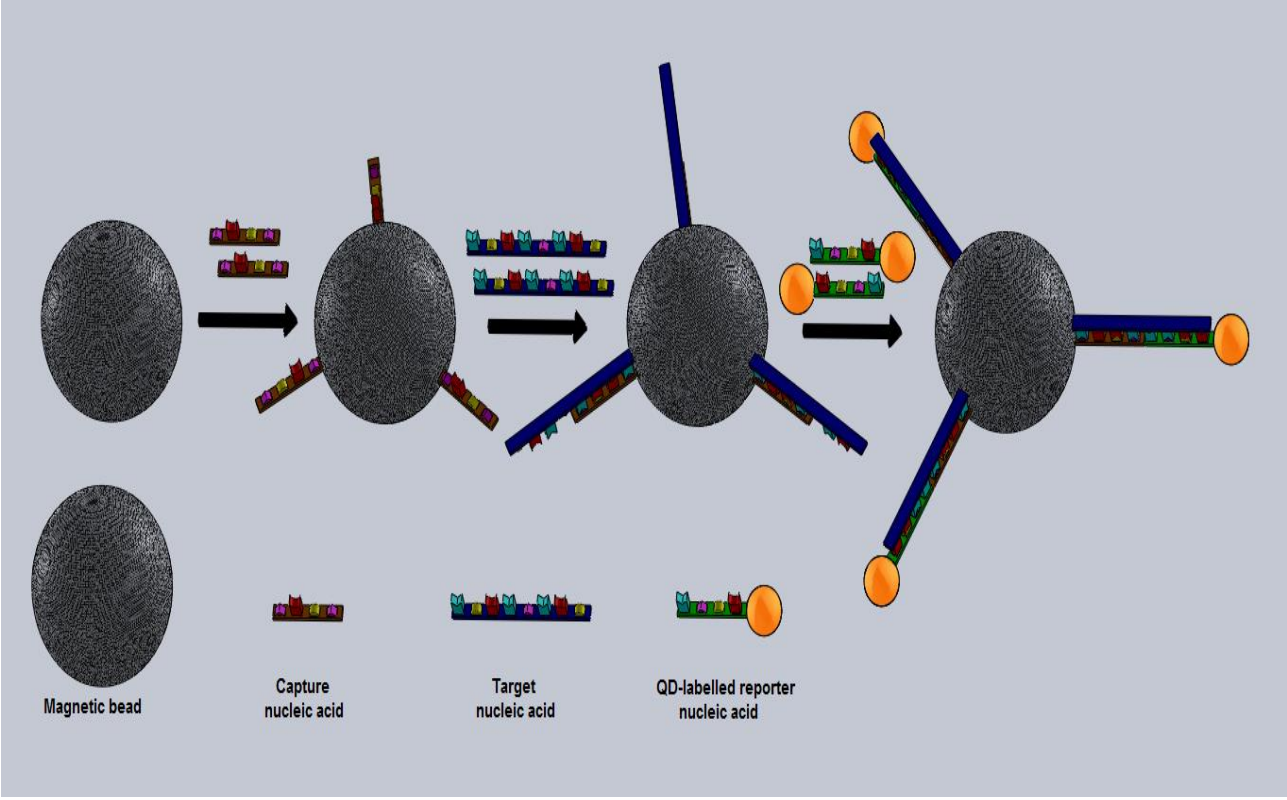

Fig. 4. Schematic representation of nucleic acid-based bioassays using a sandwich strategy with magnetic beads for immobilization of capture probes and quantum dot-labelled reporter probes for detection.

Nucleic acid-based bioassays, including gene chips, have clearly demonstrated to provide simple, fast, cost-effective, sensitive and specific detection in human health, food analysis, environmental and bioterrorism applications (Cheng et al., 2014; Cho et al., 2014; Foreman et al., 2011; Hao et al., 2011; Izadi et al., 2016; Umek et al., 2001). They seem especially promising for the high-throughput diagnosis of a wide range of pathologies at the point-of-care setting, including genetic, cancer, infectious, immunological, neurological and other diseases, although this technology still needs to bridge the gap between the laboratory and real clinical applications (Loo et al., 2015; Xu et al., 2016). One interesting characteristic is that, unlike enzymes or antibodies, the nucleic acid biorecognition elements in this type of devices can be readily prepared and regenerated for several uses (Ulianas et al., 2014). Nucleic acid-based bioassays can be coupled to optical, electrochemical (both label-based and label-free approaches) and piezoelectric detection systems, where the nucleic acid material is usually attached to different nanostructure transducers, including QDs and other nanocrystals, nanotubes, nanopolymers, nanowires, nanorods, etc. (Abu-Salah et al., 2015).

3.1. Sandwich format nucleic acid-based bioassays

3.1.1. Detection of bacteria

The first work reporting the development of a magnetic bead sandwich strategy for water and food-borne pathogens using QD-conjugated aptamers comes from 2006. This approach was implemented for the detection of *Cryptosporidium parvum* oocysts and *Campylobacter jejuni*, with a LOD of <5,000 oocysts and 10 bacteria/mL, respectively. Interestingly, the authors developed in parallel an antibody-based assay obtaining comparable results, although aptamers showed higher specificity than antibodies. This study proposed the use of a handheld and battery operated system for field applications, also with comparable results to laboratory detectors (Dwarakanath et al., 2006).

Further improvements on this strategy were introduced by Liu and colleagues, who included a biotinylated linker as a bridge between two QDs, allowing the formation of multilayers of the

semiconductor nanostructures on the same bead for signal amplification. Using a 32 base pairs DNA oligonucleotide, linear results were obtained up to a third layer of QD binding for the detection of an *E. coli* O157:H7 target DNA encoding a virulence factor, with a LOD of 250 zM (corresponding to around 150 molecules of the target DNA/mL). A mismatch test for single nucleotides confirmed the high specificity of the approach (Liu et al., 2008) (**see Fig. 2b for more details**).

Bruno et al., developed a system based on two selected DNA aptamers for detection of *C. jejuni.* Assay components were adhered to polystyrene cuvettes, enabling detection of fluorescence in one plane with a long shelf-life when lyophilized material was used (Bruno et al., 2009). The authors were able to detect as low as 2.5 CFU/mL in buffer and 10-250 CFU/mL in various food matrices both for live and heat-killed bacteria, which is below the levels recommended by current regulations. The approach showed some cross-reactivity with other *Campylobacter* species, but not outside the *Campylobacte*r genus. Efforts were put on the development of a fast (15-20 min), inexpensive and highly portable assay, by using a hand-held battery-operated fluorometer with similar results to a commercial spectrofluorometer (Bruno et al., 2009)**.**

This strategy also has promising applications for disease diagnosis. Using oligonucleotide DNA probes, one work was able to detect *Mycobacterium* species DNA previously isolated with a commercial kit in clinical samples (bronchoalveolar lavage, paraffin-embedded tissues and feces), without the need of DNA amplification. The assay was fast, cheap, reached a LOD of 0.625 ng/µL and reduced the number of false positives found in fecal samples with other techniques (Gazouli et al., 2010).

3.1.2. Detection of viruses

A great majority of nucleic acid-based devices based on the sandwich strategy with magnetic beads and QDs have been developed for viral detection. For example, Lim and coworkers developed an assay able to detect target DNA of different sizes from avian virus H5N1. The detection limit was

3 nM (Lim et al., 2009). Further devices for H5 influenza used confocal microscopy with a LOD of 0.1 ng of RNA (Zhang et al., 2010). Electrochemical methods were also applied for the detection of the neuraminidase gene from H5N1 in less than one hour using an automated nucleic acid isolation process (Krejcova et al., 2013). This system reached a LOD of subnanogram quantities with high sequence specificity, and was able to distinguish individual point mutations using RNA sequences. In the case of influenza, the use of QDs might be especially interesting for the development of multiplex devices that could detect several virus subtypes at the same time.

A more complex sandwich approach based on three types of probes was proposed by Xiang et al. for simultaneous detection of human papillomavirus (HPV)-16 and HPV-18, the strains responsible for most of the HPV-associated cancers. The bio-barcoded assay included a magnetic particle probe and two QD probes with the HPV DNA probe and fluorescent-labelled random DNA. The fluorescent signals of the dyes were measured by spectrophotometry with a LOD in the range of 10^{-11} M (Xiang et al., 2011). Interestingly, in this work magnetic beads were removed from the sandwich by heating at 95°C for 5 minutes and then by applying a magnetic field, in order to avoid the possibility that the light-scattering signal of magnetic microparticles would interfere with the fluorescent signal of the dye. A different multiplex system was proposed by Hu et al. for the simultaneous detection of human immunodeficiency virus (HIV) and hepatitis B and C viruses DNA. The device reached a LOD in the order of 100 pM for the three viruses and was validated in fetal bovine serum with similar results to a buffer system (Hu et al., 2013). Another assay for detection and serotyping of all the four-dengue virus genotypes was developed by Shen and Gao. This method achieved a significant signal enhancement by the use of duplex-specific nucleases that, after formation of RNA heteroduplexes with the different QD-probes on magnetic beads, released QDs and freed target RNA strands. These free targets were hybridized with remaining QDs on the magnetic particles by the establishment of an isothermal target cycling amplification process.

Although RNA extraction was required, this device offered excellent mismatch discrimination and a LOD of 100 viral RNA strands/µL using a simple battery-powered UV lamp (Shen and Gao, 2014).

3.1.3. Detection of other pathogens

Hushiarian et al. developed an assay based on this strategy for the detection of target DNA from *Ganoderma boninense*, a major pathogen of oil palm trees, using oligonucleotides from a ribosomal RNA gene (Hushiarian et al., 2014). Although little information is provided about the efficiency of the assay, the authors comment on the limitations caused by difficulties in sampling, extraction and denaturation of DNA from pathogens.

Aptamers were also used as biorecognition elements for the detection of other protein biomarkers involved in diseases. For instance, one study included two aptamers with different binding affinities for different isoforms of prion proteins, being able to detect as little as 85.5 pmol/L (Xiao et al., 2010). This method was able to detect the disease-associated prion protein isoform in 0.01% of mouse brain homogenate using a system that can be reused and stored.

3.2. Competitive format nucleic acid-based bioassays

Although less frequently used, the competition approach has also been applied to biodevices with nucleic acids as biorecognition elements. A competitive strategy based on a two-aspect signal amplification treatment, together with magnetic nanoparticles and the highly efficient *in vitro* process of rolling circle amplification, was developed for fluorescent detection of the abundant mycotoxin ochratoxin A (Yao et al., 2015). Rolling circle amplification consists in a unidirectional nucleic acid replication that rapidly synthesizes multiple copies of circular molecules of DNA or RNA. In 80 minutes, the system based on aptamers as recognition elements was able to detect as low as 0.13 parts

per trillion of ochratoxin A, a 10,000-fold improvement in comparison with traditional methods, with a wide linear range from 10^{-3} to 10 parts per billion.

Table 2 summarizes and compares the different strategies applied to nucleic acid-based bioassays described along the text.

Table 2. Summary of the characteristics of nucleic acid-based bioassays based in a sandwich strategy with magnetic beads and quantum dots reviewed along this work.

Biosensor format	Type of analyte	Reference	Measured analytes	Detection system	Limit of detection	Linear range	Time of assay/main incubation	Real-world samples
Sandwich	**Bacteria detection**	Dwarakanath S, et al., 2006	*Cryptosporidium parvum oocysts* and *Campylobacter jejuni*	Fluorescence (microscope)	10 bacteria/mL and <5000 oocysts, respectively	nd	<1 h	No
		Liu et al., 2008	*E. coli* O157:H7 target	Fluorescence (microscope)	250 zM (≈150 molecules of target DNA/mL)	nd	40-60 min	No
		Bruno et al., 2009	*C. jejuni*	Fluorescence (spectrofluorometer)	10 (live bacteria)-250 (dead bacteria) CFU/mL	nd	15-20 min	Different food matrices
		Gazouli et al., 2010	*Mycobacterium*species	Fluorescence (nd)	0.625 ng/µL	nd	≈2 h	Bronchoalveolar lavage, fixed tissues and feces
	Virus detection	Lim et al., 2009	Avian influenza H5N1 virus	Fluorescence (microscope)	3 nM	nd	1h	No
		Zhang et al., 2010	H5 influenza virus	Fluorescence (spectrofluorometer)	0.1 ng RNA	nd	3 h	No
		Krejcova et al., 2013	Neuraminidase from H5N1 virus	Electrochemical (voltammetry)	< ng DNA	nd	<1 h	No
		Xiang et al., 2011	Human papillomavirus (HPV)-16 and HPV-18	Fluorescence (nd)	6 (HPV-18)-7 (HPV-18) x 10^{-11} M	$8x10^{-11}$ to 8 x 10^{-9} M	75 min	No
		Hu et al., 2013	Human immunodeficiency virus and hepatitis B and C viruses	Fluorescence (spectrofluorometer)	209, 148 and 77 pM, respectively	nd	6 h	Fetal bovine serum

		Shen and Gao, 2014	Dengue virus serotypes 1-4	Fluorescence (spectrofluorometer)	100 viral RNA strands/µL	nd	≈1 h	No
	Fungi detection	Hushiarian et al., 2014	*Ganoderma boninense*	Fluorescence (spectrofluorometer)	10^{-5} M DNA assayed	nd	≈3h	No
	Others	Xiao et al., 2010	Prion protein	Fluorescence (spectrofluorometer)	85.5 pmol/L	nd	≈2 h	Serum and brain homogenate
Competitive	**Others**	Yao et al., 2015	Ochratoxin A	Fluorescence (spectrofluorometer)	0.13 ppt[a]	10^{-3} to 10 ppb[b]	80 min	No

nd = not described [a] ppt= parts per trillion [b] ppb= parts per billion

4. From the bench to the market: concerns and potential solutions for bioassay commercialization

Beside the success of the glucose meter, very few biosensor applications have arrived to the market. Versatility and low price remain key requirements for cost-effective assays, which, together with several technical issues still to be overcome, have slowed down the market viability of the current biosensors (reviewed in Luong et al. 2008). A great majority of the published works do not provide an analysis of cost-effectiveness of the proposed strategies, making difficult to assess their applicability for real-world use and constraining their immediate or near future application for example in a clinical or diagnostic setting. Commercially viable bioassays require stable biorecognition elements and a prolonged lifetime, while being able to produce a result in a few minutes. However, only a limited number of the works presented in this review analyzed the stability and reusability of the biorecognition element. Nucleic acid-based assays, although presenting the potential of sensing very low concentrations, still require time-ineffective purification steps at upstream processes. Contrarily, immunodevices need relatively fewer steps for sample preparation and can therefore be performed in shorter assays times, but present the disadvantage of requiring antibodies that are often complicated and expensive to produce and could have low affinity for the antigen (Koedrith et al., 2015).

One of the main challenges for the development of bioanalysis tools is the matrix interference, since many of the research has been developed using only laboratory samples (Sin et al., 2014). Throughout this review, emphasis has been put on works that reported the use of real-world samples for testing of the assays, some of them with promising results. Other common problems are sensor fouling due to adsorption of endogenous components in the assay sample, signal drift and potential microbial contaminations (Luong et al., 2008). Established protocols, together with validation in field samples, are required for comparison of the performance among different bioassays, an aspect that will be crucial in medical applications requiring approval from regulatory agencies (Luong et al.,

2008). Finally, successful approaches need to allow automation and integration of biosensing platforms with sampling, fluid handling, separation and other detection principles for continuous and remote detection of multiple, complex analytes, in order to transfer technologies from laboratories to the market (Luong et al., 2008; Sin et al., 2014). The integration of microfluidics and biosensor/bioassay technologies provides the ability to merge chemical and biological components into a single platform with the advantages of portability, disposability, real-time detection, unprecedented accuracy and simultaneous analysis of different analytes (Luka et al., 2015).

In this sense, several published works have gone a step further in system integration, using the double approach with magnetic beads and QDs in microfluidic devices. One of the first automated integrated systems based on QD and magnetic beads was proposed by Tennico et al. in 2010. Based on the use of two different DNA-thrombin aptamers, the authors developed a disposable microfluidic device performing on-chip washing procedures that was simple, robust and fast to operate**.** Additionally, this work showed the efficiency of the assay for removal of excess of unbound matrix and the absence of interference with serum components, working with a LOD of 10 ng/mL and acceptable reproducibility and linear range (similar to those of ELISA in well format). Other advantages were the minimized reagent consumption and the facility for multiplexing with QDs (Tennico et al., 2010).

A further approach based on microfluidic chips with different magnetic beads patterns in multiple branch channels was proposed by Yu and coworkers in 2013. The immunoassay was validated for the dual detection of the cancer biomarkers carcinoma embryonic antibody and AFP in serum in 40 minutes, with a high anti-interference capability and comparable results with hospital diagnostic tests (Yu et al., 2013). Continuous washing eliminated non-specific adsorption and allowed repeated use of the chip for at least 16 times. The LOD and linear range were in the ng/mL range for both antigens (Yu et al., 2013).

Automated multiple-step QD barcode assays based on magnetism and microfluidics have also been proposed for the simultaneous detection of several pathogenic organisms, such as HIV, hepatitis B and syphilis**.** Although allowing detection in the nM range in only 20 minutes, the authors reported a substantial difference in signal intensities for different barcodes due to variations in the hybridization efficiency of different DNA sequences determined by their size and secondary structure (Gao et al., 2013)**.**

Finally, microfluidic chips have been integrated with QDs adsorpted onto the surface of screen-printed electrodes for sensitive electrochemical detection, using an immunoassay with magnetic beads as a pre-concentration platform (Medina-Sánchez et al., 2014)**.** The authors were able to perform all conjugation steps in flow mode and achieved a LOD of 12.5 ng/mL for apolipoprotein E using wave anodic stripping voltammetry.

Last but not least, another crucial element for system integration is the detection module. A great number of optical detection strategies require bulky and expensive instruments, such as microscope and laser sources, which are not practical in many field settings where the biodevices present intended applications (Sin et al., 2014). Recently, research has focused on portable detection systems based on optical, electrical and magnetic sensing. Several works that utilized autonomous, compact, economic and portable detection systems for detection using the magnetic bead-QD approach have been described along this review (Bruno et al., 2009; Lisi et al., 2012; Wang et al., 2007). In this sense, our group has developed several robust portable optical, amperometric and/or conductometric detection instruments that have up to 6 independent cells for carrying out simultaneous tests on several types of biomarkers in sample volumes as small as 100 µL, in order to fulfill the current market demands of compact devices that can be used independently by end-users for onsite testing (Buonasera et al., 2010; Giardi et al., 2009; Scognamiglio et al., 2012).

5. One step further: towards innovative approaches

Going back to the unique characteristics of inorganic nanoparticles, such as nanometer dimensions, tunable imaging properties and multifunctionality, in the last years several works have focused in the development of biocompatible, inorganic nanoparticle-based multimodal probes. Nanoparticles mainly based on QDs, iron oxide, gold and silica have been combined with other materials such as biomolecules, polymers and radiometals to increase their functionality for molecular targeting, therapeutic delivery and multimodal imaging (reviewed in Swierczewska et al., 2011). Magnetic-fluorescent composite nanoparticles combine the fluorescent, magnetic and physical properties of the nano-size, can be guided by magnetic forces and can provide detailed information on biodistribution using, for example, a fluorescence microscope (Labiadh et al., 2015). The resulting bifunctional nanoparticles present a wide range of applications, including detection and bioseparation of proteins and DNA, bioimaging, cell localization and drug delivery (Heidari Majd et al., 2013; Lu et al., 2015; Truillet et al., 2013; Wu et al., 2012). Moreover, some works have shown their biocompatibility in cell viability and uptake assays, thus overcoming toxicity problems of QDs (Lu et al., 2015). Zhou et al. recently developed a novel dual-mode immunoassay based on surface-enhanced Raman scattering and fluorescence, designed using graphene QD labels to detect a tuberculosis antigen (CFP-10), via a newly developed sensing platform of linearly aligned magnetoplasmonic nanoparticles (Zou et al., 2015). This method presented the advantages of offering a solid platform with great multiplexing ability for fast quantitative identification of biomarkers and a LOD as low as 0.05 pg/mL (Zou et al., 2015). Efforts are now focused on overcoming the challenges of the complex preparation of these multifunctional nanoparticles that involves multistep synthesis and purification, as well as their instability and aggregation problems; and new methods have achieved a good compromise (Labiadh et al., 2015). QDs with intense electrochemiluminescent and magnetic properties have also been developed and successfully applied for detection of cancer cells via DNA cyclic amplification (Jie et al., 2013).

Conclusions

The present review provides a comprehensive compilation of bioassay strategies based on the simultaneous use of magnetic beads and QDs, highlighting the pros and the cons, the current concerns and the innovative solutions applied for sensitive detection of biomolecules. The relative complexity of sandwich strategies, their limited applicability in complex samples, their cost and the difficulties in transferring knowledge from academia to industry may constrain the short-term development of commercial biodevices based in QDs and magnetic beads. However, simultaneous use of fluorescent nanoparticles and magnetic particles could facilitate miniaturization techniques, together with multiplex detection systems and nanomaterials-based research for the development of future bioanalysis tools. New approaches based on multimodal nanoparticles and the improvement of current strategies, including direct detection, are being explored and will hopefully allow simplified and sensitive biosensing for real-world applications.

References

Abu-Salah, K.M., et al., 2015. DNA-Based Nanobiosensors as an Emerging Platform for Detection of Disease. Sensors (Basel). 15, 14539–68. doi:10.3390/s150614539

Agrawal, A., Sathe, T., Nie, S., 2007. Single-bead immunoassays using magnetic microparticles and spectral-shifting quantum dots. J. Agric. Food Chem. 55, 3778–82. doi:10.1021/jf0635006

Bally, M., Vörös, J., 2009. Nanoscale labels: nanoparticles and liposomes in the development of high-performance biosensors. Nanomedicine (Lond). 4, 447–67. doi:10.2217/nnm.09.16

Baudry, J., et al., 2006. Acceleration of the recognition rate between grafted ligands and receptors with magnetic forces. Proc. Natl. Acad. Sci. U. S. A. 103, 16076–8. doi:10.1073/pnas.0607991103

Beloglazova, N. V, et al., 2014. Novel multiplex fluorescent immunoassays based on quantum dot nanolabels for mycotoxins determination. Biosens. Bioelectron. 62, 59–65. doi:10.1016/j.bios.2014.06.021

Beyer, A., Biziuk, M., 2008. Methods for determining pesticides and polychlorinated biphenyls in food samples- problems and challenges. Crit. Rev. Food Sci. Nutr. 48, 888–904. doi:10.1080/10408390701761878

Bhunia, A.K., 2008. Biosensors and bio-based methods for the separation and detection of foodborne pathogens. Adv. Food Nutr. Res. 54, 1–44. doi:10.1016/S1043-4526(07)00001-0

Botelho, D.J., et al., 2016. Low-dose AgNPs reduce lung mechanical function and innate immune defense in the absence of cellular toxicity. Nanotoxicology 10, 118–27. doi:10.3109/17435390.2015.1038330

Bruchez, M., et al., 1998. Semiconductor nanocrystals as fluorescent biological labels. Science 281, 2013–6. doi: 10.1126/science.281.5385.2013

Bruno, J.G., et al., 2007. Reovirus Detection Using Immunomagnetic-Fluorescent Nanoparticle Sandwich Assays. J. Bionanoscience 1, 84–89. doi:10.1166/jbns.2007.015

Bruno, J.G., et al., 2009. Plastic-adherent DNA aptamer-magnetic bead and quantum dot sandwich assay for Campylobacter detection. J. Fluoresc. 19, 427–35. doi:10.1007/s10895-008-0429-8

Brus, L.E., 1984. Electron-electron and electron-hole interactions in small semiconductor crystallites: The size dependence of the lowest excited electronic state. J. Chem. Phys. 80, 4403. doi:10.1063/1.447218

Brus, L.E., 1983. A simple model for the ionization potential, electron affinity, and aqueous redox potentials of small semiconductor crystallites. J. Chem. Phys. 79, 5566. doi:10.1063/1.445676

Buonasera, K., et al., 2010. New platform of biosensors for prescreening of pesticide residues to support laboratory analyses. J. Agric. Food Chem. 58, 5982–90. doi:10.1021/jf9027602

Chan, W.C., Nie, S., 1998. Quantum dot bioconjugates for ultrasensitive nonisotopic detection. Science 281, 2016–8.

Chang, W.S., et al., 2008. Rapid detection of dengue virus in serum using magnetic separation and fluorescence detection. Analyst 133, 233–40. doi:10.1039/b710997k

Chen, A., Yang, S., 2015. Replacing antibodies with aptamers in lateral flow immunoassay. Biosens. Bioelectron. 71, 230–42. doi:10.1016/j.bios.2015.04.041

Chen, C.C., et al., 2016. Polymerase chain reaction-free detection of hepatitis B virus DNA using a nanostructured impedance biosensor. Biosens. Bioelectron. 77, 603–8. doi:10.1016/j.bios.2015.10.028

Chen, N., et al., 2012. The cytotoxicity of cadmium-based quantum dots. Biomaterials 33, 1238–44. doi:10.1016/j.biomaterials.2011.10.070

Chen, C., et al., 2013. Cation exchange-based facile aqueous synthesis of small, stable, and nontoxic near-infrared Ag_2Te/ZnS core/shell quantum dots emitting in the second biological window. ACS Appl Mater Interfaces. 5, 1149–55. doi: 10.1021/am302933x. Chen, O., et al., 2013. Compact high-quality CdSe-CdS core-shell nanocrystals with narrow emission linewidths and suppressed blinking. Nat. Mater. 12, 445–51. doi:10.1038/nmat3539

Cheng, W., et al., 2014. A novel electrochemical biosensor for ultrasensitive and specific detection of DNA based on molecular beacon mediated circular strand displacement and rolling circle amplification. Biosens. Bioelectron. 62, 274–9. doi:10.1016/j.bios.2014.06.056

Cho, M., et al., 2014. Combination of biobarcode assay with on-chip capillary electrophoresis for ultrasensitive and multiplex biological agent detection. Biosens. Bioelectron. 61, 172–6. doi:10.1016/j.bios.2014.05.018

Dobrovolskaia, M.A., McNeil, S.E., 2007. Immunological properties of engineered nanomaterials. Nat. Nanotechnol. 2, 469–78. doi:10.1038/nnano.2007.223

Du, D., et al. 2011. Magnetic electrochemical sensing platform for biomonitoring of exposure to organophosphorus pesticides and nerve agents based on simultaneous measurement of total enzyme amount and enzyme activity. Anal. Chem. 83, 3770-7. doi: 10.1021/ac200217d.

Dudak, F.C., Boyaci, İ.H., 2008. Enumeration of immunomagnetically captured Escherichia coli in water samples using quantum dot-labeled antibodies. J. Rapid Methods Autom. Microbiol. 16, 122–131. doi:10.1111/j.1745-4581.2008.00120.x

Dwarakanath S., et al., 2006. Ultrasensitive Fluorescent Nanoparticle-Based Binding Assays for Foodborne and Waterborne Pathogens of Clinical Interest. J. Clin. Ligand Assay 29, 136–142.

Ellington, A.D., Szostak, J.W., 1990. In vitro selection of RNA molecules that bind specific ligands. Nature 346, 818–22. doi:10.1038/346818a0

Erogbogbo, F., et al., 2011a. Bioconjugation of luminescent silicon quantum dots for selective uptake by cancer cells. Bioconjug. Chem. 22, 1081–8. doi:10.1021/bc100552p

Erogbogbo, F., et al., 2011b. In vivo targeted cancer imaging, sentinel lymph node mapping and multi-channel imaging with biocompatible silicon nanocrystals. ACS Nano 5, 413–23. doi:10.1021/nn1018945

Esteve-Turrillas, F.A., Abad-Fuentes, A., 2013. Applications of quantum dots as probes in immunosensing of small-sized analytes. Biosens. Bioelectron. 41, 12–29. doi:10.1016/j.bios.2012.09.025

Fomenko, V., Nesbitt, D.J., 2008. Solution control of radiative and nonradiative lifetimes: a novel contribution to quantum dot blinking suppression. Nano Lett. 8, 287–93. doi:10.1021/nl0726609

Foreman, A.L., et al., 2011. A DNA-based assay for toxic chemicals in wastewater. Environ. Toxicol. Chem. 30, 1810–8. doi:10.1002/etc.568

Galland, C., et al., 2011. Two types of luminescence blinking revealed by spectroelectrochemistry of single quantum dots. Nature 479, 203–7. doi: 10.1038/nature10569.

Gan, N., et al., 2013. An ultrasensitive electrochemiluminescent immunoassay for aflatoxin M1 in milk, based on extraction by magnetic graphene and detection by antibody-labeled CdTe quantum dots-carbon nanotubes nanocomposite. Toxins (Basel) 5, 865–83. doi:10.3390/toxins5050865

Gao, Y., et al., 2013. Automating quantum dot barcode assays using microfluidics and magnetism for the development of a point-of-care device. ACS Appl. Mater. Interfaces 5, 2853–60. doi:10.1021/am302633h

Gazouli, M., et al., 2010. Specific detection of unamplified mycobacterial DNA by use of fluorescent semiconductor quantum dots and magnetic beads. J. Clin. Microbiol. 48, 2830–5. doi:10.1128/JCM.00185-10

Giardi, M.T., et al., 2009. Optical biosensors for environmental monitoring based on computational and biotechnological tools for engineering the photosynthetic D1 protein of *Chlamydomonas reinhardtii*. Biosens. Bioelectron. 25, 294–300. doi:10.1016/j.bios.2009.07.003

Grieshaber D., et al., 2008. Electrochemical Biosensors - Sensor Principles and Architectures. Sensors (Basel) 8, 1400-1458. doi:10.3390/s8031400

Hammer, N.I., et al., 2006. Coverage-mediated suppression of blinking in solid state quantum dot conjugated organic composite nanostructures. J. Phys. Chem. B 110, 14167–71. doi:10.1021/jp062065f

Hao, R.Z., et al., 2011. DNA probe functionalized QCM biosensor based on gold nanoparticle amplification for Bacillus anthracis detection. Biosens. Bioelectron. 26, 3398–404. doi:10.1016/j.bios.2011.01.010

Hatch, G.P., Stelter, R.E., 2001. Magnetic design considerations for devices and particles used for biological high-gradient magnetic separation (HGMS) systems. J. Magn. Magn. Mater. 225, 262–276. doi:10.1016/S0304-8853(00)01250-6

Hauck, T.S., et al., 2010. In vivo quantum-dot toxicity assessment. Small 6, 138–44. doi:10.1002/smll.200900626

He, Y., et al., 2011. Ultra-photostable, non-cytotoxic, and highly fluorescent quantum nanospheres for long-term, high-specificity cell imaging. Biomaterials 32, 2133–40. doi: 10.1016/j.biomaterials.2010.11.034.

Heidari Majd, M., et al., 2013. Specific targeting of cancer cells by multifunctional mitoxantrone-conjugated magnetic nanoparticles. J. Drug Target. 21, 328–40. doi:10.3109/1061186X.2012.750325

Hohng, S., Ha, T., 2004. Near-complete suppression of quantum dot blinking in ambient conditions. J. Am. Chem. Soc. 126, 1324–5. doi:10.1021/ja039686w

Hollingsworth, J.A., 2013. Heterostructuring nanocrystal quantum dots toward intentional suppression of blinking and Auger recombination. Chem Mater. 25, 1318–1331. doi:10.1021/cm304161d

Hu, J., et al., 2013. Optically encoded multifunctional nanospheres for one-pot separation and detection of multiplex DNA sequences. Anal. Chem. 85, 11929–35. doi:10.1021/ac4027753

Hushiarian, R., et al., 2014. A Novel DNA Nanosensor Based on CdSe/ZnS Quantum Dots and Synthesized Fe3O4 Magnetic Nanoparticles. Molecules 19, 4355–4368. doi:10.3390/molecules19044355

Izadi, Z., et al., 2016. Fabrication of an electrochemical DNA-based biosensor for Bacillus cereus detection in milk and infant formula. Biosens. Bioelectron. 80, 582–589. doi:10.1016/j.bios.2016.02.032

Jangam, S.R.,et al., 2013. A point-of-care PCR test for HIV-1 detection in resource-limited settings. Biosens. Bioelectron. 42, 69–75. doi:10.1016/j.bios.2012.10.024

Jiang, X., et al., 2008. Immunosensors for detection of pesticide residues. Biosens. Bioelectron. 23, 1577–87. doi:10.1016/j.bios.2008.01.035

Jianrong, C., et al., 2004. Nanotechnology and biosensors. Biotechnol. Adv. 22, 505–18. doi:10.1016/j.biotechadv.2004.03.004

Jie, G., et al., 2013. Amplified electrochemiluminescence detection of cancer cells using a new bifunctional quantum dot as signal probe. Biosens. Bioelectron. 50, 368–72. doi:10.1016/j.bios.2013.06.048

Koedrith, P., et al., 2015. Recent trends in rapid environmental monitoring of pathogens and toxicants: potential of nanoparticle-based biosensor and applications. ScientificWorldJournal 2015, 510982. doi:10.1155/2015/510982

Kost, G.J., et al., 2015. Molecular detection and point-of-care testing in Ebola virus disease and other threats: a new global public health framework to stop outbreaks. Expert Rev. Mol. Diagn. 15, 1245–59. doi:10.1586/14737159.2015.1079776

Krejcova, L., et al., 2013. Development of a magnetic electrochemical bar code array for point mutation detection in the H5N1 neuraminidase gene. Viruses 5, 1719–39. doi:10.3390/v5071719

Kuang, H., et al., 2013. A one-step homogeneous sandwich immunosensor for Salmonella detection based on magnetic nanoparticles (MNPs) and quantum Dots (QDs). Int. J. Mol. Sci. 14, 8603–10. doi:10.3390/ijms14048603

Labiadh, H., et al., 2015. A facile method for the preparation of bifunctional Mn:ZnS/ZnS/Fe3O4 magnetic and fluorescent nanocrystals. Beilstein J. Nanotechnol. 6, 1743–51. doi:10.3762/bjnano.6.178

Law, J.W., et al., 2014. Rapid methods for the detection of foodborne bacterial pathogens: principles, applications, advantages and limitations. Front. Microbiol. 5, 770. doi:10.3389/fmicb.2014.00770

Li, N., et al., 2013. Quantum dot based fluorometric detection of cancer TF-antigen. Anal. Chem. 85, 9699-704. doi: 10.1021/ac402082s.

Lim, S.H., et al., 2009. Quantitative analysis of nucleic acid hybridization on magnetic particles and quantum dot-based probes. Sensors (Basel) 9, 5590–9. doi:10.3390/s90705590

Lisi, F., et al., 2012. Rapid detection of hendra virus using magnetic particles and quantum dots. Adv. Healthc. Mater. 1, 631–4. doi:10.1002/adhm.201200072

Liu, Y.J., et al., 2008. Magnetic bead-based DNA detection with multi-layers quantum dots labeling for rapid detection of Escherichia coli O157:H7. Biosens. Bioelectron. 24, 558–65. doi:10.1016/j.bios.2008.06.019

Loo, J.F., et al., 2015. A non-PCR SPR platform using RNase H to detect MicroRNA 29a-3p from throat swabs of human subjects with influenza A virus H1N1 infection. Analyst 140, 4566–75. doi:10.1039/c5an00679a

López-Campos, G., et al., 2012. Chapter 2. Detection, Identification, and Analysis of Foodborne Pathogens., in: Microarray Detection and Characterization of Bacterial Foodborne Pathogens, SpringerBriefs in Food, Health, and Nutrition. Springer US, Boston, MA, pp. 13-32. doi:10.1007/978-1-4614-3250-0

Lu, Y., et al., 2015. Bifunctional magnetic-fluorescent nanoparticles: synthesis, characterization, and cell imaging. ACS Appl. Mater. Interfaces 7, 5226–32. doi:10.1021/am508266p

Luka, G., et al., 2015. Microfluidics Integrated Biosensors: A Leading Technology towards Lab-on-a-Chip and Sensing Applications. Sensors (Basel) 15, 30011–31. doi:10.3390/s151229783

Luong, J.H., et al., 2008. Biosensor technology: technology push versus market pull. Biotechnol. Adv. 26, 492–500. doi:10.1016/j.biotechadv.2008.05.007

Marston, H.D., et al., 2014. Emerging viral diseases: confronting threats with new technologies. Sci. Transl. Med. 6, 253ps10. doi:10.1126/scitranslmed.3009872

Medina-Sánchez, M., et al., 2014. On-chip magneto-immunoassay for Alzheimer's biomarker electrochemical detection by using quantum dots as labels. Biosens. Bioelectron. 54, 279–84. doi:10.1016/j.bios.2013.10.069

Nirmal, M., et al., 1996. Fluorescence intermittency in single cadmium selenide nanocrystals. Nature 383, 802–804. doi:10.1038/383802a0

Oliveira, N., et al., 2015. A Sensitive and Selective Label-Free Electrochemical DNA Biosensor for the Detection of Specific Dengue Virus Serotype 3 Sequences. Sensors (Basel) 15, 15562–77. doi:10.3390/s150715562

Painuly, D., et al., 2013. Mercaptoethanol capped CdSe quantum dots and CdSe/ZnS core/shell: synthesis, characterization and cytotoxicity evaluation. J Biomed Nanotechnol. 9, 257–66. doi:10.1166/jbn.2013.1488

Park, H., et al., 2013. Quantification of cardiovascular disease biomarkers via functionalized magnetic beads and on-demand detachable quantum dots. Nanoscale 5, 8609–15. doi: 10.1039/c3nr02357e.

Resch-Genger, U., et al., 2008. Quantum dots versus organic dyes as fluorescent labels. Nat. Methods 5, 763–75. doi:10.1038/nmeth.1248

Rombach-Riegraf, V., et al., 2013. Blinking effect and the use of quantum dots in single molecule spectroscopy. Biochem. Biophys. Res. Commun. 430, 260–4. doi:10.1016/j.bbrc.2012.10.140

Sahu, D., et al., 2014. Size-dependent effect of zinc oxide on toxicity and inflammatory potential of human monocytes. J. Toxicol. Environ. Health. A 77, 177–91. doi:10.1080/15287394.2013.853224

Scognamiglio, V., et al., 2012. Towards an integrated biosensor array for simultaneous and rapid multi-analysis of endocrine disrupting chemicals. Anal. Chim. Acta 751, 161–170. doi:10.1016/j.aca.2012.09.010

Sefah, K., et al., 2009. Nucleic acid aptamers for biosensors and bio-analytical applications. Analyst 134, 1765–75. doi:10.1039/b905609m

Shen, W., Gao, Z., 2014. Quantum dots and duplex-specific nuclease enabled ultrasensitive detection and serotyping of Dengue viruses in one step in a single tube. Biosens. Bioelectron. 65C, 327–332. doi:10.1016/j.bios.2014.10.060

Sin, M.L., et al., 2014. Advances and challenges in biosensor-based diagnosis of infectious diseases. Expert Rev. Mol. Diagn. 14, 225–44. doi:10.1586/14737159.2014.888313

Su, X.L., Li, Y., 2004. Quantum dot biolabeling coupled with immunomagnetic separation for detection of Escherichia coli O157:H7. Anal. Chem. 76, 4806–10. doi:10.1021/ac049442+

Su, Y., et al., 2011. In vivo distribution, pharmacokinetics, and toxicity of aqueous synthesized cadmium-containing quantum dots. Biomaterials 32, 5855–62. doi:10.1016/j.biomaterials.2011.04.063

Swierczewska, M., et al., 2011. Inorganic nanoparticles for multimodal molecular imaging. Mol. Imaging 10, 3–16.

Tang, D., et al., 2013. Multiplexed electrochemical immunoassay of biomarkers using metal sulfide quantum dot nanolabels and trifunctionalized magnetic beads. Biosens. Bioelectron. 46, 37–43. doi:10.1016/j.bios.2013.02.027

Tang, D., et al., 2015. A sensitive electrochemiluminescence cytosensor for quantitative evaluation of epidermal growth factor receptor expressed on cell surfaces. Anal. Chim. Acta. 881,148-54. doi: 10.1016/j.aca.2015.04.008

Tennico, Y.H., et al., 2010. On-chip aptamer-based sandwich assay for thrombin detection employing magnetic beads and quantum dots. Anal. Chem. 82, 5591–7. doi:10.1021/ac101269u

Toh, S.Y., et al., 2015. Aptamers as a replacement for antibodies in enzyme-linked immunosorbent assay. Biosens. Bioelectron. 64, 392–403. doi:10.1016/j.bios.2014.09.026

Truillet, C., et al., 2013. Bifunctional polypyridyl-Ru(II) complex grafted onto gadolinium-based nanoparticles for MR-imaging and photodynamic therapy. Dalton Trans. 42, 12410–20. doi:10.1039/c3dt50946j

Tsae, P.K., DeRosa, M.C., 2015. Outlook for aptamers after twenty five years. Curr. Top. Med. Chem. 15, 1153–9.

Tuerk, C., Gold, L., 1990. Systematic evolution of ligands by exponential enrichment: RNA ligands to bacteriophage T4 DNA polymerase. Science 249, 505–10.

Ulianas, A., et al., 2014. A regenerable screen-printed DNA biosensor based on acrylic microsphere–gold nanoparticle composite for genetically modified soybean determination. Sensors Actuators B Chem. 190, 694–701. doi:10.1016/j.snb.2013.09.040

Umek, R.M., et al., 2001. Electronic detection of nucleic acids: a versatile platform for molecular diagnostics. J. Mol. Diagn. 3, 74–84. doi:10.1016/S1525-1578(10)60655-1

Vijian, D., et al., 2016. Non-protein coding RNA-based genosensor with quantum dots as electrochemical labels for attomolar detection of multiple pathogens. Biosens. Bioelectron. 77, 805–11. doi:10.1016/j.bios.2015.10.057

Wang, G., et al., 2010. Multiplex immunoassays of equine virus based on fluorescent encoded magnetic composite nanoparticles. Anal. Bioanal. Chem. 398, 805-13.

Wang, H.,et al., 2014. Rapid and Simultaneous Detection of Salmonella and Campylobacter in Poultry Samples Using Quantum Dots Based Fluorescent Immunoassay Coupled with Magnetic Immunoseparation. Int. J. Poult. Sci. 13, 611–618. doi:10.3923/ijps.2014.611.618

Wang, H., et al., 2007. Rapid detection of Listeria monocytogenes using quantum dots and nanobeads-based optical biosensor. J. Rapid Methods Autom. Microbiol. 15, 67–76. doi:10.1111/j.1745-4581.2007.00075.x

Wang, H., et al., 2011. Rapid, sensitive, and simultaneous detection of three foodborne pathogens using magnetic nanobead-based immunoseparation and quantum dot-based multiplex immunoassay. J. Food Prot. 74, 2039–47. doi:10.4315/0362-028X.JFP-11-144

Wang, J., Mountziaris, T.J., 2013. Homogeneous immunoassays based on fluorescence emission intensity variations of zinc selenide quantum dot sensors. Biosens. Bioelectron. 41, 143–9. doi:10.1016/j.bios.2012.08.003

Wang, L., et al., 2012. Detection of Escherichia coli O157:H7 and Salmonella in ground beef by a bead-free quantum dot-facilitated isolation method. Int. J. Food Microbiol. 156, 83–7. doi:10.1016/j.ijfoodmicro.2012.03.003

Wang, X., et al., 2009. A novel CdSe/CdS quantum dot-based competitive fluoroimmunoassay for the detection of clenbuterol residue in pig urine using magnetic core/shell Fe3O4/Au nanoparticles as a solid carrier. Anal. Sci. 25, 1409–13.

Wegner, K.D., Hildebrandt, N., 2015. Quantum dots: bright and versatile in vitro and in vivo fluorescence imaging biosensors. Chem. Soc. Rev. 44, 4792–834. doi:10.1039/c4cs00532e

Wei, B., et al., 2012. Magnetic beads-based enzymatic spectrofluorometric assay for rapid and sensitive detection of antibody against ApxIVA of Actinobacillus pleuropneumoniae. Biosens. Bioelectron. 35, 390–3. doi:10.1016/j.bios.2012.03.027

World Health Organization, 2014. Preventing diarrhoea through better water, sanitation and hygiene.

World Health Organization, 2015. WHO Technical Report. WHO estimates of the global burden of foodborne diseases.

Wu, F., et al., 2015. Multiplexed detection of influenza A virus subtype H5 and H9 via quantum dot-based immunoassay. Biosens. Bioelectron. 77, 464–470. doi:10.1016/j.bios.2015.10.002

Wu, Y., et al., 2012. A new type of silica-coated $Gd_2(CO_3)_3$:Tb nanoparticle as a bifunctional agent for magnetic resonance imaging and fluorescent imaging. Nanotechnology 23, 205103. doi:10.1088/0957-4484/23/20/205103

Xiang, D., et al., 2011. Magnetic microparticle-based multiplexed DNA detection with biobarcoded quantum dot probes. Biosens. Bioelectron. 26, 4405–10. doi:10.1016/j.bios.2011.04.051

Xiao, S.J., et al., 2010. Sensitive discrimination and detection of prion disease-associated isoform with a dual-aptamer strategy by developing a sandwich structure of magnetic microparticles and quantum dots. Anal. Chem. 82, 9736–42. doi:10.1021/ac101865s

Xu, H., et al., 2015. Multiplex biomarker analysis biosensor for detection of hepatitis B virus. Biomed. Mater. Eng. 26 Suppl 1, S2091–100. doi:10.3233/BME-151515

Xu, J., et al., 2016. Double-stem Hairpin Probe and Ultrasensitive Colorimetric Detection of Cancer-related Nucleic Acids. Theranostics 6, 318–27. doi:10.7150/thno.13533

Yang, K., et al., 2016. A novel biosensor based on competitive SERS immunoassay and magnetic separation for accurate and sensitive detection of chloramphenicol. Biosens. Bioelectron. 80, 373–377. doi:10.1016/j.bios.2016.01.064

Yang, L., Li, Y., 2006. Simultaneous detection of Escherichia coli O157:H7 and Salmonella Typhimurium using quantum dots as fluorescence labels. Analyst 131, 394–401. doi:10.1039/b510888h

Yang, L., Li, Y., 2005. Quantum dots as fluorescent labels for quantitative detection of Salmonella typhimurium in chicken carcass wash water. J. Food Prot. 68, 1241–5.

Yao, L., et al., 2015. Integrated platform with magnetic purification and rolling circular amplification for sensitive fluorescent detection of ochratoxin A. Biosens. Bioelectron. 74, 534–8. doi:10.1016/j.bios.2015.06.056

Yaohua, H., et al., 2014. Detection of Staphylococcus Aureus using quantum dots as fluorescence labels. Int. J. Agric. Biol. Eng. doi:10.3965/ijabe.v7i1.883

Yong, K.T., et al., 2009. Imaging pancreatic cancer using bioconjugated InP quantum dots. ACS Nano 3, 502–10. doi:10.1021/nn8008933

Yong, K.T., Swihart, M.T., 2012. In vivo toxicity of quantum dots: no cause for concern? Nanomedicine (Lond). 7, 1641–3. doi:10.2217/nnm.12.152

Yu, H.W., et al., 2011. Bead-based competitive fluorescence immunoassay for sensitive and rapid diagnosis of cyanotoxin risk in drinking water. Environ. Sci. Technol. 45, 7804-11. doi: 10.1021/es201333f.

Yu, X., et al., 2013. On-chip dual detection of cancer biomarkers directly in serum based on self-assembled magnetic bead patterns and quantum dots. Biosens. Bioelectron. 41, 129–36. doi:10.1016/j.bios.2012.08.007

Yue, Z., et al., 2013. Quantum-dot-based photoelectrochemical sensors for chemical and biological detection. ACS Appl. Mater. Interfaces 5, 2800–14. doi:10.1021/am3028662

Zahavy, E., et al., 2012. Application of nanoparticles for the detection and sorting of pathogenic bacteria by flow-cytometry. Adv. Exp. Med. Biol. 733, 23–36. doi:10.1007/978-94-007-2555-3_3

Zhang, B., et al., 2009. Quantum dots/particle-based immunofluorescence assay: synthesis, characterization and application. J. Photochem. Photobiol. B. 94, 45–50. doi:10.1016/j.jphotobiol.2008.09.008

Zhang, W., et al., 2010. A new method for the detection of the H5 influenza virus by magnetic beads capturing quantum dot fluorescent signals. Biotechnol. Lett. 32, 1933–7. doi:10.1007/s10529-010-0379-5

Zhang, X., et al., 2013. Preparation, characterization of Fe3O4 at TiO2 magnetic nanoparticles and their application for immunoassay of biomarker of exposure to organophosphorus pesticides. Biosens. Bioelectron. 41, 669–74. doi:10.1016/j.bios.2012.09.047

Zhang, Y., et al., 2012. Magnetic beads-based electrochemiluminescence immunosensor for determination of cancer markers using quantum dot functionalized PtRu alloys as labels. Analyst 137, 2176–82. doi:10.1039/c2an16170b

Zhao, Y., et al., 2009. Simultaneous detection of multifood-borne pathogenic bacteria based on functionalized quantum dots coupled with immunomagnetic separation in food samples. J. Agric. Food Chem. 57, 517–24. doi:10.1021/jf802817y

Zhelev, Z., et al., 2006. Single quantum dot-micelles coated with silica shell as potentially non-cytotoxic fluorescent cell tracers. J Am Chem Soc. 128, 6324–5. doi: 10.1021/ja061137d

Zhu, Y.D., et al., 2014. Fluorescent immunosensor based on CuS nanoparticles for sensitive detection of cancer biomarker. Analyst 139, 649–55. doi:10.1039/c3an01987j

Zou, F., et al., 2015. Dual-Mode SERS-Fluorescence Immunoassay Using Graphene Quantum Dot Labeling on One-Dimensional Aligned Magnetoplasmonic Nanoparticles. ACS Appl. Mater. Interfaces 7, 12168–75. doi:10.1021/acsami.5b02523

FINAL CONCLUSIONS

The discharge of wastewater containing various contaminants into the aquatic ecosystems is a major concern as it can be a threat to public health

In the context of environmental biotechnology, sensitive microalgae species are useful as a biological tool for assessment and monitoring of environmental toxicants such as heavy metals, pesticides and pharmaceuticals. While chemical assays are used to determine the contents of the pollutants, only bioassays can really assess the biological effects on living organisms. Adverse impacts of environmental toxicants on microalgae can be far-reaching as they form the basis of the food chain. Thus, microalgae are often included in the bioassays of environmental pollutants.

Micro-algae are microscopic photosynthetic organisms that are found in both marine and freshwater environments. Several species having a range of specific requirements for their living environment appear to be especially suited for biosensor applications. These requirements are nutrients, salinity, temperature, light, depth, and currents. They constantly face the threat of photo-oxidative stress from fluctuating light conditions and environmental stress. Algae have developed an array of defences to protect the chloroplast from reactive oxygen species. Unfortunately, nearly every imaginable environmental change can upset this balance, resulting in the production of reactive oxygen species (ROS). Photo-oxidative stress can lead to loss of protein function, membrane integrity, and eventual cell death. Therefore, it is necessary to propose new biomediators that can operate in harsh environmental conditions.

In chapter two, we suggested a novel microfluidic biosensor that can detect quickly and accurately the pesticide concentration in seawater based on chlorophyll fluorescence emitted from *Chlorella vulgaris* and *Tetrahymena pyroformis* symbiotic association. The system is composed of 500µmol photons m^{-2} s^{-1} red light for 11 s at 650nm as excitation light source, white survival light, a photodiode detector at 680nm, a signal analysis circuit and a microfluidic chip as a symbiotic *Chlorella vulgaris-Tetrahymena pyroformis* transportation platform. To demonstrate the utility of this

system, real samples spiked with different pesticides were tested in comparison to LC-MS. The developed biosensor can detect the presence of pesticides. The lowest concentration that can be detected by using this biosensor are varies between 0.13-1.35µg/L for different analytes. Even smaller analyte concentrations could be detected by increasing the exposure time. The developed microfluidic biosensor has great potential for in situ marine monitoring. Most of the algal biosensors published to date has focused on applications in freshwater and wastewater. In contrast to them, the proposed biosensor developed directly for marine toxicity detection on microfluidic chip. It confers also novel features by employing symbiotic association between *Chlorella vulgaris* and the ciliate *Tetrahymena pyriformis* as biomediator, showing enhanced resistance to the salinity of marine water.

In chapter three, an optical and amperometric biosensor for rapid quantification of the photoprotective effect of xanthophylls on the PSII macromolecular assembly was reported. The proof-of-concept of this novel-designed biosensor is based on the knowledge that in the presence of excess absorbed energy the D1 protein is photodamaged determining a reduction of the amperometric/fluorescence signals; that damage in the presence of xanthophylls could be prevented or reduced. The measurements was performed on the immobilized *Chlamydomonas reinhardtii* strains mutated at the level of photosynthetic D1 protein after short-term exposure of saturated light. The presence of chlorophyll and carotenoids in mutated *Chlamydomonas reinhardtii* cells was confirmed spectrometrically and further with thin layer silica gel-silufol chromatography analysis. The responses of the cells to high light in the absence and presence of endogenous astaxanthin was confirmed optically by measuring the photosynthetic quantum yield and amperometrically by measuring O_2 reduction currents produced by the light-induced electron transfer chain and water splitting in PSII. The biosensor was proved to be suitable for the determination of the exogenous supplied astaxanthin, showing in a short time a reliable response with a detection limit of 3 µM. The present results suggest that in algae, astaxanthin exploits both filtering andantioxidant effects in

different light conditions. The proposed multitransduction biosensor based on algae was novel, cheap and convenient for the evaluation of astaxanthin physiological effect and its detection.

Algal biomediators can also be employed for the design of biosensing systems for the detection of photosynthetic herbicides, in addition to enzymes for different classes of pesticides, insecticides and organophosphorus compounds

In chapter four, we aimed to develop and validate a sensitive method to optically detect a set of chemical classes in raw milk samples hence an optical biosensor, involving an array of biomediators, for the multiplex screening of diuron, chlorpyrifos, cathecol, urea, lactose, D-Lactic acid in milk are reported for the first time. The multiplexed detection relies on the use of a target specific enzymes modified with fluorescein 5(6)-isothiocyanate or 5(6)-carboxynaphthofluorescein and *C. reinhardtii* cells. The analyses were performed by fluorescence that for the algal cells was based on chlorophyll a fluorescence emission while for enzymes was guaranteed by the use of fluorescein 5(6)-isothiocyanate or 5(6)-carboxynaphthofluorescein. The usefulness of the multiarray biosensor was demonstrated by analyzing spiked milk samples with minimal sample preparation, namely ½ dilution of the sample, in only 10 min. The results demonstrated that a clear discrimination of milk samples contaminated with a set of chemicals at their maximum residue limits level allowing the identification of milk not complying with current legislation. These features make the developed methodology a promising alternative in the development of user-friendly devices for on-site analysis to ensure quality control for dairy milk products.

Amperometric biosensors based on measurement of photosynthetic oxygen generated by microalgae on screen printed electrodes for monitoring and assessment of environmental toxicants is another application that has attracted much interest. Biosensors based on screen-printed electrodes (SPE) are especially attractive for on-site monitoring because of their small-size and portability. The easy of production and low-cost materials involved in the screen-printing technology have lead to the massive production of such devices. SPEs are also disposable devices, which is an important feature

for clinical applications. Amperometric measurements often need a buffering solution to be pumped inside a detection cell and mechanical pumping in dynamic mode. The use of peristaltic pumps as fluidic distribution microsystems in electrochemical biosensor devices operating with amperometric transducers can result in periodic spikes affecting the output signal. Mechanical components rotating inside the pumps are the main cause of this kind of disturbing noise. In this sense, reducing signal to noise ratio and increasing the sensitivity of the biosensor is primary interest.

In chapter five, a novel fluidic approach for electrochemical measurements based on a test fluid for readout signal cleanliness has been presented. Comparisons with other commercial fluidic systems used in the targeted field have been carried out. Evidence has been shown of an enhanced performance of a novel pumping system resulting in an improved reading of the final signal. The experimental characterization of the system confirmed the theoretical findings and a first functioning prototype device has been built. This device combines the absolute stability of the flow rate feeding the sensor with the non-contamination of the test fluid. In addition, the absence of moving mechanical parts and need for external power supply, not only simplifies the system but it allows to reduce malfunctions and to considerably contain the cost.

Apart from being important in environmental monitoring and food control, unicellular green microalgae is also essential element of bioregenerative life support systems. Bioregenerative life support systems (BLSS) are complex systems based on biological elements which aim at recreating within confined spaces a biosphere similar to Earth's. For the space arena, the issue is related to human space exploration and colonization of the solar system. On ground, the issue is directly related and of interest for agriculture in confined and extreme environments and in the construction industry, with a very high space-to-ground transfer potential and with the expectation of a significant contribution to the issues of environmental sustainability, resource conservation, and energy efficiency.

Within BLSS, as well as in the terrestrial ecosystem, the growth of algae plays a key functional role, for the production of food with high nutritional characteristics especially in terms of

antioxidants, release of oxygen and reduction of carbon dioxide etc. On the other hand, in confined environments and away from Earth, microalgae can play a positive impact also on the psychological well-being of astronauts. However, the cultivation of microalgae in confined environments and under reduced gravity conditions is extremely complex. Scientific knowledge on microalgae in space should be advanced, and several key technologies required for the cultivation of microalgae in space should be brought to a higher level of development and qualified for their use in the space environment.

Thus in chapter six, biologic research focus are related to the production of the most suitable microalgae species to be grown in a harsh environment under multi-stressor conditions such as the abiotic stress, gravity reduction, radiation and magnetic field. Furthermore, development of fluorometric systems consist of photodiodes and LED lighting with the most effective wavelengths for monitoring the fluorescence induction kinetics of microalgae. In the current project we produced two set of like to *Chlamydomonas* strains which (i) express antioxidative peptides and (ii) are adapted to increased doses of UV radiation. Their physiological characteristics were examined and some important metabolites, which plays important role in antioxidant activities, such as phenols and lipids were analyzed using the Folin-Ciocalteu method and gravimetric method respectively. The in-vitro antioxidant activity of the algae extracts of the different *Chlamydomonas reinhardtii* mutants culture was evaluated by two different methods: TEAC and DPPH assay. Beside, a study with mutants to assess their general in-vivo antioxidant activity was performed in the presence of $_1O^2$ precursors such as a photosynthesizer dye Rose Bengal and hydrogen peroxide. Finally, the algal cultures were integrated in developed automatic multicell fluorescence instrument to measure and store chlorophyll fluorescence induction data. The mutant strains showed physiological characteristics similar to control strain IL. The UV180 mutant strain, which was exposed to UV-B light (312nm) for 180 min over a period of 12 month, clumped in tris-acetate-phosphate medium. Measurement of in-vivo antioxidant activity showed that antiox and UV mutants have improved their survival rate in the presence of singlet oxygen precursor (rose bengal and H_2O_2), which exceeds the survival rate of

control algae. The half-life of UV-mutants was also increased. Obtained results clearly revealed that the produced mutant strains are promising to be used as biosensor for ground-based research and as life support systems for the ISS modules for development towards space exploration. Keeping all this interesting results in mind, the produced mutants revealed to be a worthy for environmental monitoring and beyond that for next mission to ISS station.

Finally, in the sense of commercial biosensor applications photosynthetic whole cell-based biosensors preserve photosystem functionality, but provide a slow response and sometimes low sensitivity. Although the use of thylakoid membranes or isolated protein complexes provides high sensitivity, their extraction, purification or in vitro reconstitution procedures are often laborious, expensive and in some cases not always reliable. Thus under the shadow of nanotechnology and molecular biology improvements, it is desirable to design a novel biomimetic molecules able to simulate biological processes, such as the binding of specific analytes, for use as bioreceptor in environmental monitoring. These novel products can be exploited as molecular tools for finding applications in the development of analytical devices and accelerate the commercialization of biosensors and biochips. In this context, the chloroplast psbA gene-encoded D1 protein has received particular attention due to its involvement in the PSII assembly and repair cycle, and capability to bind anthropogenic pollutants.

In chapter seven, the *Chlamydomonas reinhardtii* D1 primary structure was used as a template to computationally design novel peptides enabling the binding of the herbicide atrazine. Three biomimetic molecules, containing the Q_B-binding site in a loop shaped by two a-helices, were reconstituted by automated protein synthesis and evaluated as bioreceptor for atrazine detection. We reported preliminary results about a technology using QDs-D1 biomimetic peptide conjugation acting as sensing element and its application for the detection of atrazine and diuron. Standing out among the others, the biomimetic mutant peptide, D1pepS268C, showed high ability to mimic the D1 protein in binding atrazine. The fluorescence emission intensity of CdSe quantum dots (QDs) conjugated to

biomimetic D1 peptide to form QD-based biomolecular sensor increases significantly upon binding of the sensors to target atrazine. This phenomenon enables the development of homogenous, separation-free bioassay for quantitative detection of atrazine in solution. Proof-of-principle assays were developed by dosing a solution containing a biomolecular target with a solution containing the corresponding QD-based sensor and monitoring the changes in the fluorescence emission intensity of the QDs. Moreover, this work demonstrates the interest to replace whole microalgae cells or their photosynthetic apparatus (thylakoids, isolated reaction centers) by much smaller fragments such as D1 peptide mimics. This approach might improve the system in terms of sensitivity, but also in terms of stability (oligopeptides being much more stable than the whole three-dimensional protein molecule)